OUKA
The University of Osaka
Institutional Knowledge Archive

Title	Identification and Overexpression of Genes in Escherichia coli that Enhances the Growth of Chlorella sorokiniana under Co-cultivation
Author(s)	Yi Tong, Cheah
Citation	大阪大学, 2026, 博士論文
Version Type	VoR
URL	https://doi.org/10.18910/105407
rights	
Note	

The University of Osaka Institutional Knowledge Archive : OUKA

https://ir.library.osaka-u.ac.jp/

The University of Osaka

Doctoral Dissertation

(Double Degree Program)

Identification and Overexpression of Genes in *Escherichia coli* that Enhances the Growth of *Chlorella sorokiniana* under Co-cultivation

CHEAH YI TONG

December 2025

Biotechnology Global Human Resource Development Program

Division of Biology

Graduate School of Engineering

The University of Osaka

Table of Contents

CHAPTER 1: Introduction 5

1.1 Algae-bacteria mutualistic interaction: Symbiotic relevance in phycosphere 5

1.2 Major cooperative mechanisms in mutualistic co-cultures 6

1.3 Adoption of bacteria in promoting microalgal metabolite production 10

1.4 Exploring beneficial bacteria from metabolic engineering: Insights beyond symbiosis 14

1.5 Problem statement and research objectives 16

CHAPTER 2: KEIO Knockout Collection Reveals Metabolomic Crosstalk in *Chlorella sorokiniana- Escherichia coli* Co-cultures 17

2.1 Introduction 17

2.2 Materials and methods 18

2.2.1 Establishment of microalgal and bacterial culture 18

2.2.2 Co-cultivation of *C. sorokiniana*-KEIO Knockout collection and KEGG matching 19

2.2.3 Validation test of shortlisted bacterial determinants 21

2.2.4 Statistical analysis 21

2.3 Results and discussion 22

2.3.1 Establishment of a screening approach for identifying bacterial genes responsible for algal growth 22

2.3.2 Investigation and mapping of the shortlisted functional genes derived from bacteria in potential metabolic biosynthesis pathways 31

2.3.3 Impact assessment of synthetic metabolites on *C. sorokiniana* growth 38

2.4 *S*ummary 42

CHAPTER 3: Impacts of Riboflavin-overproducing Engineered *Escherichia coli* towards *Chlorella sorokiniana* Growth in Optimized Co-cultivation Approach 44

3.1 Introduction 44

3.2 Materials and methods 45

3.2.1 Strains, plasmids, media, and cultivation conditions 45

3.2.2 Gene overexpression and plasmid construction 46

3.2.3 Riboflavin production under different isopropyl β -d-1-thiogalactopyranoside (IPTG) concentrations 48

3.2.4 Quick assessment of co-cultivation approaches in microscale set-ups 49

3.2.5 Long-term shaking-flask co-cultivation and cell growth assessment 50
3.2.6 Extra- and intra-cellular metabolite concentration measurement 51
3.2.7 Statistical analysis and Pearson correlation 51
3.3 Results and discussions 52
3.3.1 Impact of induced riboflavin production from different recombinant systems on bacterial cell growth and microscale co-cultivation performance 52
3.3.2 Cell growth assessment and pigment content analysis in the optimum co-cultivation approach 56
3.3.3 Accumulation of metabolites from flask cultures 62
3.3.4 Proposed interaction mechanisms between microalgae and engineered bacteria from co-culture systems 65
3.4 Summary 69
CHAPTER 4: Synergistic Enhancement of Biomass and Lipid Productivity in *Chlorella sorokiniana* Co-cultured with Vitamins-overproducing *Escherichia coli* 70
4.1 Introduction 70
4.2 Materials and methods 71
4.2.1 Strains, plasmids, and cultivation conditions 71
4.2.2 Gene cloning and construction of recombinants 72
4.2.3 Co-cultivation medium preparation and conditions 74
4.2.4 Quantification of targeted metabolites secreted into the extracellular medium 74
4.2.5 Determination of growth profile 75
4.2.6 Determination of photosynthetic pigment content 75
4.2.7 Determination of biochemical composition 76
4.2.8 Determination of antioxidant enzyme activity 76
4.2.9 Determination of fatty acid methyl esters (FAMEs) 77
4.2.10 Evaluation of biofuel properties 77
4.2.11 Statistical analysis 78
4.3 Results and discussions 78
4.3.1 Recombinant strains screening and long-term cultures growth assessment 78
4.3.2 Vitamin profiles in extracellular medium throughout long-term cultivation 83
4.3.3 Effect of engineered bacterial strain onto photosynthetic pigment and intracellular organic matters composition 86
4.3.4 Effect of engineered bacterial strain onto the oxidative stress responses in the cultures 88
4.3.5 FAME contents and fatty acids-based biodiesel properties evaluation 91

4.4 Summary 96
CHAPTER 5: Conclusion and Future Perspectives 97
5.1 Conclusion 97
5.2 Future perspectives 98
References……..... 100
Supplementary Data 111
List of Publications 151
Acknowledgement 154

CHAPTER 1: Introduction

1.1 Algae-bacteria mutualistic interaction: Symbiotic relevance in phycosphere

Microalgae is a large group of photosynthetic organisms that are autotrophic in nature and well-acknowledged as living bioreactors to produce valuable bio-products such as proteins, lipids, carbohydrates, and pigments, to fulfill the global biochemical demand [1]. They exhibit growth rates three to ten times higher than terrestrial plants, exceptional adaptability for cultivation on non-arable lands, and widespread presence across all aquatic habitats on Earth. Nevertheless, monoculture of microalgae is always associated with insufficient cell density, high contamination risk, and low metabolite concentration [2]. These downsides have then rekindled interest in researchers to optimize microalgal cultivation conditions and design novel photobioreactors. One of the promising approaches is to co-culture microalgae with symbiotic bacteria for algal biomass enhancement and bio-compounds production. The main idea in microalgal-bacterial co-cultivation is to mimic the natural environmental systems, thus rendering the co-cultivation system higher robustness, scalability, and self-resilience.

Microalgae was found to actively interact with surrounding bacteria via a multitude of interfaces, such as physical contact between cells, bilateral transfer of dissolved organic compounds, and communication via signaling molecules [3]. All these microscale interactions happen within a micro-region, termed as phycosphere, an extracellular zone that extends outward from an algal colony or individual cell to an undefined distance, which is constrained by the diffusion of algal organic matter and inorganic nutrients [4]. Bacterial groups living within the phycosphere normally thrive on the extracellular products derived from microalgae and present at high concentrations [5]. In return, algae could obtain the necessary vitamin directly from synthesizing bacteria to support their own growth. Such a bi-directional positive interaction

between microalgae and bacteria, regardless of which colonies stand largely benefitted from another, is defined as "mutualism". This type of interaction marks the greatest number of examples reported in archival literatures, particularly the key collaborative mechanisms in mutualistic co-cultures [6-8].

1.2 Major cooperative mechanisms in mutualistic co-cultures

This section aims to provide a bigger body of information about the main mutualistic associations, all of which have been demonstrated through past experiments conducted by other researchers under controlled laboratory conditions. As illustrated in **Figure 1**, key cooperative mechanisms include (a) gas exchange and compensation; (b) growth stimulation via phytohormones secretion; (c) nutrient acquisition promotion; (d) production of antibiotics for host defense; (e) organic products biodegradation; and (f) communication through signal transduction. In the phycosphere, carbon dioxide and oxygen concentrations are pivotal factors influencing the cellular respiration of both microalgae and bacteria. Microalgae typically convert the captured bicarbonate (HCO_3^-) into CO_2 via energy-intensive enzymatic reactions in periplasm, but bacteria can alleviate this energy burden by directly supplying the CO_2 to microalgae for improved photosynthesis efficiency [9]. For example, O_2-CO_2 gaseous exchange in microalgae-bacteria consortium remarkably enhanced the biomass concentration by at least five times in a 120 h cultivation [10]. In a different study, evidence of symbiotic gas exchange between co-immobilized *Pseudomonas putida* and *Chlorella vulgaris* was also observed by a stable of dissolved oxygen profile, in the absence of external aeration [11]. In the presence of bacteria, the issue of abiotic CO_2 stripping (carbon loss that impedes algal growth and nutrient assimilation) also becomes negligible in microalgal-bacterial wastewater treatment systems [12, 13].

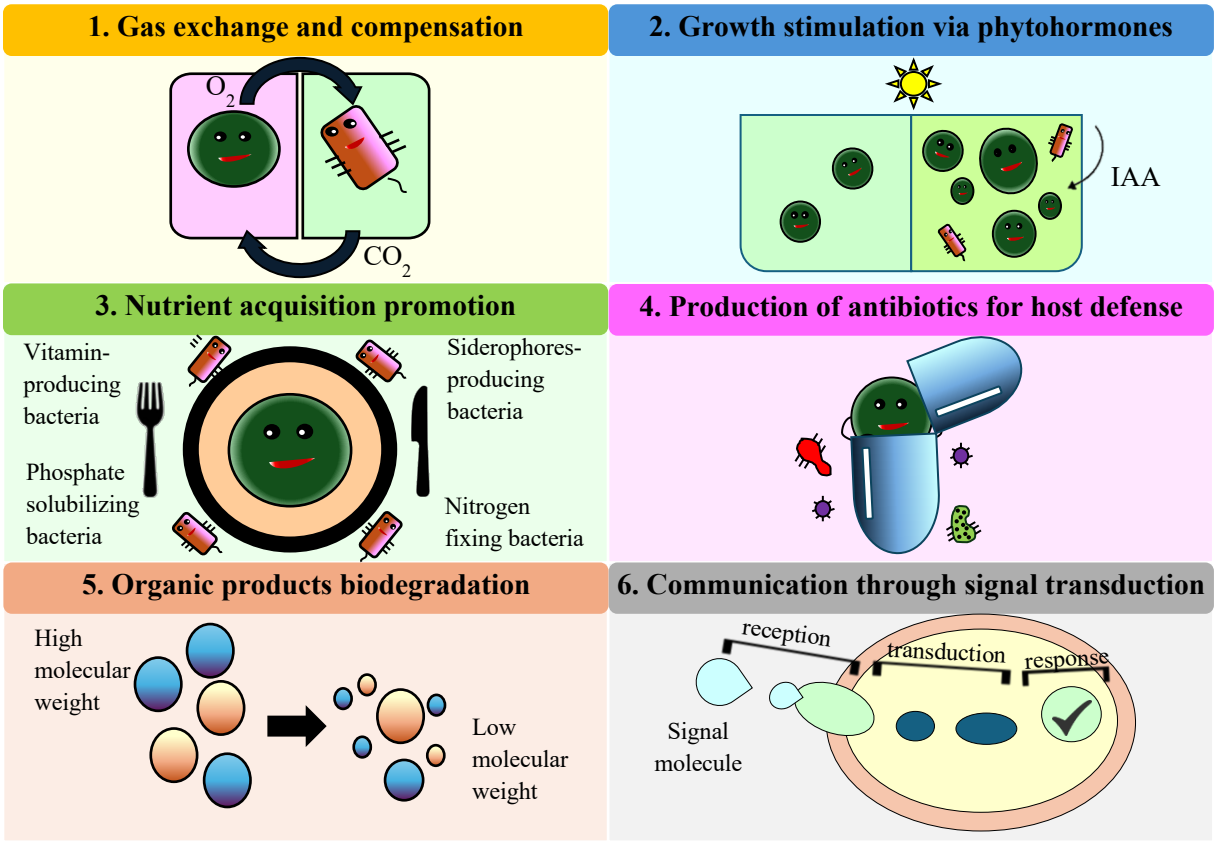

Figure 1 *Coordinating mechanisms involved in mutualistic co-cultures of microalgae and bacteria.*

Phytohormones, or sometimes called as natural or synthetic chemical messengers, are popular in stimulating plant growth by coordinating the adaptive metabolism and environmental responses, even at trace concentrations [14]. They comprise of auxins, cytokinins, gibberellins, abscisic acid, ethylene, brassinosteroids, jasmonates, salicylic acid, and strigolactones. These hormones could act individually or influence other hormone signaling pathways through feedback regulation, known as "hormonal crosstalk" [15]. While their roles in microalgae remain poorly understood, studies suggested they affected algal growth similarly to plants. For instances, meta-transcriptome analyses revealed that *Sulfitobacter* sp. promoted diatom cell division by secreting elevated indole-3-acetic acid levels (~113% - 265%, with microalgae), and enhancing tryptophan biosynthesis in diatoms, eventually attracting more bacteria closer to microalgae [16, 17].

During cell reproduction, microalgae release metabolites to the phycosphere and began the nutrient exchange with bacteria existing near each algal cells (92-98%, up to eight bacteria per algae) [18, 19]. Amid nutrient recycling, microalgal exudates, being relatively diffusible, prompt nearby unattached bacteria to subsidize on the organic matters through bacterial chemotaxis [18]. For example, extracellular carbohydrates from *Coelastrella* sp. was utilized by *Rhodobacter sphaeroides* as energy source for respiratory activity, subsequently allowing this nitrogen-fixing bacteria to supply CO_2 and NH_3 in return [20]. A perfect self-sustaining nitrogen cycle enabled a 2-years-long co-cultivation of *Synechoccus* sp. PCC7002 and natural heterotrophic bacteria, ensuring the healthy survival of the cyanobacteria without any external nutrient supply throughout this period [21]. Similarly, a wide spectrum of bacteria such as *Escherichia coli*, *Pseudomonas* sp., and *Bacillus* sp., were found to be capable in transferring inorganic phosphate (an essential ingredient of adenosine triphosphate and nucleic acids in microalgal cells) to their host microalgae [22, 23].

Dynamic microalgal-bacterial interactions could have their outcomes changed by both abiotic and biotic cues. The right signals can prompt bacteria to suppress antagonistic or growth-inhibiting bacteria. To exemplify this, co-cultivating *Cylindrotheca closterium* with the growth-inhibiting Marinobacter SRVMe reduced microalgal growth, but this inhibition was alleviated when co-cultured with intertidal marine bacteria, suggesting a shift toward beneficial bacteria [24]. Such co-adapted bacteria can fend off foreign hosts, but the underlying mechanisms remain in the dark, and no one is able to predict to what extent the bacteria are able to hinder the foreign host attack. For example, bacterial community associated with *Scenedesmus vacuolatus* exhibited commensal or mutualistic interactions with the microalgae in the absence of aphelid infection, but shifted to a pathogenic behavior once *Amoebaaphelidium protococcarum* was introduced [25].

Bacteria act as natural mineralizers, contributing to the breakdown of organic materials that enhances microalgal adaptation to stressful environments, such as exposure to strong chemicals or pollutants in contaminated aqua systems. Symbiotic bacteria, particularly those exposed to pollutants over time, can help surviving microalgae due to their increased pollutant tolerance [26]. While some bacteria may have an algicidal effect, they can also alleviate toxicity or promote metal availability to microalgae through pesticide breakdown or metal immobilization [27]. During metabolism, bacteria also degrade high-molecular-weight algal organics, such as carbohydrates, lipids, and proteins, into volatile fatty acids, small amino acids, and alcohols [28]. These substances, along with dominant organic matters like tryptophan, humic acids, and chlorophyll *a*, can be further oxidized by electrochemically active bacteria [29]. In a concentrated piggery digestate treatment system, organic-degrading and nitrifying bacteria were deliberately inoculated alongside *Desmodesmus* sp. CHX1, resulting in high $NH4^+$ removal and algal biomass of three-fold higher [30]. Wang and others (2020) cited that complex microalgal-bacterial interconnections were robust enough to resist harmful invasion by efficiently reducing available nutrients for invaders. Indigenous bacteria is capable to break down excessive soluble algal products, alleviating algal growth inhibition in nutrient-over rich wastewater [31].

Last but not least, another significant mechanism of synergistic mutualism between microalgae and bacteria is signal transduction, where chemical substances facilitate communication to alter gene expression or cell metabolism, instead of serving as nutrients. Bacterial quorum sensing (QS), or sometimes defined as a type of “molecular circuit”, allows bacteria to coordinate community-wide physiological processes via autoinducers [32]. Popular QS signals in microalgal-bacterial interactions include N-acyl-homoserine lactone (AHL), 2-alkyl-4-quinolone, furanosyl borate diester, and tetramic acid [32]. For instance, long-chain AHL (C14-

HSL) enhanced the growth of benthic diatom *Seminavis robusta*, whereas oco-C14-HSL and tetramic acid (TA14) were linked to growth inhibition as these two QS molecules trigger a shift in lipid metabolism [33].

1.3 Adoption of bacteria in promoting microalgal metabolite production

Generally, as illustrated in **Figure 2**, dynamic configuration of a microalgal-bacterial consortium can be divided into four basic steps: (1) the consortium is facilitated by exopolysaccharides that extend the territory of activated bacterial flocs; (2) newly growing bacteria attach to the algal surface, particularly within the phycosphere or its surroundings; (3) bacterial and microalgal cells distribute evenly within the particles; and (4) a balance between biomass aggregation and separation is established, indicating a cooperative relationship between microalgae and bacteria [19]. Building on these mechanisms, Palacious and co-authors (2022) further outlined some essential characteristics for microalgal growth-promoting bacteria: (1) the bacteria must exhibit multiple mutualistic mechanisms or metabolic alterations beyond providing CO_2 through natural catabolism; (2) they must be species-specific and highly adaptable to environmental factors such as nutrient composition, pH, and temperature; (3) they should sustain beneficial interactions with most microalgae over extended periods, including logarithmic and stationary growth phases; (4) bacteria that do not directly promote microalgal growth should mitigate biotic or abiotic stressors; and (5) physical attachment to microalgae is unnecessary, but the bacteria must produce volatile organic compounds that can penetrate the phycosphere and influence microalgal metabolism [34].

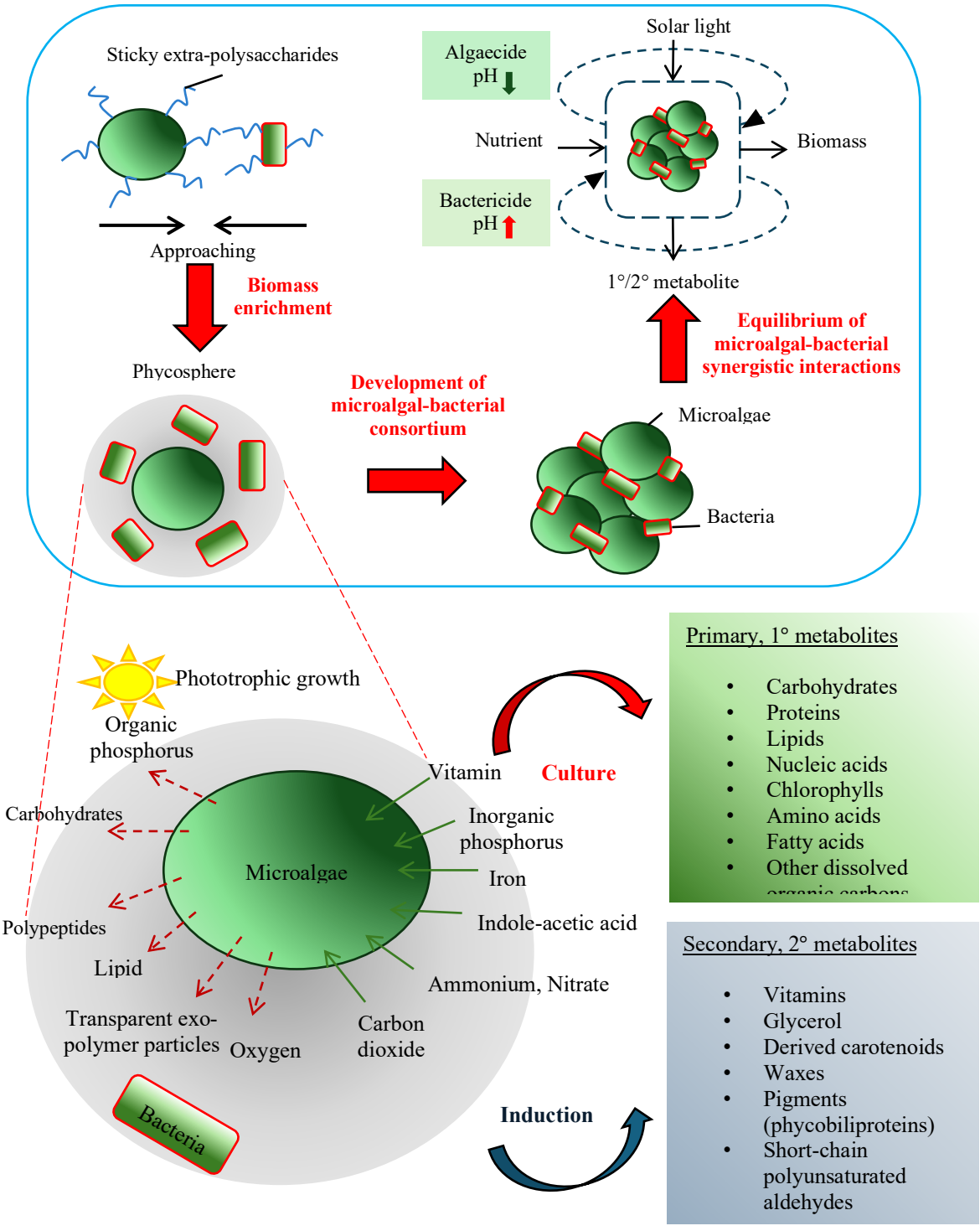

Figure 2 *Development of microalgal-bacterial consortia and their nutritional exchange with primary and secondary metabolite production.*

Microalgae benefit from symbiotic bacteria by synthesizing primary metabolites (e.g., carbohydrates, proteins, lipids, and chlorophylls) for cell maintenance and secondary metabolites (e.g., terpenes, lutein, and astaxanthin) for ecological interactions [15]. **Table 1** summarizes some recent microalgal-bacterial systems that have successfully enhanced microalgal metabolites production. Suitable pairing of specific microalgae and bacteria in a co-cultivation system not only renders higher algal biomass productivity, but also elevates intra-/extra-cellular metabolite synthesis and signaling molecule concentration, improving overall production and system efficiency. High stability of these partnerships eventually brings promising applications such as efficient biomass harvesting that resolve the hassle of downstream processing.

Associating with that, two widely recognized applications are wastewater bioremediation and biofuel production. For example, a satisfactory wastewater treatment efficiency was observed from a microalgae-bacteria consortia over a broad temperature range, leading to a maximum energy yield of 87.4 kJ L^{-1} and lipid production of 1.9 g L^{-1}, driven by the predominance of microalgae [35]. In treating marine aquaculture streams, microalgal-bacterial consortium grown in photobioreactors removed 52%-97% of the organic matter concentrations in the recirculating aquaculture stream [36]. Additionally, bacterial companions can aggregate microalgae without affecting the total lipid content of the cultured cells, as demonstrated by a novel bacterium from Permian groundwater that aggregated potential biofuel-producing *Nannochlropsis oceanica* IMET1 [37]. Other studies also emphasized the potential for a timed-release mechanism in a pond environment, where bacteria initially stimulate algal growth using phytohormones and later shift to produce lysing compounds once the algae reach a certain density, thus aid in lipid harvesting.

Table 1 *Examples of positive microalgal-bacterial interactive systems and their microalgal metabolite production.*

Microalgae	Bacteria	Medium source	Mediators from microalgae	Mediators from bacterium	1° /2° metabolites from microalgae	Ref.
Auxenochlorella protothecoides	*Escherichia coli*	Specific culture medium	Pyruvate	Thiamine derivatives and degradation products	High neutral lipid content	[38]
Chlorella sorokiniana	*Ralstonia pickettii*	Specific culture medium	Extracellular monosaccharide	Solubilized iron	Higher extracellular monosaccharides	[6]
Chlorella sorokiniana	*Azospirillum brasilense*	Specific culture medium	Oxygen	IAA, Vitamin B, lumichrome, riboflavin, CO_2	Higher chlorophyll and lipid (<72 h of cultivation)	[39]
Chlorella sorokiniana	*Melaminivora Jejuensis*	Specific culture medium	Soluble carbon	Soluble carbon	High lipid yield and fatty acid (C16:0, C16:1, C18:1, C18:2) content	[40]
Chlorella sp.	*Pseudomonas* sp., *Proteiniphilum* sp. *and Brevundimonas* sp.	Swine wastewater	Oxygen	Degraded soluble microalgal EPS	High chlorophyll, carotenoid and bounded EPS content	[41]
Chlorella sp.	Ammonium- or nitrite-oxidizing bacteria	Pond wastewater	Carbon dioxide	Oxygen	High chlorophyll content	[42]
Chlorella variabilis ATCC 12198	*Idiomarina loihiensis* RS14	Specific culture medium	Internal organic matter after cell lysis	Siderophores	Higher lipid content (7% of increase in co-culture) and protein content (30% of increase in co-culture)	[43]
Coelastrella sp. KGU-HN001	*Rhodobacter sphaeroides*	Specific culture medium	Carbohydrate	Nitrogenase	Higher extracellular polysaccharide	[20]
Marinichlorella kaistiae KAS603	*Erythrobacter* sp.	Specific culture medium	Dissolved organic carbon	Vitamin B12, carbon dioxide	High chlorophyll content	[44]
Scenedesmus obliquus	*Acidovorax facilis*	Specific culture medium	Carbon dioxide EPS	Oxygen/ Oxidative stress EPS	Bounded polysaccharides was lower in co-cultures, whereas the opposite for bounded protein	[45]

Note: EPS extrapolymeric substances; HRT hydraulic retention time; IAA indole-3-acetic acid

1.4 Exploring beneficial bacteria from metabolic engineering: Insights beyond symbiosis

Undeniably, the cooperation between two different biological kingdoms offers promising potential for the induction of high-value metabolites production with significant commercial interest in pharmaceutical, nutraceutical, and cosmetics industries[46]. To optimize key traits such as biomass yield and nutritional content for large-scale co-culture productions, potential approaches involve: (i) species selection, (ii) harnessing trait plasticity or evolution through DNA alterations or targeted genetic engineering, and (iii) bioprocess optimization of the developed strain [47]. While microalgae are typically a primary focus over decades, attention can also be directed toward bacteria to benefit co-culture systems. This section explores the possibility of metabolic engineering in bacteria to redirect pathways or optimize metabolic flux to produce targeted compounds, such as cofactors or phytohormones, to enhance algal growth.

Bacteria, especially *Escherichia coli*, the workhorse in molecular biology laboratories, are frequently employed as host organism in metabolic engineering due to their exceptional genetic tractability, favorable growth conditions, and well characterized biochemistry [48]. For example, recombinant *E. coli* MG1655 recorded an indole acetic acid titer of 7.1 g L^{-1} via heterologous indole-3-acetamide pathway, with 10 g L^{-1} tryptophan as the substrate [49]. Mutating the FeS-cluster binding in *E. coli* BW25113 benefitted biotin, thiamine, and lipoic acid production by 2.2-fold, 1.3-fold, and 1.8-fold, respectively [50]. Furthermore, a recombinant *E. coli* strain achieved a riboflavin yield approximately 250 times greater following optimization of fermentation conditions [51]. All these bacterial-derived compounds serve as important cofactors for carboxylation reactions, carbohydrate metabolism, and redox reactions in microalgae. While the metabolic capabilities have been well-documented in bacteria, their potential effects on microalgal growth remain largely unexplored.

Apart from that, some promising industrially important bacteria such as *Corynebacterium glutamicum*, *Zymomonas mobilis*, *Lactococcus lactis*, *Bacillus subtilis*, and *E. coli*, stand out due to their extensive use and optimization [52]. *E. coli* has achieved triacylglycerols levels of 399.4 mg L^{-1} with 43.8% medium-chain fatty acids under shake flask conditions after being introduced a complete Kennedy pathway [53]. For oleaginous bacterium *Rhodococcus opacus*, it was successfully engineered to produce 82.9 g L^{-1} of triacylglycerols from glucose and 50.2 g L^{-1} of free fatty acids after having the acyl-coenzyme A synthetases deleted and three lipases overexpressed [54]. Heterogenous expression of the *araBAD* operon from *E. coli* into *Rhodococcus jostii* RHA1, combined with an overexpression of *atf1* encoding a diglyceride acyltransferase showed the improvement of biomass yield and a lipid content by around 8.9% (of the cell dry weight), when grown solely on L-arabinose [55].

While these bacteria independently synthesize commercially important metabolites, exploring their co-cultivation with suitable microalgal strains or engineering them to induce lipid accumulation before co-culture offers an intriguing possibility. For instances, a co-culture of *Synechococcus elongatus* with *Rhodococcus* sp. AF2108 achieved an 8.5-fold increase in cyanobacterial chlorophyll content compared to monoculture [56]. Similarly, *E. coli* has demonstrated compatibility with *Chlorella* sp., suggesting significant potential for total lipid accumulation [57]. These findings have served as a baseline for establishing novel engineered consortia, rather than relying on wild-type states for both entities.

1.5 Problem statement and research objectives

There have been studies demonstrating the enhancement of microalgal growth in the presence of symbiotic bacteria over the years however most of the studies were application-focused with preliminary analyses involved, lacking detailed investigation into the metabolic crosstalk between two [31, 58, 59]. Those past studies were mainly revolving around the role of cultivation regimes [7], nitrogen limitation in cultivation medium [60], or exogenous addition of growth-promoting chemicals [61]. Moreover, plethora works have solely engineered the microalgae for better understanding of gene expression and elucidation of related metabolic pathways but none so far on the bacteria for co-cultivation purposes [62, 63]. Therefore, this research work proposes an in-depth study to investigate the role of bacteria and its streamlined genomes in this intricate cross-kingdom signaling pathways, particularly on the upregulation of potential bio-compounds (vitamins, auxins etc.) from bacteria. It includes the utilization of metabolic engineering to modify the symbiotic bacteria for microalgal proliferation spur. Insight gained can be further incorporated for a theoretical proposal of working mechanisms in transporting the biomolecules generated from bacteria to microalgae, principally developing predictive formulations to enhance the growth of targeted biological entities.

Research objectives are as follows:

- To set-up a genome-wide screening system for the identification of bacterial determinants that improve the algal growth.
- To conduct a preliminary investigation and optimize the metabolic capacity of engineered bacteria in promoting the wild type microalgal growth in co-cultivation.
- To evaluate the impact of effective engineered bacteria on the intracellular metabolite and lipid accumulation of co-cultures.

CHAPTER 2: KEIO Knockout Collection Reveals Metabolomic Crosstalk in *Chlorella sorokiniana- Escherichia coli* Co-cultures

2.1 Introduction

It has come to a general agreement that an interplay between microalgae and bacteria are mostly governed by cell adhesion, chemotaxis, secretion systems, and synthesis of growth promoters. However, the holistic role of symbiotic bacteria inhabiting the algal cell wall is not well documented. It is hypothesized that a much broader set of molecules could be secreted from bacteria, perceived, and utilized by the microalgae. While for bacteria, high-throughput DNA sequencing and functional genes analysis are preferred to uncover the mechanism of metabolites provision and energy transfer in this symbiotic community. The ever-expanding strain repositories or mutant libraries such as completed ASKA library (focuses on over-expression effects) or KEIO Knockout Collection (focuses on loss-of-function effects) could serve as a great starting point to investigate co-occurrence correlations between microalgae and bacteria [64]. Such genome-wide library tools enable the elucidation of functional genes and identification of molecular mechanisms underlying symbiotic interactions, hence tackling the challenges of exploring the algal growth-promoting factors originating from bacteria in this complex cell assemblages. While both approaches are valuable, KEIO was eventually chosen as it offers a straightforward insight, without the interference of overexpression-related effects. In contrast, the ASKA library involving artificial upregulation might potentially induce metabolic stress, altered protein folding, or unintended phenotypic effects, that do not accurately reflect the gene's natural function, necessitating more in-dept analysis to account for these secondary effects [65].

Study in **Chapter 2** is going to reveal new bacterial factors involved in substrate exchange that could be harnessed to engineer more efficient bacterial strains for algal growth promotion.

Collectively, it is hypothesized that a complete set of KEIO Knockout Collection, a comprehensive *E. coli* gene knockout mutant library, could serve as an ideal screening tool to detect specific beneficial metabolites derived from bacteria in the co-culture system. In contrast to the research objective by Heo *et al.* (2020) who aimed to mitigate the algal blooming issues through bacterial interactions [66], the objectives of this current study were: (i) to screen for bacterial genes that positively (or negatively) affect the algal growth, and (ii) to assess the bacterial metabolites that promote algal growth via gene mapping and pathway analysis.

2.2 Materials and methods

2.2.1 Establishment of microalgal and bacterial culture

Being one of the most well-known microalgal genera, *Chlorella sorokiniana* 211/8K (Culture Collection of Algae and Protozoa, United Kingdom) were selected due to its high ability to metabolize carbon sources and synthesize value-added metabolites such as lipids and proteins [67-69]. To completely remove any possible heterotrophic bacterial contamination, they were first treated with a mixture of gentamycin sulfate, kanamycin sulfate, and neomycin sulfate (each at a concentration of 250 mg L^{-1}) for 3 days, and then transferred to antibiotics-free BG-11 medium. For subculture purpose, stock cultures were axenically maintained in 200 mL of autoclaved BG-11 medium (121 ℃, 20 min) in 500 mL Erlenmeyer flask at 25±2℃ under ~120 $\mu mol\ m^{-2}s^{-1}$ of continuous cool-white, fluorescent light. *Escherichia coli* BW25113, the parent strain of KEIO Knockout Collection (National BioResource Project, NBRP, Japan), was cultured overnight in Luria-Bertani (LB) Lennox broth (Nacalai Tesque, Japan) at 37℃ with continuous shaking at 250 rpm in 96-well deep well plates on a Taitech (Saitama, Japan) DWMax MBR-034 microplate shaker.

2.2.2 Co-cultivation of *C. sorokiniana*-KEIO Knockout collection and KEGG matching

The entire study was divided into two main stages: KEIO Knockout Collection wide screening (95 96-well plates, total 3,985 deletions in duplicate, total 7,970 knockout mutants, as described by Barrick lab [70]), and validation of potential metabolites (**Figure 3**). At first, *C. sorokiniana* was pre-cultured in liquid BG-11 medium (17.6 mM $NaNO_3$, 0.23 mM K_2HPO_4, 0.3 mM $MgSO_4 \cdot 7H_2O$; 0.24 mM $CaCl_2 \cdot 2H_2O$; 0.031 mM citric acid·H_2O: 0.021 mM ferric ammonium citrate; 0.0027 mM $Na_2EDTA \cdot 2H_2O$; 0.19 mM Na_2CO_3; 46 μM H_3BO_3; 9 μM $MnCl_2 \cdot 4H_2O$; 0.77 μM $ZnSO_4 \cdot 7H_2O$; 1.6 μM $Na_2MoO_4 \cdot 2H_2O$; 0.3 μM $CuSO_4 \cdot 5H_2O$; 0.17 μM $Co(NO_3)_2 \cdot 6H_2O$) for about one week to achieve a cell density of 5×10^6 cells mL^{-1}. *E. coli* BW25113 and each KEIO mutant strain were pre-cultured in 96 deep well plates containing fresh LB medium (1 mL broth for every well and 30 μg mL^{-1} kanamycin for mutants) under the same conditions as described in **Section 2.2.1,** to reach an optical density about 0.6-0.7 at OD 600 i.e., ca. 10^7 CFU mL^{-1}. About 1 mL of each prepared algal and bacterial cultures were mixed in a 2 mL centrifuge tube, followed by centrifugation at 19,000 ×g for 2 min. Supernatant was carefully discarded and the remaining cell pellets were re-suspended in an equal volume of BG11. No exogenous glucose was supplemented, as the organic products released from the microalgae through photosynthesis could also serve as the alternative carbon source.

Subsequently, co-cultivation was performed by dispensing 200 μL of prepared samples into 96-well microplates and placed on orbital shaker (Mix-EVR, Taitec, Saitama, Japan) at 250 rpm. *E. coli* K-12 BW25113 served as the wild-type control. All the plates were incubated in a growth cabinet (MLR 352, Panasonic, Japan) at 25 ℃ for 45-48 h. Subsequently, the chlorophyll-*a* content (the primary pigment in algal cells) of each individual well was assessed using a microplate reader

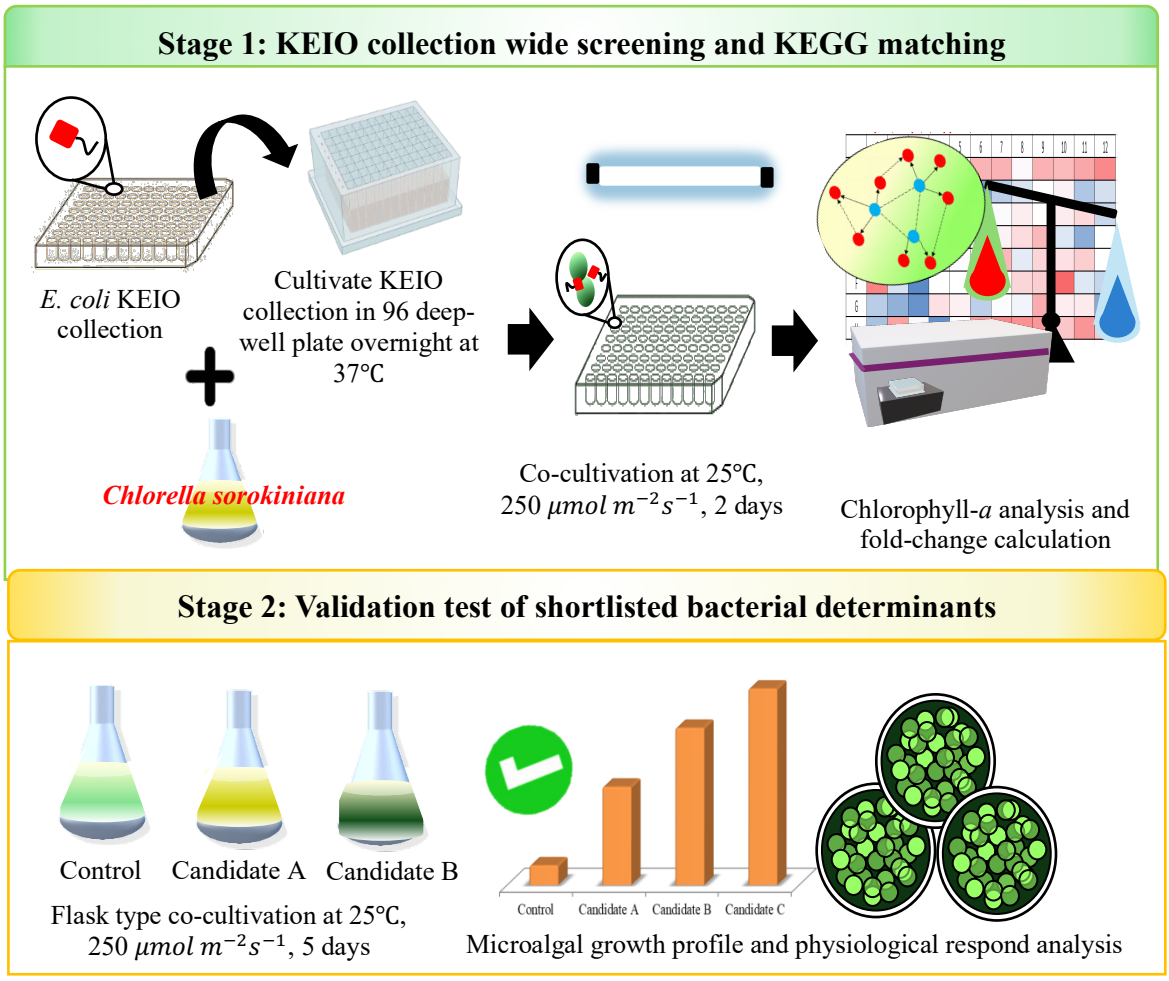

Figure 3 *Schematic overview of the entire research workflow.*

(SpectraMax M2, Molecular Device, Sunnyvale, CA, USA) under operating conditions (Ex 490 nm, Em 650 nm, detector gain 40, reader temperature 25 °C). Based on the acceptable level of this screening experiment, knockout clones demonstrating a 1.25-fold change in relative fluorescence values compared to those of wild-type control were shortlisted to be matched with Kyoto Encyclopedia of Genes and Genomes (KEGG) pathway database (https://www.genome.jp) and UnitProt (https://www.uniprot.org). Potential genes facilitating (≥1.25) and constraining algal growth (≤ 0.8, inverse of 1.25) were concurrently identified.

2.2.3 Validation test of shortlisted bacterial determinants

To validate the findings of the KEGG database pathway analysis, potential bacterial metabolites (riboflavin, biotin, 2,3-butanediol, and cobalamin) obtained from commercial sources (FUJIFILM Wako Pure Chemical Corporation, Osaka, Japan) were supplemented into fresh medium at concentrations of 1, 5, and 10 mg L^{-1}. A pure algal culture served as the control group in the absence of supplemented metabolites. These concentrations were chosen based on the range identified in previous studies involving the similar overexpressing clones [64]. Algae cultivation with the supplemented metabolites took place in 40 mL fresh medium in 250 mL Erlenmeyer flasks, kept under ~120 $\mu mol\ m^{-2}s^{-1}$ of continuous cool-white fluorescent light at 25±2 ℃ for 5 days (exponential growth phase of microalgae, as shown in **Supplementary data 1**). Subsequently, the algal growth responses under different concentrations of commercial metabolites were assessed by measuring the dry weight of algal cells at the end of the experiment. 15 ml of culture was centrifuged to collect cell pellet and subsequently dried at 60℃ until a constant weight was achieved. The difference between the final and initial weight gave the biomass dry weight as expressed in mg L^{-1}.

2.2.4 Statistical analysis

All experiments in this study were performed in triplicate (n=3). Mean values along with their respective standard deviations were reported. The analysis of variance for the triplicates was conducted using SPSS software (IBM SPSS Statistics 25). Significant treatment effects were identified based on a p-value less than 0.05, using one-way analysis of variance (ANOVA). Where any significant differences were spotted, Tukey's post hoc test was utilized to ascertain significant differences among the various groups for multiple comparison purposes.

2.3 Results and discussion

2.3.1 Establishment of a screening approach for identifying bacterial genes responsible for algal growth

With *C. sorokiniana* as a test indicator algal strain, the KEIO Knockout Collection was screened using 96-well plate format, aiming to identify genes that affect algal growth. As illustrated by the experimental workflow in **Figure 4**, color bars that code for each individual effects were integrated into the original 96-well plate layouts from the KEIO Knockout Collection, to accurately depict a large data set. With a fold-change threshold set at 1.25, any increase in algal growth was visually represented by varying shades of red, while a decrease in growth was indicated by blue hues of varying intensity. However, given the study' focus on specific gene knockout effects, it is crucial to highlight that genes exhibiting higher fluorescence values were indicative of their role in impeding algal growth, and vice versa. Each strain carries a single-gene knockout; therefore, the observed fluorescence reflected the microalgal response to the absence of that specific gene. Coupling with fold-change tables sharing the same 96-well plate layouts, such a wide screening method facilitated a comprehensive evaluation of both promoters and inhibitors of algal growth concurrently, directly enhancing the data transparency in an efficient manner. A complete data profile of mean chlorophyll-*a* fluorescence values represented by color bars, and their corresponding fold-changes was provided in **Supplementary data 2**, and **3**, respectively.

The entire knockout gene collection was further filtered to generate a table consisting of genes demonstrating a fold change (in terms of chlorophyll-*a* fluorescence values) of equal to or greater than 1.25 (potential algal growth promoting genes), as well as equal to or less than 0.8 (potential algal growth inhibiting genes). In **Table 2**, the fold change values were ranked in decreasing order, starting from the highest at 1.55 to the lowest at 0.662, with values falling between 0.8 and 1.25 disregarded. Out of the 3,985 clones screened, a total of 87 hit wells were

Gene distribution in original 96-well plate from KEIO collection

	1	2	3	4	5	6	7	8	9	10	11	12
A	JW2035 *wcaI*	JW2118 *yehY*	JW2204 *rcsD*	JW2516 *yfhQ*	JW5922 *ypjL*		JW0436 *cof*	JW1936 *dsrB*		JW3067 *yqjB*	JW5892 *yadB*	
B		JW2124 *yohD*	JW2243 *yfaY*	JW2522 *hcaE*			JW0536 *ninE*	JW2133 *yeiT*	JW2411 *pdxK*	JW3402 *yhhW*	JW0193 *metQ*	JW0409 *yajO*
C	JW2040 *wcaE*	JW2125 *yohF*	JW2287 *yfbQ*	JW2546 *yfhL*		JW2781 *csdA*	JW0600 *uspG*	JW2164 *rtn*	JW2422 *murP*	JW0005 *yaaA*	JW0216 *dinJ*	JW0424 *yajG*
D	JW2045 *wzc*	JW2153 *yeiC*	JW2339 *yfcY*	JW2561 *yfiE*	JW2705 *ygbI*		JW0605 *citG*	JW5378 *dedD*	JW2431 *yffI*	JW0010 *yaaW*		JW0437 *ybaO*
E	JW2049 *asmA*	JW2160 *yeiQ*	JW2376 *yfdZ*	JW2565 *yfiF*	JW2736 *ygcN*	JW2833 *ygeR*	JW0619 *crcB*	JW2314 *dedA*	JW2440 *cchB*	JW0065 *thiQ*	JW0308 *yahB*	JW0443 *ybaY*
F	JW2087 *yegV*	JW2166 *yejB*	JW2430 *yfeG*	JW2586 *yfiB*	JW2737 *ygcO*	JW0184 *rof*	JW0697 *ybgA*	JW2318 *flk*	JW2441 *cchA*	JW0125 *yadI*	JW0309 *yahC*	JW0474 *ybaS*
G	JW2093 *yohM*	JW2167 *yejE*	JW2438 *eutJ*	JW2615 *yfjR*		JW0210 *ivy*	JW1395 *paaY*	JW2381 *ypdE*	JW2515 *iscR*	JW0131 *yadC*	JW0317 *yahK*	
H	JW2116 *yehW*	JW2168 *yejF*		JW2619 *yfjU*		JW0325 *prpD*	JW1823 *yebT*	JW2383 *ypdG*	JW2640 *ygaU*	JW0137 *yadN*	JW0360 *tauD*	JW0534 *ybcM*

Data incorporation

96-wellplate layout showcasing gene distribution from the KEIO collection, accompanied by mean chlorophyll-*a* fluorescence values for each gene when co-cultured with microalgae

	1	2	3	4	5	6	7	8	9	10	11	12
A	JW2035 *wcaI*	JW2118 *yehY*	JW2204 *rcsD*	JW2516 *yfhQ*	JW5922 *ypjL*		JW0436 cof	JW1936 *dsrB*		JW3067 *yqjB*	JW5892 *yadB*	
B	BW25113 **Wild type**	JW2124 *yohD*	JW2243 *yfaY*	JW2522 *hcaE*			JW0536 *ninE*	JW2133 *yeiT*	JW2411 *pdxK*	JW3402 *yhhW*	JW0193 *metQ*	JW0409 *yajO*
C	JW2040 *wcaE*	JW2125 *yohF*	JW2287 *yfbQ*	JW2546 *yfhL*		JW2781 *csdA*	JW0600 *uspG*	JW2164 *rtn*	JW2422 *murP*	JW0005 *yaaA*	JW0216 *dinJ*	JW0424 *yajG*
D	JW2045 *wzc*	JW2153 *yeiC*	JW2339 *yfcY*	JW2561 *yfiE*	JW2705 *ygbI*		JW0605 *citG*	JW5378 *dedD*	JW2431 *yffI*	JW0010 *yaaW*		JW0437 *ybaO*
E	JW2049 *asmA*	JW2160 *yeiQ*	JW2376 *yfdZ*	JW2565 *yfiF*	JW2736 *ygcN*	JW2833 *ygeR*	JW0619 *crcB*	JW2314 *dedA*	JW2440 *cchB*	JW0065 *thiQ*	JW0308 *yahB*	JW0443 *ybaY*
F	JW2087 *yegV*	JW2166 *yejB*	JW2430 *yfeG*	JW2586 *yfiB*	JW2737 *ygcO*	JW0184 *rof*	JW0697 *ybgA*	JW2318 *flk*	JW2441 *cchA*	JW0125 *yadI*	JW0309 *yahC*	JW0474 *ybaS*
G	JW2093 *yohM*	JW2167 *yejE*	JW2438 *eutJ*	JW2615 *yfjR*		JW0210 *ivy*	JW1395 *paaY*	JW2381 *ypdE*	JW2515 *iscR*	JW0131 *yadC*	JW0317 *yahK*	
H	JW2116 *yehW*	JW2168 *yejF*		JW2619 *yfjU*		JW0325 *prpD*	JW1823 *yebT*	JW2383 *ypdG*	JW2640 *ygaU*	JW0137 *yadN*	JW0360 *tauD*	JW0534 *ybcM*



❑ **Low** fluoro. values

❑ **High** fluoro. values

❑ **Enhanced** algal

Fold change= $\frac{Fluoroscence\ values_{WT}}{Fluorescence\ values_{X}}$

Fold-change determination:

- Lower growth expectation for algal growth promoting gene **(≥1.25 fold)**
- Higher growth expectation for algal growth inhibiting gene **(≤0.80 fold)**

	1	2	3	4	5	6	7	8	9	10	11	12
A	1.125	1.071	1.201	0.971	1.012		0.991	0.902		0.983	0.815	
B	1.000	1.287	1.012	0.888			0.965	1.221	1.075	0.875	0.711	0.804
C	1.165	1.036	1.413	0.922		0.877	0.950	0.881	0.837	0.992	0.803	0.809
D	0.860	1.104	1.146	1.142	0.964		0.986	0.987	0.854	0.972		0.826
E	0.882	1.100	1.420	1.020	0.881	0.930	0.930	0.933	0.808	0.989	0.817	0.800
F	0.828	1.122	1.006	1.048	0.913	0.956	0.971	0.961	0.862	0.892	0.826	0.812
G	1.020	1.166	1.318	0.995		0.940	1.069	0.919	0.917	0.998	0.955	
H	0.882	1.128		1.175		1.266	1.021	1.073	0.804	0.991	0.838	0.814

Figure 4 *The screening of bacterial genes from KEIO collection. In order to ease the data visualization and potential genes identification, data acquired was incorporated into every single cell, coupling with heatmap. Similar approaches were adapted during fold-change determination.*

Averages values derived from three replicates are represented (n=3). Note: Figure only provides a glimpse into one random 96-well plate from the KEIO collection. Full spectrum is provided in ***Supplementary data 2-3****.*

identified, comprising of 31 potential algal growth promoting genes and 56 potential algal growth inhibiting genes were identified, respectively. These hits were determined based on significant microalgae-bacteria interactions using a predefined threshold as the selection criterion. However, upon further analysis, among the 87 hit wells, only 20 corresponded to unique genes that clustered tightly within the metabolite networks. Of these 20 unique clones, 11 were from the subset of 31 algal growth-promoting hits (35%), and 9 were from the 56 algal growth-inhibiting hits (16%). These 20 genes have also been highlighted in bold in **Table 2** for clarity. The functions of each shortlisted genes were then delineated together with their associated metabolic pathways in the biosynthesis of specific compounds.

Table 2 *Identified bacterial genes showing ≥1.25-fold increased and ≤0.8-fold decreased C. sorokiniana growth than control via KEIO collection-mediated high throughput screening test. Fold changes determined are sorted in a descending order to facilitate data interpretation. The functions of shortlisted genes (E. coli K-12 MG1655 (U00096.3))were searched via UniProt database (https://www.uniprot.org/) and KEGG pathways (https://www.genome.jp/kegg/pathway.html) .*

No.	Fold change value	Knockout gene	Related metabolic pathway	Gene function
Potential algal growth promoting genes (≥1.25)				
1	1.55	*yae*B	tRNA methylation	Responsible for the addition of the methyl group in the formation of N6-methyl-N6-threonylcarbamoyladenosine
2	1.54	*yhh*F	rRNA methylation	Methylates the guanine in position 966 of 16S rRNA in the assembled 30S particle
3	1.54	***fbp***	**Riboflavin biosynthesis**/ Sucrose biosynthesis	Catalyzes the decomposition of fructose 1,6-diphosphate into 6-phosphate fructose and inorganic phosphorus
4	1.48	***gua*B**	**Riboflavin biosynthesis**/ Purine biosynthesis	Catalyzes the conversion of inosine 5'-phosphate (IMP) to xanthosine 5'-phosphate (XMP)
5	1.47	*yhc*H	DNA damage response	Opens both the alpha- and beta-forms of N-acetylneuraminate (sialic acid; Neu5Ac) to provide aceneuramate, the preferred substrate for NanA.
6	1.44	***bio*B**	**Biotin biosynthesis**	Catalyzes the conversion of dethiobiotin (DTB) to biotin by the insertion of a sulfur atom into dethiobiotin via a radical-based mechanism
7	1.42	*yfd*Z	Alanine biosynthesis	Catalyzes the transamination of pyruvate by glutamate, leading to the formation of L-alanine and 2-oxoglutarate
8	1.41	*yfb*Q	-	Hypothetical protein
9	1.35	*yia*K	Vitamin C degradation	Catalyzes the reduction of 2,3-diketo-L-gulonate in the presence of NADH, to form 3-keto-L-gulonate.
10	1.34	*ego*	Quorum sensing	Responsible for energy coupling to the transport system
11	1.34	*yga*V	Transcription regulation	Functions as a transcription repressor
12	1.33	*tig*	Protein transport	Acts as a chaperone by maintaining the newly synthesized secretory and non-secretory proteins in an open conformation
13	1.32	*yec*R	-	Hypothetical protein

14	1.32	*eut*J	Ethanolamine degradation	Assembling the bacterial microcompartment and/or in refolding EAL
15	1.31	*ybi*S	Cell-shape regulation	Anchor the major outer membrane lipoprotein to the peptidoglycan via a meso-diaminopimelyl-L-Lys- bond on the terminal residue of Lpp
16	1.30	*ybj*D	-	Hypothetical protein
17	1.30	*yci*H	-	Hypothetical protein
18	1.30	yobB	-	Hypothetical protein
19	1.30	*dkg*B	Vitamin C biosynthesis	Catalyzes the reduction of 2,5-diketo-D-gluconic acid (25DKG) to 2-keto-L-gulonic acid
20	1.29	*yfj*W	-	Hypothetical protein
21	1.29	*yoh*D	-	Hypothetical protein
22	1.27	*prp*D	Tricarboxylic acid cycle	Catalyzes the dehydration of 2-methylcitrate (2-MC) to yield the cis isomer of 2-methyl-aconitate
23	1.26	***bio*F**	**Biotin biosynthesis**	Catalyzes the decarboxylative condensation of pimeloyl-[acyl-carrier protein] and L-alanine to produce 8-amino-7-oxononanoate (AON), [acyl-carrier protein], and carbon dioxide
24	1.26	***gnd***	**Riboflavin biosynthesis**/ Glucose metabolism	Catalyzes the oxidative decarboxylation of 6-phosphogluconate to ribulose 5-phosphate and CO_2, with concomitant reduction of NADP to NADPH
25	1.26	***gua*A**	**Riboflavin biosynthesis**/ Purine biosynthesis	Catalyzes the synthesis of GMP from XMP
26	1.26	*cob*B	Chemotaxis	A protein-lysine deacylase by mediating protein desuccinylation and de-2-hydroxyisobutyrylation
27	1.26	***cob*U**	**Cobalamin biosynthesis**	Catalyzes ATP-dependent phosphorylation of adenosylcobinamide and addition of GMP to adenosylcobinamide phosphate
28	1.25	***cob*C**	**Cobalamin biosynthesis**	Catalyzes the conversion of adenosylcobalamin 5'-phosphate to adenosylcobalamin
29	1.25	***zwf***	**Riboflavin biosynthesis**/ Glucose metabolism	Catalyzes the oxidation of glucose 6-phosphate to 6-phosphogluconolactone

30	1.25	***bio*C**	**Biotin biosynthesis**	Converts the free carboxyl group of a malonyl-thioester to its methyl ester by transfer of a methyl group from S-adenosyl-L-methionine
31	1.25	***bio*D**	**Biotin biosynthesis**	Catalyzes a mechanistically unusual reaction, the ATP-dependent insertion of CO2 between the N7 and N8 nitrogen atoms of 7,8-diaminopelargonic acid (DAPA, also called 7,8-diammoniononanoate) to form a ureido ring
Potential algal growth inhibiting genes (≤0.80)				
1	0.80	***fum*B**	**2,3-butanediol biosynthesis**/ Tricarboxylic acid cycle	Catalyzes the reversible hydration of fumarate to (S)-malate
2	0.80	***fab*F**	**Biotin biosynthesis**/ Fatty acid biosynthesis	Catalyzes the elongation of a wide range of acyl-ACP by the addition of two carbons from malonyl-ACP to an acyl acceptor
3	0.80	***adh*E**	**2,3-butanediol biosynthesis**/ Ethanol biosynthesis	Catalyzes the sequential NADH-dependent reduction of acetyl-CoA to acetaldehyde and then to ethanol
4	0.80	***mdh***	**2,3-butanediol biosynthesis**/ Tricarboxylic acid cycle	Catalyzes the reversible oxidation of malate to oxaloacetate
5	0.79	*ace*A	Tricarboxylic acid cycle	Catalyzes the reversible formation of succinate and glyoxylate from isocitrate
6	0.79	*pho*B	Phosphate ion transport/ transcription regulation	A positive regulator for the phosphate regulon
7	0.79	*hch*A	DNA repair	Repairs methylglyoxal- and glyoxal-glycated proteins, and also releases repaired proteins
8	0.79	*pur*K	Purine biosynthesis	Catalyzes the ATP-dependent conversion of 5-aminoimidazole ribonucleotide (AIR) and HCO3- to N5-carboxyaminoimidazole ribonucleotide
9	0.79	*ymf*L	-	Hypothetical protein
10	0.79	***frd*B**	**2,3-butanediol biosynthesis**/ Tricarboxylic acid cycle	Responsible for the catalysis of fumarate and succinate interconversion
11	0.79	*ada*	DNA damage response/ DNA dealkylation in DNA repair	Repairs the methylated nucleobase in DNA by stoichiometrically transferring the methyl group to a cysteine residue in the enzyme
12	0.79	*asnc*	DNA binding/	Activator of asnA transcription

			transcription regulation	
13	0.79	***pta***	**2,3-butanediol biosynthesis**/ acetate biosynthesis	Catalyzes the reversible interconversion of acetyl-CoA and acetyl phosphate
14	0.79	*glc*B	Tricarboxylic acid cycle	Catalyzes the condensation and subsequent hydrolysis of acetyl-coenzyme A (acetyl-CoA) and glyoxylate to form malate and CoA
15	0.79	***fab*H**	**Biotin biosynthesis**/ fatty acid biosynthesis	Catalyzes the condensation reaction of fatty acid synthesis by the addition to an acyl acceptor of two carbons from malonyl-ACP
16	0.79	*pyr*E	Pyrimidine biosynthesis	Catalyzes the transfer of a ribosyl phosphate group from 5-phosphoribose 1-diphosphate to orotate
17	0.78	*pyr*D	Pyrimidine biosynthesis	Catalyzes the conversion of dihydroorotate to orotate with quinone as electron acceptor
18	0.78	*yeb*C	Transcription regulation	DNA binding
19	0.78	*yfj*Y	Proteolysis	Putative DNA repair protein
20	0.77	*ykf*J	-	Hypothetical protein
21	0.77	*app*Y	DNA binding/ transcription regulation	Induces the synthesis of appA and other polypeptides during the decelerating growth phase
22	0.77	*yda*T	-	Hypothetical protein
23	0.77	***pur*A**	**Riboflavin biosynthesis**/ Purine biosynthesis	Catalyzes the first committed step in the biosynthesis of AMP from IMP
24	0.77	*nar*K	Nitrate assimilation	Catalyzes nitrate uptake, nitrite uptake and nitrite export across the cytoplasmic membrane
25	0.77	*yfj*F	RNA methylation	RNA methyltransferase
26	0.77	*ace*B	Tricarboxylic acid cycle	Catalyzes the irreversible condensation of acetyl-CoA with glyoxylate to form (S)-malate
27	0.77	*cai*D	Fatty acid beta-oxidation/ Carnitine catabolic process	Catalyzes the reversible dehydration of L-carnitinyl-CoA to crotonobetainyl-CoA
28	0.76	*pgp*B	Phosphatidylglycerol biosynthesis	Catalyzes the dephosphorylation of diacylglycerol diphosphate (DGPP) to phosphatidate (PA) and the subsequent dephosphorylation of PA to diacylglycerol (DAG)
29	0.76	*pst*B	Phosphate ion transport	Responsible for energy coupling to the transport system

30	0.76	*ren*D	-	Putative defective protein Ren from DLP12 prophage, hypothetical protein
31	0.76	*yfb*P	-	Hypothetical protein
32	0.76	*cai*A	Fatty acid beta-oxidation/ Carnitine catabolic process	Catalyzes the reduction of crotonobetainyl-CoA to gamma-butyrobetainyl-CoA
33	0.76	*gpt*	Purine biosynthesis	catalyzes the transfer of the ribosyl-5-phosphate group from 5-phospho-alpha-D-ribose 1-diphosphate (PRPP) to the N9 position of the 6-oxopurines guanine and xanthine to form the corresponding ribonucleotides GMP
34	0.76	*yae*H	-	Hypothetical protein
35	0.76	*car*A	Pyrimidine biosynthesis	Catalyzes the formation of carbamoyl phosphate from the ammonia moiety of glutamine, carbonate, and phosphate donated by ATP
36	0.76	*nar*L	Nitrate assimilation/ Transcription regulation	Activates the expression of the nitrate reductase (narGHJI) and formate dehydrogenase-N (fdnGHI) operons
37	0.76	*cpd*A	Metal-binding	Hydrolyzes cAMP to 5'-AMP
38	0.76	*ycg*B	-	Hypothetical protein
39	0.75	*pol*B	DNA replication	DNA binding
40	0.75	*ybe*A	rRNA methylation	Specifically methylates the pseudouridine at position 1915 (m3Psi1915) in 23S rRNA
41	0.75	*yaa*J	-	Hypothetical protein
42	0.74	*yei*R	Zinc ion binding	Zinc chaperone that directly transfers zinc cofactor to target proteins
43	0.73	*yci*S	Lipopolysaccharide biosynthesis	Lipopolysaccharide assembly protein A
44	0.73	*pho*R	Phosphate ion transport	A membrane-associated protein kinase that phosphorylates PhoB in response to environmental signals
45	0.73	*ymd*B	Purine biosynthesis	Deacetylates O-acetyl-ADP ribose to yield ADP-ribose and free acetate
46	0.73	*ycd*C	Transcription regulation	regulates the synthesis of pyrimidine nucleotides and arginine from glutamine (carAB) and the supply of glutamate

47	0.72	*rel*E	Transcription regulation	A sequence-specific, ribosome-dependent mRNA endoribonuclease that inhibits translation during amino acid starvation
48	0.72	*ycg*R	Cell motility regulation	Acts as a flagellar brake, regulating swimming and swarming in a bis-(3'-5') cyclic diguanylic acid (c-di-GMP)-dependent manner
49	0.72	*ybd*M	-	Hypothetical protein
50	0.71	*met*Q	Methionine biosynthesis	A binding protein-dependent, ATP-driven transport system
51	0.71	***sdh*C**	**2,3-butanediol biosynthesis**/ Tricarboxylic acid cycle	Membrane-anchoring subunit of succinate dehydrogenase
52	0.70	*iad*A	Proteolysis	Catalyzes the hydrolytic cleavage of a subset of L-isoaspartyl (L-beta-aspartyl) dipeptides
53	0.70	*fim*B	Transcription regulation	Control the phase variation of type 1 fimbriae in *E.coli*.
54	0.68	*ycd*M	Thymine, pyrimidine, and uracil catabolic process/ nitrogen utilization	Catalyzes the pyrimidine ring opening between N-3 and C-4 by an unusual flavin hydroperoxide-catalyzed mechanism
55	0.67	*met*J	Methionine biosynthesis	Regulatory protein that combines with S-adenonsylmethionine to represses the expression of the methionine regulon
56	0.66	*yej*A	-	Hypothetical protein

Among the 31 genes, attention was drawn to 11 genes, such as *fbp*, *gua*B, *gnd*, *gua*A, and *zwf* which were responsible for riboflavin–biosynthesis; *bio*B, *bi*oF, *bio*C, and *bio*D which were responsible for biotin biosynthesis; and *cob*U and *cob*C which were responsible for cobalamin biosynthesis. On the other hand, from the 56 genes, 9 genes were highlighted, namely *fum*B, *adh*E, *mdh*, *frd*B, *pta*, and *sdh*C which compete with 2,3-butanediol biosynthesis; *fab*F and *fab*H which compete with biotin biosynthesis; and *pur*A which compete with riboflavin biosynthesis.

Apart from these genes belonging to the same metabolite biosynthetic pathways, some of the remaining genes (as listed in **Table 2**) were assumed to be involved in the following functions, quorum sensing, protein transport, tricarboxylic acid cycle, glucose metabolism, and DNA damage/transcription regulation. Various interaction or metabolic complementation may occur between prokaryotes and eukaryotes, thus developing a mechanistic understanding of their effects, such as cell-signaling process and nutrient transport. However, despite their involvement at the genomic level, it was speculated that these genes might have minor importance in the co-culture pair used in the current work. As mentioned earlier, since the primary objective of this study is to narrow down the main beneficial metabolites derived from bacteria for algal growth, the focus is exclusively directed towards those bacterial metabolites sharing the same network of shortlisted regulatory genes or enzymes, induced by the presence of microalgae.

2.3.2 Investigation and mapping of the shortlisted functional genes derived from bacteria in potential metabolic biosynthesis pathways

Utilizing KEGG information system and capturing knowledge reported in archival literature, all the molecular interactions and reaction networks were presented in **Figure 5**. Potential associations among the related genes in the same pathways were depicted, with particular emphasis placed on the red- (potential algal growth promoting genes) and black-colored (potential algal

growth inhibiting gene) dots in the visual representations. For example, *fbp* (encoding fructose 1,6-bisphosphatase) was identified as algal growth promoting gene from the screening results. This enzyme catalyzes the hydrolysis of fructose 1,6-diphosphate into fructose-6-phosphate in glyconeogenesis. This is consistent with a previous study reporting that an endogenous *fbp* over-expression was found to divert more upstream glycolytic intermediates likes fructose-6-phosphate and glyceraldehyde-3-phosphate into the pentose phosphate pathway, enhancing both the availability of key precursors (ribulose-5-phoshpate) and reducing power required for riboflavin biosynthesis [71].

Associating with the same bio-compound production, glucose 6-phosphate 1-dehydrogenase encoded by *zwf* gene, catalyzes the oxidation of glucose-6-phosphate to phosphogluconolactone in the reductive pentose phosphate pathway. This can enhance the riboflavin production [72]. In the pentose phosphate pathway, ribulose 5-phosphate is generated after the oxidative decarboxylation of 6-phosphogluconate by 6-phosphogluconate dehydrogenase (encoded by *gnd*, another identified algal growth promoting gene). Ribulose 5-phosphate is subsequently converted by 3,4-dihydroxy 2-butanone 4-phosphatase (encoded by *ribB*) to L-3,4-dihydroxybutan-2-one 4-phosphate (DHPB), guiding the riboflavin biosynthetic pathway. At meantime, ribulose 5-phosphate is also the precursor of the purine biosynthetic pathway consisting of *guaB* and *guaA* encoding inosine 5'-monophosphate cyclohydrolase and inosine 5'-monophosphate dehydrogenase, respectively, which were also successfully identified as one of the potential algal growth promoting genes in the previous screening result. Being a side product of the purine biosynthetic pathway, GTP is considered as another immediate precursor of riboflavin biosynthesis via enzymatic

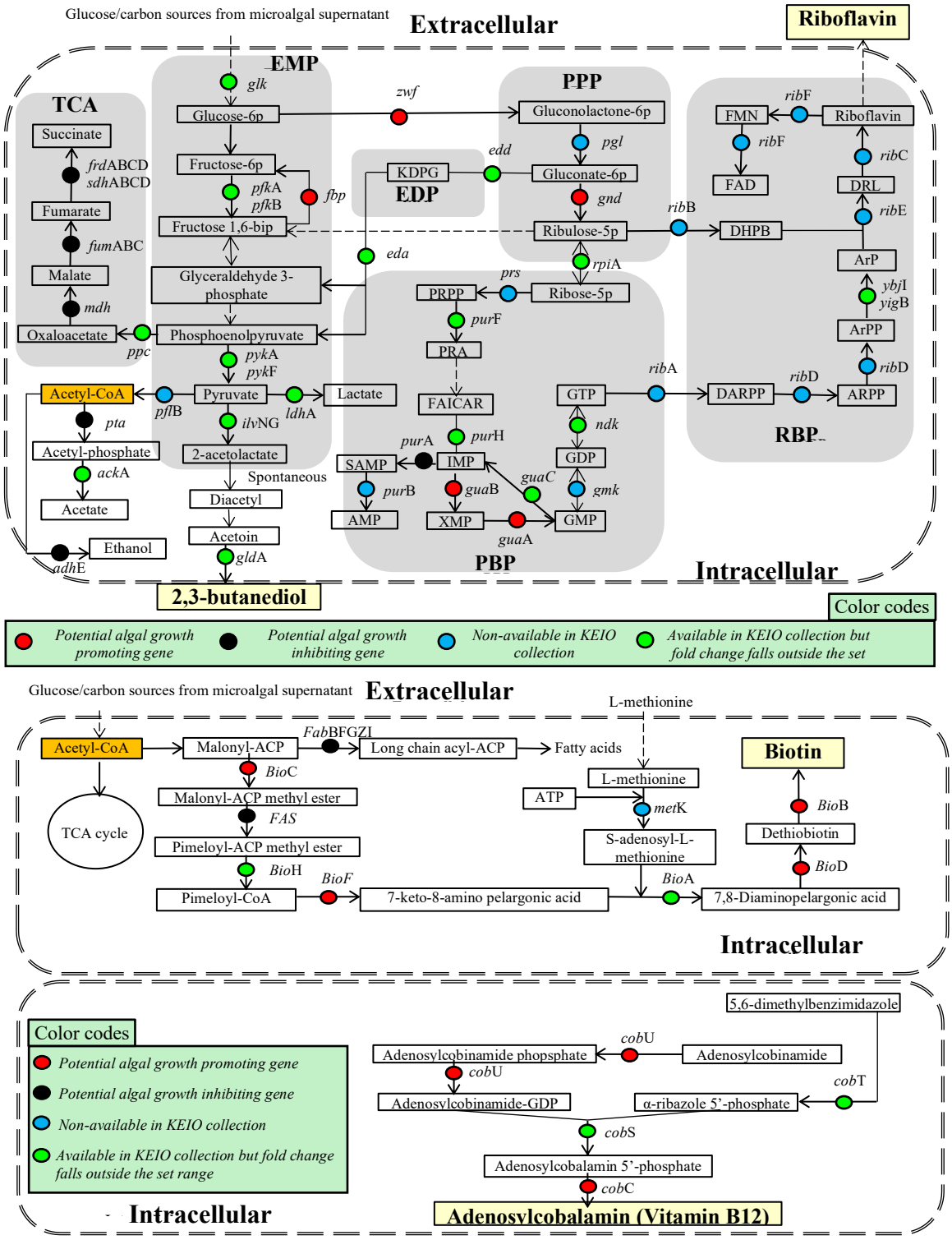

Figure 5 *Schematic location of the shortlisted genes in three potential metabolism pathways, namely riboflavin, 2,3-butanediol, biotin, and adenosylcobalamin biosynthesis.* ***Pathways: PPP****, pentose-phosphate pathway;* ***EDP****, Entner–Doudoroff pathway;* ***TCA****, tricarboxylic acid cycle;* ***EMP****, glycolytic pathway;* ***PBP****, purine biosynthesis pathway;* ***RBP****, riboflavin biosynthetic*

pathway. ***Enzymes:*** ***Pgl****, 6-phosphogluconolactonase;* ***pfkA****, 6-phosphofructokinase I;* ***pfkB****, 6-phosphofructokinase II;* ***fbp****, fructose-1,6-biphosphatase I;* ***zwf****, glucose-6-phosphate 1-dehydrogenase;* ***gnd****, 6-phosphogluconate dehydrogenase;* ***rpiA****, allose-6-phosphate isomerase;* ***prs****, ribose-phosphate diphosphokinase;* ***purF****, amidophosphoribosyltransferase;* ***guaB****, IMP dehydrogenase;* ***guaA****, GMP synthase;* ***gmk****, guanylate kinase;* ***ndk****, nucleoside-diphosphate kinase;* ***ribA****, GTP cyclohydrolase II;* ***ribB****, 3,4-dihydroxy 2-butanone 4-phosphate synthase;* ***ribD****, diaminohydroxyphosphoribosylaminopyrimidine deaminase/5-amino-6-(5-phosphoribosylamino)uracil reductase;* ***ybjI*** *and* ***yigB****, FMN hydrolase/5-amino-6-(5-phospho-D-ribitylamino)uracil phosphatase;* ***ribE****, 6,7-dimethyl-8-ribityllumazine synthase;* ***ribC****, riboflavin synthase;* ***ribF****, bifunctional riboflavin kinase/FMN adenylyltransferase;* ***purH****, bifunctional AICAR transformylase/IMP cyclohydrolase;* ***purA****, adenylosuccinate synthase;* ***purB****, adenylosuccinate lyase;* ***guaA****, GMP synthase;* ***guaB****, IMP dehydrogenase;* ***guaC****, GMP reductase;* ***Glk****, glucokinase;* ***pykA*** *and* ***pykF****, pyruvate kinase;* ***ldhA****, lactate dehydrogenase A;* ***ilvNG****, acetohydroxy acid synthase;* ***gldA****, glycerol dehydrogenase;* ***pflB****, pyruvate formate lyase;* ***pta****, phosphotransacetylase;* ***ppc****, phosphoenolpyruvate carboxylase;* ***ackA****, acetate kinase A;* ***adhE****, bifunctional aldehyde-alcohol dehydrogenase;* ***mdh****, malate dehydrogenase;* ***fumABC****, fumarase;* ***frdABCD****, fumarate reductase iron-sulfur subunit;* ***sdhABCD****, succinate dehydrogenase complex subunit;* ***FAS****, fatty acid synthase;* ***BioC****, malonyl-ACP O-methyltransferase;* ***BioH****, pimeloyl-ACP methyl ester esterase;* ***BioF****, 7-keto-8-amino pelargonic acid synthase;* ***BioA****, 7,8-diaminopelargonic acid aminotransferase;* ***BioD****, desthiobiotin synthase;* ***BioB****, biotin synthase;* ***fabBFGZI****, 3-oxoacyl-[acyl-carrier-protein] synthase;* ***metK****, S-adenosylmethionine synthase;* ***ATP****, adenosine triphosphate;* ***cobU****, bifunctional adnosylcobalamin biosynthesis protein;* ***cobS****, adenosylcobinamide-GDP ribazoletransferase;* ***cobT****, nicotinate-nucleotide-dimethylbenzimidazole phosphoribosyltransferase;* ***cobC****, adenosylcobalamin/alpha-ribazole phosphatase.* ***Compounds:*** ***PRPP****, 5-phospho-alpha-D-ribose 1-diphosphate;* ***PRA****, 5-phosphoribosylamine;* ***IMP****, iInosine monophosphate;* ***XMP****, xanthosine 5'-phosphate;* ***GMP****, guanosine 5'-phosphate;* ***GDP****, guanosine 5'-diphosphate;* ***GTP****, guanosine 5'-triphosphate;* ***DARPP****, 2,5-diamino-6-(5-phospho-D-ribosylamino)pyrimidin-4(3H)-one;* ***ARPP****, 5-amino-6-(5'- phosphoribosylamino)uracil;* ***ArPP****, 5-amino-6-(5'-phospho-D-ribitylamino)uracil;* ***ArP****, 5-amino-6-(1-D-ribitylamino)uracil;* ***DHPB****, L-3,4- dihydroxybutan-2-one 4-phosphate;* ***DRL****, 7-dimethyl-8-(D-ribityl)lumazine;* ***FMN****, flavin mononucleotide;* ***FAD****, flavin adenine dinucleotide;* ***SAMP****, N6 -(1,2-dicarboxyethyl) AMP;* ***AMP****, adenosine 5'-monophosphate;* ***FAICAR****, 5-formamido-1- (5-phospho-D-ribosyl)-imidazole-4-carboxamide.*

reaction of GTP cyclohydrolase II encoded by *rib*A, an essential gene in riboflavin biosynthetic pathway. In this study, the screening results also indicate that adenylosuccinate synthase (encoded by *pur*A) does not contribute to riboflavin biosynthesis and should therefore be deleted or downregulated. This hypothesis is consistent with an earlier study reporting that reducing the expression levels of *rib*F, *pur*A, and *gua*C genes, which are involved in downstream or branch reactions of the riboflavin biosynthesis pathway, could enhance carbon flux towards riboflavin accumulation [73].

In a separate metabolic network, at the junction between the glycolysis and the tricarboxylic acid cycle lies the phosphoenolpyruvate and pyruvate-oxaloacetate node. Phosphoenolpyruvate (PEP), an intermediate in glycolysis, is irreversibly converted to oxaloacetate by PEP carboxylase encoded by *ppc*. While the main function of PEP carboxylase is not directly tied to oxaloacetate, it is still crucial in generating oxaloacetate. In contrast, most genes involved in the TCA cycle (*mdh*, *fum*B, *frd*B, and *sdh*C) were identified to inhibit the algal growth. With similarities to phosphotransacetylase (encoded by *pta*, responsible for acetate production) and bifunctional aldehyde-alcohol dehydrogenase (encoded by *adh*E, responsible for acetyl-CoA conversion in ethanol production), they are the candidates too for gene deletion to minimize the byproduct formation during 2,3-butanediol synthesis [74]. Therefore, it underscores the necessity to delete those inhibiting genes coding for pyruvate-consuming side reactions, branching from phosphoenolpyruvate (succinate) and pyruvate (ethanol) [75]. With this, a larger amount of pyruvate could be shunted to 2,3-butanediol production at a higher titer. However, it is important to highlight that *E. coli* strain itself lacks a functional 2,3-butanediol synthesis pathway and does not prioritize its production after glucose uptake in its wild form, but it can be altered by either amplifying the gene expression linked to its biosynthesis pathway or by eliminating genes (as identified in this study) that hinder its production [74, 76]. Despite *E. coli*'s inherent metabolic pathways not favoring substantial 2,3-butanediol production, the intriguing results indicate a worthy exploration on the potential benefits of externally supplying 2,3-butanediol to validate their positive effects on the algal growth. It is hard to elucidate the interesting result discovered without clear understanding of the underlying mechanisms. However, this unexpected outcome warrants further investigation as discussed in the subsequent **Section 2.3.3**.

Extending from acetyl-CoA, the genes *bio*B, *bio*C, *bio*D, and *bio*F were determined as algal growth promoting genes. They collectively hold a significant position in synthesizing pimeloyl-CoA and constructing the biotin ring. In biotin biosynthesis, the last phase is the insertion of sulfur into desthiobiotin, which is catalyzed by biotin synthase (encoded by *bio*B). A particular biotin ligase (*bir*A) is tasked with covalently attaching biotin to biotin-dependent enzymes and regulating the expression of *bio* operon. Hence, an overexpression of *bir*A or *bio* operon directly corresponds to enhanced biotin production, highlighting the advantageous metabolites originating from bacteria for algal growth, namely biotin [77, 78]. Nevertheless, despite *E. coli* can synthesize biotin *de novo*, biotin is generally not released extracellularly into the growth media but typically retained within the cells for use of fatty acid synthesis and other internal metabolic requirements. Therefore, results speculate that some cross-feeding mechanisms such as bacterial cell lysis or active metabolite externalization/induction could happen in a co-culture environment [79], causing the biotin leaked into the surrounding medium to be potentially taken up by the microalgae. For example, metabolite induction was observed when the authors discovered that *Botryococcus braunii* secretes more biotin into its surroundings, induced by the biotin-auxotrophic *Brevundimonas* sp. Bb-A [80]. A similar mechanism could occur in reverse, where the roles of microalgae and bacteria switch. It underscores that the direction of induction depends entirely on which organism has a greater vitamin demand, at any given time. Microalgae which usually will dominate the whole co-culture system at the end, could be considered as a competitive recipient to stimulate the metabolite externalization. Algal secondary metabolites or allelopathic compounds could also exhibit antibacterial properties that potentially alter the bacterial membrane permeability and damage the cell membrane, eventually leading to the leakage of internal cell

contents. For instance, phenol, hexadecenoic acid, phytol, octadecadienoic acid and bicyclo[3.1.1]heptane from *Chlorella* sp. were found to possess antimicrobial activity [81].

In a separated metabolic network, biosynthetic enzymes, bifunctional adenosylcobalamin biosynthesis protein (encoded by *cob*U) and adenosylcobalamin/alpha-ribazole phosphatase (encoded by *cob*C) from the endogenous *E. coli* cobalamin salvage pathway, were also identified to render positive effects onto algal growth. However, *E. coli* BW25113 or K12 lacks the complete genetic machinery required for the *de novo* biosynthesis of adenosylcobalamin, but can synthesize it when supplied with exogenous corrinoids, such as cobinamide, an intermediate precursor [82]. While there is no exogenous supply of cobinamide in the growth medium, the results obtained was surprising, although this bacterial strain has the potential to produce cobalamin. One possible explanation is that the microalgae might have contributed precursors or analogs that facilitate the cobalamin accumulation within the *E. coli* cells. Earlier research that revealed the presence of cobalamin-active compounds in *Chlorella* sp. grown without an external source of cobalamin suggested that the corrinoid derivatives detected in algal cell extracts may serve essential physiological and possibly coenzyme functions [83]. However, no subsequent research has replicated this discovery, making it difficult to pinpoint the underlying mechanism. Additionally, in this experimental setup, cobinamide may primarily originate from the LB medium carried over from the pre-culture as there was no cell-washing step in between. Residual components of the LB medium, such as cobinamide, can remain associated with the cells and further introduced into the main co-culture set-up, potentially impacting the experimental results. One recent study cited that complete cofactor synthesis pathways in the microbial community might not be necessary to support auxotrophic algae growth, given the prevalence of partial synthesis and salvage pathways in algae [84]. It highlights the complexity of the microalgal-bacterial complementarity, yet related

evidence could still lend credence to the speculation. In fact, adenosylcobalamin itself is not crucial for bacterial growth, but having another principal role in the metabolism of compounds which serve as the important sources of carbon, nitrogen, and energy in specific environments [85]. It indirectly supports the recognition of bacteria-derived cobalamin as a potential growth promoter for the co-partner organism. Overall, results speculated that the generation of riboflavin, 2,3-butaneiol, biotin, and cobalamin may enhance the chlorophyll-*a* production by the *C. sorokiniana.*

2.3.3 Impact assessment of synthetic metabolites on *C. sorokiniana* growth

To confirm the nature of identified bacterial metabolites that potentially enhanced the microalgal chlorophyll-*a* fluorescence, growth responses of the axenic microalgae *C. sorokiniana* to varying concentrations (0, 1, 5, and 10 ppm) of synthetic cobalamin, biotin, riboflavin, and 2,3-butanediol were tested. As displayed in **Figure 6(a)**, it is evident that there is a noticeable variation in color across different concentrations of commercial metabolites, with the axenic control (0 ppm) exhibiting the lightest hue compared to others. In line with the quantitative data in **Figure 6(b)**, microalgal biomass productivities for metabolites-supplemented cultures was at least 1.5-fold higher than that of the un-supplemented culture. In a concentration dependent manner, 2,3-butanediol significantly increased algal growth ($df=3$, $F=28.044$, $p<0.05$), with its most prominent effect on 10 ppm supplementation (6.86 ± 1.29 mg L^{-1} d^{-1}). On the contrary, algae survived the best in 1 ppm of cobalamin-supplemented medium around 8.28 ± 0.01mg L^{-1} d^{-1}, and its growth gradually declined afterwards, possibly due to vitamin overdose that might causes toxicity to the algal cells or feedback inhibition in the algae. In parallel with a previous study, *Chlorella* sp. grew well in food waste-derived digestate (ranging from 0.06 to 1.16 ppm) and algal cells only managed to accumulate around 26% of the cobalamin-rich surrounding medium, suggesting that the cells have a limited capacity to take up and store the vitamin [86, 87]. Demonstrating a different trend,

riboflavin-supplemented cultures have its biomass productivity peaked at 5 ppm of supplementation at approximately 7.64 ± 1.21mg L^{-1} d^{-1}, whereas there was no remarkable difference ($p>0.05$) of biomass productivity across varying concentrations for biotin-supplemented cultures. It is possible that low biotin concentration was already sufficient to meet the metabolic needs of *C. sorokiniana*, thereby increasing its concentration did not provide any additional benefit for biomass productivity. Additionally, the cells might require more time to uptake biotin since the entry of biotin into cells is by passive diffusion. Likewise, microbial biotin transport systems of biotin are often stimulated by the presence of an energy-rich carbon source [88, 89].

(a)

Dosage conc. (mg L^{-1})	**0**	**1**	**5**	**10**
Cobalamin		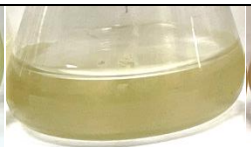		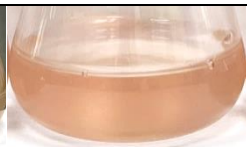
Biotin		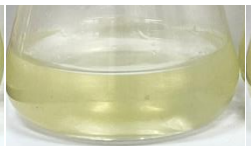	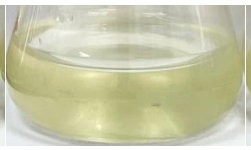	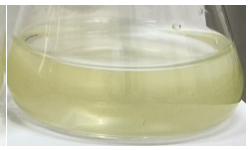
Riboflavin				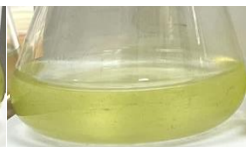
2,3-butanediol				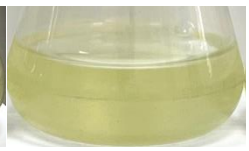

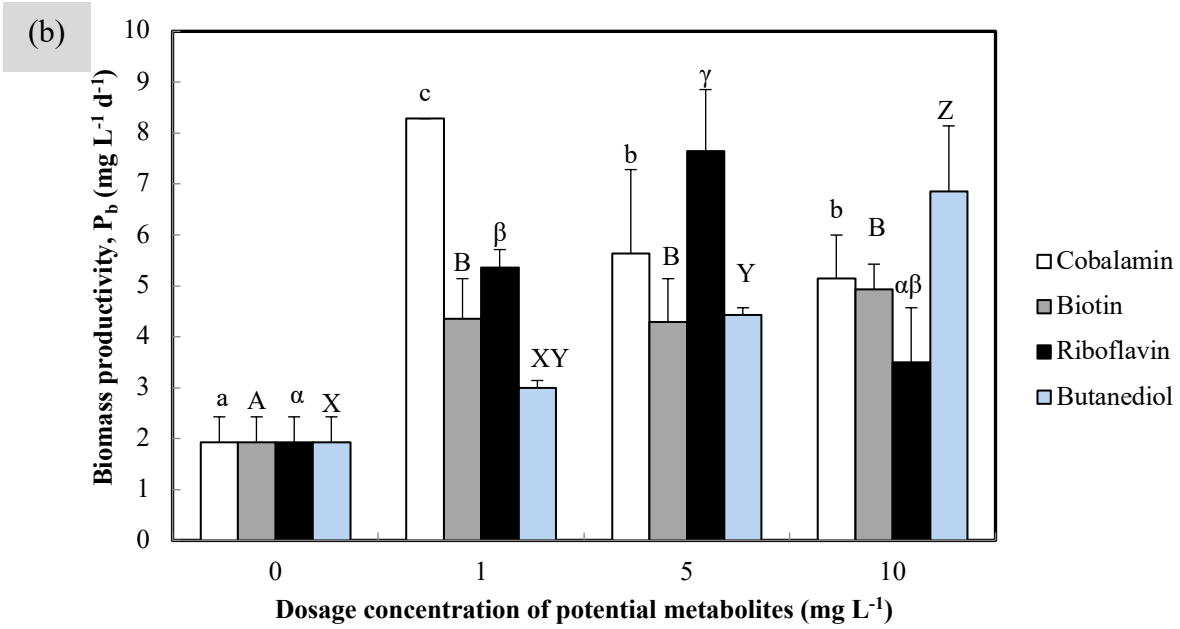

Figure 6 *Validation test of shortlisted bacterial determinants. (a) Morphological appearance of Chlorella sorokiniana grown in medium supplemented with different concentration of potential metabolites after 5 days of cultivation, and (b) their respective biomass productivity (n=3). Error bars depict mean± standard deviation (SD). Different forms of letters indicate significant level variation across different dosage amount of potential metabolites within the group, as determined by ANOVA and post-hoc analysis.*

It can be inferred that diverse bacterial metabolites exert differing impacts on algal growth, with effects varying across different concentrations. To fully understand the dynamics, it becomes essential to investigate the individual function and role of each metabolite within the context of real microalgae-bacteria consortia. For instances, *C. sorokiniana* exhibited enhanced growth and accumulation of total carbohydrates, lipids, and chlorophyll with *Azospirillum brasilense*, attributing to the hormonal-like effect rendered by 2,3-butanediol [90]. It can enhance the expression of photosynthetic genes in microalgae and trigger cell-signaling cascades, leading to an improved algal cell vitality. On the other hand, growing *Tisochrysis lutea* with bacterial consortium in cobalamin/vitamin B_{12}-deprived medium partially restored its algal growth, emphasizing the significance of microbial interactions involving direct exchange of vitamin for central cellular metabolism. Authors also verified that an exogenous provision of

cobalamin/vitamin B_{12} to xenic cultures led to a 5.5-fold greater biomass increase, compared to the control [91]. More than half of the surveyed microalgal species in archival literature showcase a strict necessity for an external supply of cobalamin for their growth, suggesting the effectiveness of its artificial supplementation in enhancing the algal productivity or further shaping the algal community [92-94]. Similarly, some microalgae depend upon a combination of B-complex vitamins such as cobalamin, biotin, pyridoxine, and thiamine as a growth factor, which algae are not able to produce them. For example, biotin acts as a coenzyme in carbon dioxide fixation to assist the synthesis of fatty acids and amino acids. As only prokaryotes possess the ability to synthesize such vitamins, microalgae must rely on external sources such as bacteria for these nutrients. Consistent with the findings of this work, prior research has identified a set of predicted functional genes suggesting that *Chlorella*-associated bacteria have the enzymes involved in vitamin metabolism. However, the accessibility of vitamins to *Chlorella* appeared to be constrained by the absence of genes encoding vitamin transporter genes [95].

Similarly, the impact of synthetic riboflavin on microalgae was dependent on its concentration in the culture media when one discovered a lower concentration bolstered the growth of *Chlorella sorokiniana*, whereas a higher concentration exhibited no discernible effect. Riboflavin-rich *Azospirillum brasilense* extracellular product not only heightened the algal growth, but meantime stimulating pigment and carbohydrate production from the algae [96]. Although riboflavin is known as a cofactor in antioxidation and peroxidation processes during osmotic stress, its precise mechanism in augmenting algal growth remains unclear [97]. Despite that, it is now undeniable that presence of identified metabolites effectively improved the performance of algal growth.

2.4 *Summary*

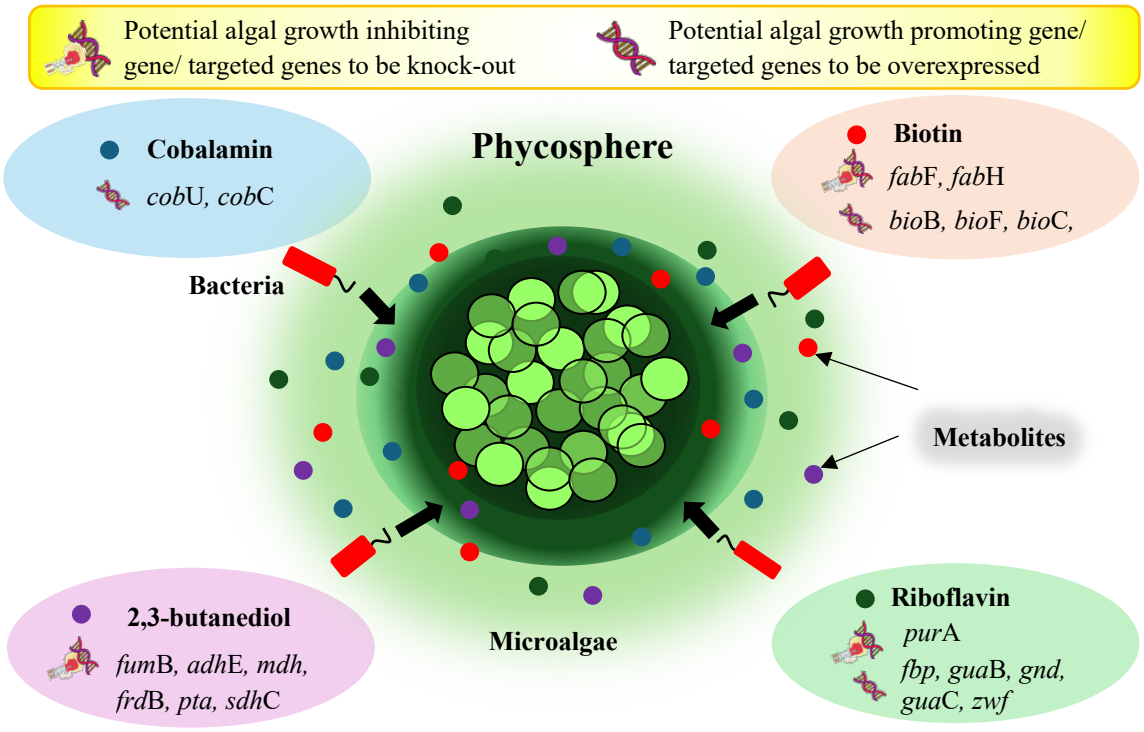

Figure 7 *Summary of Chapter 2.*

As summarized in **Figure 7**, a genome-wide high-throughput screening technique using KEIO Knockout Collection was demonstrated to be an effective strategy for identification of beneficial bacterial metabolites in algal-bacterial co-cultures. Study of **Chapter 2** utilized a comprehensive approach by considering both the potential algal growth-promoting and inhibiting genes into the metabolic network derived from KEGG database. Screening results have revealed the key roles of four potential bacteria-derived metabolites, namely cobalamin, biotin, riboflavin, and 2,3-butanediol in the co-cultures. A higher titer of metabolites amounts can exert a minimum of 1.5-fold enhancement onto the algal biomass productivity, although it was concentration-dependent. However, a considerable drawback is that gene deletion does not always accurately reflect the impact of gene overexpression. Some knockout effects may stem from indirect regulatory disruptions instead of direct metabolic contributions. Therefore, while the KEIO library is a powerful tool to execute function-driven screening and hypothesis building, validation of the

proposed method through gene overexpression or any related complementation studies. The findings obtained serve as a foundation for developing an engineered bacterial strain that benefit algal growth or optimizing nutrient supplementation in longer-term microalgal-engineered bacterial cultivation, which will be discussed in the next chapter.

CHAPTER 3: Impacts of Riboflavin-overproducing Engineered *Escherichia coli* towards *Chlorella sorokiniana* Growth in Optimized Co-cultivation Approach

3.1 Introduction

Stemming from the findings acquired in **Chapter 2**, it is intriguing to introduce metabolic engineering techniques onto *E. coli* to assess its impact onto co-existing algal growth. Among four identified bacteria-derived metabolites, riboflavin stands out for its broad role in critical cellular processes like energy metabolisms, redox reactions, and stress responses. While cobalamin and biotin are indispensable in their respective pathways, their roles are more specialized and less directly linked to the broad metabolic activity seen in algal growth and photosynthesis. Meanwhile, 2,3-butanediol's role is ancillary compared to the vitamins. This distinction directly supports the rationale for focusing on riboflavin at first, as its effects are likely to have the most far-reaching advantages on algal growth and metabolism. Starting with single metabolite also helps to create a reliable framework due to elimination of confounding factors from other metabolites. Other than that, it allows a focus on refining co-cultivation conditions. Such decision can be regarded as a stepwise approach to complexity, which is the incorporation of multiple metabolites in future studies. It reflects a strategic, hypothesis-driven approach to generate fundamental knowledge before exploring synergistic effects.

Therefore, study in **Chapter 3** is going to evaluate the impact of the riboflavin-overproducing engineered *E. coli* strain on microalgae across various co-culture setups. The objectives of this current study were: (i) to determine the optimal co-cultivation strategy between recombinant *E. coli* and microalgae, (ii) to assess the algal growth performance under the influence of engineered bacteria, and (iii) to propose a potential interaction mechanism in the novel co-

cultures during long-term cultivation. Understanding the extent to which their interaction is regulated is crucial before considering future scaling up and applications.

3.2 Materials and methods

3.2.1 Strains, plasmids, media, and cultivation conditions

Microalgae, *Chlorella sorokiniana* 211/8K (Culture Collection of Algae and Protozoa, United Kingdom) was cultivated in BG11 medium and maintained at 25±2℃ under continuous white light ~120 $\mu mol\ m^{-2}s^{-1}$ from fluorescent lamps. All the bacteria strains and plasmids used in this study are listed in **Table 3**. *E. coli* DH5α was used to propagate vector DNA, whereas *E. coli* BL21 (DE3) was used as the expression host strain for riboflavin production and co-culture purposes. pETDuet-1 (Merck Millipore, State, USA) was used for gene expression. LB medium (Lennox, Nacalai Tesque, Kyoto, Japan) supplemented with ampicillin (Amp) at a concentration of 50 μg mL^{-1} was used for the seed culture and other standard procedures. *E. coli* cells were cultivated at 37℃ and 180 rpm.

Table 3 *Escherichia coli strains and plasmids used in this study.*

Strain/plasmid	Description and genotype	Source
Strain		
Escherichia coli DH5α	Wild type, *F$^-$, _Φ80d lacZ ΔM15, Δ(lacZYA-argF)U169, deoR , recA1, endA 1, hsdR17(r K$^-$, m K$^+$), phoA , supE 44, λ$^-$, thi-1, gyrA96, relA1*	New England Biolabs
Escherichia coli BL21 (DE3)	Wild type, *fhuA2 [lon] ompT gal (λ DE3) [dcm] ΔhsdS λ DE3 = λ sBamHIo ΔEcoRI-B int::(lacI::PlacUV5::T7 gene1) i21 Δnin5*	New England Biolabs
R1	*E. coli* BL21(DE3) with pET-*zwf*	This study
R2	*E. coli* BL21(DE3) with pET-*fbp*	This study
R3	*E. coli* BL21(DE3) with pET-*zwf-fbp*	This study
Plasmid		
pETDuet-1	Expression vector, two multiple cloning sites, T7 promoter, Amp^R	Merck-Millipore
pET-*zwf*	pETDuet-1 with *zwf* gene	This study
pET-*fbp*	pETDuet-1 with *fbp* gene	This study
pET-*zwf-fbp*	pETDuet-1 with *zwf* and *fbp* genes	This study

3.2.2 Gene overexpression and plasmid construction

Based on the native *de novo* riboflavin synthesis as illustrated in the study of **Chapter 2**, two specific endogenous genes, *zwf* and *fbp* that encode glucose-6-phosphate 1-dehydrogenase and fructose-1,6-biphosphatase I, respectively, were selected for overexpression in this study due to their promising effects in elevating riboflavin titers [71-73]. The former gene is responsible for increasing the carbon metabolism level and facilitating the carbon flow in the pentose phosphate pathway (PPP), whereas the latter is responsible for attenuating the glycolysis pathway (EMP). *E. coli* DH5α genomic DNAs were extracted with Wizard Genomic DNA Purification Kit (Promega, Madison, WI, USA). The target gene fragments were amplified from the extracted genome by PCR (KOD One PCR master mix, TOYOBO, Japan) using corresponding primers as listed in **Supplementary data 4**.

Vectors were also PCR-amplified essentially the same procedure. Amplicons were separated by agarose gel electrophoresis and purified using FastGene Gel/PCR Extraction Kit (Nippon Genetics, Japan). Three recombinant plasmids were designed as shown in **Figure 8**. The *zwf* and *fbp* genes were amplified through PCR with the primer pairs *zwf*-MCS2-Fwd/Rev and *fbp*-MCS2-Fwd/Rev, respectively. Each fragment was then inserted into the multiple cloning site-2 of the pETDuet-1 vector. To this end, pETDuet-1 was PCR-amplified with the primer pairs pET-*zwf*-MCS2-Fwd/Rev and pET-*fbp*-MCS2-Fwd/Rev, respectively. The insert and vector fragments were then fused by Gibson assembly (NEBuilder HIFI DNA Assembly Master Mix, New England Biolabs). The resultant plasmids were named pET-*zwf* (or denoted as recombinant R1 for *E. coli* BL21(DE3) transformant) and pET-*fbp* (R2), respectively. Subsequently, the *zwf* gene was re-amplified using a different primer pair, *zwf*-MCS1-Fwd/Rev, to clone into the multiple cloning site-1 site. The gene was amplified using primer pair, pET-*fbp*-MCS1-Fwd/Rev, and pET-*fbp* as

the template. The resultant vector was named pET-*zwf-fbp* (R3). These three plasmids were then used to transform *E. coli* BL21(DE3) competent cells, and transformants were selected on LB/Amp agar plates at 37 ℃. Recombinant strains were sub-cultured in LB/Amp medium at 37 ℃ to mid-exponential phase at 180 rpm and frozen at -80 ℃ in 50% (v/v) glycerol as the seed for subsequent experiments.

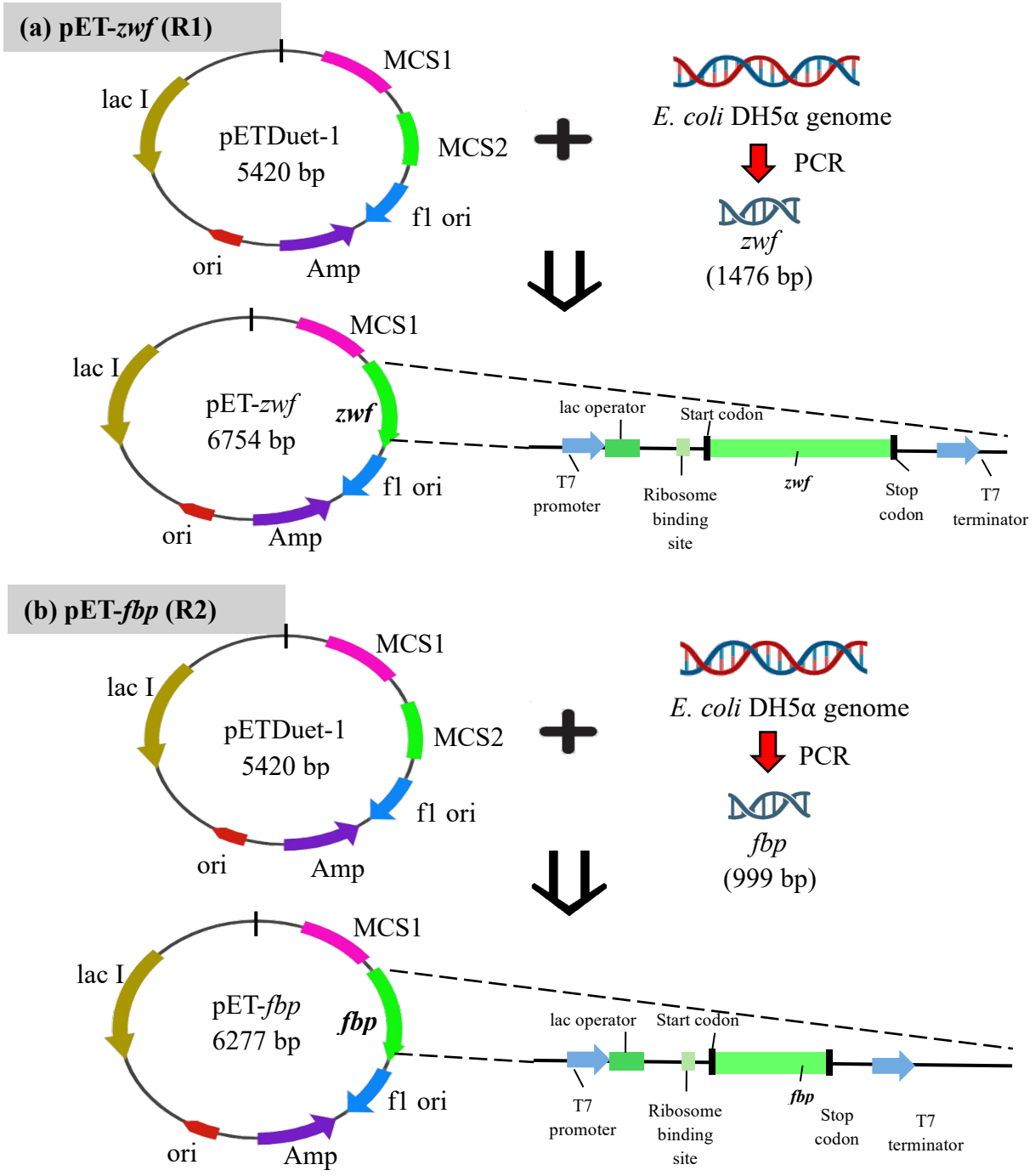

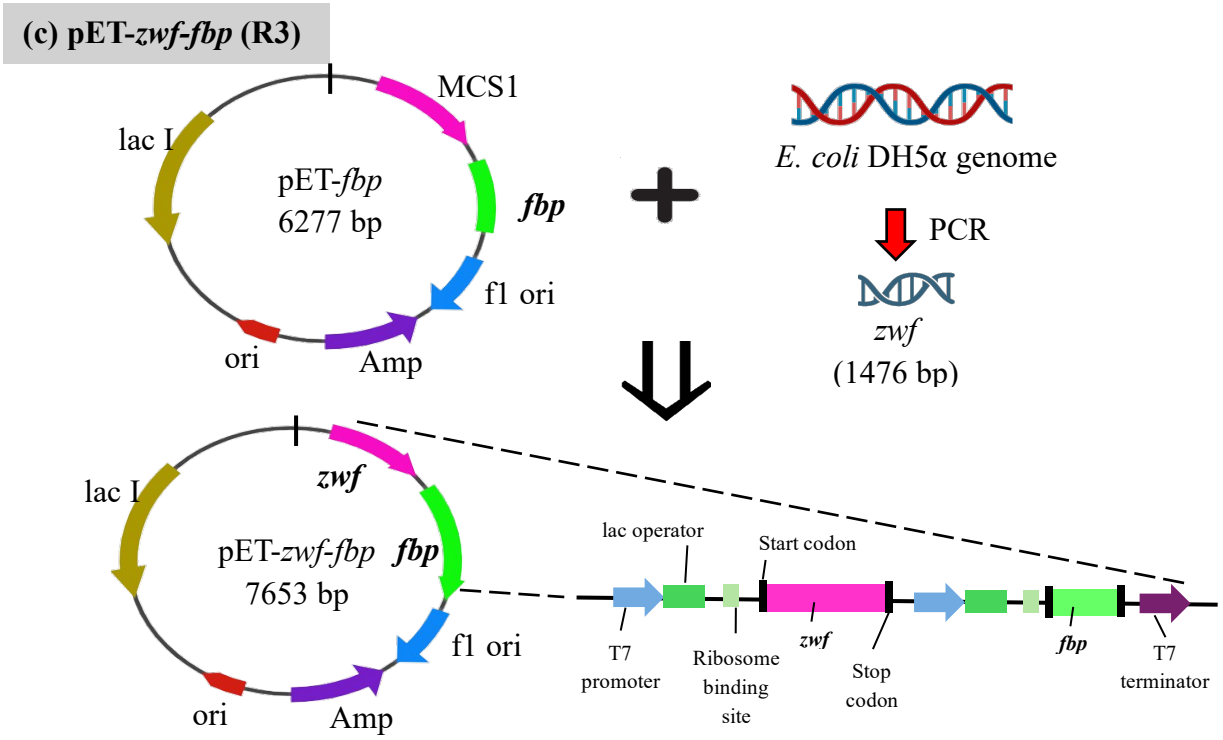

Figure 8 *Schematic map of the construction of the plasmids (a) pET-zwf, (b) pET-fbp, and (c) pET-zwf-fbp. These plasmids are also denoted as R1, R2, and R3, respectively.*

3.2.3 Riboflavin production under different isopropyl β-d-1-thiogalactopyranoside (IPTG) concentrations

The inoculum was prepared from frozen seed stocks in LB/Amp medium, grown to mid-exponential phase, and then used to inoculate 1% (v/v) *E. coli* BL21(DE3) of the seed culture. When OD_{600} reached 0.6, the gene was expressed by adding various concentrations (0.01-0.3 mM) of IPTG. After cultivation at 18°C for 18 h, cell density was measured at OD_{600} and then pelleted by centrifugation at 19,000 × g for 2 min. The supernatant was taken, and the riboflavin concentration was immediately determined on a SpectraMax M2 (Molecular Devices, Sunnyvale, CA, USA) microplate reader at A_{444}.

3.2.4 Quick assessment of co-cultivation approaches in microscale set-ups

IPTG induction was applied to the pre-cultured recombinant *E. coli* strains and co-cultured with one-week-old microalgae pre-culture at a cell density around 5×10^6 cells mL^{-1} in a microscale set-up. It allowed quick exploration of three different proposed co-cultivation approaches, namely physical cell interaction (approach A-direct method), nutrient-based strategy (approach B-indirect method), and synergistic effect of combining both physical cells and bacterial medium supernatant (approach C-mixed method).

In approach A, bacterial strains were inoculated to an initial density of $OD_{600} \approx 0.6$ in test tubes and immediately harvested through high-speed centrifugation, then mixed with microalgal cells harvested from an equal volume of microalgal cultures. Mixed cultures were then re-suspended in sterile BG11 medium, and gene expression was induced by adding varying concentrations of IPTG. Next, the mixtures were carefully distributed into 96-well microplates and placed on an orbital shaker (Mix-EVR, Taitec, Saitama, Japan). The plates were agitated at 250 rpm to grow bacterial and algal cells under microalgal growth conditions (25±2°C) for 2 days. In Approach B, instead of involving physical bacterial cells during the co-cultivation, the bacterial medium supernatant was opted, with physical bacterial cells omitted from the co-culture system.. Bacterial cultures were prepared following **Section 3.2.3**. After the incubation, cells were harvested to gather the supernatant. The bacterial supernatant was mixed with an equal volume of sterile BG11 medium to make up a new culture medium. Only the algal cells were re-suspended with this prepared culture medium and then carefully dispensed into microplates for co-culture purposes. Approach C integrated the first two approaches by co-cultivating microalgal and bacterial physical cells in microplates using a 1:1 volume ratio of BG11 medium and bacterial medium supernatant as the culture medium. All the co-culture experiments were performed in

triplicates, with monoculture, non-transformant, and empty plasmid groups as the controls. Fluorescent intensity of the chlorophyll-*a* (the main pigment in algal cells) of each well was measured using a microplate reader (SpectraMax M2, Molecular Devices, Sunnyvale, CA, USA) at excitation and emission wavelengths of 490 nm and 650 nm, respectively.

3.2.5 Long-term shaking-flask co-cultivation and cell growth assessment

The optimum co-cultivation approach identified from the microscale experiments was selected as the basis for a 10-days long shaking-flask experiment. The co-culture volume was scaled up to a working volume of 60 mL per 100 mL flask (the initial organic substrate present in the medium was tabulated in **Supplementary data 5**), and sampling of 5 mL culture was conducted every 2 days to monitor algal cell growth by fluorescence measurement. Algal growth was further assessed with changes in the specific growth rate during the exponential growing phase (0-4 days) and doubling time using the equations below:

$$Specific\ growth\ rate, \mu\ (d^{-1}) = \frac{lnX - lnX_0}{t - t_0} \quad (1)$$

$$Doubling\ time, t_d = \frac{ln2}{\mu} \quad (2)$$

where X and X_0 are the cell density (in terms of fluorescence value) at t and t_0, respectively.

Algal cell sizes of at least 20 individual cells from each sample were measured under a light microscope (Axio Observer, Zeiss, Germany), and the average values were determined. To count colony forming units (CFUs), the co-cultures were serially diluted and evenly spread on LB-agar plates using glass beads. The plates were kept in the incubator overnight, and the number of colonies was counted.

3.2.6 Extra- and intra-cellular metabolite concentration measurement

On each sampling day, cultures were harvested by centrifugation, where the resulting supernatant was collected as extracellular metabolites, while the remaining cell pellet was resuspended in an equal volume of medium and lysed to release intracellular metabolites. Chl-*a/b* and total chlorophyll were extracted and quantified following the protocol reported by a previous study [98]. The extracellular proteins and carbohydrates were also recovered from the planktonic cells after centrifugation at 19,000 × g for 10 min. Carbohydrate concentration was determined using the phenol-sulfuric acid assay described by Dubois *et al.* [99], whereas protein concentration was determined using standard Bradford's Protein Assay (500-0006, BIO-RAD Laboratories Inc., California, USA) according to the manufacturer's recommendations. For rapid quantification of total lipid contents, the sulfo-phospho-vanillin method was referred [100].

3.2.7 Statistical analysis and Pearson correlation

Statistical analyses were conducted using IBM SPSS Statistics 25 and Graphpad Prism 10. Analysis of variances was performed to detect the significant differences in the relative riboflavin production, cell growth performance, biochemical content across different IPTG effects, and cultivation time for each bacterial strain and co-culture group, respectively. Data for relative biochemical content was previously normalized to the control group and then illustrated as adjusted mean ±95% confidence interval obtained from Tukey's post hoc test (ANOVA). Each data point is represented as mean±SD (n=3). Pearson correlation matrix was plotted to assess the correlations between the cell growth performance and all the physiochemical parameter tested.

3.3 Results and discussions

3.3.1 Impact of induced riboflavin production from different recombinant systems on bacterial cell growth and microscale co-cultivation performance

With IPTG as a model inducer, the effect of different recombinant systems on the bacterial cell growth dynamics and riboflavin production level is presented in **Figure 9(a)** and **Figure 9(b)**. All the transformants exhibited at least a 5-fold increase in riboflavin production compared to the non-transformant (NT) strain (~1.2 ± 0.1 mg L^{-1}), demonstrating the effectiveness of the recombinant design. Not only in riboflavin production, transformants also showed a trend of increase in cell growth, particularly in the R3 strain co-expressing *zwf* and *fbp*. This observation was in good agreement with previous reports demonstrating the positive effect of riboflavin in the medium on cell growth [72, 101]. Riboflavin, which serves as a precursor for the coenzymes flavin adenine dinucleotide (FAD) and flavin mononucleotide (FMN), plays an indispensable role in redox reactions across all organisms, thereby additional riboflavin in the medium could definitely enhance the initial cell growth [102].

In general, greater riboflavin production was observed across three recombinant strains, although a significant increase in riboflavin production was observed even without chemical induction probably due to a leaky expression of the target genes. Strain R3 showed the highest riboflavin titer (9.3 ± 0.2 mg L^{-1}) at 0.1 mM IPTG, followed by R2, and R1.

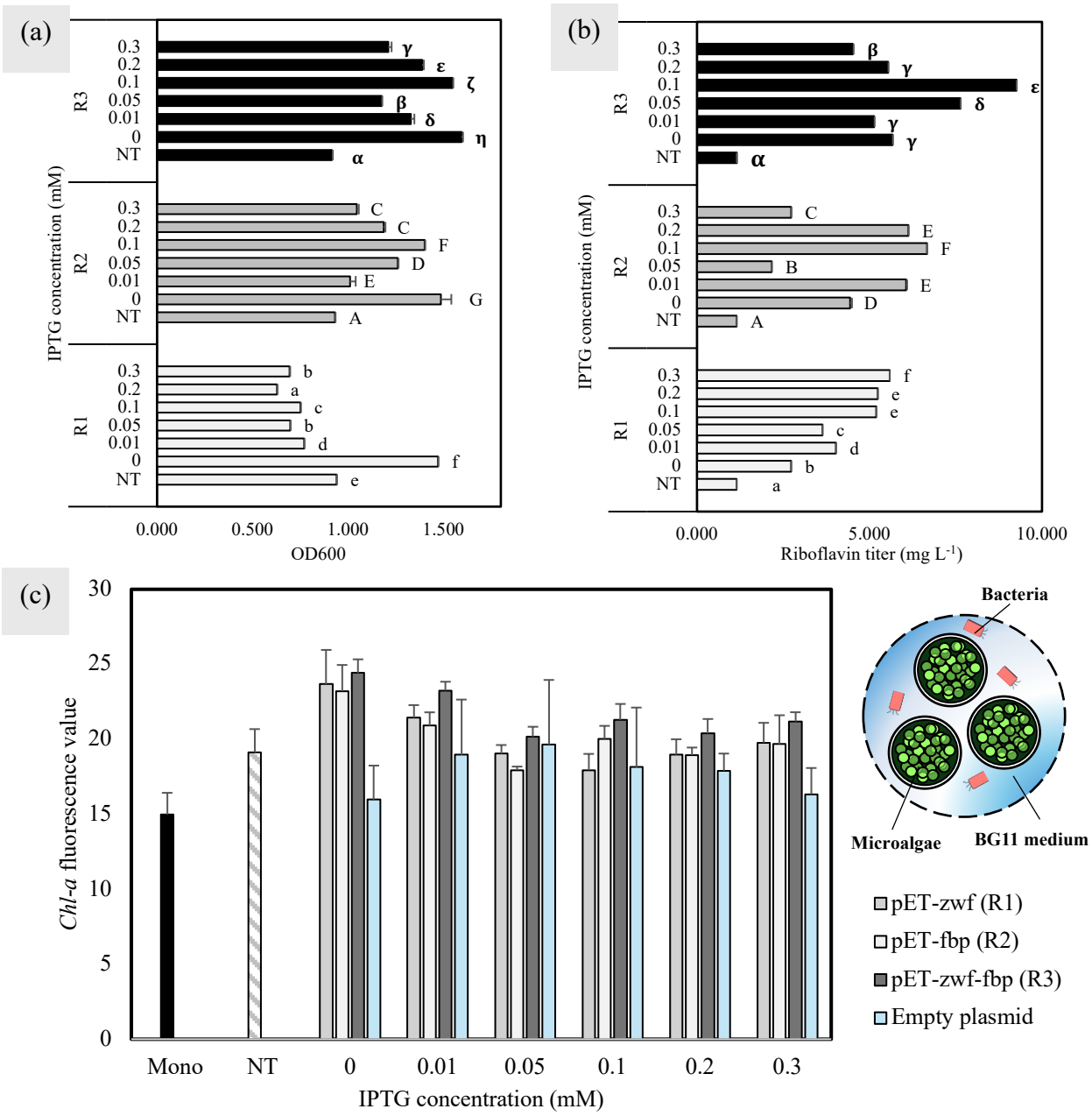
(a)
IPTG concentration (mM)
R3
R2
R1
0.3
0.2
0.1
0.05
0.01
0
NT
γ
ε
ζ
β
δ
η
α
C
C
F
D
E
G
A
b
a
c
b
d
f
e
0.000
0.500
1.000
1.500
OD600
(b)
IPTG concentration (mM)
β
γ
ε
δ
γ
γ
α
C
E
F
B
E
D
A
f
e
e
c
d
b
a
0.000
5.000
10.000
Riboflavin titer (mg L-1)
(c)
Chl-a fluorescence value
30
25
20
15
10
5
0
Mono
NT
0
0.01
0.05
0.1
0.2
0.3
IPTG concentration (mM)
Bacteria
Microalgae
BG11 medium
pET-zwf (R1)
pET-fbp (R2)
pET-zwf-fbp (R3)
Empty plasmid

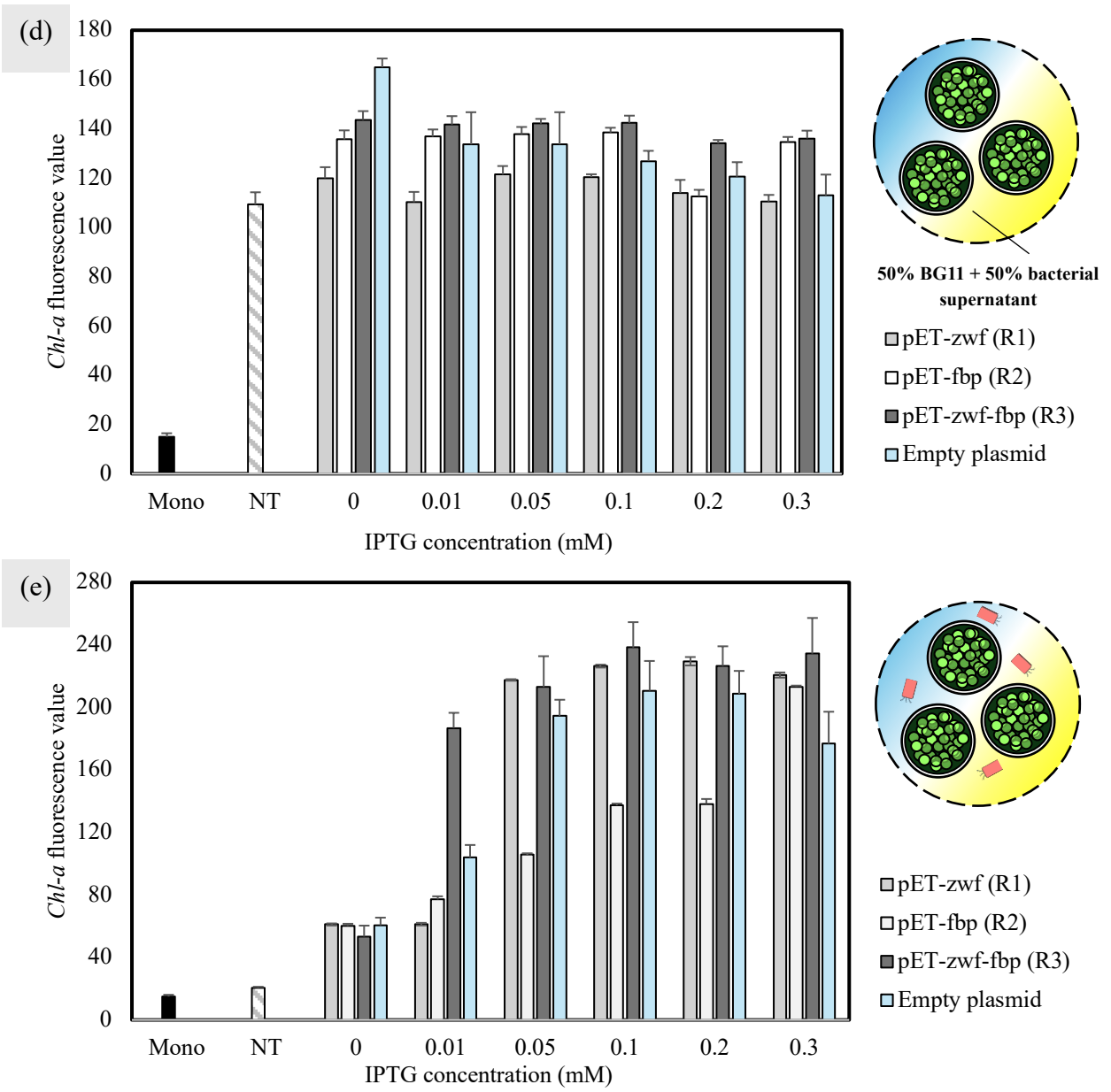

Figure 9 *Effect of IPTG concentration on (a) bacterial growth, (b) riboflavin titer, algal-derived chl-a fluorescence value in co-cultivation (c) approach A, (d) approach B, and (e) approach C. Inset images illustrate types of co-cultivation approaches. NT= non-transformant group; Mono= monoculture control group. All data are presented as mean ± standard deviation of triplicate, with lower-case alphabet letters, upper-case alphabet letters, and Greek alphabet letters representing the statistical comparison across different IPTG concentration within each individual engineered strain, as a threshold of* $p \leq 0.05$.

Despite increased riboflavin production with appropriate chemical induction, the recombinant strain designed in this current work was not able to achieve an extremely high riboflavin titer, as achieved in previous studies, where the levels exceeded 100 mg L^{-1} or even far

beyond that [71, 73]. This limitation is probably due to the absence of exogenous glucose supplementation for bacterial cultures, thereby lowering the overall efficiency of overexpression and causing slower growth. Furthermore, large amounts of riboflavin were found to be unnecessary in the co-culture medium because microalgae showed a high affinity to riboflavin only during the early growth phase, which lasted only a few hours [103]. Riboflavin's supplementation must be taken with caution as it was not stable under light and could be converted to lumichrome via photolysis [104]. In a *Chlorella sorokiniana-Azospirillum brasilense* co-culture, lumichrome was found to induce growth in early stage of cultivation. However, this effect was temporary, as no additional consumption of riboflavin or lumichrome was noted in the co-cultures after 36 h. By the end of the experiment, the riboflavin levels in the medium were nearly the same as the initial amount provided through synthetic riboflavin supplementation [103]. This statement was further supported by the fact that *C. sorokiniana* grown in a high-concentration riboflavin-supplemented medium exhibited a similar growth effect to that of the base medium, yet lower riboflavin concentration resulted in significantly higher growth rates [96].

In view of this, a 48 h-long co-cultivation in microplate was further assessed. Focus was paid onto three different proposed co-cultivation approaches A (direct method), B (indirect method), and C (mixed method), by comparing the growth performance under varying induction conditions. As presented in **Figure 9(c)**, no significant differences were spotted between recombinant strains; however, algal growth declined as IPTG concentration increased. With the inclusion of bacterial supernatant but without bacterial cells (**Figure 9(d)**), the *chl-a* value unexpectedly rose to around 140, which was about 5.6-fold higher than that obtained by the first approach. Following the incorporation of physical bacterial cells into the mixed medium (**Figure 9(e)**), a strikingly different trend emerged: algae grew better with increasing IPTG levels, generally

peaking at 0.1 mM for most strains, and notably with strain R3 achieving a maximum value of 238.4 ±10.9. While the reasons behind such a growth trend are not yet fully understood, it is likely due to the intricate interactions inherent in co-culture systems. Overall, the results pointed to an augmented effect of recombinant bacteria on the growth of *C. sorokiniana* in a culture medium half-mixed with bacterial supernatant. The riboflavin effect was particularly significant in R3, coupled with an improvement beginning from 0.01 mM IPTG induction up to 0.1 mM, which was in concordance with the riboflavin production as discussed previously. Considering the well-acknowledged positive microalgal-bacterial interaction via physical contact, along with a former study demonstrating the superior stimulation of microalgal growth by bacterial supernatant [105], approach C was then speculated to have a promising impact on algal growth rates and metabolite status. This is the first study to evaluate the unique performance of freshwater microalgae under the influence of bacterial supernatant, assisted by the recombinant *E. coli*.

3.3.2 Cell growth assessment and pigment content analysis in the optimum co-cultivation approach

Based on approach C, co-culture growth (*C. sorokiniana* and R3) was further analyzed over a 10-day incubation period in culture flasks, as displayed in **Figure 10(a)**. As expected, monoculture control consistently showed the lowest growth rates across the entire experiment. Due to the co-existence of bacteria in the cultures, it was observed that the liquid media became slightly milky-white for the rest of the groups. However, its presence did not inhibit the microalgal growth, as evidenced by the medium's color change from pale green to dark green by the end of the experiment, particularly in the case of R3-0.1 mM. Treatment effect of R3 under suitable IPTG induction was also significant ($p<0.05$) to the algal mean cell size (**Figure 10(b)**). For co-culture under IPTG induction, both the cell size (full data in **Supplementary data 6**) and cell surface area were approximately 1.89 times greater than that of the control groups. The maximum cell diameter

(5.2 ± 0.8 μm) and cell surface area (21.6± 6.5 μm^2) were attained at 0.1 mM IPTG. Early experiment suggested that, in a typical cell cycle commonly observed in green microalgae, a cell under illumination actively divides by increasing cell volume until reaching a commitment point (CP) and the first DNA replication-cell division is allowed [106]. According to Bišová and Zachleder (2014), this CP triggered a simultaneous entry into a second growth phase, where the cell continues to enlarge, leading to a four-fold increase in its initial size; attainment of the second CP will lead to another round of cell divisions with the same repeating process. Depending on the growth conditions, cells may either undergo immediate division or continue growing through additional CPs, until reaching a critical size. With improved growth conditions in this study, such as supplementation of additional energy from co-cultured bacteria and increased production of riboflavin at higher IPTG concentrations (riboflavin is a cofactor in the photoreduction and precursor to the cellular respiration in microalgae), the same culture may increase the extent of overlapping cell cycles and shift the division pattern from producing two daughter cells to eight or even more [106].

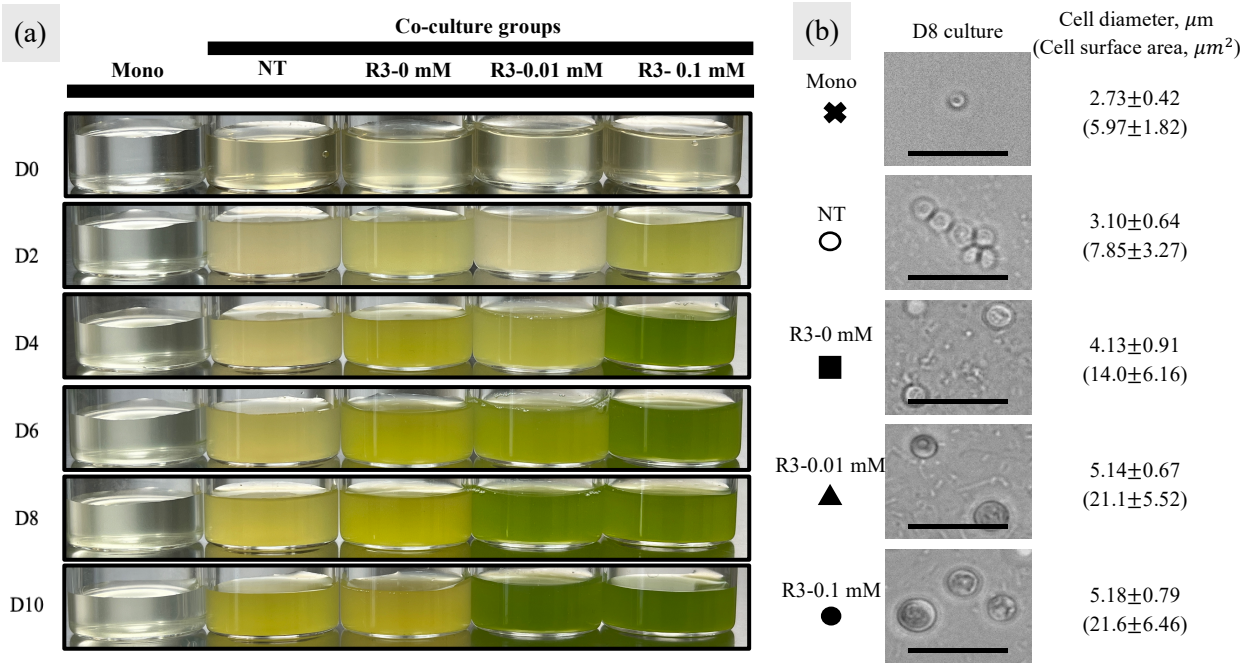

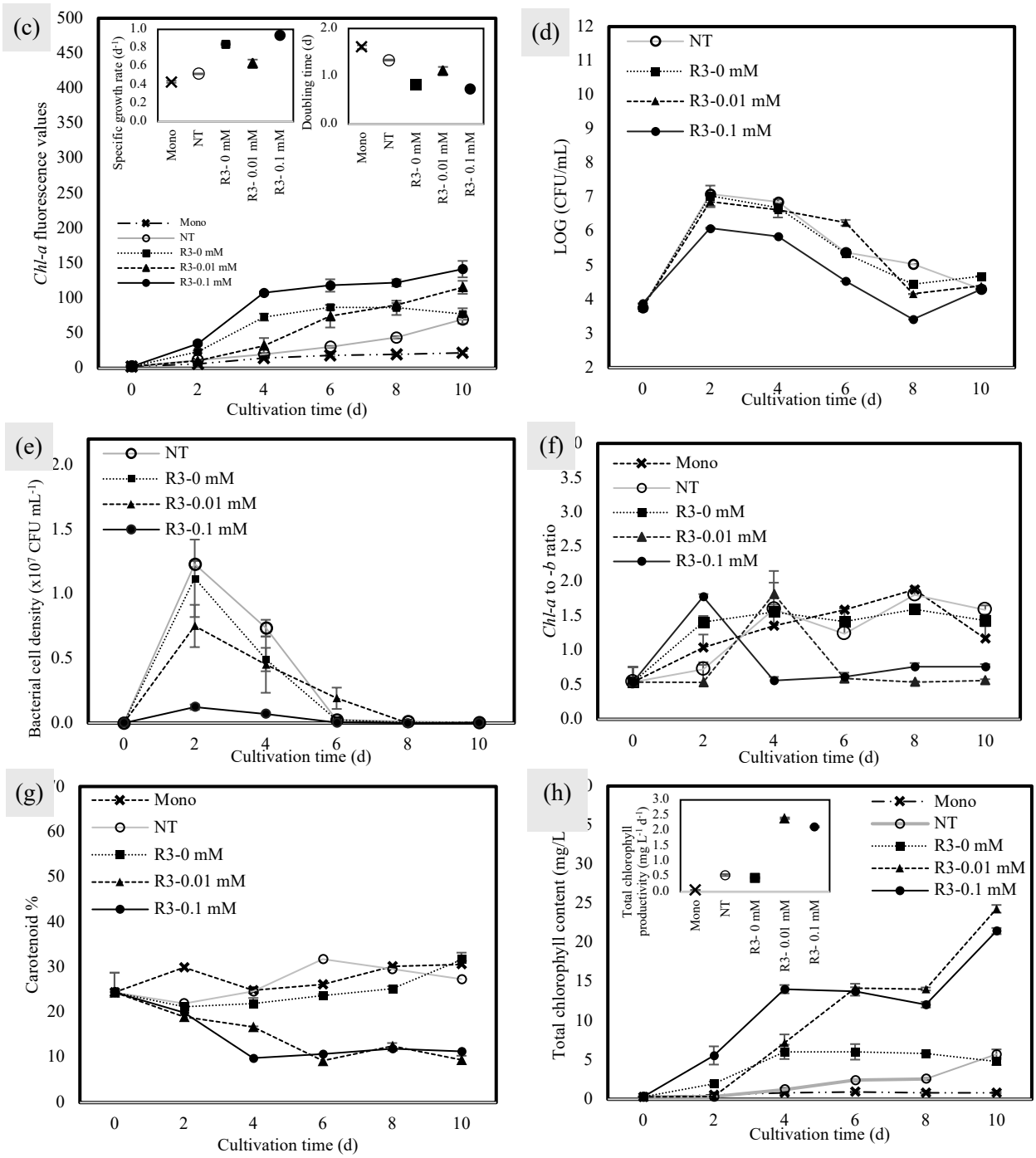
(c)
Chl-a fluorescence values
Cultivation time (d)
Specific growth rate (d-1)
Doubling time (d)
Mono
NT
R3-0 mM
R3-0.01 mM
R3-0.1 mM
(d)
LOG (CFU/mL)
Cultivation time (d)
(e)
Bacterial cell density (x10^7 CFU mL-1)
Cultivation time (d)
(f)
Chl-a to -b ratio
Cultivation time (d)
(g)
Carotenoid %
Cultivation time (d)
(h)
Total chlorophyll content (mg/L
Total chlorophyll productivity (mg L-1 d-1)
Cultivation time (d)

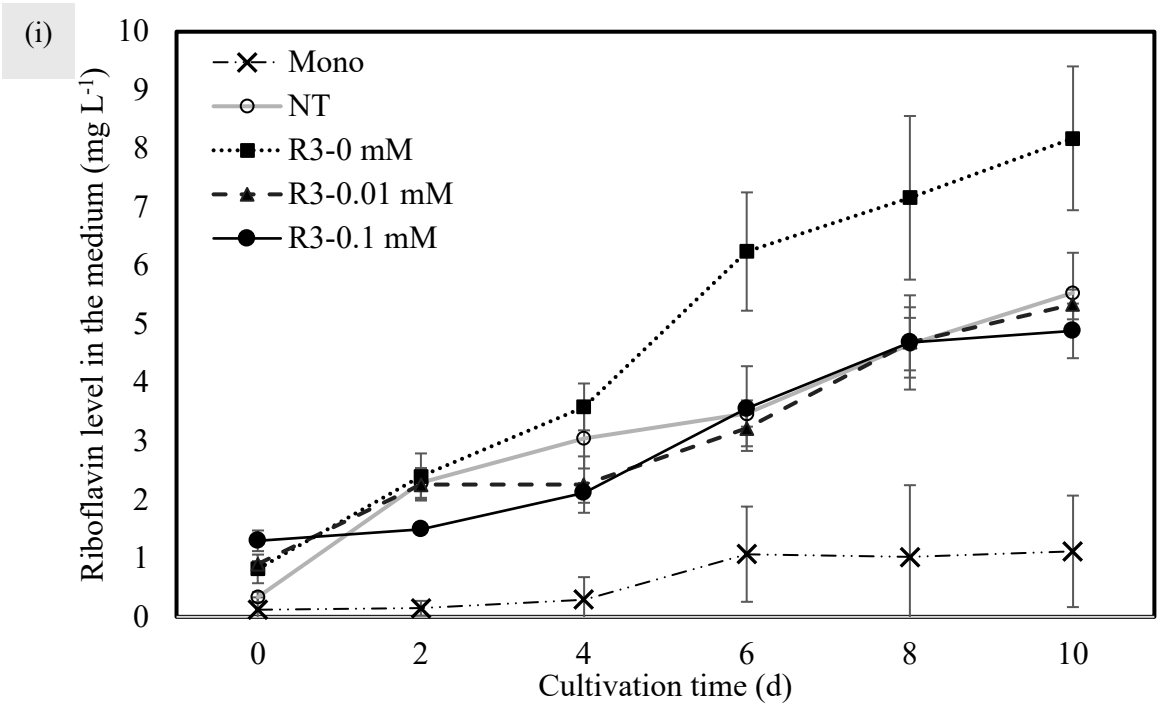

Figure 10 *Assessment of cell growth in the algal-bacterial phototrophic community. (a) Photographs of the co-culture experiments depicts algal growth which was arrested by color change across 10 days. (b) Morphology change of algal cells at D8 as a magnification of ×400. Scale bar: 20 μm. Cell growth of (c) microalgae C. sorokiniana and bacteria E. coli in (d) log-scale and (e) linear scale. Inset images show the specific growth rate and doubling time of microalgae during the exponential growing phase. Photosynthetic pigments obtained from the culture groups, in terms of (f) ratio of chlorophyll a to chlorophyll b (Chl-a/Chl-b); (g) carotenoid content percentage; and (h) total chlorophyll content. Inset image shows the confidence interval plot representing the total chlorophyll productivity in the studied groups. (i)Riboflavin level measurement in the medium over time, n=3. Reduced riboflavin level at D0 is due to the dilution with BG11 medium during the experimental set-up. NT= non-transformant group; Mono= monoculture control group; R3-0/0.01/0.1 mM= co-culture of microalgae with recombinant strain R3 under different IPTG concentrations. All data are presented as mean ± standard deviation of triplicate.*

As shown in **Figure 10(c)**, *chl-a* fluorescence value in the co-culture system was remarkably enhanced compared to the parental-type and monoculture control ($p<0.05$). During the exponential growing phase (up to D4, **Supplementary data 7**), R3-0.1 mM recorded its highest *chl-a* value of 107.8±2.0, which is a >5.4-fold and >7.5-fold increase over NT (20.1±1.6) and Mono (14.3±1.8). Although the algal growth in R3-0.01 mM started slower than in R3-0 mM, the algae recovered and began to grow rapidly, catching up to R3-0.1 mM and surpassing R3-0 mM towards the end

of the experiment. In contrast, algal growth in R3-0 mM remained constant after D4 and gradually ceased towards the end. Overall, algae co-cultivated in R3-0.1 mM (0.94±0.022 d^{-1}) showed the maximum specific growth rate and shortest doubling time (0.74±0.01 d^{-1}) among all tested, confirming the positive effect of riboflavin-overproducing strain on the algal growth. Nevertheless, *E. coli* growth was restricted after 2 days of incubation (**Figure 10(d)** and **(e)**), most likely due to insufficient exogenous carbon sources or suboptimal co-cultivation temperature. Bacterial count was ranked in descending order as follows: NT (1.2±0.02 $\times 10^7$ CFU mL^{-1}), R3-0 mM (1.1±0.3 $\times 10^7$ CFU mL^{-1}), R3-0.01 mM (0.8 ±0.2 $\times 10^7$ CFU mL^{-1}), and R3-0.1 mM (0.1±0.02 $\times 10^7$ CFU mL^{-1}) the least. The induction agent IPTG may have been toxic to the bacteria [107], leading to reduced bacterial growth, with colony counts at least 33% lower compared to the R3-0 mM group on D2. Since IPTG is not hydrolyzed by the cells, it likely remained constant until the end of the experiment, and this prolonged exposure may explain its detrimental effects on cell viability [108].

The differences in photosynthetic pigments and behaviors between the studied groups also actively contribute to the observed variation. Being the most abundant natural pigment supporting oxygenic photosynthesis in microalgae, *chl-a* always derives energy for metabolism and reproduction purposes. When paired with *chl-b* (found in the photosynthetic antenna proteins), which serves as an important accessory pigment to facilitate the excitation energy transfer, *chl a*/*chl b* ratio is positively correlating with the ratio of PSII cores to the light-harvesting chlorophyll-protein complex (LHCII) [109]. It can reflect the physiological state of cultures and their light-harvesting capacity, with the ratio increasing, particularly under high-light conditions [110], as seen in the current study. Apparently, recombinant strains had a marked effect on the *chl a*/*chl b* ratio for microalgae (**Figure 10(f)**) at every time point ($p<0.005$). All the treated cultures presented different periodic changes, but both the R3-0.01 mM and R3-0.1 mM groups recovered to a similar

ratio (as in D0) from D6 and D4 onwards ($p>0.05$), respectively. This is probably because of the mutual self-shading effects due to the extremely high cell densities, where scattering cells absorb incident light and reduce overall light penetration through the medium [111]. The antenna protein size typically increased to capture a broader spectrum of light wavelengths under low-light conditions, compensating for the reduced light availability [112]. Cultures with the lowest cell density, like Mono, which showed an increasing *chl a*/*chl b* ratio ($df=5$; $F=24.4$; $p<0.001$), often suggested that the culture was adapting to higher light irradiance/stress and shifting towards greater *chl-a* production. It could be part of a protective mechanism while reducing the risk from reactive oxygen species caused by excessive light [113]. This adaptive response, especially in terms of pigment changes, could also relate to carotenoid production as a secondary defense strategy.

Oxidative damage could also be alleviated by generating additional amounts of carotenoids. For the carotenoid content (**Figure 10(g)**), all the cultures depicted a constant build-up over time; however, both R3-0.01 mM and R3-0.1 mM groups showed a gradual decline from D2 onwards. Such a significant reduction was likely due to the cell adaptation mechanisms in response to nutrient-rich supernatant and riboflavin. Since both riboflavin and carotenoids are biosynthesized from common precursors (like fructose-6-phosphate), enhanced riboflavin production might be preferentially reallocate the resource away from the carotenoid biosynthesis, leading to a decrease in carotenoid content [114, 115]. Furthermore, riboflavin also plays a protective role against photo-oxidative stress, hence further alleviating the need for additional carotenoid production [103]. Moreover, considering the substantial increase in algal density from D2 and D4 onwards in these groups, a large algal population could rapidly consume the available riboflavin until reaching the saturation value per cell, leaving minimal amounts in the medium and thus reducing oxidative stress in the later growth phase (**Figure 10(i)**). A similar observation was noted in other studies,

where carotenoid content in riboflavin-treated cultures decreased over time and was significantly lower than in the monoculture control during the late growth phase [103]. In summary, it is presumed that the effects of riboflavin were most prominent during the early growth phase (< 48 h) and depended on cell density, with the impact more pronounced at higher biomass levels. If summing up all the photosynthetic pigments as displayed in **Figure 10(h)**, the overall trend basically reflected the actual algal growth profile over time. High chlorophyll productivities of both R3-0.01 mM (2.4±0.1 mg L^{-1} d^{-1}) and R3-0.1 mM (2.1±0.1 mg L^{-1} d^{-1}), were achieved due to their respective higher algal cell densities, which corresponded well with the naked-eye observation.

3.3.3 Accumulation of metabolites from flask cultures

Since the main physiological response in microalgae was frequently associated with the metabolite status in the function of time, detailed comparisons regarding three major metabolites (total soluble carbohydrate, soluble protein, and lipid) were performed. In **Figure 11(a)**, co-cultures treated with recombinant bacteria accumulated more soluble carbohydrate through the 10 days of experiment duration. Interestingly, all the co-culture groups depicted a gradual decline in production from D2, followed by a rapid recovery after D6 until D10, with a minimum of about a 3-fold leap. The highest production of soluble carbohydrate was obtained in co-cultures in R3-0.1 mM (224 ±15 mg L^{-1}), followed by R3-0.01 mM (217 ±14 mg L^{-1}), R3-0 mM (173 ±28 mg L^{-1}), NT (88±36 mg L^{-1}), and Mono (39±26 mg L^{-1}). Meanwhile, the total soluble protein content fluctuated at each time point (**Figure 11(b)**). Nevertheless, protein production was relatively higher

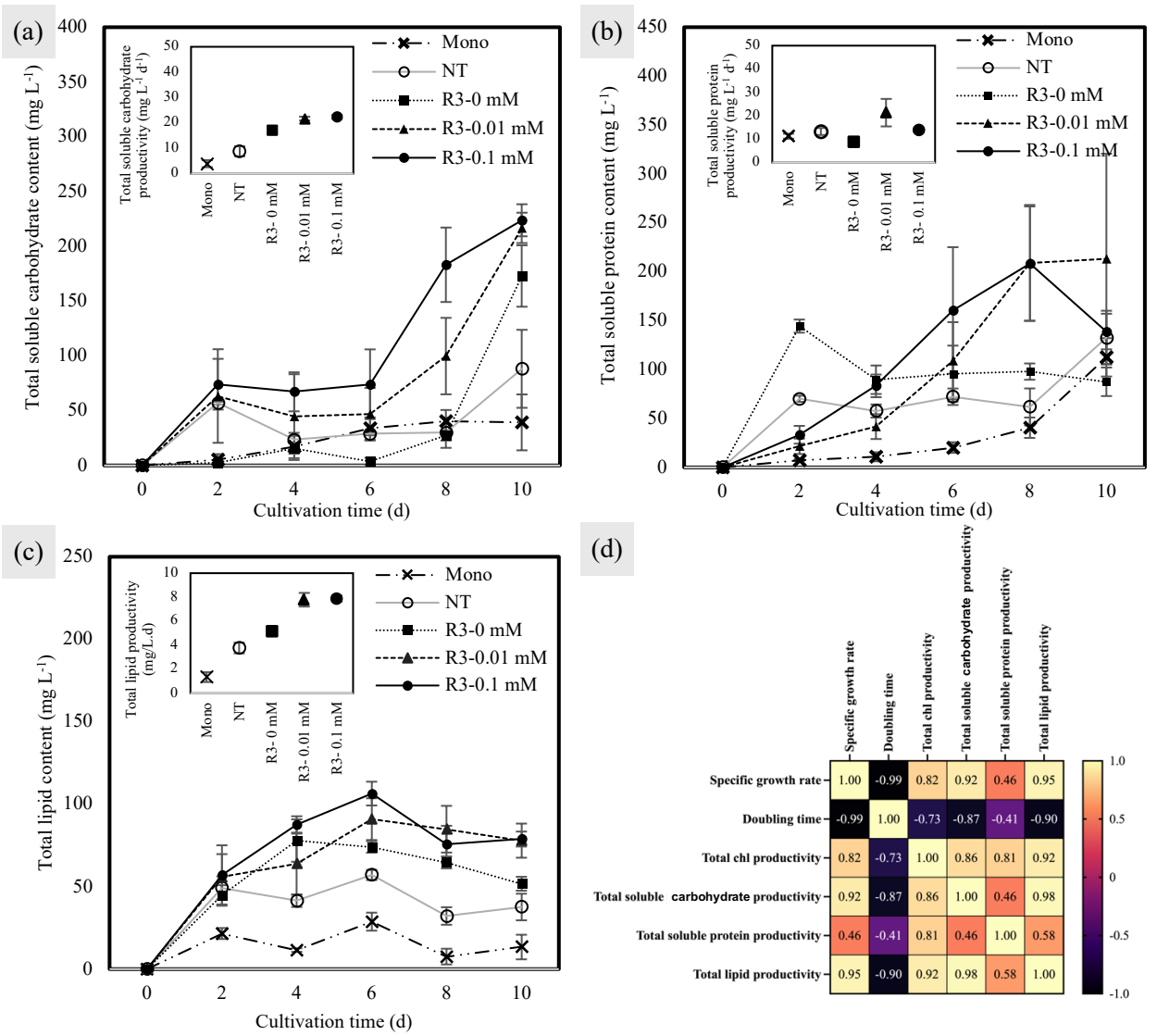

Figure 11 *Biochemical composition of co-culture communities throughout 10 days of cultivation. (a) Total soluble carbohydrate content (inset; total soluble carbohydrate productivity), (b) total soluble protein content (inset; total soluble protein productivity), (c) total lipid content (inset; total lipid productivity), and (d) Pearson correlation heatmaps of specific growth rate, doubling time, total chlorophyll productivity, total soluble carbohydrate productivity, total soluble protein productivity, and total lipid productivity for C. sorokiniana-E. coli co-cultures.*

in cultures with IPTG supplementation and showed an increasing trend, whereas both the R3-0 mM and NT groups remained unchanged throughout the experimental period. On the other hand, in **Figure 11(c)**, co-cultures with the IPTG-induced recombinant strains showed enhanced total lipid production within the cells compared to both NT and Mono, at different incubation times. R3-0.1 mM-treated cultures presented the highest production of total lipid at D6 (106.4±7.2 mg

L^{-1}). Generally, total lipid content peaked at D6 for all the groups, and the values gradually decreased afterwards.

These changes in the constituents agreed with Hamouda *et al.* who mentioned that *C. vulgaris* cultivated in the riboflavin-supplemented medium typically showed a proportional increase in carbohydrate content relative to the riboflavin amount. In the same study, the protein content exhibited an irregular pattern in response to the riboflavin levels [116]. Extracellular carbohydrates were found as the intermediary reserves in algae because their more readily available form can be broken down quickly and used as the precursors for lipid synthesis, as indicated by the opposite trend displayed from D2 to D6. However, lipid accumulation within the algae bodies usually occurred during the nutrient starvation phase [117], making this explanation unsuitable for the early phase observed. Additionally, the reduction in total lipid content and the slight increase in algal density over subsequent days suggested that the co-culture system had not yet reached a state of nutrient depletion. The most plausible explanation is that riboflavin likely enhances both metabolic efficiency and carbon utilization, leading to an early onset of lipid accumulation as a cellular response to the presence of riboflavin-overproducing recombinant bacteria. As the bacterial population was nearly eliminated from D8 onwards (**Figure 10(d)** and **(e)**), allowing the algae to dominate the entire co-culture system, the carbon allocation appeared to revert to its original state, resulting in the continued accumulation of extracellular carbohydrates alongside the increasing biomass. Meanwhile, bacterial supernatant represented a more complex nutrient environment, containing not only riboflavin but many other molecules such as phytohormone, thiamine, indole-acetic-acid, and tryptophan; the ongoing accumulation of soluble carbohydrates suggested a synergistic effect between riboflavin and other signal compounds presented in these supernatants [96].

Most extracellular proteins function as enzymes that catalyze various reactions and hydrolyze organic matter, providing energy to support cell growth [118]. Under sufficient nitrogen availability supplied by $NaNO_3$ in BG11 medium, optimal growth was expected from the cultures, where extracellular nitrogen augmented proteins and pigment biosynthesis [119], as observed in the current study. In the function of time, the soluble protein profile may also mirror the growth pattern of the co-culture. As displayed in **Figure 11(d)**, Pearson correlation of the key physio-chemical parameters confirmed that optimal growth was achieved when riboflavin was present, as evidenced by an enhanced specific growth rate, shortened doubling time, and increased total chlorophyll, soluble carbohydrates, and internal lipid accumulation.

3.3.4 Proposed interaction mechanisms between microalgae and engineered bacteria from co-culture systems

This study clarified that riboflavin positively influenced cell growth and metabolite accumulation. However, algal growth was species-dependent and likely relied on the symbiotic dynamics between recombinant bacteria and *C. sorokiniana* wild-type. Although algae can grow by scavenging excess riboflavin from both bacterial extracts and recombinant cells, such a nutrient addition can perturb the equilibrium of mutualistic co-cultures, particularly in response to a chemical-based inducer. As illustrated in **Figure 12**, microalgal-bacterial ratio tended to be minimized in the absence of IPTG. In this study, 8.2 ± 1.2 mg L^{-1} riboflavin was detected in the cultivation medium at D10 (**Figure 10 (i)**), indicating a leaky expression where a small amount of the target gene was transcribed and translated [120]. As a result, the released riboflavin can be sufficient for enhanced bacterial growth or a faster-growing rate compared to its ancestral line. Over time, such circumstances can suppress the algal growth when bacterial members began to dominate the system, transitioning the bacterial role from a mutualistic partner to a mild competitor, as evidenced by an algal growth decline observed in co-cultures containing R3-0 mM. However,

as the amount of microalgae decreased, the rate of riboflavin uptake slowed down while the growing recombinant bacteria continued to synthesize riboflavin, eventually leading to a stable accumulation of riboflavin in the medium (**Figure 10 (i)**). Under specific stress conditions such as nutrient competition, *C. sorokiniana* cells can even occasionally exude riboflavin into the medium, thereby contributing to the built-up of total riboflavin amount [121].

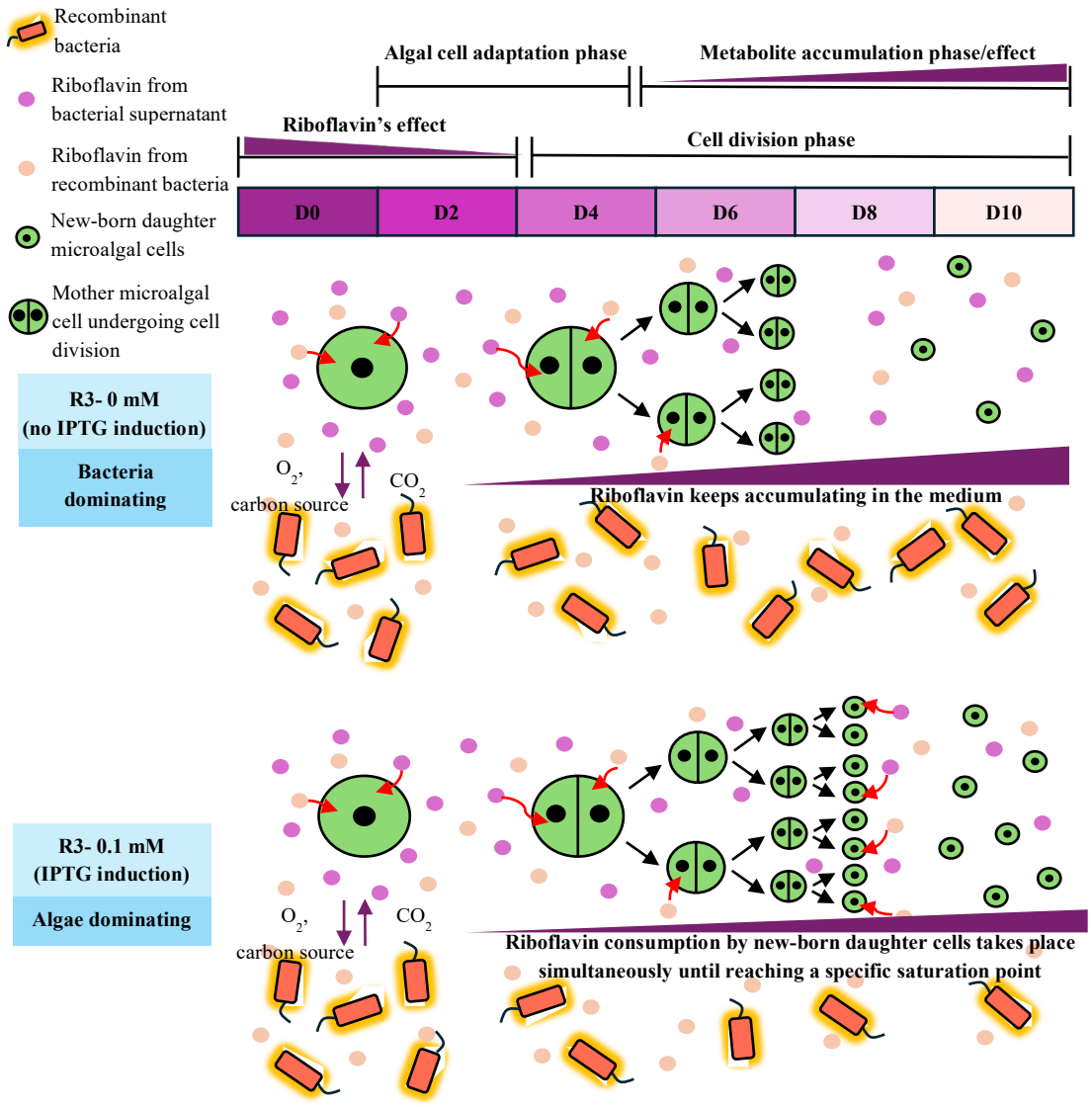

Figure 12 *Proposed mechanisms of co-culturing microalgae with riboflavin-overproducing engineered bacteria in comparison to monoculture and non-transformant controls, along with the underlying mechanisms by which recombinant bacteria influence microalgal metabolism.*

In the case of IPTG presence, a contrasting trend was discovered in which algae benefit from the recombinant strains, particularly at the early growing phase (< D2). Unfortunately, remaining IPTG in the medium was considered a negative impact for bacterial growth over a long period of time [108]. Although there was a direct relationship between the initial inducer concentrations and the initial inducer transport rate together with the specific activity, a majority of the inducer remained in the medium once reaching equilibrium with the intracellular level (~17% to 25% of IPTG uptake efficiency) [122]. High concentrations of IPTG eventually halted bacterial growth, resulting in a co-culture with a higher microalgae-to-bacteria ratio. Such a gradual decline in bacterial growth (**Figure 10(d)** and **(e)**) suggested that excess riboflavin consumption by bacteria was unlikely over a long cultivation period. In contrast, the algal cells exhibited active growth. Although higher riboflavin levels were anticipated in both the R3-0.01 mM and R3-0.1 mM groups, these levels declined towards the end of the experiment as algal growth significantly increased (**Figure 10 (i)**), indirectly indicating that the actively growing daughter algal cells were primarily responsible for riboflavin consumption, until achieving a specific saturation point.

In this study, we identified the rate-limiting factor for prolonging the elevated microalgal growth rate is the bacterial amount in the co-culture system. Generally, as the bacterial population decreased, microalgal growth compensated by slowing down over time, implying an interdependence between these two microorganisms. A recent study highlighted microalgae-bacteria interactions require direct contact for improved nutrient uptake [123]. The synergistic interactions between microalgae and bacteria have directly underscored the importance of having both in the co-culture system with a proper ratio. Nevertheless, it is evident that both parental-type and engineered bacterial strains, due to their extremely short doubling times, require sufficient exogenous carbon sources to sustain their growth. The metabolites produced solely by the

microalgae were inadequate for this purpose, leading to premature cessation. Therefore, future experiments could consider (a) replacing IPTG with lactose, which could serve as both carbon source and inducer, but it is easily metabolized and not stable enough for gene overexpression [124]; (b) replenishing fresh bacterial inoculum into the co-culture system using a fed-batch approach, but again, this poses a challenge in controlling the ratio to prevent uncontrollable bacterial overgrowth, which eventually disrupt the system and make it facultative [125]; and (c) batch-operating the system with IPTG pulse induction, but the cell growth rate has to be closely monitored to enable an induction at a desired cell density [126]; (d) using lactose/IPTG-based auto-induction medium batch cultivations [127].

With a limiting bacterial growth, as seen in this study, riboflavin's effect only took place within the first 48 h (with a more significant impact at earlier phase and diminishing thereafter). It was followed by an algal cell adaptation phase (D2-D4), during which cells re-adjusted their own metabolite production in an unusual way for nutrient assimilation in a new environment. In the cell division phase (> D4), growth occurred at a slower rate and cells typically relied on available external nutrients or internally accumulated metabolites, leading to minimal changes in cell size. From D6 onwards, a metabolite accumulation phase began, where cells actively produced extracellular products to create a more favorable environment for growth or due to saturated metabolic pathways, resulting in the release of metabolites extracellularly. In short, the overall findings allow a speculation of phase characterization as a function of time over these 10 days.

3.4 Summary

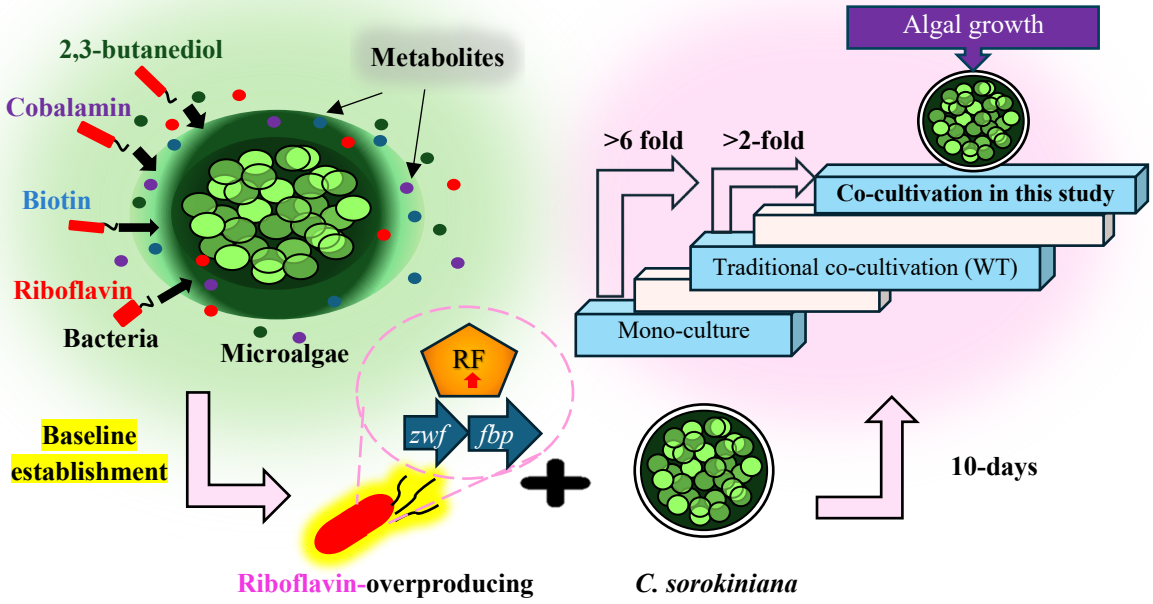

Figure 13 *Summary of Chapter 3.*

To our knowledge, **Chapter 3** shows the first study to evaluate the growth performance of *C. sorokiniana* with the assistance of riboflavin-overproducing recombinant *E. coli* and its bacterial supernatant. As shown in **Figure 13**, riboflavin-overproducing *E. coli* was co-cultivated with *Chlorella sorokiniana* at a bacteria: algae ratio of 5:1 (dry wt/wt) in BG11 medium supplemented with *E. coli* supernatant (an equal-volume mixture of BG11 medium and bacterial supernatant, 0.1 mM IPTG). The algal specific growth rate, cell size, pigment productivity, extracellular carbohydrate productivity, and lipid productivity all showed at least a two-fold increase compared to the parental control. However, due to the limited bacterial growth, riboflavin's effect was most significant during the first two days, followed by cell adaptation phase (D2-D4), slower cell division phase (D4-D10), and metabolite accumulation phase (D6-D10). Building upon the positive findings from this study, the synergistic effect of more than two upregulated metabolites within a single bacterial host on algal growth, along with the estimation of derived biofuel properties, will be discussed in the next chapter.

CHAPTER 4: Synergistic Enhancement of Biomass and Lipid Productivity in *Chlorella sorokiniana* Co-cultured with Vitamins-overproducing *Escherichia coli*

4.1 Introduction

Study in **Chapter 3** have demonstrated the advantage of engineered *de-novo* riboflavin production from bacteria in nourishing microalgal growth. This metabolic approach extends beyond natural interactions between two kingdom species by enabling precise regulation of targeted metabolites in the microbial co-partner, thereby strategically enhancing biotechnological applications, such as biomass productivity in this current research. Recognizing microalgae as a third-generation biofuel feedstock, the next phase of research will incorporate metabolic engineering of symbiotic co-partner with an in-depth assessment of biodiesel-relevant lipid profiles in co-cultures. It will provide crucial insights into the industrial feasibility of microalgal-bacterial consortia for sustainable biofuel production. Since majority of the green microalgae such as *Chlorella* spp. are vitamin auxotroph, the bacterial strain will be further engineered to concurrently over-synthesize three essential vitamins identified in **Chapter 2** (riboflavin, cobalamin, and biotin).

Study in **Chapter 4** will rigorously investigate the extent of their synergistic effects on microalgal lipid biosynthesis and overall productivity. Moreover, to ensure the long-term viability and robustness of the engineered co-culture system, systematic evaluations of stability will be conducted under extended cultivation periods. Therefore, objectives of this chapter were: (i) to elucidate the synergistic effects between vitamins-overproducing recombinant *E. coli* and microalgae under prolonger cultivation, (ii) to assess the co-culture system stability by tracking biochemical fluctuations, microbial population dynamics, and metabolic resilience, and (iii) to

evaluate the fatty acids-derived biodiesel properties in accordance to international standards. The entire analysis could illuminate more paths in genetic engineering techniques tailored to sustainable bioprocess development in microalgal biotechnology.

4.2 Materials and methods

4.2.1 Strains, plasmids, and cultivation conditions

Microalgae, *Chlorella sorokiniana* 211/8K (CCAP, Scotland, UK) was cultivated in BG11 medium and incubated at 25±2℃ under cool fluorescent white light around 120 μmol photon m^{-2} s^{-1}. All the bacterial strains and plasmids used in this work are described in **Table 4**. *E. coli* DH5α was used for plasmid construction and cloning, whereas *E. coli* BL21 (DE3) was used for overexpression. *E. coli* cells were cultivated in LB medium (Lennox, Nacalai Tesque, Kyoto, Japan) at 37℃ and 180 rpm. Gene overexpression was performed using pETDuet-1, pACYCDuet-1, and pCDFDuet-1.

Table 4 *Escherichia coli strains and plasmids used in this study.*

Strain/plasmid	Description and genotype	Source
Strain		
Escherichia coli DH5α	Wild type, *F- , _Φ80d lacZ ΔM15, Δ(lacZYA-argF)U169, deoR , recA1, endA 1, hsdR17(r K- , m K+), phoA , supE 44, λ- , thi-1, gyrA96, relA1*	New England Biolabs
Escherichia coli BL21 (DE3)/ parental strain (PS)	Wild type, *fhuA2 [lon] ompT gal (λ DE3) [dcm] ΔhsdS λ DE3 = λ sBamHIo ΔEcoRI-B int::(lacI::PlacUV5::T7 gene1) i21 Δnin5*	New England Biolabs
RS01	*E. coli* BL21(DE3) with pETDuet-1-*zwf-fbp*	This study
RS02	*E. coli* BL21(DE3) with pACYCDuet-1-*cob*U-*cob*C	This study
RS03	*E. coli* BL21(DE3) with pCDFDuet-1-*bio*F-*bio*D	This study
RS04	*E. coli* BL21(DE3) with pETDuet-1-*zwf-fbp,* pACYCDuet-1-*cobU-cobC*, and pCDFDuet-1-*bio*F-*bio*D	This study
RSE01	*E. coli* BL21(DE3) with empty pETDuet-1	This study
RSE02	*E. coli* BL21(DE3) with empty pACYCDuet-1	This study
RSE03	*E. coli* BL21(DE3) with empty pCDFDuet-1	This study

RSE04	*E. coli* BL21(DE3) with empty pETDuet-1, pACYCDuet-1, and pCDFDuet-1	This study
Plasmid		
pETDuet-1	Expression vector, ColE1 replication, two multiple cloning sites, T7 promoter, Amp^R	Merck-Millipore
pACYCDuet-1	Expression vector, p15A replication, two multiple cloning sites, T7 promoter, CmR^R	Merck-Millipore
pCDFDuet-1	Expression vector, ColDF13 replication, two multiple cloning sites, T7 promoter, SmR^R	Merck-Millipore
pETDuet-1-*zwf-fbp*	pETDuet-1 carrying *zwf* gene in MCS1 and *fbp* gene in MCS2	This study
pACYCDuet-1-*cobU-cobC*	pACYCDuet-1 carrying *cob*U gene in MCS1 and *cob*C gene in MCS2	This study
pCDFDuet-1-*bioF-bioD*	pCDFDuet-1 carrying *bio*F gene in MCS1 and *bio*D gene in MCS2	This study

[a]Abbreviations: *Amp* ampicillin; *CmR* chloramphenicol; *SmR* streptomycin; *R* resistance; *MCS* multiple cloning site.

4.2.2 Gene cloning and construction of recombinants

Plasmid construction idea in this study was adapted from our previous work in **Chapter 2**, which has successfully identified algal growth-promoting genes and beneficial bacterial-derived metabolites. Building upon the shortlisted genes deemed suitable for overexpression to upregulate synthesis levels, this study concentrates on vitamin-based metabolites, specifically riboflavin, cobalamin, and biotin. Three different plasmids carrying different antibiotic resistance genes were employed to overexpress two key genes responsible at two cloning sites, to produce these metabolites, as illustrated in **Figure 14.** Primers used in this work are listed in **Supplementary data 8.**

To construct riboflavin-overproducing plasmid, *zwf* (encoding glucose-6-phosphate 1-dehydrogenase) and *fbp* (encoding fructose-1,6-biphosphatase I) genes were amplified using *zwf*-MCS1-Fwd/Rev and *fbp*-MCS2-Fwd/Rev. Corresponding vectors were also amplified using pET-*fbp*-MCS1-Fwd/Rev and pET-*fbp*-MCS2-Fwd/Rev. Each gene fragments were then inserted into

their corresponding cloning sites by Gibson assembly (NEBuilder HIFI DNA Assembly Master Mix, New England Biolabs), yielding a resultant plasmid named pETDuet-1-*zwf-fbp*. With the corresponding primers, same protocol was applied to the other four target gene fragments: *cob*U (encoding bifunctional adnosylcobalamin biosynthesis protein), *cob*C (encoding adenosylcobalamin/alpha-ribazole phosphatase), *bio*F (encoding 7-keto-8-amino pelargonic acid synthase), and *bio*D (encoding desthiobiotin synthase). It yielded two additional plasmids, namely pACYCDuet-1-*cob*U-*cob*C, and pCDFDuet-1-*bio*F-*bio*D. All the corresponding plasmids were transformed into *E. coli* BL21 (DE3), resulting in RS01, RS02, and RS03. Finally, all three plasmids were sequentially integrated into a single expression host, producing the strain RS04.

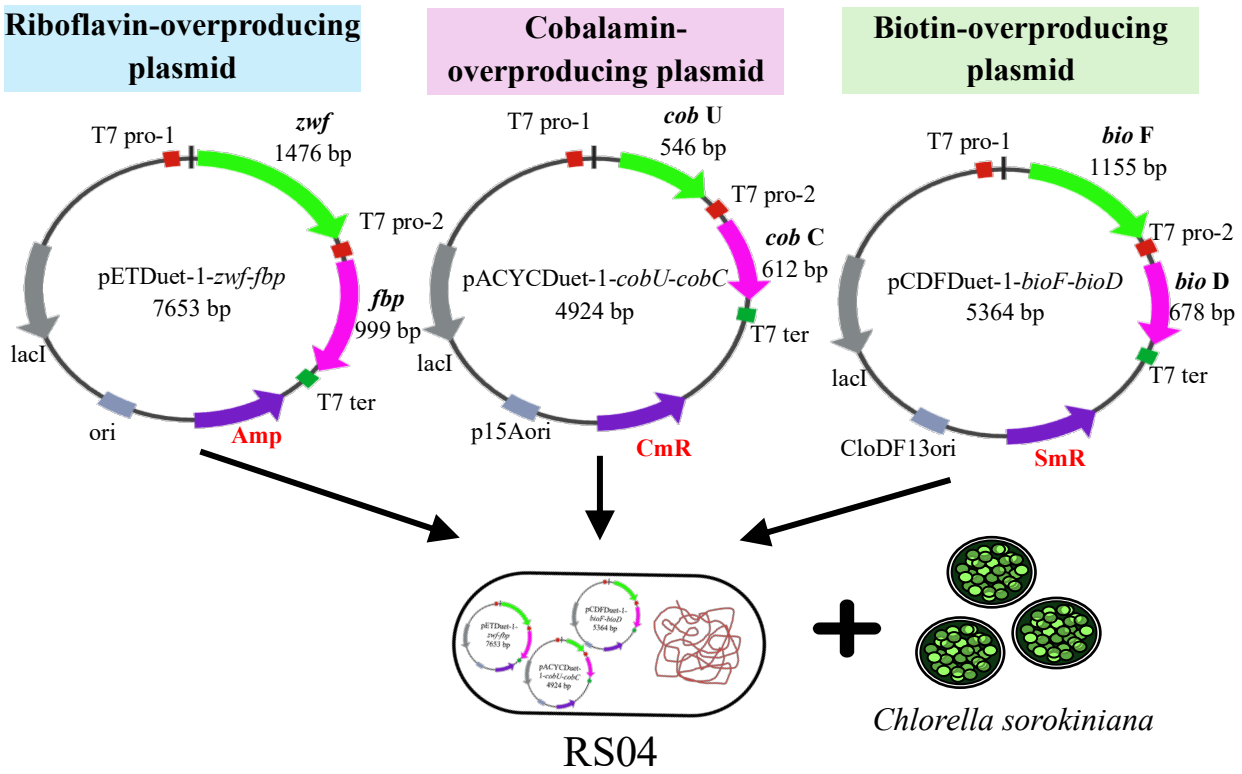

Figure 14 *Construction of recombinant E. coli RS04 harboring three separate plasmids, which are corresponding to riboflavin, cobalamin, and biotin synthesis, respectively. zwf, glucose-6-phosphate 1-dehydrogenase; fbp, fructose-1,6-biphosphatase I; cobU, bifunctional adnosylcobalamin biosynthesis protein; cobC, adenosylcobalamin/alpha-ribazole phosphatase; BioF, 7-keto-8-amino pelargonic acid synthase; BioD, desthiobiotin synthase; Amp, ampicillin resistance gene; CmR, chloramphenicol resistance gene; SmR, streptomycin resistance gene.*

4.2.3 Co-cultivation medium preparation and conditions

All the constructed recombinant strains were routinely grown in LB broth or agar at 37℃. Where necessary, respective antibiotics were added to the final concentration of 50 μg mL^{-1}. 1 mL overnight seed cultures of recombinant strains were used to inoculate 250 mL shake flasks containing 100 mL of LB medium supplemented with appropriate antibiotics and incubated at 37℃ in a rotary shaker at 180 rpm until reaching OD_{600} about 0.6. Then, 0.1 mM isopropyl-β-D-1-thiogalactopyranoside (IPTG) was added to induce expression at 18°C for 18 h. On the other hand, 90 mL one-week old microalgal cultures were pelleted at ~2,300 ×g for 10 min and the supernatant was discarded. The algal cell pellets were then re-suspended with an equal volume of sterile BG11 medium and subsequently mixed with 90 mL of IPTG-induced bacterial cultures. Such a co-cultivation approach was adapted from our previous optimized findings, utilizing a 1:1 ratio of BG11 to bacterial exudate (v/v) as the co-cultivation medium and a bacteria-to-microalgae inoculum size of 5:1 on a dry weight basis [128].

The mixture was divided among three separate shaking flasks and incubated under microalgal culture conditions for one week (strains screening purpose), and 28 days (long-term culture stability assessment purpose). Data collection was performed at seven-days intervals.

4.2.4 Quantification of targeted metabolites secreted into the extracellular medium

5 mL of sample was harvested at every data collection points for all the analysis. Gathered samples were centrifuged at 19,000 ×g for 10 min and supernatant was transferred into another clean sample tube. For the quantification of riboflavin, measurement was carried out with the supernatant at A444 immediately. To determine the concentration of cobalamin, 10 μL aqueous supernatant was subjected to HPLC analysis via Nexera Lite HPLC System (Shimadzu, Japan)

equipped with a reversed-phase column (Cosmosil 5C18-AR-II, Φ 4.6 × 250 mm, Nacalai Tesque Inc, Kyoto, Japan) and photo diode array detector set at 361 nm. The HPLC system was implemented using solvent A (0.025% trifluoroacetic acid in water, pH 2.6) and solvent B (100% acetonitrile), combined in a linear gradient. Elution was performed with solvent B from 0%-70% (0.21 min-10 min) at 30°C, with a flow rate of 1 mL min^{-1}. A standard cyanocobalamin solution was prepared between the range 0.625 to 10 mg L^{-1}. Quantification of biotin was carried out using bioassay method, employing *Lactobacillus plantarum* NBRC 3070 (National Institute of Technology and Evaluation biological resource center, Japan) as the indicator organism. *L. plantarum* was cultured in 30 mL biotin spiked-Difco biotin assay medium (final concentration of 1 ng d-biotin mL^{-1}) for over approximately 45 hours at 37°C to obtain an OD_{600} of approaching 2.0. The cells are centrifuge under aseptic conditions and washed at least three times with sterile 0.85% saline solution, eventually re-suspended with 15 mL biotin free-assay medium. Samples or various biotin concentrations were added and incubated at a similar. Condition for turbidimetric analysis at 600 nm. It is essential that a standard curve must be constructed each time an assay was run.

4.2.5 Determination of growth profile

Algal growth was assessed with fluorescent intensity of chlorophyll-*a* at excitation and emission wavelengths of 490 nm and 650 nm, respectively, using a microplate reader (SpectraMax M2, Molecular Devices, Sunnyvale, CA, USA). Aliquots of harvested samples were serially diluted for bacterial colony forming units.

4.2.6 Determination of photosynthetic pigment content

Remaining cell pellets from **Section 4.2.4** were re-suspended with 3 mL of 2:1 chloroform: methanol (v/v) and left the mixture to stand at 4°C overnight for chlorophyll extraction. After that,

2 mL 0.9% NaCl solution was pipetted into the mixture to induce phase separation, resulting in two distinct layers: the lower chloroform phase was again transferred to a clean tube, whereas the upper aqueous phase was gathered as intracellular organic materials (IOM) for further analysis. Using the greenish lower phase, Chl-*a/b*, carotenoid, and total chlorophyll concentration were quantified based on all the key equations listed in previous work [98]. All the data were adjusted by incorporating the relevant dilution factors.

4.2.7 Determination of biochemical composition

IOM acquired was characterized for its total carbohydrate, protein, and lipid content using phenol-sulfuric acid method [99], Bradford's Protein Assay (500-0006, BIO-RAD Laboratories Inc. California, USA, according to the manufacturer's instructions), and sulfo-phospho-vanillin method [100], respectively.

4.2.8 Determination of antioxidant enzyme activity

For catalase (CAT) activity determination, reaction mixture was prepared with 2.5 mL of 10 mM phosphate buffer (pH 7.0), 0.5 mL of 30 mM H_2O_2, and 0.2 mL of cell lysate (IOM). The reaction immediately started after adding H_2O_2 at 30°C, and the decrease in the absorbance at 240 nm was calculated. One unit of catalase activity (U) was defined as the amount of enzyme that decomposed 1 μmol H_2O_2 mg^{-1} soluble protein per minute. Superoxide (SOD) activities were determined using SOD assay kit (Dojindo Laboratories, Japan) according to the manufacturer's instructions. Peroxidase (POD) activities were determined based on guaiacol oxidation method. Reaction mixture was prepared with 0.5 mL of cell lysate mixed with equal volume of 50 mM PBS containing 20 mM guaiacol and 40 mM H_2O_2. A_{470} was recorded every 1 min, until getting a stable absorbance value. Similarly, one enzyme unit of POD was defined as the amount of enzyme that

catalyzed the oxidation of guaiacol per minute and calculated using the molar extinction coefficient of guaiacol (26.6 mM^{-1} cm^{-1}).

4.2.9 Determination of fatty acid methyl esters (FAMEs)

The organic phase acquired in **Section 4.2.6** was volatilized and methylated using a fatty acid methylation kit (Nacalai Tesque, Kyoto, Japan). Resulting supernatant was then analyzed using a gas chromatograph equipped with FID detector (Nexis GC-2030, Shimadzu Corporation, Kyoto, Japan) and TC-70 column (0.25 mm I.D. x 60 m, df= 0.25 μm). Chromatographic conditions were as follows: injection volume 1 μL; split ratio 1:50; air 300 mL min^{-1}; H_2 35 mL min^{-1}; gas carrier (N_2) 30 mL min^{-1}; detector temperature 250 °C; oven temperature started at 140°C for 3.5 min and raised to 180°C at a rate of 8°C min^{-1}, then ramped at 4°C min^{-1} to 200°C, followed by a slower ramp of 1°C min^{-1} to 220°C. The final ramping was 25°C min^{-1} to 240°C and held for 3 minutes. The FAMEs contents were quantified by comparing their peak areas with that of 37-component FAME mix CRM47885 (Supelco, Bellefonte, PA, USA).

4.2.10 Evaluation of biofuel properties

To further assess the suitability of the fatty acid components from both mono- and co-cultures for biodiesel production, some pivotal properties of biodiesel derived from these fatty acids were evaluated. This evaluation involved theoretical calculations of various biodiesel properties as follows [129]:

$$\text{Average degree of unsaturation (ADU, \%)} = \sum N \times Mf \quad (3)$$

where N is the number of carbon-carbon double bonds in each fatty acid, and Mf is the mass fraction of each fatty acid.

$$\text{Cetane number (CN)} = -6.6684 \times ADU + 62.876 \quad (4)$$

Iodine value (IV, g I_2 100 g^{-1} oil) = $74.373 \times ADU + 12.710$ (5)

Kinematic viscosity (vi, $mm^2\ s^{-1}$) = $-0.613 \times ADU + 5.2065$ (6)

Specific gravity (ρ, g m^{-3}) = $0.0055 \times ADU + 0.8276$ (7)

Cloud point (CP, °C) = $-3.356 \times ADU + 19.994$ (8)

Higher heating value (HHV, MJ kg^{-1}) = $1.7601 \times ADU + 38.534$ (9)

Long chain saturation factor (LCSF, wt%) = $(0.1 \times C16{:}0) + (0.5 \times C18{:}0)$ (10)

Cold filter plugging point (CFPP, °C) = $(3.1417 \times LCSF) - 16.477$ (11)

where C16:0 and C18:0 is the percentage of the saturated fatty acids.

Oxidation stability (Y, h) = $\frac{117.9295}{X} + 2.5905$ (12)

where X is the content of linoleic and linolenic acids (wt%) (0<X<100).

4.2.11 Statistical analysis

Statistical analysis was conducted with SPSS Statistics 25 (SPSS Inc,. Chicago, IL, USA). A one-way ANOVA and post-hoc Tukey-test were used to confirm the differences between experimental groups and controls, with significance indicated by a $p < 0.05$.

4.3 Results and discussions

4.3.1 Recombinant strains screening and long-term cultures growth assessment

A one-week long co-culture system was preliminarily established to screen for the best recombinant strain with the best growth-enhancing effect. According to **Figure 15**, three recombinant strains, namely RS01, RS02, and RS03 exhibited at least a twofold increase in algal

growth compared to the parental strain control, but the growth of *C. sorokiniana* with these three recombinant strains remained insignificant between each other ($p>0.5$). As shown in **Supplementary data 9**, although riboflavin production in RS01 (7.8 ± 0.4 mg L^{-1}) was approximately 10 times higher than that of PS, its highest production did not give significant algal growth promotion effect when compared with RS02 and RS03, which exhibited lower riboflavin concentrations (4.3 ± 3.0 mg L^{-1} and 3.5 ± 3.0 mg L^{-1}, respectively). Interestingly, a slight increase in cobalamin concentration in RS02 (0.10 ± 0.00 mg L^{-1}, 1.1% higher than PS) and biotin concentration in RS03 (0.38 ± 0.04 ng mL^{-1}, 24% higher than PS) resulted in a comparable growth-promoting effect for *C. sorokiniana*. This outcome was likely due to the algae's prioritization of vitamin assimilation, which will be discussed further in **Section 4.3.2.**

In the case of RS04, the synergistic effect of three vitamins further enhanced its cobalamin and biotin concentrations to 0.12 ± 0.06 mg L^{-1} and 0.39 ± 0.08 ng mL^{-1}, respectively, but riboflavin production was downregulated to 1.8 ± 0.22 mg L^{-1}, suggesting a potential metabolic burden within the cell (**Supplementary data 9**). Despite that, a striking color intensity change, as seen in **Figure 15(a)** for RS04, highlighted its most significant algal growth-boosting effect, achieving a fourfold increase in algal growth compared to PS (**Figure 15(b)**). It was initially expected that RS04, harboring three plasmids responsible for the overproduction of three key vitamins, would result in approximately a sixfold increase in algal growth, assuming a cumulative effect. However, this was not observed, with a fourfold increase appearing to be the maximum growth achieved. Such a maximum algal growth capacity could be attributed to several factors: (a) the micronutrient utilization threshold has been reached in a resource-saturated state [130]; (b) the synergistic effects have plateaued; (c) the vitamin uptake may have been inefficient due to a low abundance of suitable vitamin transport genes [95], ending up with limited vitamin availability to *C. sorokiniana*.

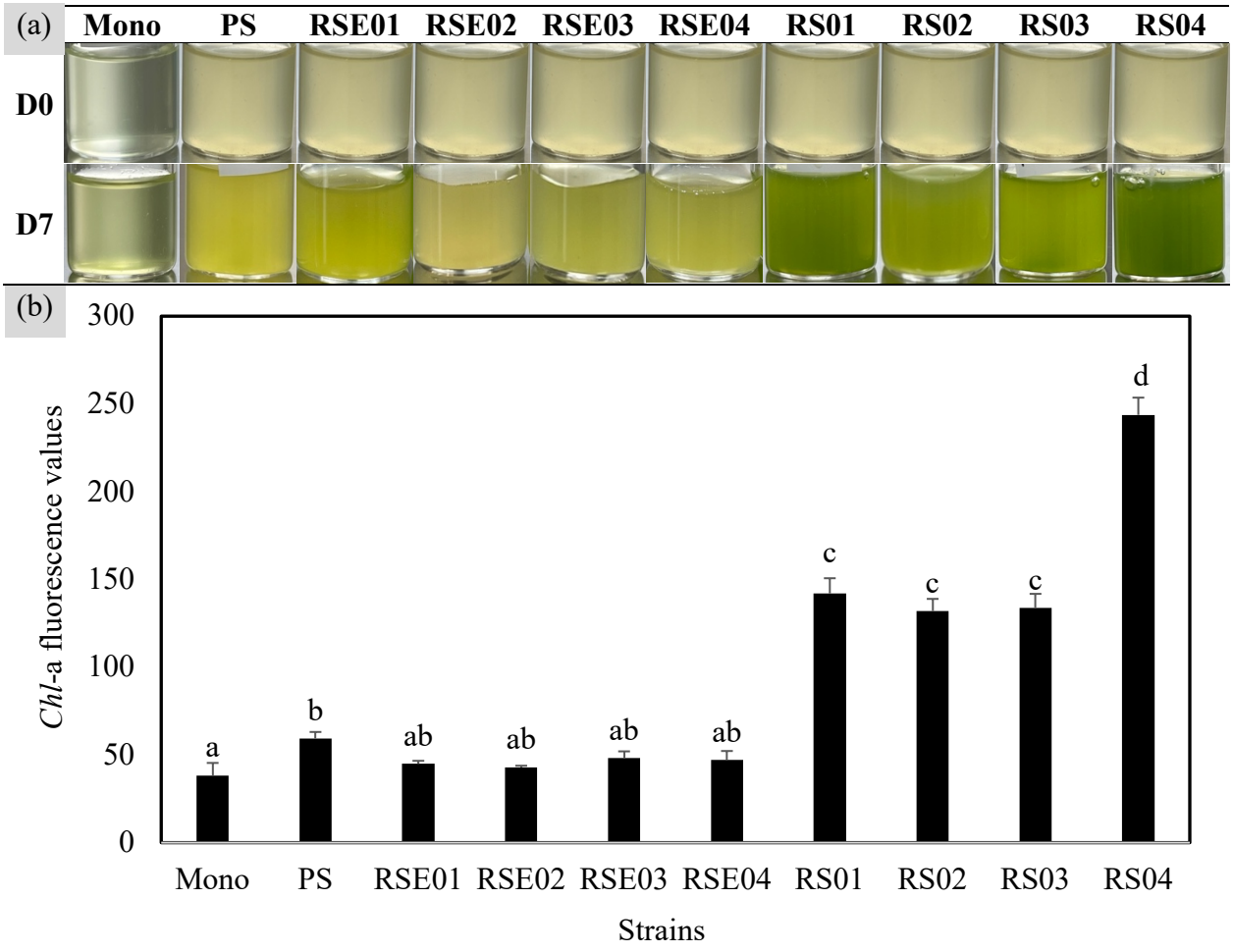

Figure 15 *Short-week one-week C. sorokiniana-E. coli co-cultures. (a) Images of cultures demonstrating the change in the culture color after two days. (b) chl-a fluorescence measurement after two days of cultivation. Data are stated as mean±standard deviation, n=3. Alphabets stand for significant differences between strains, detected by Tukey test. Mono: axenic microalgae; PS: parental strain; RSE01: E. coli BL21(DE3) with empty pETDuet-1; RSE02: E. coli BL21(DE3) with empty pACYCDuet-1; RSE03: E. coli BL21(DE3) with empty pCDFDuet-1; RSE04: E. coli BL21(DE3) with empty pETDuet-1, pACYCDuet-1, and pCDFDuet-1; RS01: E. coli BL21(DE3) with pETDuet-1-zwf-fbp; RS02: E. coli BL21(DE3) with pACYCDuet-1-cobU-cobC; RS03: E. coli BL21(DE3) with pCDFDuet-1-zwf-fbp; RS04: E. coli BL21(DE3) with pETDuet-1-zwf-fbp, pACYCDuet-1-cobU-cobC, and pCDFDuet-1-bioF-bioD.*

The most positive results from RS04 made it the best candidate for the subsequent one-month long experiment, aiming to confirm that the findings are not temporary under short-term conditions and to observe lipid accumulation under non-stressful conditions, making its application more relevant for large-scale set-up. **Figure 16(a)** showed a drastic color change between three studied groups, with results demonstrating the algae grew the fastest with RS04 during the first 7 days,

without any obvious lag, implying its good adaptability to the cultivation environment. In **Figure 16(b)**, the growth of *C. sorokiniana* with PS conformed to an S-shaped growth curve with the logarithmic growth period starting around D14, which was later than that of RS04. Both RS04 and PS had their chl-*a* fluorescence values peak around 309 and 230, respectively, at D21, whereas Mono peaked earlier at D7 with a value of only 47. Generally, all three groups exhibited an exponential growth phase, followed by the onset of stationary phase.

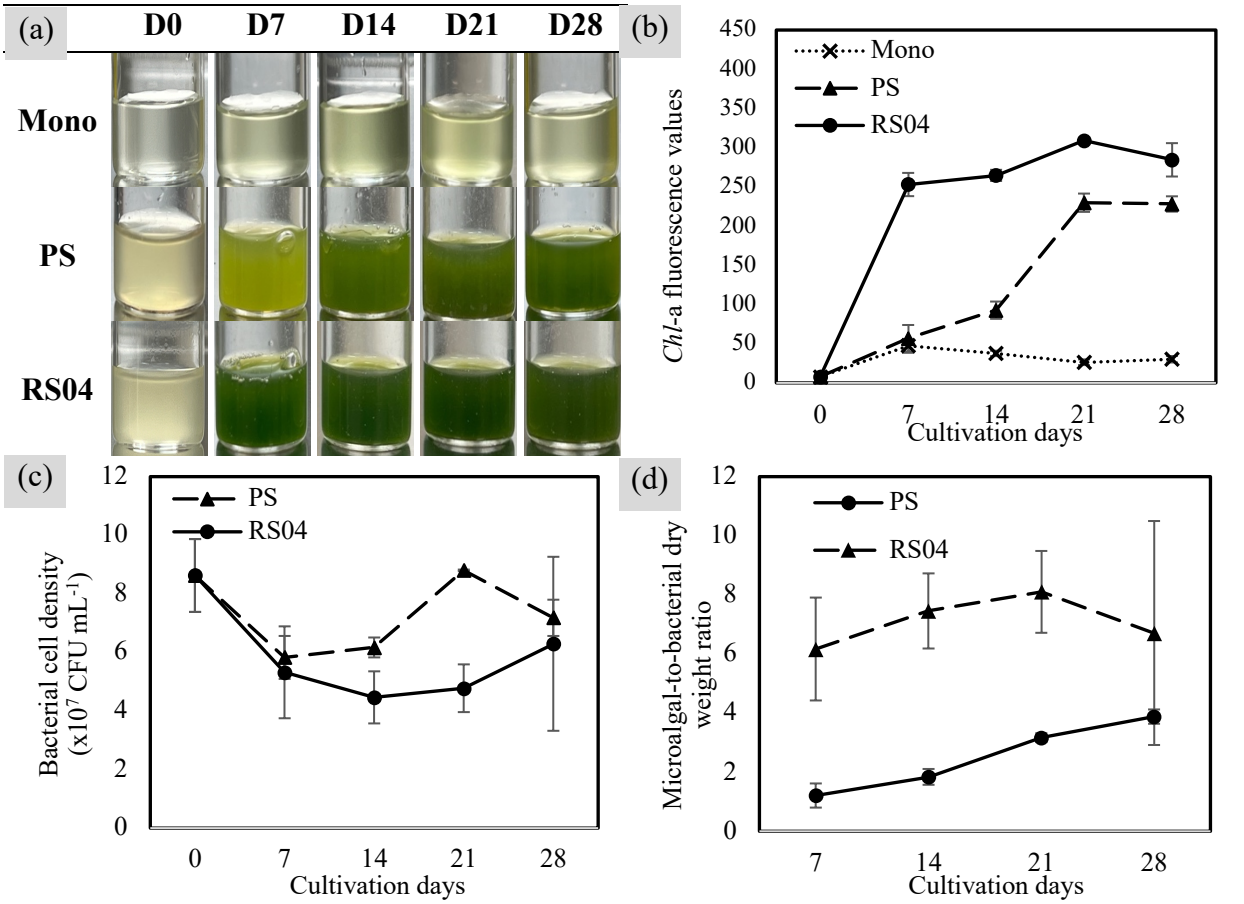

Figure 16 *Long-term 28-days C. sorokiniana-E. coli co-cultures. (a) Images of cultures demonstrating the change in the culture color over time. (b) chl-a fluorescence measurement over time. (c) Colony-forming units (CFU) per mL from the co-cultures over time. (d) Microalgal-to-bacteria ratio (dry weight basis) over time. Data are stated as mean±standard deviation, n=3. Alphabets stand for significant differences across different time points within the same strain, detected by Tukey test. Mono: axenic microalgae; PS: parental strain; RS04: E. coli BL21(DE3) with pETDuet-1-zwf-fbp, pACYCDuet-1-cobU-cobC, and pCDFDuet-1-bioF-bioD.*

However, in **Figure 16(c)**, the bacterial densities in all groups have drastically reduced in the first 7 days, continued to decline until D14, and then slowly recovered thereafter. It indicated that *C. sorokiniana* and PS or RS04 could grow in symbiosis in organic carbon containing medium. Findings in this study was in an agreement to Han *et al.* (2016) citing that the concentration of bacterium declined in the first 9 days, but steadily rose back as the incubation time prolonged [131]. In the initial phase of the co-culture, exponentially growing algae tend to compete actively for more resources to dominate the entire system, thereby inhibiting bacterial growth. However, once algae entered the stationary phase, algal by-products would have been released into the medium to allow a subsequent recovery of bacterial growth. For RS04, there could be an initial burden on recipient bacterial metabolism but recovered slowly once they adapted to the metabolic load. Another possible explanation lies in the efficiency of phycosphere, where bacterial cells attach to the algal cell wall, ingest algal lysates (in close proximity) to support bacterial binary fission or plasmid replication, and finally release their offsprings from the algal host cells to continue the cycle [132, 133]. A well-maintained phycosphere could sustain the bacterial cells even when they are in low quantities or inactive state.

Throughout the cultivation period, as displayed in **Figure 16(d)**, microalgae consistently dominated the co-culture system, maintaining a minimum microalgae-to-bacteria dry weight ratio of 1.2 and 6.2 in PS and RS04, respectively from D7 onwards. The ratio in RS04 showed minimal fluctuations over time, attaining a peak of 8.1 at D21, whereas PS achieved a maximum ratio of 3.9 at D28 (during the algal stationary phase). It indicates a stable co-culture system without any issues of bacterial overgrowth.

4.3.2 Vitamin profiles in extracellular medium throughout long-term cultivation

Representative profiles of riboflavin, cobalamin, and biotin assimilation were shown in **Figure 17**. While *C. sorokiniana* could grow by scavenging vitamins from bacterial extracts, co-culture experiments demonstrated different assimilation trends across 28 days. With the presence of bacteria, riboflavin titer in the medium was upregulated at least three-fold higher than Mono at D0 (**Figure 17(a)**). The amount of riboflavin released into the medium remained consistent in Mono, whereas its production depicted an increasing trend for both PS and RS04. Notably, in RS04, the

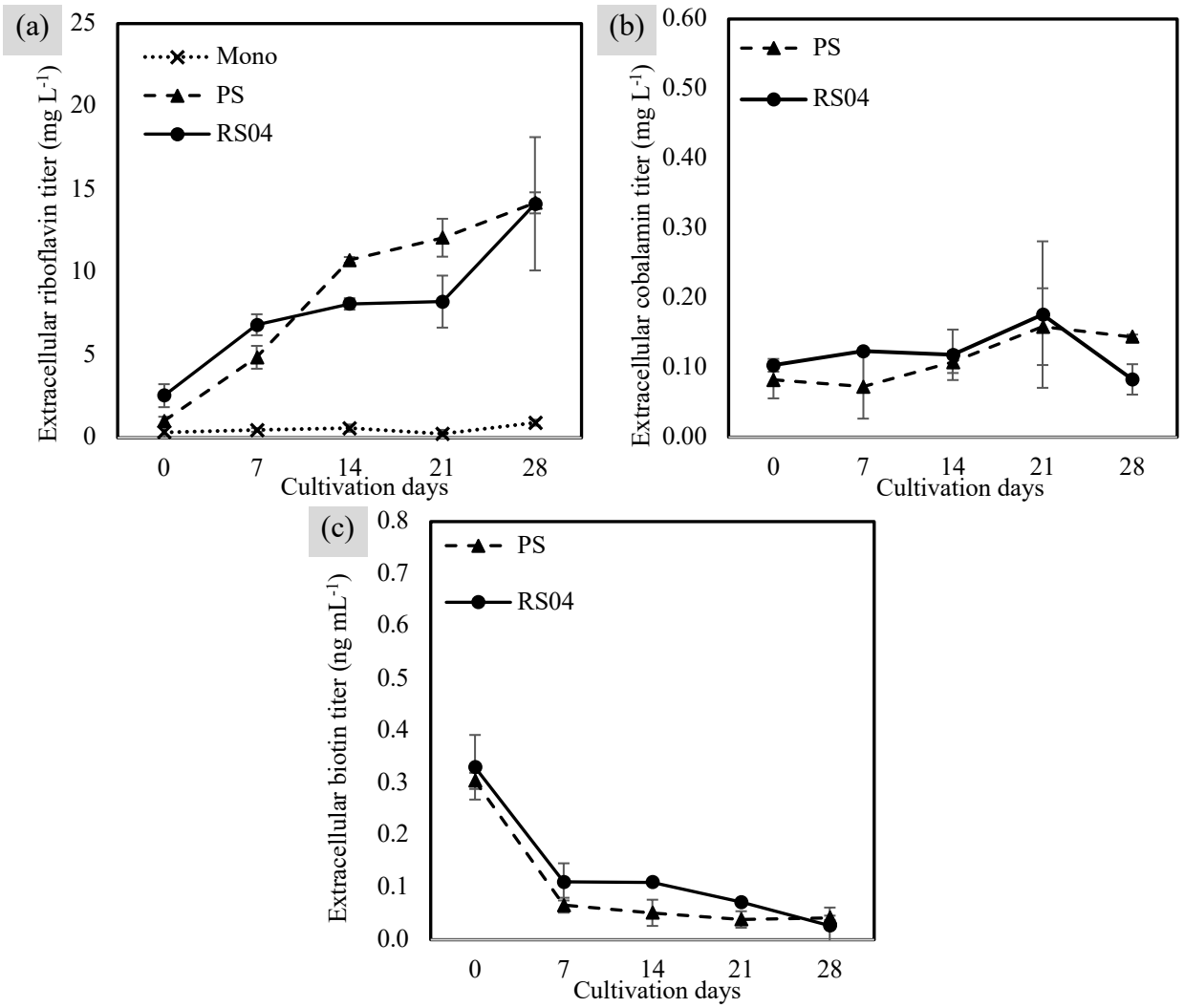

Figure 17 *Vitamin profiles of the extracellular medium across 28-days C. sorokiniana-E. coli co-cultures. (a) Riboflavin. (b) Cobalamin. (c) Biotin. Data are stated as mean±standard deviation, n=3.*

riboflavin concentration remained constant between D7 and D21 (6.8 mg L^{-1} to 8.2 mg L^{-1}), but then increased further, eventually reaching the same level as PS (14.1±4.0 mg L^{-1}) by D28. The increasing microalgae-to-bacteria ratio from D7 to D21 indirectly indicated an active riboflavin assimilation by the cultures to support cell growth, as riboflavin plays a critical role as a cofactor in biological redox and radical metabolism [97]. Given that riboflavin production is generally bacterial cell density-driven, the attenuated rate of riboflavin uptake by the microalgae accounts for the observed accumulation from D21 onwards [96]. It simultaneously implied that riboflavin assimilation was governed by metabolic demand, with its utilization being selectively prioritized rather than constitutive.

Unlike cobalamin in **Figure 17(b)**, there was no measurable cobalamin in *C. sorokiniana* cell extracts, confirming its vitamin B_{12}-auxotriphic nature. Cobalamin permits the enzymatic activities of methionine synthase, class II ribonucleotide reductase (RNR II), and methylmalonyl-CoA-mutase (MMCM). In eukaryotic metabolism, microalgae generally require two different active forms of vitamin B_{12}: methylcobalamine (*MeCbl*) for catalysis in protein synthesis within the cytosol and adenosylcobalamin (*AdoCbl*) for enzymatic activity in citric acid cycle within the mitochondrion [134]. Nonetheless, while *E. coli* lacks the methylation pathway necessary for *MeCbl* synthesis, the cobalamin detected predominantly exists in its native *AdoCbl* form. It then serves as a cofactor in TCA cycle, powering cellular processes and efficiently channeling more carbon into microalgal biomass production. The minor fluctuations as noted in **Figure 17(b)** might reflect a consistent demand for cobalamin by the cultures throughout the co-cultivation period. Such a dynamic equilibrium was also evidenced by *Chlorella vulgaris*-anaerobic bacteria grown in tris acetate phosphate medium, where the uptake of cobalamin in the non-axenic culture system was attributed to biosynthesis of symbiotic bacteria [86]. Previous research cited that microalgae

require only a minimum cobalamin of 10 ng L^{-1} for growth, whereas ~0.1 mg L^{-1} achieved in the medium appeared to be more than sufficient [135-137]. As cobalt serves as a critical precursor for cobalamin synthesis and only becomes limiting at <0.01 mM, 0.17 mM cobalt nitrate hexahydrate from BG11 medium (~10 mg L^{-1} cobalt ions) effectively supported high production noted in this study, which aligns with expectations. As a result, this level was likely adequate to maintain a balance between bacterial production and algal uptake.

Interestingly, in **Figure 17(c)**, biotin uptake was statistically significant ($p<0.05$) during the first seven days as it is another important coenzyme for carboxylation reactions and fatty acid synthesis during algae's rapid proliferation phase [93]. Since *C. sorokiniana* does not produce biotin *de novo*, an initial burst in algal growth likely involved the scavenging of substantial biotin amount from external sources to support cell division and this early uptake could also be associated to nutrient storage for subsequent growth. As the culture progresses, the uptake might be stabilized, as indicated in **Figure 17(c)**. However, a previous research showed that 1 ng mL^{-1} biotin was optimal for green microalgal growth, while the current study found only a maximum of 0.3 ng mL^{-1} biotin, still below the algae's full uptake capacity [130]. This directly explained the continuous uptake of biotin after D7. Aside from that, Suneerat and others (2018) also discovered that a 50: 0.5: 1 ng mL^{-1} mixture of thiamine: biotin: cobalamin managed to achieve 1.86 g L^{-1} algal biomass, highlighting an equivalent importance of both biotin and cobalamin for algal growth, which was in line with the current findings. In short, the entire co-culture system revealed distinct temporal patterns in the vitamin assimilation, shaped by the metabolic demands of the algae and vitamin availability in the medium. Biotin was rapidly taken up during the early growth phase, cobalamin maintained a steady profile throughout the cultivation, while riboflavin uptake was more gradual and closely tied to bacterial production and algal density. Therefore, the overall synergistic

interactions between three different vitamins allows a proposal of sequential vitamin assimilation model as follows: biotin (initial uptake)< cobalamin (consistent need)< riboflavin (slowest).

4.3.3 Effect of engineered bacterial strain onto photosynthetic pigment and intracellular organic matters composition

Microalgae produce and accumulate different compounds depending on the cultivation environment that are applied during their growth. As shown in **Figure 18(a)** and **(b)**, two main groups of pigments: Chl-*a*,*b* (most abundant in green microalgae) and carotenoids- were quantified in cultivated *C. sorokiniana* under the effect of RS04. Chl-*a* is a principal photosynthetic pigment to capture light energy whereas Chl-*b* acts as an accessory pigment that responsible for energy transfer to Chl-*a* for light harvesting efficiency enhancement [138]. In **Figure 18(a)**, low chl-*a*-to-*b* ratio (~0.45 to ~0.55) found in RS04 across the entire cultivation timeframe indicates that the co-cultures were subjected to low light intensities or shaded conditions due to high-dense cultures as noted in RS04 from D7 onwards. In parallel with the findings of this study, Chl-*a* content in *Tetraselmis suecica* was reduced because of lower light penetration within the culture [139]. Expectedly, the chl *a*/*b* ratio increased to support more photosynthesis in less dense Mono, whereas exponentially growing PS depicted a decline in the ratio after D7.

Since there was no excess light energy to be dissipated in RS04 groups (due to shaded conditions), no photoprotection from carotenoids is needed. As a result, in **Figure 18(b)**, its carotenoid content remained significantly low (4.2% to 5.45%) from D7 onwards [140]. As anticipated, carotenoid production was the highest in Mono, followed by PS. In **Figure 18(c)**, the similarity between the total pigment production and growth profile mirrors a direct correlation between two. Additional vitamins supplementation from RS04 rendered a 3.5-times higher total pigment production than PS at D7, confirming their roles in promoting the biological activity of

algal cells. It has also been evidenced by a *Chlorella vulgaris-Bacillus licheniformis* co-culture system grown in synthetic wastewater with exogenous vitamin B, where differential protein enrichment in GO terms was significant for chloroplast, lipid synthesis, intracellular protein metabolism, material transports, and transmembrane transport [87].

Intracellular biochemical composition from the cultures was also summarized in **Figure 18(d)**. Lipids typically constitute the largest proportion within the algal cells, followed by carbohydrate, protein, and pigment. Notably, carbohydrate content gradually decreased over time, accompanied by a slow rise in lipid content. Results are consistent with a previous study reporting that during

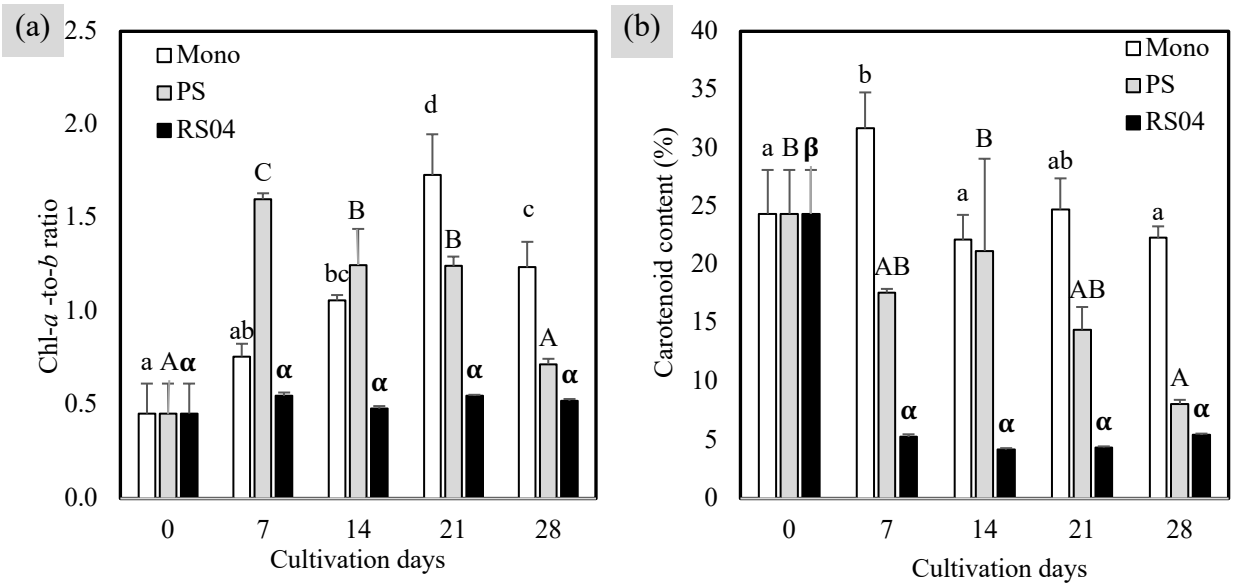

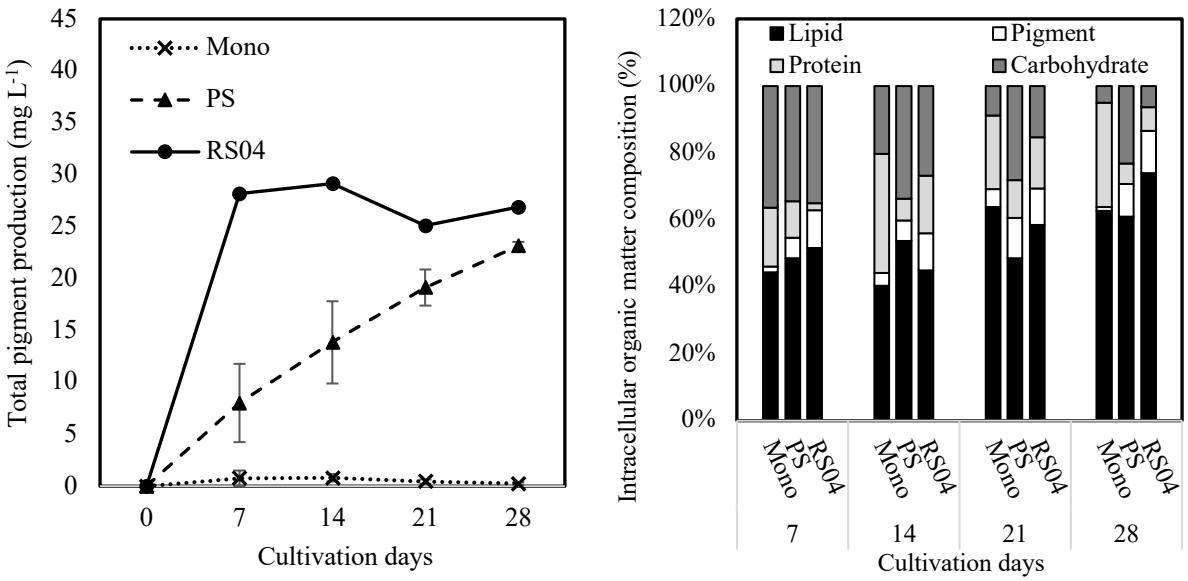

Figure 18 *Photosynthetic pigments in C. sorokiniana-E. coli co-cultures over 28-days of co-cultivation. (a) Ratio of chlorophyll a to chlorophyll b. (b) Carotenoid content. (c) Total chlorophyll production. (d) Intracellular metabolites profile in the co-culture system. Data are stated as mean±standard deviation, n=3. Lowercase alphabets, uppercase alphabets, and Greek letters stand for significant differences across different time points within the same strain, detected by Tukey test.*

reduced CO_2 fixation, *Chlamydomonas* sp. KOR1 exhibited rapid carbohydrate degradation alongside increased lipid accumulation [141]. Carbohydrates typically serve as short-term energy reserves due to their faster synthesis and metabolism during the active cell division phase. However, under nutrient-depleted conditions, central carbon metabolism is shifted toward lipid accumulation for long-term energy storage [142]. It is also coupled with the onset of oxidative stress, a phenomenon that will be detailed in the subsequent **Section 4.3.4**.

4.3.4 Effect of engineered bacterial strain onto the oxidative stress responses in the cultures

Microalgae generate reactive oxygen species (ROS) such as O_2^- and H_2O_2 under stress while antioxidants could effectively scavenge these ROS to safeguard the microalgal cellular components from oxidative damage [143]. As depicted schematically in **Figure 19**, at D7, the activities of CAT, SOD, and POD were relatively lower in PS but comparably higher in RS04, as

compared to Mono. It is common to report lower antioxidant enzyme activities in co-cultures compared to monocultures of the same species as less O_2^- and H_2O_2 were produced in co-cultures, owing to their capability in balancing intracellular antioxidation systems for oxidative stress mitigation while achieving the desired biomass yield, preventing lipid oxidation and enhancing lipid productivity [129].

However, an exceptionally high antioxidant activities observed in RS04 at D7 and significant drop afterwards in this study might warrants careful attention. While metabolic activity in algal cultures with RS04 was likely at its peak at D7, an oxidative burst was stemming from biotic stress, such as heightened mitochondrial electron transport chain (in microalgae) and oxidative phosphorylation (in bacteria) [144]. Excess oxygen accumulation during active photosynthesis in microalgae could have formed more ROS, eventually exceeding the ROS scavenging capacity of auto-oxidizing enzymes (superoxide dismutase, ascorbate peroxidase, catalase, glutathione peroxidase etc.) present in the chloroplast. The same effect could also be seen when the algal population has attained its peak in the case of PS. Despite so, the ROS produced did not appear to overwhelm the microalgal protective mechanisms, as no severe growth reduction was observed afterwards. Instead, a rapid decline following that suggested a cellular self-adjustment to maintain physiological homeostasis [145]. This scenario could also be interpreted as a stress-priming effect during the optimum growth stages, enabling the cells to handle ROS more efficiently throughout the subsequent growth phase.

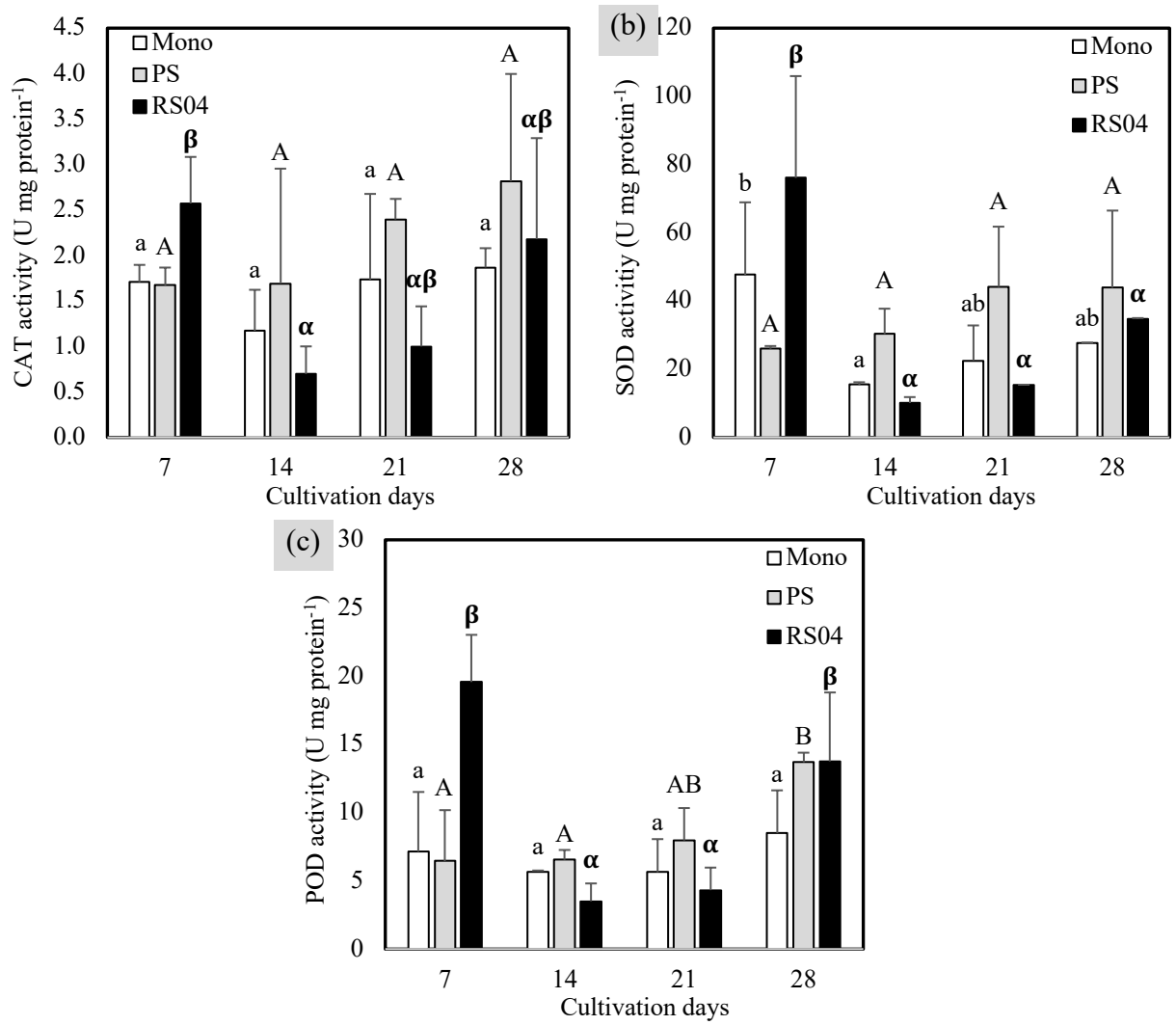

Figure 19 *Antioxidant enzyme activities of C. sorokiniana-E. coli co-cultures over 28-days of co-cultivation. (a) Catalase. (b) Superoxide dismutase. (c) Peroxidase. Data are stated as mean±standard deviation, n=3. Lowercase alphabets, uppercase alphabets, and Greek letters stand for significant differences across different time points within the same strain, detected by Tukey test.*

Evidently, antioxidation activities in RS04 were comparatively lower than both Mono and PS from D14 onwards. A gradual rise of those activities for all the studied sample groups were attributed to the abiotic stress such as nutrient limitation as seen in many former studies [146, 147]. Cells experiencing interspecies competition or nutritional stress would typically activate the synthesis of reserve compounds like lipid, as part of their survival strategy. Upregulating diacylglycerol acyltransferase (DGAT) and inhibiting ADP-glucose pyrophosphorylase were some

key regulatory mechanisms that are activated under environmental stress [148]. The overall antioxidant activities have indirectly validated the lipid accumulation trend observed in the biochemical indices.

4.3.5 FAME contents and fatty acids-based biodiesel properties evaluation

The fatty acid profile of algae determines its potential as a biodiesel feedstock. As tabulated in **Table 5**, the biomass lipids obtained from the pure algal culture (Mono condition) consisted mainly of C16:0, C18:0, and C18:2. At least 80% of the fatty acids were saturated. Notably, a percentage rise of the only PUFA (C18:2) in Mono from D7 (4.5±1.4%) to D14 (13.7±7.8%) could indicate the adaptive stress response in the cultures from D14 onwards. As the culture ages, cultures introduced a lipid remodeling by increasing their PUFA content in the membrane lipids to maintain the cellular membrane fluidity and functionality [149, 150]. While being non-polar lipids, triacylglycerols which contain C16:0 and C18:0, serve as energy storage molecules. Their gradual decline over time confirmed a trend of lipid remodeling [149]. A similar profile was also observed in both PS and RS04 across the cultivation time.

However, when comparing to that of Mono group, co-cultures offered a great variety of fatty acids, namely C12:0, C13:0, C14:0, C15:0, C15:1, C16:1, C17:0, C17:1, C18:1, and C18:3. All these fatty acids primarily originated from the symbiotic bacterium *E. coli*, as supported by a previous findings [40]. Although a higher fatty acid contribution was anticipated from the microalgae in co-cultures with a high microalgae-to-bacteria ratio, the lower-than-expected findings (up to 57%) was likely due to the incorporation of bacteria-derived fatty acids into the microalgae's lipid pool from the exogenous medium [151, 152]. Despite that, both the PS and RS04 were able to accumulate a significant amount of MUFA but exhibiting a contrast trend between two over time, most likely due to their huge difference in algal specific growth rate. While

high MUFA content is beneficial for biodiesel production [153], PS required 21 days to reach its maximum MUFA content (12.0±1.4%), whereas RS04 attained the same level in just 7 days (11.10±0.2%). A combination of C16-C18 fatty acids accounted for a maximum of 67% and 64% for PS and RS04, respectively, which were comparatively higher than that of Mono (61%).

To better align with the desired biodiesel standards, **Table 6** presents an assessment of the estimated properties of fatty acids-based biodiesel. The theoretical values of all biodiesel parameters fully met the criteria set by both ASTM D6751, and EN 14214 standards. Cetane number (CN) is a major indicator of biodiesel quality associating with combustion quality and ignition delay time, with a higher value signifying a better engine performance. In this study, all the groups have shown a similar CN of ~60. Iodine value (IV), a rough measure of oxidative stability, with high IV indicating lower stability, unfortunately shows that both PS and RS04 have poorer oxidative stability. The same applies to the average degree of unsaturation (ADU) and oxidation stability (Y), which reflects the oxidative stability of biodiesel during long-term storage. A higher ADU value in both PS and RS04 was significantly associated with their high PUFA content [130].

A qualified biodiesel should have low kinematic viscosity (νi), as depicted by both PS and RS04 in **Table 6**. Simultaneously, a specific gravity (ρ) of 0.9 g m^{-3} reflects the ease of transportability of these fatty acids-based biodiesel. Cloud point (CP), is the lowest temperature at which biodiesel starts to form crystals. An average value of ~18℃, across all the groups and time suggests an

Table 5 *Fatty acid profiles in monocultures and co-cultures over time.*

Fatty acid profiles	Mono				PS				RS04			
	D7	D14	D21	D28	D7	D14	D21	D28	D7	D14	D21	D28
Lauric acid (C12:0)	-	-	-	-	1.1±0.1	0.6±0.2	0.4±0.0	0.3±0.1	0.7±0.1	0.7±0.1	0.5±0.1	0.5±0.1
Tridecanoic acid (C13:0)	-	-	-	-	0.6±0.1	2.6±0.3	1.9±0.3	2.8±0.0	4.0±0.1	4.8±0.1	4.7±0.1	4.8±0.2
Myristic acid (C14:0)	-	-	-	-	1.9±0.1	1.3±0.2	1.0±0.0	1.2±0.0	0.9±0.0	0.8±0.1	0.9±0.0	0.9±0.1
Pentadecanoic acid (C15:0)	-	-	-	-	1.0±0.1	0.8±0.1	0.7±0.1	0.8±0.1	1.1±0.1	0.8±0.1	0.7±0.1	0.7±0.1
cis-10-pentadecenoic acid (C15:1)	-	-	-	-	1.4±0.1	1.6±0.8	2.1±0.3	3.0±0.1	5.1±0.3	6.4±0.2	6.0±0.1	5.6±0.4
Palmitic acid (C16:0)	52.0±0.9	43.5±3.2	42.0±2.9	44.3±3.4	35.6±0.9	30.9±2.1	27.3±0.9	26.8±0.4	28.9±0.8	23.3±0.3	24.8±0.5	24.5±0.4
Palmitoleic acid (C16:1)	-	-	-	-	1.3±0.1	2.4±0.1	3.9±0.7	4.7±0.4	5.5±0.2	5.8±0.1	5.2±0.2	5.2±0.1
Heptadecanoic acid (C17:0)	-	-	-	-	2.1±0.6	3.9±1.3	4.7±0.2	4.6±0.1	7.1±0.3	9.0±0.3	9.2±0.2	9.2±0.2
Heptadecenoic acid (C17:1)	-	-	-	-	20.7±0.9	17.3±0.8	14.9±1.0	14.8±0.6	6.9±0.1	7.0±0.2	7.1±0.1	8.0±0.4
Stearic acid (C18:0)	43.5±0.7	42.8±5.4	38.6±5.9	44.5±2.3	15.6±1.4	12.5±2.2	7.5±0.3	7.5±0.5	13.4±0.8	8.5±0.1	8.2±0.3	6.8±0.7
Oleic acid (C18:1)	-	-	-	-	4.9±0.2	5.3±1.4	8.2±0.8	6.9±0.3	5.5±0.0	5.4±0.1	3.5±0.2	3.0±0.1
Linoleic acid (C18:2)	4.5±1.4	13.7±7.8	19.5±3.4	11.2±5.7	5.2±1.7	12.2±2.0	19.1±1.2	18.2±0.9	14.3±0.7	20.4±0.4	21.5±0.2	21.7±0.7
Linolenic acid (C18:3)	-	-	-	-	8.5±0.5	8.6±0.6	8.4±0.2	8.5±0.1	6.6±0.1	7.2±0.4	7.7±0.4	9.1±0.6
∑ C16	52.0±0.9	43.5±3.2	42.0±2.9	44.3±3.4	36.9±1.0	33.3±2.0	31.1±1.6	31.5±0.4	34.4±0.6	29.1±0.3	30.0±0.4	29.7±0.5
∑ C18	4.5±1.4	13.7±7.8	19.5±3.4	11.2±5.7	18.7±1.9	26.0±3.5	35.7±0.3	33.6±1.1	26.4±0.7	32.9±0.1	32.6±0.3	33.8±1.0
∑ C16 + C18	56.5±0.7	57.2±5.4	61.4±5.9	55.5±2.3	55.5±0.9	59.4±1.8	66.8±1.3	65.1±0.8	60.8±0.1	62.0±0.3	62.6±0.5	63.5±0.6
∑ SFA	95.5±1.4	86.3±7.8	80.5±3.4	88.8±5.7	54.1±2.2	45.3±4.3	36.2±0.6	35.8±0.8	43.9±1.6	33.3±0.3	34.5±0.7	32.7±1.2
∑ MUFA	-	-	-	-	6.2±0.3	7.7±1.6	12.0±1.4	11.5±0.5	11.1±0.2	11.2±0.1	8.6±0.4	8.2±0.1
∑ PUFA	4.5±1.4	13.7±7.8	19.5±3.4	11.2±5.7	13.7±2.1	20.8±2.1	27.5±1.1	26.8±0.9	20.8±0.7	27.6±0.1	29.2±0.3	30.8±1.1
Others	-	-	-	-	25.9±0.7	26.2±2.3	24.2±1.1	25.9±0.5	24.3±0.7	27.9±0.2	27.7±0.4	28.3±0.2

SFA, MUFA, and PUFA indicate saturated fatty acids, monounsaturated fatty acids, and polyunsaturated fatty acids, respectively. Other represented the components other than C12, C14, C16, and C18. The data are shown as the mean value of three independent biological replicates (n=3) ± the standard deviation.

Table 6 *The estimated properties of monoculture and co-cultures fatty acids-based biodiesel in comparison with the international standards over time.*

Biodiesel parameters	Units	Mono				PS				RS04				International standards	
		D7	D14	D21	D28	D7	D14	D21	D28	D7	D14	D21	D28	ASTM D6751	EN 14214
Cetane number (CN)	N/A	62.3	61.1	60.3	61.4	60.1	59.0	57.8	58.0	58.9	58.0	57.9	57.6	≥ 47	≥ 51
Iodine value (IV)	g I_2 100 g oil^{-1}	19.4	33.0	41.7	29.4	44.1	55.7	68.9	67.4	56.8	67.3	68.2	71.4	N/A	≤ 120
Average degree of unsaturation (ADU)	N/A	0.1	0.3	0.4	0.2	0.4	0.6	0.8	0.7	0.6	0.7	0.7	0.8	N/A	N/A
Oxidation stability (Y)	h	28.9	11.2	8.7	13.1	11.2	8.3	6.9	7.0	8.3	6.9	6.6	6.4	N/A	≥ 6
Kinematic viscosity (νi)	mm^2 s^{-1}	5.2	5.0	5.0	5.1	4.9	4.9	4.7	4.8	4.8	4.8	4.7	4.7	1.9-6.0	3.5-5.0
Specific gravity (ρ)	g m^{-3}	0.9	0.9	0.9	0.9	0.9	0.9	0.9	0.9	0.9	0.9	0.9	0.9	0.878	0.86-0.90
Cloud point (CP)	℃	19.7	19.1	18.7	19.2	18.6	18.1	17.5	17.5	18.0	17.5	17.5	17.3	N/A	>4
Long chain saturation factor (LCSF)	wt%	0.3	0.3	0.2	0.3	0.1	0.1	0.1	0.1	0.1	0.1	0.1	0.1	N/A	N/A
Cold filter plugging point (CFPP)	℃	-15.6	-15.7	-15.7	-15.6	-16.1	-16.2	-16.3	-16.3	-16.2	-16.3	-16.3	-16.3	N/A	≤ 5 or ≥ -20
Higher heating value (HHV)	MJ kg^{-1}	38.7	39.0	39.2	38.9	39.3	39.6	39.9	39.8	39.6	39.8	39.8	39.9	N/A	N/A

improved biodiesel applicability under colder climates. Associating with this, long chain saturation factor (LCSF) and cold filter plugging point (CFPP), are another biodiesel parameters to indicate the flow performance at low temperature, with lower value predicting a better flow performance. All the co-cultures demonstrated a lower value, showing that symbiotic bacteria could improve this specific biodiesel property. A high HHV (higher heating value) derived from all the groups has represent a higher power output delivery per unit of fuel, and the average value (~40 MH kg^{-1}) acquired in this study was in line with the previous recommendation [129, 154].

Although *C. sorokiniana* co-cultured with RS04 did not show significant improvements in biodiesel properties compared to the controls, all theoretical values still met international criteria and remained competitive with fossil fuels. Remarkably, RS04 group exhibited an exceptionally high algal growth rate and required minimal cultivation time to achieve high biomass and lipid productivity. The synergistic effects of the vitamin-overproducing bacteria primarily enhanced lipid yield without compromising cell viability, reflecting a high cultivation system stability in long-term.

4.4 Summary

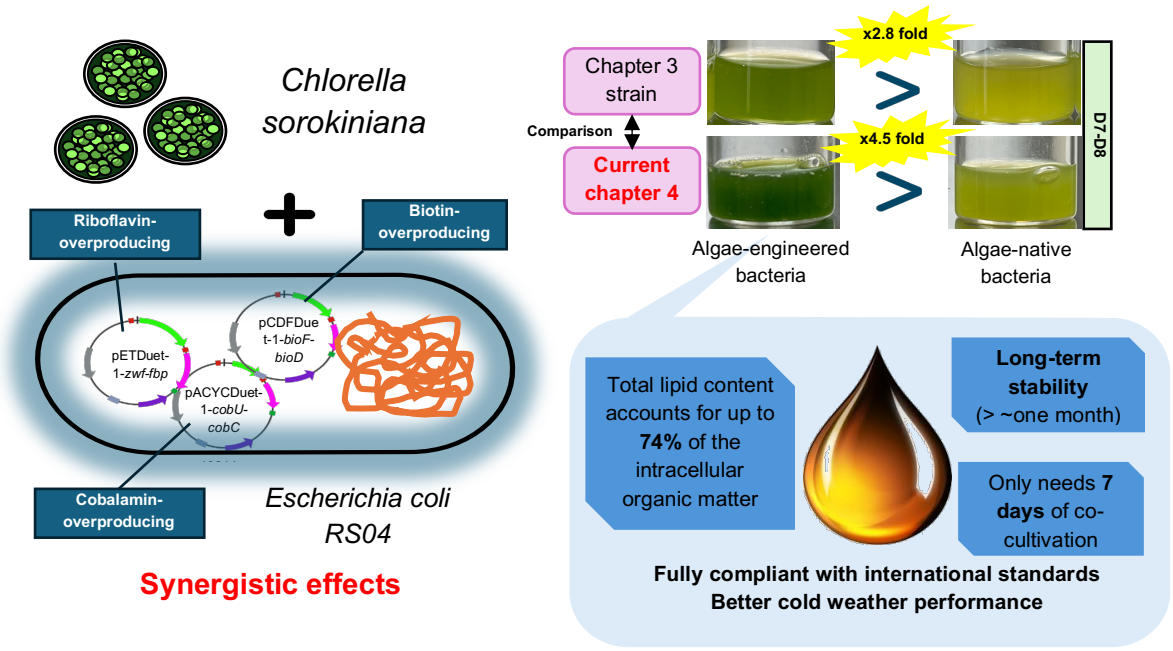

Figure 20 *Summary of Chapter 4.*

As summarized in **Figure 20**, RS04 harboring riboflavin, cobalamin, and biotin-related genes was found to remarkably enhance the *C. sorokiniana* growth by at least five times just within seven days, when compared to both Mono and PS control groups. The synergistic effects were encouraging when comparing the strain performance in **Chapter 4** to that of in **Chapter 3**, which involved only a single metabolite. The findings also suggest that co-cultures exhibited a prioritized vitamin assimilation pattern, with biotin being taken up early, followed by a sustained demand of cobalamin, while riboflavin was only required when needed at a later phase. From D14 onwards, all the culture groups appeared to experience environmental stress, as reflected by a rising trend in total lipid after a potential metabolic shift. Co-cultures yielded a huge variety of fatty acids, with C16-C18 more than 56%. However, further efforts are still necessary as RS04 did not significantly impact the biodiesel properties, although its extraordinarily high biomass and lipid productivity could potentially offset the limitation.

CHAPTER 5: Conclusion and Future Perspectives

5.1 Conclusion

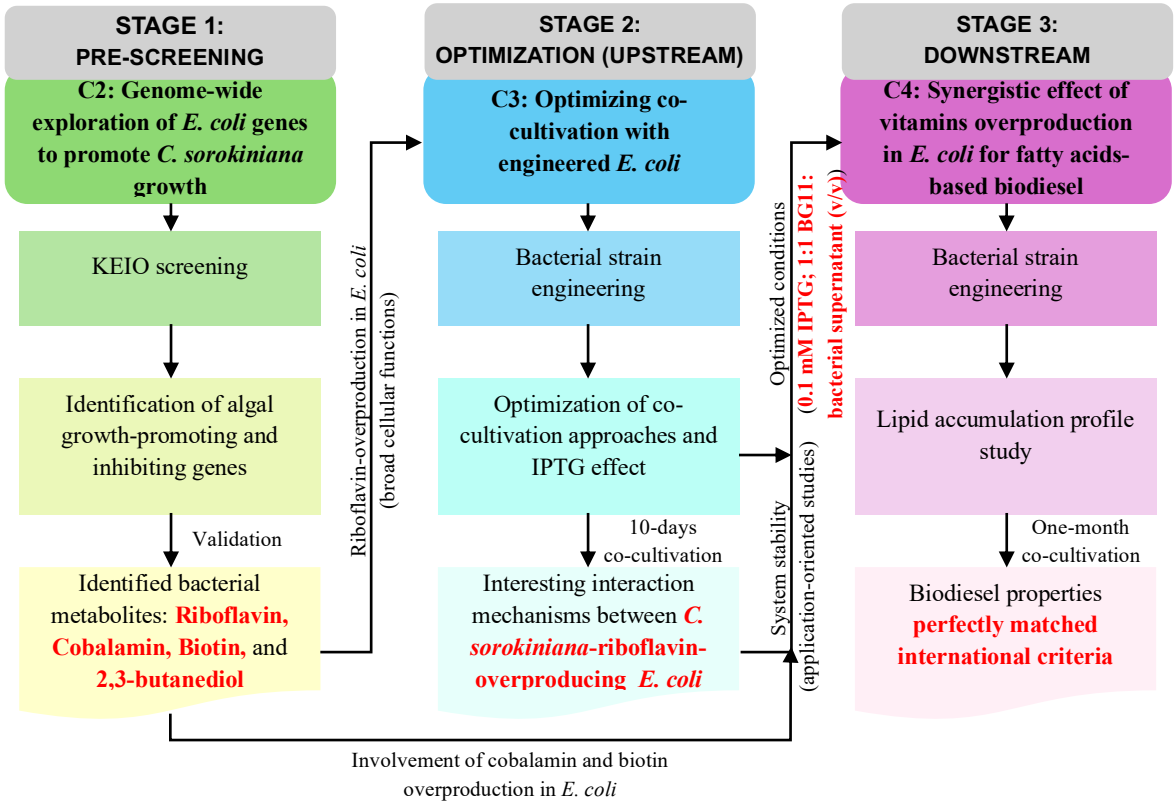

Figure 21 *Schematic flow of the entire study.*

As illustrated in **Figure 21**, three key experimental phases conclusively demonstrated that the metabolically engineered *E. coli* strain significantly promoted co-surviving algal growth, greatly outperforming conventional co-cultivation systems that rely solely on natural interactions and available nutrients. This novel co-cultivation system was shown to be relatively stable over four weeks and highly effective. It is crucial to stress that perceptions could be altered by shifting the focus from the host microalgae to the co-existing bacteria, which serves as an ideal partner over decades for creating the beneficial enzymes, cofactors and vitamins required for microalgae. Bacteria have a far simpler cellular structure than microalgae, and a wide spectrum of molecular

tools are accessible for in-depth research, hence facilitating the gene alterations or metabolism reconstruction.

5.2 Future perspectives

The findings acquired in the entire study have demonstrated that microalgal-engineered bacterial symbiotic systems are promising and have the potential for scaling up to larger applications. Nevertheless, some challenges of microalgal-engineered bacterial interactions studies must not be overlooked:

1) Bacteria remained inactive during the first two weeks, with gradual growth recovery thereafter. While this was intriguing, the mutualistic effect could not be claimed during that time;
2) Significant reduction in bacterial-to-microalgal ratio may not be able to sustain long-term co-cultivation when the bacterial population is playing a positive symbiotic role in promoting algal growth.
3) It is difficult to establish appropriate analysis methodologies that efficiently separates microalgae and bacteria from co-cultures, especially when certain downstream products require a pure separation to ensure product safety (nutraceuticals, food additives etc.);
4) Cellular physiology, intracellular product recovery or nutrient expenditure is often dynamics and unpredictable; and
5) Usage of high-cost IPTG at large scales is not practical.

Therefore, integration of robust microalgal and engineered bacterial cells must be obtained prior to scale-up applications to secure the economic and environmental feasibility. Co-culture monitoring and adjustment is always needed. If the bacterial activity is low for an extended period, a phased approach design could be adapted by introducing bacteria at different stages that align

with their growth cycle, allowing a better synchronization between bacterial and algal growth over time. A more stable bacterial population could be achieved if implementing closed or semi-closed cultivation systems. Next, efficient separation techniques, such as size-exclusion membranes filtration, density-based separation or advanced microfluidics could be explored to enhance cells separation in co-cultures. Refining genome-scale metabolic models through multi-omics integration (genomics, transcriptomics, and metabolomics) could improve the prediction of complicated metabolic interactions between microalgae and engineered bacteria. In addition, real-time physiological monitoring with AI-driven predictive models is possible to assist tracking cellular dynamics or even optimize nutrient utilization. Particularly, metabolically engineered cells must be stable and safe enough to allow their practical mutations to be integrated into larger scale set-ups. This is necessary so that the cells could withstand harsh operating conditions of industrial processes, which is different from the mild and well controlled laboratory conditions. To alternatively replace expensive chemical inducer, temperature, nutrient, pH, or light-inducible promoters could be utilized to allow the gene expression in engineered strain responsive to the culture environment.

References

[1] Medipally, S.R., F.M. Yusoff, S. Banerjee, and M. Shariff, Microalgae as Sustainable Renewable Energy Feedstock for Biofuel Production. *BioMed Research International*, 2015. **2015**: p. 519513.

[2] Ray, A., M. Nayak, and A. Ghosh, A review on co-culturing of microalgae: A greener strategy towards sustainable biofuels production. *Science of The Total Environment*, 2022. **802**: p. 149765.

[3] Kimbrel, J.A., T.J. Samo, C. Ward, D. Nilson, M.P. Thelen, A. Siccardi, P. Zimba, T.W. Lane, and X. Mayali, Host selection and stochastic effects influence bacterial community assembly on the microalgal phycosphere. *Algal Research*, 2019. **40**: p. 101489.

[4] Bell, W. and R. Mitchell, Chemotactic and growth responses of marine bacteria to algal extracellular products. *The Biological Bulletin*, 1972. **143**(**2**): p. 265-277.

[5] Azam, F. and F. Malfatti, Microbial structuring of marine ecosystems. *Nature Reviews Microbiology*, 2007. **5**(**10**): p. 782-791.

[6] Rawat, D., U. Sharma, P. Poria, A. Finlan, B. Parker, R.S. Sharma, and V. Mishra, Iron-dependent mutualism between *Chlorella sorokiniana* and *Ralstonia pickettii* forms the basis for a sustainable bioremediation system. *ISME Communications*, 2022. **2**(**1**): p. 83.

[7] Guo, Z. and Y.W. Tong, The interactions between *Chlorella vulgaris* and algal symbiotic bacteria under photoautotrophic and photoheterotrophic conditions. *Journal of Applied Phycology*, 2014. **26**(**3**): p. 1483-1492.

[8] Tong, C.Y., K. Honda, and C.J.C. Derek, A review on microalgal-bacterial co-culture: The multifaceted role of beneficial bacteria towards enhancement of microalgal metabolite production. *Environmental Research*, 2023. **228**: p. 115872.

[9] Singh, S.K., S. Sundaram, S. Sinha, M.A. Rahman, and S. Kapur, Recent advances in CO_2 uptake and fixation mechanism of cyanobacteria and microalgae. *Critical Reviews in Environmental Science and Technology*, 2016. **46**(**16**): p. 1297-1323.

[10] Goswami, G., B.B. Makut, and D. Das, Sustainable production of bio-crude oil via hydrothermal liquefaction of symbiotically grown biomass of microalgae-bacteria coupled with effective wastewater treatment. *Scientific Reports*, 2019. **9**(**1**): p. 15016.

[11] Shen, Y., J. Gao, and L. Li, Municipal wastewater treatment via co-immobilized microalgal-bacterial symbiosis: Microorganism growth and nutrients removal. *Bioresource Technology*, 2017. **243**: p. 905-913.

[12] Nagarajan, D., D.-J. Lee, S. Varjani, S.S. Lam, S.I. Allakhverdiev, and J.-S. Chang, Microalgae-based wastewater treatment – Microalgae-bacteria consortia, multi-omics approaches and algal stress response. *Science of The Total Environment*, 2022. **845**: p. 157110.

[13] Zhang, H., W. Gong, L. Bai, R. Chen, W. Zeng, Z. Yan, G. Li, and H. Liang, Aeration-induced CO_2 stripping, instead of high dissolved oxygen, have a negative impact on algae–bacteria symbiosis (ABS) system stability and wastewater treatment efficiency. *Chemical Engineering Journal*, 2020. **382**: p. 122957.

[14] Rubio, V., R. Bustos, M.L. Irigoyen, X. Cardona-López, M. Rojas-Triana, and J. Paz-Ares, Plant hormones and nutrient signaling. *Plant Mol Biol*, 2009. **69**(**4**): p. 361-73.

[15] Stirk, W.A. and J. van Staden, Potential of phytohormones as a strategy to improve microalgae productivity for biotechnological applications. *Biotechnology Advances*, 2020. **44**: p. 107612.
[16] Amin, S.A., L.R. Hmelo, H.M. van Tol, B.P. Durham, L.T. Carlson, K.R. Heal, R.L. Morales, C.T. Berthiaume, M.S. Parker, B. Djunaedi, A.E. Ingalls, M.R. Parsek, M.A. Moran, and E.V. Armbrust, Interaction and signalling between a cosmopolitan phytoplankton and associated bacteria. *Nature*, 2015. **522**(**7554**): p. 98-101.
[17] Dao, G.-H., G.-X. Wu, X.-X. Wang, T.-Y. Zhang, X.-M. Zhan, and H.-Y. Hu, Enhanced microalgae growth through stimulated secretion of indole acetic acid by symbiotic bacteria. *Algal Research*, 2018. **33**: p. 345-351.
[18] Samo, T.J., J.A. Kimbrel, D.J. Nilson, J. Pett-Ridge, P.K. Weber, and X. Mayali, Attachment between heterotrophic bacteria and microalgae influences symbiotic microscale interactions. *Environmental Microbiology*, 2018. **20**(**12**): p. 4385-4400.
[19] Sial, A., B. Zhang, A. Zhang, K. Liu, S.A. Imtiaz, and N. Yashir, Microalgal–bacterial synergistic interactions and their potential influence in wastewater treatment: A review. *BioEnergy Research*, 2021. **14**(**3**): p. 723-738.
[20] Aburai, N., T. Tsukagoshi, S. Sekiguchi, H. Arakawa, Y. Imamura, and K. Abe, Mutual supply of carbon and nitrogen sources in the co-culture of aerial microalgae and nitrogen-fixing bacteria. *Algal Research*, 2021. **70**: p. 103001.
[21] Zhang, Z., S. Nair, L. Tang, H. Zhao, Z. Hu, M. Chen, Y. Zhang, S.-J. Kao, N. Jiao, and Y. Zhang, Long-term survival of *Synechococcus* and heterotrophic bacteria without external nutrient supply after changes in their relationship from antagonism to mutualism. *mBio*, 2021. **12**(**4**): p. e01614-21.
[22] Jiang, L., L. Yang, L. Xiao, X. Shi, G. Gao, and B. Qin, Quantitative studies on phosphorus transference occuring between *Microcystis aeruginosa* and its attached bacterium (*Pseudomonas* sp.), in Eutrophication of Shallow Lakes with Special Reference to Lake Taihu, China, B. Qin, Z. Liu, and K. Havens, Editors. 2007, Springer Netherlands: Dordrecht. p. 161-165.
[23] Zhang, B., W. Li, Y. Guo, Z. Zhang, W. Shi, F. Cui, P.N.L. Lens, and J.H. Tay, Microalgal-bacterial consortia: From interspecies interactions to biotechnological applications. *Renewable and Sustainable Energy Reviews*, 2020. **118**: p. 109563.
[24] Stock, W., L. Blommaert, M. De Troch, S. Mangelinckx, A. Willems, W. Vyverman, and K. Sabbe, Host specificity in diatom–bacteria interactions alleviates antagonistic effects. *FEMS Microbiology Ecology*, 2019. **95**(**11**).
[25] Hoeger, A.-L., N. Jehmlich, L. Kipping, C. Griehl, and M. Noll, Associated bacterial microbiome responds opportunistic once algal host *Scenedesmus vacuolatus* is attacked by endoparasite *Amoeboaphelidium protococcarum*. *Scientific Reports*, 2022. **12**(**1**): p. 13187.
[26] Bauer, N., H.-P. Grossart, and S. Hilt, Effects of bacterial communities on the sensitivity of *Stephanodiscus minutulus* and *Desmodesmus armatus* to tannic acid. *Aquatic Microbial Ecology*, 2010. **59**: p. 295-306.
[27] Fouilland, E., A. Galès, I. Beaugelin, E. Lanouguère, O. Pringault, and C. Leboulanger, Influence of bacteria on the response of microalgae to contaminant mixtures. *Chemosphere*, 2018. **211**: p. 449-455.

[28] Wirth, R., B. Pap, T. Böjti, P. Shetty, G. Lakatos, Z. Bagi, K.L. Kovács, and G. Maróti, *Chlorella vulgaris* and its phycosphere in wastewater: Microalgae-bacteria interactions during nutrient removal. *Frontiers in Bioengineering and Biotechnology*, 2020. **8**.
[29] Wang, H., L. Lu, D. Liu, F. Cui, and P. Wang, Characteristic changes in algal organic matter derived from *Microcystis aeruginosa* in microbial fuel cells. *Bioresource Technology*, 2015. **195**: p. 25-30.
[30] Wang, M., S.-C. Zhang, Q. Tang, L.-D. Shi, X.-M. Tao, and G.-M. Tian, Organic degrading bacteria and nitrifying bacteria stimulate the nutrient removal and biomass accumulation in microalgae-based system from piggery digestate. *Science of The Total Environment*, 2020. **707**: p. 134442.
[31] Li, D., R. Liu, X. Cui, M. He, S. Zheng, W. Du, M. Gao, and C. Wang, Co-culture of bacteria and microalgae for treatment of high concentration biogas slurry. *Journal of Water Process Engineering*, 2021. **41**: p. 102014.
[32] Dow, L., How do quorum-sensing signals mediate algae–bacteria interactions? *Microorganisms*, 2021. **9**(**7**): p. 1391.
[33] Stock, F., G. Bilcke, S. De Decker, C.M. Osuna-Cruz, K. Van den Berge, E. Vancaester, L. De Veylder, K. Vandepoele, S. Mangelinckx, and W. Vyverman, Distinctive growth and transcriptional changes of the diatom *Seminavis robusta* in response to quorum sensing related compounds. *Frontiers in Microbiology*, 2020. **11**.
[34] Palacios, O.A., B.R. López, and L.E. de-Bashan, Microalga growth-promoting bacteria (MGPB): A formal term proposed for beneficial bacteria involved in microalgal–bacterial interactions. *Algal Research*, 2022. **61**: p. 102585.
[35] Zhang, C., X. Chen, M. Han, X. Li, H. Chang, N. Ren, and S.-H. Ho, Revealing the role of microalgae-bacteria niche for boosting wastewater treatment and energy reclamation in response to temperature. *Environmental Science and Ecotechnology*, 2023. **14**: p. 100230.
[36] Perales-Pérez, Á., M.D. Macías-Sánchez, J. Ruiz, J.A. Perales, and C. Garrido-Pérez, Process for nutrient recycling from intensive aquaculture through microalgae-bacteria consortium. *Science of The Total Environment*, 2023. **901**: p. 165848.
[37] Wang, H., D. Laughinghouse Haywood, A. Anderson Matthew, F. Chen, E. Willliams, R. Place Allen, O. Zmora, Y. Zohar, T. Zheng, and T. Hill Russell, Novel Bacterial Isolate from Permian Groundwater, Capable of Aggregating Potential Biofuel-Producing Microalga Nannochloropsis oceanica IMET1. *Applied and Environmental Microbiology*, 2012. **78**(**5**): p. 1445-1453.
[38] Higgins, B.T., I. Gennity, S. Samra, T. Kind, O. Fiehn, and J.S. VanderGheynst, Cofactor symbiosis for enhanced algal growth, biofuel production, and wastewater treatment. *Algal Research*, 2016. **17**: p. 308-315.
[39] Peng, H., L.E. de- Bashan, and B.T. Higgins, Comparison of algae growth and symbiotic mechanisms in the presence of plant growth promoting bacteria and non-plant growth promoting bacteria. *Algal Research*, 2021. **53**: p. 102156.
[40] Kim, D.H., H.S. Yun, Y.S. Kim, and J.G. Kim, Effects of co-culture on improved productivity and bioresource for microalgal biomass using the floc-forming bacteria *Melaminivora Jejuensis*. *Front Bioeng Biotechnol*, 2020. **8**: p. 588210.
[41] Liu, X.-Y., Y. Hong, Q.-Y. Zhai, G.-P. Zhao, H.-K. Zhang, and Q. Wang, Performance and mechanism of *Chlorella* in swine wastewater treatment: Roles of nitrogen-phosphorus ratio adjustment and indigenous bacteria. *Bioresource Technology*, 2022. **358**: p. 127402.

[42] Akao, P.K., B. Singh, P. Kaur, A. Sor, A. Avni, A. Dhir, S. Verma, S. Kapoor, U.G. Phutela, S. Satpute, S. Sharma, D. Avisar, K.S. Sandha, and H. Mamane, Coupled microalgal–bacterial biofilm for enhanced wastewater treatment without energy investment. *Journal of Water Process Engineering*, 2021. **41**: p. 102029.

[43] Rajapitamahuni, S., P. Bachani, R.K. Sardar, and S. Mishra, Co-cultivation of siderophore-producing bacteria *Idiomarina loihiensis* RS14 with *Chlorella variabilis* ATCC 12198, evaluation of micro-algal growth, lipid, and protein content under iron starvation. *Journal of Applied Phycology*, 2019. **31**(**1**): p. 29-39.

[44] Martin, N., T. Bernat, J. Dinasquet, A. Stofko, A. Damon, D.D. Deheyn, F. Azam, J.E. Smith, M.P. Davey, A.G. Smith, S. Vignolini, and D. Wangpraseurt, Synthetic algal-bacteria consortia for space-efficient microalgal growth in a simple hydrogel system. *Journal of Applied Phycology*, 2021. **33**(**5**): p. 2805-2815.

[45] Wang, R., S. Xue, D. Zhang, Q. Zhang, S. Wen, D. Kong, C. Yan, and W. Cong, Construction and characteristics of artificial consortia of *Scenedesmus obliquus*-bacteria for *S. obliquus* growth and lipid production. *Algal Research*, 2015. **12**: p. 436-445.

[46] Stavridou, E., L. Karapetsi, G.M. Nteve, G. Tsintzou, M. Chatzikonstantinou, M. Tsaousi, A. Martinez, P. Flores, M. Merino, L. Dobrovic, J.L. Mullor, S. Martens, L. Cerasino, N. Salmaso, M. Osathanunkul, N.E. Labrou, and P. Madesis, Landscape of microalgae omics and metabolic engineering research for strain improvement: An overview. *Aquaculture*, 2024. **587**: p. 740803.

[47] Torres-Tiji, Y., F.J. Fields, and S.P. Mayfield, Microalgae as a future food source. *Biotechnology Advances*, 2020. **41**: p. 107536.

[48] Pontrelli, S., T.-Y. Chiu, E.I. Lan, F.Y.H. Chen, P. Chang, and J.C. Liao, *Escherichia coli* as a host for metabolic engineering. *Metabolic Engineering*, 2018. **50**: p. 16-46.

[49] Wu, H., J. Yang, P. Shen, Q. Li, W. Wu, X. Jiang, L. Qin, J. Huang, X. Cao, and F. Qi, High-level production of indole-3-acetic acid in the metabolically engineered *Escherichia coli*. *Journal of Agricultural and Food Chemistry*, 2021. **69**(**6**): p. 1916-1924.

[50] Bali, A.P., D. Lennox-Hvenekilde, N. Myling-Petersen, J. Buerger, B. Salomonsen, L.S. Gronenberg, M.O.A. Sommer, and H.J. Genee, Improved biotin, thiamine, and lipoic acid biosynthesis by engineering the global regulator IscR. *Metabolic Engineering*, 2020. **60**: p. 97-109.

[51] Fang, H., D. Li, J. Kang, P. Jiang, J. Sun, and D. Zhang, Metabolic engineering of *Escherichia coli* for de novo biosynthesis of vitamin B12. *Nature Communications*, 2018. **9**(**1**): p. 4917.

[52] Aamer Mehmood, M., A. Shahid, S. Malik, N. Wang, M. Rizwan Javed, M. Nabeel Haider, P. Verma, M. Umer Farooq Ashraf, N. Habib, A. Syafiuddin, and R. Boopathy, Advances in developing metabolically engineered microbial platforms to produce fourth-generation biofuels and high-value biochemicals. *Bioresource Technology*, 2021. **337**: p. 125510.

[53] Xu, L., L. Wang, X.-R. Zhou, W.-C. Chen, S. Singh, Z. Hu, F.-H. Huang, and X. Wan, Stepwise metabolic engineering of *Escherichia coli* to produce triacylglycerol rich in medium-chain fatty acids. *Biotechnology for Biofuels*, 2018. **11**(**1**): p. 177.

[54] Kim, H.M., T.U. Chae, S.Y. Choi, W.J. Kim, and S.Y. Lee, Engineering of an oleaginous bacterium for the production of fatty acids and fuels. *Nature Chemical Biology*, 2019. **15**(**7**): p. 721-729.

[55] Xiong, X., X. Wang, and S. Chen, Engineering of an L-arabinose metabolic pathway in Rhodococcus jostii RHA1 for biofuel production. *Journal of Industrial Microbiology and Biotechnology*, 2016. **43**(**7**): p. 1017-1025.
[56] Tan, P.Y., Y. Kato, and M. Konishi, A Novel Strain of the Cyanobacterial Growth-promoting Bacterium, Rhodococcus sp. AF2108, Enhances the Growth of Synechococcus elongatus. *Microbes and Environments*, 2024. **39**(**4**).
[57] Tong, C.Y., K. Honda, and C.J.C. Derek, Enhanced microalgal growth and metabolites through co-cultivation with *Escherichia coli* in algal organic matter solution. *Algal Research*, 2024. **77**: p. 103351.
[58] Liu, B., E.E. Eltanahy, H. Liu, E.T. Chua, S.R. Thomas-Hall, T.J. Wass, K. Pan, and P.M. Schenk, Growth-promoting bacteria double eicosapentaenoic acid yield in microalgae. *Bioresource Technology*, 2020. **316**: p. 123916.
[59] Qi, W., S. Mei, Y. Yuan, X. Li, T. Tang, Q. Zhao, M. Wu, W. Wei, and Y. Sun, Enhancing fermentation wastewater treatment by co-culture of microalgae with volatile fatty acid- and alcohol-degrading bacteria. *Algal Research*, 2018. **31**: p. 31-39.
[60] Wei, Z., H. Wang, X. Li, Q. Zhao, Y. Yin, L. Xi, B. Ge, and S. Qin, Enhanced biomass and lipid production by co-cultivation of Chlorella vulgaris with Mesorhizobium sangaii under nitrogen limitation. *Journal of Applied Phycology*, 2020. **32**(**1**): p. 233-242.
[61] Kong, W., J. Kong, H. Lyu, J. Ma, Z. Wang, Z. Zhang, S. Feng, and B. Shen, Application of indole-3-acetic acid in microalgae cultivation to improve the feasibility of simultaneously purifying wastewater, fixing CO_2 and producing fatty acids under Hg stress. *Journal of Cleaner Production*, 2022. **358**: p. 132028.
[62] Oyama, T., Y. Kato, K. Satoh, Y. Oono, M. Matsuda, T. Hasunuma, and A. Kondo, Development of mutant microalgae that accumulate lipids under nitrate-replete conditions. *Algal Research*, 2021. **60**: p. 102544.
[63] Sreenikethanam, A., S. Raj, R.B. J, P. Gugulothu, and A.K. Bajhaiya, Genetic engineering of microalgae for secondary metabolite production: Recent developments, challenges, and future prospects. *Front Bioeng Biotechnol*, 2022. **10**: p. 836056.
[64] Heo, J., S. Kim, D.-H. Cho, G.C. Song, H.-S. Kim, and C.-M. Ryu, Genome-wide exploration of *Escherichia coli* genes to promote *Chlorella vulgaris* growth. *Algal Research*, 2019. **38**: p. 101390.
[65] Chen, H., S. Venkat, J. Wilson, P. McGuire, A.L. Chang, Q. Gan, and C. Fan, Genome-Wide Quantification of the Effect of Gene Overexpression on Escherichia coli Growth. *Genes (Basel)*, 2018. **9**(**8**).
[66] Heo, J., K. Cho, U. Kim, D.-H. Cho, S. Ko, Q.-G. Tran, Y.J. Lee, C.-M. Ryu, and H.-S. Kim, Genome-wide high-throughput screening of interactive bacterial metabolite in the algal population using *Escherichia coli* K-12 Keio collection. *Scientific Reports*, 2020. **10**(**1**): p. 10647.
[67] Piasecka, A. and A. Baier, Metabolic and proteomic analysis of *Chlorella sorokiniana*, *Chloroidium saccharofilum*, and *Chlorella vulgaris* cells cultured in autotrophic, photoheterotrophic, and mixotrophic cultivation modes. *Molecules*, 2022. **27**(**15**): p. 4817.
[68] Asadi, P., H.A. Rad, and F. Qaderi, Lipid and biodiesel production by cultivation isolated strain *Chlorella sorokiniana* pa.91 and *Chlorella vulgaris* in dairy wastewater treatment plant effluents. *Journal of Environmental Health Science and Engineering*, 2020. **18**(**2**): p. 573-585.

[69] Yun, H.S., Y.S. Kim, and H.S. Yoon, Characterization of *Chlorella sorokiniana* and *Chlorella vulgaris* fatty acid components under a wide range of light intensity and growth temperature for their use as biological resources. *Heliyon*, 2020. **6**(**7**): p. e04447.
[70] Barrick, J. Keio and ASKA collections. 2014 2014-05-30; Available from: https://barricklab.org/twiki/bin/view/Lab/ReferenceKeioASKACollection.
[71] Liu, S., W. Hu, Z. Wang, and T. Chen, Rational engineering of *Escherichia coli* for high-level production of riboflavin. *Journal of Agricultural and Food Chemistry*, 2021. **69**(**41**): p. 12241-12249.
[72] Fu, B., J. Ying, Q. Chen, Q. Zhang, J. Lu, Z. Zhu, and P. Yu, Enhancing the biosynthesis of riboflavin in the recombinant *Escherichia coli* BL21 strain by metabolic engineering. *Front Microbiol*, 2022. **13**: p. 1111790.
[73] Lin, Z., Z. Xu, Y. Li, Z. Wang, T. Chen, and X. Zhao, Metabolic engineering of *Escherichia coli* for the production of riboflavin. *Microbial Cell Factories*, 2014. **13**(**1**): p. 104.
[74] Erian, A.M., M. Gibisch, and S. Pflügl, Engineered *E. coli W* enables efficient 2,3-butanediol production from glucose and sugar beet molasses using defined minimal medium as economic basis. *Microbial Cell Factories*, 2018. **17**(**1**): p. 190.
[75] Ghadermazi, P., A. Re, L. Ricci, and S.H.J. Chan, Metabolic engineering interventions for sustainable 2,3-butanediol production in gas-fermenting *Clostridium autoethanogenum*. *mSystems*, 2022. **7**(**2**): p. e0111121.
[76] Nielsen, D.R., S.H. Yoon, C.J. Yuan, and K.L. Prather, Metabolic engineering of acetoin and meso-2, 3-butanediol biosynthesis in *E. coli*. *Biotechnol J*, 2010. **5**(**3**): p. 274-84.
[77] Delli-Bovi, T.A., M.D. Spalding, and S.T. Prigge, Overexpression of biotin synthase and biotin ligase is required for efficient generation of sulfur-35 labeled biotin in *E. coli*. *BMC Biotechnology*, 2010. **10**(**1**): p. 73.
[78] Lévy-Schil, S., L. Debussche, S. Rigault, F. Soubrier, F. Bacchetta, D. Lagneaux, J. Schleuniger, F. Blanche, J. Crouzet, and J.-F. Mayaux, Biotin biosynthetic pathway in recombinant strains of *Escherichia coli* overexpressing bio genes: evidence for a limiting step upstream from KAPA. *Applied Microbiology and Biotechnology*, 1993. **38**(**6**): p. 755-762.
[79] McKinlay, J.B., Are bacteria leaky? Mechanisms of metabolite externalization in bacterial cross-feeding. *Annu Rev Microbiol*, 2023. **77**: p. 277-297.
[80] Blifernez-Klassen, O., V. Klassen, D. Wibberg, E. Cebeci, C. Henke, C. Rückert-Reed, S. Chaudhari, O. Rupp, J. Blom, A. Winkler, A. Al-Dilaimi, A. Goesmann, A. Sczyrba, J. Kalinowski, A. Bräutigam, and O. Kruse, Phytoplankton consortia as a blueprint for mutually beneficial eukaryote-bacteria ecosystems based on the biocoenosis of Botryococcus consortia. *Scientific Reports*, 2021. **11**: p. 1726.
[81] Shaima, A.F., N.H. Mohd Yasin, N. Ibrahim, M.S. Takriff, D. Gunasekaran, and M.Y.Y. Ismaeel, Unveiling antimicrobial activity of microalgae *Chlorella sorokiniana* (UKM2), *Chlorella* sp. (UKM8) and *Scenedesmus* sp. (UKM9). *Saudi Journal of Biological Sciences*, 2022. **29**(**2**): p. 1043-1052.
[82] Lawrence, J.G. and J.R. Roth, The cobalamin (coenzyme B12) biosynthetic genes of *Escherichia coli*. *J Bacteriol*, 1995. **177**(**22**): p. 6371-80.
[83] Halina Y. Neujahr, L.F., On the occurrence of light-sensitive corrinoids in axenic cultures of unicellular algae. *Acta Chemica Scandinavica*, 1966. **20**: p. 347-360.

[84] Higgins, B.T., I. Gennity, P.S. Fitzgerald, S.J. Ceballos, O. Fiehn, and J.S. VanderGheynst, Algal–bacterial synergy in treatment of winery wastewater. *npj Clean Water*, 2018. **1**(**1**): p. 6.
[85] Fowler, C.C., E.D. Brown, and Y. Li, Using a riboswitch sensor to examine coenzyme B12 metabolism and transport in *E. coli*. *Chemistry & Biology*, 2010. **17**(**7**): p. 756-765.
[86] Papadopoulos, K.P., M.F. de Souza, L. Archer, A.C.Z. Illanes, E.L. Harrison, F. Taylor, M.P. Davey, D.A. Gallardo, A.J. Komakech, S. Radmehr, A. Holzer, E. Meers, A.G. Smith, and P. Mehrshahi, Vitamin B12 bioaccumulation in *Chlorella vulgaris* grown on food waste-derived anaerobic digestate. *Algal Research*, 2023. **75**: p. 103290.
[87] Ji, X., X. Luo, J. Zhang, and D. Huang, Effects of exogenous vitamin B12 on nutrient removal and protein expression of algal-bacterial consortium. *Environmental Science and Pollution Research*, 2021. **28**(**13**): p. 15954-15965.
[88] Piffeteau, A. and M. Gaudry, Biotin uptake: influx, efflux and countertransport in *Escherichia coli* K12. *Biochimica et Biophysica Acta (BBA) - Biomembranes*, 1985. **816**(**1**): p. 77-82.
[89] Magdouli, S., T. Guedri, T. Rouissi, S.K. Brar, and J.-F. Blais, Sync between leucine, biotin and citric acid to improve lipid production by *Yarrowia lipolytica* on crude glycerol-based media. *Biomass and Bioenergy*, 2020. **142**: p. 105764.
[90] Amavizca, E., Y. Bashan, C.-M. Ryu, M.A. Farag, B.M. Bebout, and L.E. de-Bashan, Enhanced performance of the microalga *Chlorella sorokiniana* remotely induced by the plant growth-promoting bacteria *Azospirillum brasilense* and *Bacillus pumilus*. *Scientific Reports*, 2017. **7**(**1**): p. 41310.
[91] Nef, C., S. Dittami, R. Kaas, E. Briand, C. Noël, F. Mairet, and M. Garnier, Sharing vitamin B(12) between bacteria and microalgae does not systematically occur: Case study of the haptophyte *Tisochrysis lutea*. *Microorganisms*, 2022. **10**(**7**): p. 1337.
[92] Cooper, M. and A. Smith, Exploring mutualistic interactions between microalgae and bacteria in the omics age. *Current opinion in plant biology*, 2015. **26**: p. 147-153.
[93] Croft Martin, T., J. Warren Martin, and G. Smith Alison, Algae need their vitamins. *Eukaryotic Cell*, 2006. **5**(**8**): p. 1175-1183.
[94] Seymour, J.R., S.A. Amin, J.-B. Raina, and R. Stocker, Zooming in on the phycosphere: the ecological interface for phytoplankton–bacteria relationships. *Nature Microbiology*, 2017. **2**(**7**): p. 17065.
[95] Madhubalaji, C.K., S. Ravi, and S.N. Mudliar, Unraveling of *Chlorella*-associated bacterial load, diversity, and their imputed functions at high- and low-yield conditions through metagenome sequencing. *J Phycol*, 2022. **58**(**1**): p. 133-145.
[96] Lopez, B.R., O.A. Palacios, Y. Bashan, F.E. Hernández-Sandoval, and L.E. de-Bashan, Riboflavin and lumichrome exuded by the bacterium *Azospirillum brasilense* promote growth and changes in metabolites in *Chlorella sorokiniana* under autotrophic conditions. *Algal Research*, 2019. **44**: p. 101696.
[97] Palacios, O.A., Y. Bashan, and L.E. de-Bashan, Proven and potential involvement of vitamins in interactions of plants with plant growth-promoting bacteria—an overview. *Biology and Fertility of Soils*, 2014. **50**(**3**): p. 415-432.
[98] Chai, S., J. Shi, T. Huang, Y. Guo, J. Wei, M. Guo, L. Li, S. Dou, L. Liu, and G. Liu, Characterization of *Chlorella sorokiniana* growth properties in monosaccharide-supplemented batch culture. *PLOS ONE*, 2018. **13**(**7**): p. e0199873.

[99] Dubois, M., K.A. Gilles, J.K. Hamilton, P.A. Rebers, and F. Smith, Calorimetric method for determination of sugars and related substances. *Analytical Chemistry*, 1956. **28**: p. 350-356.
[100] Park, J., H.J. Jeong, E.Y. Yoon, and S.J. Moon, Easy and rapid quantification of lipid contents of marine dinoflagellates using the sulpho-phospho-vanillin method. *Algae*, 2016. **31**(**4**): p. 391-401.
[101] Langer, S., M. Hashimoto, B. Hobl, T. Mathes, and M. Mack, Flavoproteins are potential targets for the antibiotic roseoflavin in *Escherichia coli*. *Journal of bacteriology*, 2013. **195**(**18**): p. 4037-4045.
[102] Averianova, L.A., L.A. Balabanova, O.M. Son, A.B. Podvolotskaya, and L.A. Tekutyeva, Production of vitamin B2 (riboflavin) by microorganisms: An overview. *Frontiers in Bioengineering and Biotechnology*, 2020. **8**: p. 570828.
[103] Palacios, O.A., B.R. López, A. Palacios-Espinosa, F.E. Hernández-Sandoval, and L.E. de-Bashan, The immediate effect of riboflavin and lumichrome on the mitigation of saline stress in the microalga *Chlorella sorokiniana* by the plant-growth-promoting bacterium *Azospirillum brasilense*. *Algal Research*, 2021. **58**: p. 102424.
[104] Huang, R., H.J. Kim, and D.B. Min, Photosensitizing effect of riboflavin, lumiflavin, and lumichrome on the generation of volatiles in soy milk. *Journal of Agricultural and Food Chemistry*, 2006. **54**(**6**): p. 2359-2364.
[105] Sauvage, J., G.H. Wikfors, M.S. Dixon, D. Kapareiko, K. Sabbe, X. Li, and A. Joyce, Bacterial exudates as growth-promoting agents for the cultivation of commercially relevant marine microalgal strains. *Journal of the World Aquaculture Society*, 2022. **53**(**6**): p. 1101-1119.
[106] Bišová, K. and V. Zachleder, Cell-cycle regulation in green algae dividing by multiple fission. *Journal of Experimental Botany*, 2014. **65**(**10**): p. 2585-2602.
[107] Larentis, A.L., J.F. Nicolau, S. Esteves Gdos, D.T. Vareschini, F.V. de Almeida, M.G. dos Reis, R. Galler, and M.A. Medeiros, Evaluation of pre-induction temperature, cell growth at induction and IPTG concentration on the expression of a leptospiral protein in *E. coli* using shaking flasks and microbioreactor. *BMC Res Notes*, 2014. **7**: p. 671.
[108] Gomes, L., G. Monteiro, and F. Mergulhão, The impact of IPTG induction on plasmid stability and heterologous protein expression by *Escherichia coli* biofilms. *Int. J. Mol. Sci.*, 2020. **21**(**2**): p. 576.
[109] Kitajima, K. and K.P. Hogan, Increases of chlorophyll a/b ratios during acclimation of tropical woody seedlings to nitrogen limitation and high light. *Plant Cell Environ*, 2003. **26**(**6**): p. 857-865.
[110] da Silva Ferreira, V. and C. Sant'Anna, Impact of culture conditions on the chlorophyll content of microalgae for biotechnological applications. *World Journal of Microbiology and Biotechnology*, 2016. **33**(**1**): p. 20.
[111] Zhu, S., L. Qin, P. Feng, C. Shang, Z. Wang, and Z. Yuan, Treatment of low C/N ratio wastewater and biomass production using co-culture of *Chlorella vulgaris* and activated sludge in a batch photobioreactor. *Bioresource Technology*, 2019. **274**: p. 313-320.
[112] Negi, S., Z. Perrine, N. Friedland, A. Kumar, R. Tokutsu, J. Minagawa, H. Berg, A.N. Barry, G. Govindjee, and R. Sayre, Light regulation of light-harvesting antenna size substantially enhances photosynthetic efficiency and biomass yield in green algae. *The Plant Journal*, 2020. **103**(**2**): p. 584-603.

[113] Meagher, E., P. Rangsrikitphoti, B. Faridi, G. Zamzam, and D.G. Durnford, Photoacclimation to high-light stress in *Chlamydomonas reinhardtii* during conditional senescence relies on generating pH-dependent, high-quenching centres. *Plant Physiology and Biochemistry*, 2021. **158**: p. 136-145.
[114] Guan, N., J. Li, G. Du, J. Chen, and L. Liu, Microbial production of nutraceuticals: Challenges and prospects, in Systems and Synthetic Biotechnology for Production of Nutraceuticals, L. Liu and J. Chen, Editors. 2019, Springer Singapore: Singapore. p. 203-208.
[115] Stra, A., L.O. Almarwaey, Y. Alagoz, J.C. Moreno, and S. Al-Babili, Carotenoid metabolism: New insights and synthetic approaches. *Front Plant Sci*, 2022. **13**: p. 1072061.
[116] Hamouda, R.A., A. Abd El Latif, E.M. Elkaw, A.S. Alotaibi, A.M. Alenzi, and H.A. Hamza, Assessment of antioxidant and anticancer activities of microgreen alga *Chlorella vulgaris* and its blend with different vitamins. *Molecules*, 2022. **27**(**5**): p. 1602.
[117] Gifuni, I., G. Olivieri, A. Pollio, and A. Marzocchella, Identification of an industrial microalgal strain for starch production in biorefinery context: The effect of nitrogen and carbon concentration on starch accumulation. *New Biotechnology*, 2018. **41**: p. 46-54.
[118] Flemming, H.-C., E.D. van Hullebusch, T.R. Neu, P.H. Nielsen, T. Seviour, P. Stoodley, J. Wingender, and S. Wuertz, The biofilm matrix: multitasking in a shared space. *Nature Reviews Microbiology*, 2023. **21**(**2**): p. 70-86.
[119] Zhang, Y., H. Wu, C. Yuan, T. Li, and A. Li, Growth, biochemical composition, and photosynthetic performance of *Scenedesmus acuminatus* during nitrogen starvation and resupply. *Journal of Applied Phycology*, 2019. **31**(**5**): p. 2797-2809.
[120] Fu, B., M. Chen, X. Bao, J. Lu, Z. Zhu, F. Guan, C. Yan, P. Wang, L. Fu, and P. Yu, Site-directed mutagenesis of bifunctional riboflavin kinase/FMN adenylyltransferase via CRISPR/Cas9 to enhance riboflavin production. *Synthetic and Systems Biotechnology*, 2024. **9**(**3**): p. 503-512.
[121] Palacios, O.A., Y. Bashan, M. Schmid, A. Hartmann, and L.E. de-Bashan, Enhancement of thiamine release during synthetic mutualism between *Chlorella sorokiniana* and *Azospirillum brasilense* growing under stress conditions. *Journal of Applied Phycology*, 2016. **28**(**3**): p. 1521-1531.
[122] Fernández-Castané, A., G. Caminal, and J. López-Santín, Direct measurements of IPTG enable analysis of the induction behavior of *E. coli* in high cell density cultures. *Microb Cell Fact*, 2012. **11**: p. 58.
[123] Fan, J., X. Du, H. Zhao, and W. Yao, Allelochemicals-mediated interaction between algae and bacteria: Direct and indirect contact. *Bioresource Technology*, 2024. **398**: p. 130525.
[124] Dvorak, P., L. Chrast, P.I. Nikel, R. Fedr, K. Soucek, M. Sedlackova, R. Chaloupkova, V. de Lorenzo, Z. Prokop, and J. Damborsky, Exacerbation of substrate toxicity by IPTG in *Escherichia coli* BL21(DE3) carrying a synthetic metabolic pathway. *Microbial Cell Factories*, 2015. **14**(**1**): p. 201.
[125] Fang, J., Y. Sun, Z. Zhu, J. Li, P. Cheng, S.N. Agathos, Y. Fu, L. Zhang, C. Zhou, and J. Han, Algae-bacteria consortia promotes the cell growth of marine microalgae *Phaeodactylum tricornutum* and *Chrysotila roscoffensis*. *Algal Research*, 2024. **80**: p. 103535.

[126] Pinsach, J., C. de Mas, and J. López-Santín, Induction strategies in fed-batch cultures for recombinant protein production in *Escherichia coli*: Application to rhamnulose 1-phosphate aldolase. *Biochemical Engineering Journal*, 2008. **41**(**2**): p. 181-187.
[127] Faust, G., A. Stand, and D. Weuster-Botz, IPTG can replace lactose in auto-induction media to enhance protein expression in batch-cultured *E. coli*. *Engineering in Life Sciences*, 2015. **15**(**8**): p. 824-829.
[128] Tong, C.Y., H. Tomita, K. Miyazaki, C.J.C. Derek, and K. Honda, Impacts of riboflavin-overproducing engineered Escherichia coli towards Chlorella sorokiniana growth in co-cultivation approach. *Algal Research*, 2025: p. 103938.
[129] Li, Y., Y. Luo, R. Zhou, X. Zuo, Y. Zhang, Z. Wang, X. Li, X. Zhang, Z. Qin, and C.S.K. Lin, Coculture of Chlorella protothecoides and Coccomyxa subellipsoidea enhances cell growth and lipid accumulation: An effective strategy for biodiesel production. *Chemical Engineering Journal*, 2024. **486**: p. 150302.
[130] Ruangsomboon, S., P. Sornchai, and N. Prachom, Enhanced hydrocarbon production and improved biodiesel qualities of Botryococcus braunii KMITL 5 by vitamins thiamine, biotin and cobalamin supplementation. *Algal Research*, 2018. **29**: p. 159-169.
[131] Han, J., L. Zhang, S. Wang, G. Yang, L. Zhao, and K. Pan, Co-culturing bacteria and microalgae in organic carbon containing medium. *J Biol Res (Thessalon)*, 2016. **23**: p. 8.
[132] Soo, R.M., B.J. Woodcroft, D.H. Parks, G.W. Tyson, and P. Hugenholtz, Back from the dead; the curious tale of the predatory cyanobacterium Vampirovibrio chlorellavorus. *PeerJ*, 2015. **3**: p. e968.
[133] Serra, V., L. Gammuto, G. Petroni, A. Ciurli, and C. Chiellini, Identification of the bacteria associated to the phycosphere of the Chlorella-like strain SEC_LI_ChL_1. *Algal Research*, 2022. **67**: p. 102869.
[134] Nef, C., S. Jung, F. Mairet, R. Kaas, D. Grizeau, and M. Garnier, How haptophytes microalgae mitigate vitamin B12 limitation. *Scientific Reports*, 2019. **9**(**1**): p. 8417.
[135] Sañudo-Wilhelmy, S.A., C.J. Gobler, M. Okbamichael, and G.T. Taylor, Regulation of phytoplankton dynamics by vitamin B12. *Geophysical Research Letters*, 2006. **33**(**4**).
[136] Panzeca, C., A. Tovar-Sanchez, S. Agustí, I. Reche, C.M. Duarte, G.T. Taylor, and S.A. Sañudo-Wilhelmy, B vitamins as regulators of phytoplankton dynamics. *Eos, Transactions American Geophysical Union*, 2006. **87**(**52**): p. 593-596.
[137] Tandon, P., Q. Jin, and L. Huang, A promising approach to enhance microalgae productivity by exogenous supply of vitamins. *Microbial Cell Factories*, 2017. **16**(**1**): p. 219.
[138] da Silva, J.C. and A.T. Lombardi, Chlorophylls in Microalgae: Occurrence, Distribution, and Biosynthesis, in Pigments from Microalgae Handbook, E. Jacob-Lopes, M.I. Queiroz, and L.Q. Zepka, Editors. 2020, Springer International Publishing: Cham. p. 1-18.
[139] Jakhwal, P., E. Daneshvar, K. Skalska, L. Matsakas, A. Patel, Y. Park, and A. Bhatnagar, Nutrient removal and biomass production of marine microalgae cultured in recirculating aquaculture systems (RAS) water with low phosphate concentration. *Journal of Environmental Management*, 2024. **358**: p. 120859.
[140] Razzak, S.A., Comprehensive overview of microalgae-derived carotenoids and their applications in diverse industries. *Algal Research*, 2024. **78**: p. 103422.
[141] Kato, Y., T. Oyama, K. Inokuma, C.J. Vavricka, M. Matsuda, R. Hidese, K. Satoh, Y. Oono, J.-S. Chang, T. Hasunuma, and A. Kondo, Enhancing carbohydrate repartitioning

into lipid and carotenoid by disruption of microalgae starch debranching enzyme. *Communications Biology*, 2021. **4**(**1**): p. 450.
[142] Esteves, A.F., E.M. Salgado, V.J.P. Vilar, A.L. Gonçalves, and J.C.M. Pires, A growth phase analysis on the influence of light intensity on microalgal stress and potential biofuel production. *Energy Conversion and Management*, 2024. **311**: p. 118511.
[143] Tsai, T.-Y., I. Khozin-Goldberg, A. Vonshak, and T.-M. Lee, Ascorbate-glutathione cycle alleviates low-temperature-induced oxidative stress for augmented growth of Nannochloropsis oceanica Rose Bengal mutants. *Physiologia Plantarum*, 2024. **176**(**1**): p. e14168.
[144] Zhu, J., Y. Cai, M. Wakisaka, Z. Yang, Y. Yin, W. Fang, Y. Xu, T. Omura, R. Yu, and A.L.T. Zheng, Mitigation of oxidative stress damage caused by abiotic stress to improve biomass yield of microalgae: A review. *Science of The Total Environment*, 2023. **896**: p. 165200.
[145] Sudarshan, S., V.S. Bharti, S. Harikrishnan, S.P. Shukla, and G. RathiBhuvaneswari, Eco-toxicological effect of a commercial dye Rhodamine B on freshwater microalgae Chlorella vulgaris. *Archives of Microbiology*, 2022. **204**(**10**): p. 658.
[146] Zhang, Y.M., H. Chen, C.L. He, and Q. Wang, Nitrogen starvation induced oxidative stress in an oil-producing green alga Chlorella sorokiniana C3. *PLoS One*, 2013. **8**(**7**): p. e69225.
[147] Ruiz-Domínguez, M.C., I. Vaquero, V. Obregón, B. de la Morena, C. Vílchez, and J.M. Vega, Lipid accumulation and antioxidant activity in the eukaryotic acidophilic microalga Coccomyxa sp. (strain onubensis) under nutrient starvation. *Journal of Applied Phycology*, 2015. **27**(**3**): p. 1099-1108.
[148] Shi, T.Q., L.R. Wang, Z.X. Zhang, X.M. Sun, and H. Huang, Stresses as First-Line Tools for Enhancing Lipid and Carotenoid Production in Microalgae. *Front Bioeng Biotechnol*, 2020. **8**: p. 610.
[149] Alishah-Aratboni, H., N. Rafiei, R. Garcia-Granados, A. Alemzadeh, and J.R. Morones-Ramirez, Biomass and lipid induction strategies in microalgae for biofuel production and other applications. *Microb. Cell Fact.*, 2019. **18**(**1**): p. 178.
[150] Morales-Sánchez, D., P.S.C. Schulze, V. Kiron, and R.H. Wijffels, Production of carbohydrates, lipids and polyunsaturated fatty acids (PUFA) by the polar marine microalga Chlamydomonas malina RCC2488. *Algal Research*, 2020. **50**: p. 102016.
[151] Kato, N., G. Nelson, and K.J. Lauersen, Subcellular Localizations of Catalase and Exogenously Added Fatty Acid in Chlamydomonas reinhardtii. *Cells*, 2021. **10**(**8**).
[152] Yukino, T., M. Hayashi, I. Maruyama, and H. Murata, Incorporation of Exogenous Docosahexaenoic Acid into Triacyiglycerols and Polar Lipids of Chlorella vulgaris. *Journal of Oleo Science*, 2005. **54**: p. 15-19.
[153] Dasan, Y.K., M.K. Lam, S. Yusup, J.W. Lim, P.L. Show, I.S. Tan, and K.T. Lee, Cultivation of Chlorella vulgaris using sequential-flow bubble column photobioreactor: A stress-inducing strategy for lipid accumulation and carbon dioxide fixation. *Journal of CO2 Utilization*, 2020. **41**: p. 101226.
[154] Wang, H., X. Hu, C. Shao, M. Elshobary, F. Zhu, Y. Cui, C. Zhang, J. Ni, and S. Huo, Optimizing mixotrophic cultivation of oil-rich Tribonema minus using volatile fatty acids and glycerin: A promising approach for pH-controlling and enhancing lipid productivity. *Journal of Cleaner Production*, 2023. **402**: p. 136733.

Supplementary Data

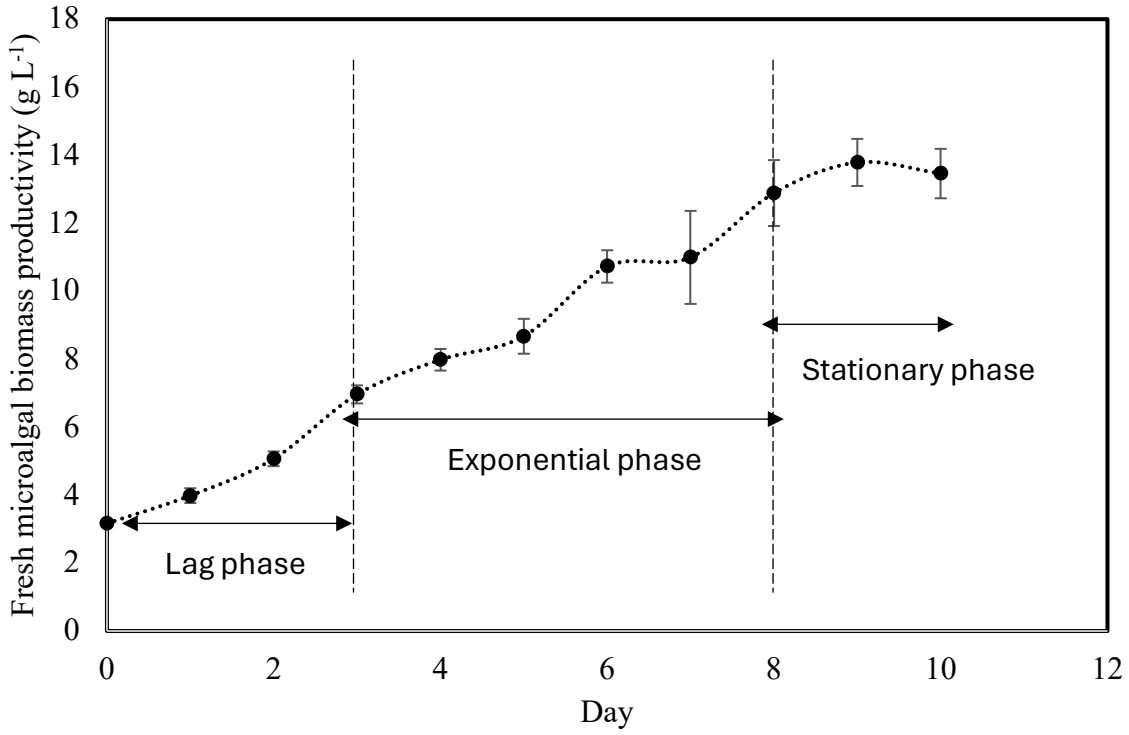

Supplementary data 1 *Growth curve of C. sorokiniana in flasks over 10 days (n=3).*

Plate #1/2

	1	2	3	4	5	6	7	8	9	10	11	12
A	JW1950 *hch*A	JW3701 *bgl*G	JW3905 *cyt*R	JW1328 *fnr*	JW0430 *hup*B		JW0662 *nag*C	JW3877 *rha*R	JW1316 *tyr*R	JW5917 *rcs*C	JW0111 *ace*F	JW0711 *sdh*C
B	BW25113 **Wild type**	JW1262 *btu*R	JW0824 *deo*R	JW2776 *fuc*R	JW2883 *arg*P		JW3195 *nan*R		JW1610 *uid*R		JW0114 *acn*B	JW0712 *sdh*D
C	JW2201 *ada*	JW4094 *cad*C	JW2361 *dsd*C	JW2805 *gal*R	JW4221 *idn*R	JW4079 *mel*R	JW0019 *nha*R	JW4024 *sox*R	JW4287 *uxu*R	JW0078 *fru*R	JW0324 *prp*C	JW0713 *sdh*A
D	JW4077 *adi*Y	JW1966 *cbl*	JW3046 *ebg*R	JW2138 *gal*S	JW3746 *ilv*Y	JW3909 *met*J	JW0109 *pdh*R	JW4023 *sox*S	JW2396 *xap*R	JW1702 *ihf*A	JW0419 *cyo*D	JW0714 *sdh*B
E	JW0553 *app*Y	JW1724 *chb*R	JW3232 *env*R		JW0075 *leu*O	JW3804 *met*R	JW0244 *per*R	JW2644 *stp*A	JW3254 *znt*R	JW3732 *rbs*R	JW0420 *cyo*C	JW0715 *suc*A
F	JW3206 *arg*R	JW5702 *crp*	JW0555 *env*Y	JW0895 *ihf*B	JW0872 *lrp*	JW0337 *mhp*R	JW4063 *phn*F	JW3089 *tdc*A	JW0198 *yaf*C	JW1901 *sdi*A	JW0421 *cyo*B	JW0716 *suc*B
G	JW3721 *asn*C	JW1023 *csg*D	JW1176 *fad*R		JW2807 *lys*R	JW1967 *nac*		JW4200 *tre*R	JW0596 *ybd*O	JW2676 *srl*R	JW0422 *cyo*A	JW0717 *suc*C
H	JW0305 *bet*I	JW5894 *cyn*R	JW3229 *fis*	JW3964 *hup*A	JW1612 *mal*I		JW1650 *pur*R	JW4356 *trp*R	JW0624 *ybe*F	JW0007 *tal*B	JW0506 *fdr*A	JW0739 *gal*M

Plate #3/4

	1	2	3	4	5	6	7	8	9	10	11	12
A	JW0807 *ybi*W	JW1228 *adh*E	JW1692 *pps*	JW2273 *nuo*L	JW5875 *nuo*B	JW3205 *mdh*	JW3923 *pfl*D	JW4112 *frd*D		JW1115 *pho*Q	JW1872 *che*B	JW2213 *ato*S
B		JW1268 *acn*A	BW25113 **Wild type**	JW2274 *nuo*K	JW2283 *nuo*A	JW3343 *yhf*W	JW3924 *pfl*C	JW4113 *frd*C	JW0611 *cit*A	JW1116 *pho*P	JW1877 *che*A	JW2214 *ato*C
C	JW0885 *pfl*A	JW1413 *gap*C	JW1841 *zwf*	JW2275 *nuo*J	JW2385 *glk*	JW3349 *rpe*	JW3928 *ppc*	JW4114 *frd*B	JW0612 *cit*B	JW1212 *nar*L	JW1899 *uvr*Y	JW2366 *evg*A
D	JW0886 *pfl*B	JW5906 *gap*C	JW1843 *pyk*A	JW2276 *nuo*I	JW2447 *mae*B	JW3366 *pck*	JW3974 *ace*B	JW4115 *frd*A		JW1213 *nar*X	JW1951 *yed*V	JW2367 *evg*S
E			JW2011 *gnd*	JW2277 *nuo*H	JW2448 *tal*A	JW3587 *gpm*I	JW3975 *ace*A	JW4346 *deo*B	JW0683 *kdp*D	JW1223 *rss*B		JW2453 *nar*Q
F	JW0960 *app*C	JW1603 *fum*C	JW2198 *mqo*	JW2278 *nuo*G	JW2449 *tkt*B	JW3887 *pfk*A		JW4358 *ytj*C	JW0797 *dps*	JW1600 *rst*A	JW2063 *bae*S	JW2538 *yfh*A
G	JW0961 *app*B	JW1604 *fum*A	JW2271 *nuo*N	JW2279 *nuo*F	JW0563 *cus*B	JW3890 *tpi*A	JW4051 *rpi*B	JW0389 *pho*B		JW1601 *rst*B	JW2181 *nar*P	
H	JW1122 *icd*	JW1666 *pyk*F	JW2272 *nuo*M	JW2280 *nuo*E	JW2943 *glc*B	JW3918 *fsa*B	JW4083 *fum*B	JW0390 *pho*R	JW0980 *tor*R	JW1871 *che*Y	JW2205 *rcs*B	

Plate #5/6

	1	2	3	4	5	6	7	8	9	10	11	12
A	JW2757 *bar*A	JW3644 *uhp*A	JW4074 *bas*R	JW1186 *tre*A	JW0855 *pox*B	JW5478 *tkt*A	JW0401 *tsx*	JW3043 *aer*	JW0100 *coa*E	JW0560 *cus*R		
B	JW2993 *qse*B	JW3839 *gln*G	JW4085 *dcu*R	JW2034 *cps*B	JW1375 *ldh*A	JW2334 *yfc*T	JW2096 *yeh*B	JW1874 *tap*	JW0243 *ykf*A	JW3367 *env*Z	JW2497 *yfg*M	JW2629 *ypj*B
C	JW2994 *qse*C	JW3840 *gln*L	JW4086 *dcu*S	JW3730 *rbs*B	JW2121 *dld*	JW2342 *yfd*F	JW2044 *wca*A			JW3393 *glg*C		
D	JW3169 *rpo*N	JW3882 *cpx*A	JW4361 *cre*B	JW1235 *opp*A	JW3580 *lld*D			JW0945 *hel*D		JW2486 *ppk*		
E	JW5536 *arc*B	JW3883 *cpx*R	JW4362 *cre*C	JW3077 *yha*K	JW0675 *pgm*	JW0564 *cus*A		JW5905 *hrp*A	JW0318 *yah*L	JW2293 *ack*A	JW2585 *yfi*N	JW2633 *yqa*D
F	BW25113 **Wild type**	JW3967 *zra*S	JW4364 *arc*A	JW1644 *rnt*	JW0710 *glt*A	JW1771 *mip*A	JW3285 *gsp*A	JW0764 *moa*A	JW0110 *ace*E	JW2369 *yfd*V		
G	JW3624 *rpo*Z	JW3968 *zra*R	JW3021 *glg*S		JW0723 *cyd*B	JW0146 *fhu*A	JW3354 *hof*Q	JW0117 *spe*E	JW0112 *lpd*	JW2373 *ypd*I		JW0449 *hha*
H	JW3643 *uhp*B	JW4073 *bas*S		JW2294 *pta*		JW3703 *pst*B	JW3454 *yhi*I	JW0530 *ren*D	JW4191 *fbp*	JW2421 *yfe*U	JW2621 *yfj*V	

Plate #7/8

	1	2	3	4	5	6	7	8	9	10	11	12
A		JW2142 *cir*A	JW0755 *ybh*C		JW2047 *wza*			JW5896 *ybh*D	JW1587 *ynf*L	JW0104 *ppd*D	JW0483 *tes*A	JW1113 *pep*T
B		BW25113 **Wild type**	JW1010 *ycd*S	JW1088 *fhu*E	JW0790 *fiu*	JW3113 *yra*J	JW2824 *yge*L		JW1337 *dbp*A			
C		JW2784 *mlt*A	JW3556 *yia*T		JW0561 *cus*C			JW1788 *yea*T	JW0058 *hep*A		JW0627 *dac*A	JW1172 *umu*D
D		JW2671 *mlt*B	JW1795 *yea*Y	JW2462 *nlp*B	JW3996 *lam*B		JW0120 *gcd*	JW2144 *yei*E	JW0144 *hrp*B	JW0227 *pep*D	JW0823 *dac*C	JW1181 *ldc*A
E			JW3474 *slp*	JW0940 *omp*A	JW1499 *yde*T	JW2762 *yqc*B			JW1645 *lhr*	JW0322 *prp*R	JW0840 *pot*H	JW1264 *soh*B
F		JW0731 *pal*		JW2203 *omp*C	JW4275 *fim*B	JW2815 *yqe*I	JW4195 *cyb*C	JW3557 *yia*U	JW3753 *rhl*B	JW0427 *clp*P	JW0866 *clp*A	
G		JW1270 *pgp*B	JW0188 *nlp*E	JW0912 *omp*F	JW5780 *fim*D			JW3689 *yid*Z	JW2560 *srm*B	JW0428 *clp*X	JW0915 *pep*N	
H	JW1502 *yde*U	JW0554 *omp*T	JW2341 *fad*L	JW1371 *omp*N	JW4276 *fim*E	JW2818 *yge*F	JW3896 *glp*X	JW4290 *yji*E	JW1797 *yoa*A	JW0429 *lon*	JW0957 *hya*D	JW1431 *ydc*P

Plate #9/10

	1	2	3	4	5	6	7	8	9	10	11	12
A	JW1489 *pqq*L	BW25113 **Wild type**	JW2712 *nlp*D	JW3100 *aga*R	JW3903 *hsl*V	JW3495 *yhj*J	JW4132 *hfl*K	JW2169 *yej*G	JW2238 *yfa*D	JW2270 *yfb*P	JW2352 *yfd*M	JW2394 *yfe*D
B	JW1755 *spp*A	JW2325 *mep*A	JW2723 *iap*	JW3098 *soh*A	JW3869 *frv*X	JW3465 *prl*C	JW4133 *hfl*C	JW2219 *yfa*P	JW5964 *ypa*A	JW2288 *yfb*R	JW2355 *yfd*O	JW2412 *yfe*K
C	JW1818 *htp*X	JW2382 *ypd*F	JW2789 *ptr*	JW3127 *yhb*U	JW3823 *pep*Q	JW3434 *znt*A	JW4217 *pep*A	JW2220 *yfa*Q	JW2239 *yfa*U	JW2296 *yfc*D	JW2357 *yfd*Q	JW2425 *yfe*Y
D	JW1819 *prc*	JW2476 *hyf*R	JW2840 *yge*Y	JW3149 *dac*B		JW3412 *ggt*		JW2221 *yfa*S		JW2302 *yfc*I	JW2358 *yfd*R	JW2426 *yfe*Z
E	JW1834 *ptr*B	JW2507 *pep*B	JW2903 *ygg*G	JW3203 *deg*Q	JW5595 *yij*K	JW3359 *mrc*A	JW4291 *iad*A	JW2222 *yfa*S	JW2250 *yfb*H	JW2322 *yfc*L		JW2432 *eut*L
F		JW2669 *rec*A	JW2911 *spr*T		JW3670 *dgo*K	JW3297 *gsp*O	JW4352 *rad*A	JW2223 *yfa*T	JW2252 *yfb*W	JW2330 *yfc*P	JW2372 *yfd*X	JW2435 *eut*A
G	JW2005 *his*H	JW2688 *hyc*H	JW2939 *ppp*A	JW3930 *arg*C		JW3981 *pep*E	JW2150 *yei*L	JW2224 *yfa*A		JW2332 *yfc*R	JW2387 *ype*C	JW2443 *eut*T
H	JW2066 *yeg*Q	JW2687 *hyc*I	JW2961 *hyb*D	JW3902 *hsl*U	JW3504 *bcs*E	JW4131 *hfl*X	JW2152 *yei*N	JW2232 *yfa*H	JW2267 *yfb*M	JW2350 *yfd*K	JW2393 *yfe*C	JW2444 *eut*Q

Plate #11/12

	1	2	3	4	5	6	7	8	9	10	11	12
A	JW2445 *eut*P		JW2608 *yfj*K	JW2624 *yfj*X	JW2702 *ygb*A	JW1560 *ydf*X	JW1599 *ydg*C	JW1659 *ydh*T		JW1800 *yoa*H	JW1835 *yeb*E	JW1894 *yec*H
B	JW2446 *ypf*E		JW2609 *yfj*L	JW2627 *ypj*F	JW2719 *ygb*E	JW1563 *ydf*A	JW1617 *ydg*T	JW1662 *ydh*W	JW1749 *ynj*H	JW1809 *yob*D	JW1837 *yeb*G	JW1900 *yec*F
C	JW2450 *ypf*G	JW2570 *yfi*M	JW2610 *yfj*M	JW2631 *yga*R		JW1565 *ydf*C	JW1618 *ydg*K	JW1675 *ydi*H		JW1814 *yeb*O		JW1913 *yed*D
D	JW2457 *ypf*N		JW2611 *yfj*N		JW2725 *ygb*T	JW1567 *ydf*D	JW1631 *ydh*A	JW1695 *ydi*E	JW1766 *yea*C		JW1857 *yec*E	JW1914 *yed*E
E	BW25113 **Wild type**	JW2584 *yfi*R		JW2645 *yga*W	JW2726 *ygc*H	JW1575 *ynf*B	JW1637 *ydh*K	JW1697 *ydi*V	JW1776 *yea*K			
F	JW2504 *yfh*M	JW2600 *yfj*G	JW2614 *yfj*Q	JW2646 *yga*C				JW1711 *ydi*Y	JW1782 *yoa*F	JW1828 *yeb*Y		JW1940 *yod*C
G	JW2520 *hca*T	JW2603 *yfj*H	JW2623 *yfj*W	JW2647 *yga*M	JW1547 *ydf*R	JW1590 *ydg*D	JW1657 *ydh*R	JW1715 *yni*B	JW1785 *yoa*G	JW1829 *yeb*Z	JW1891 *yec*J	JW1946 *yed*R
H	JW2539 *yfh*G	JW2605 *yfj*I		JW2658 *yga*H	JW5909 *ydf*U	JW1596 *ydg*H	JW1658 *ydh*S		JW1786 *yea*R	JW1832 *yob*B	JW1892 *yec*R	JW1988 *yee*W

Plate #13/14

	1	2	3	4	5	6	7	8	9	10	11	12
A	JW1990 *yee*A	JW2099 *yeh*E	JW2112 *yeh*S	JW0986 *ycc*E		JW1101 *ycf*T		JW1250 *yci*F	JW5804 *ycj*Y	JW1354 *yda*U	JW1408 *ynb*D	
B	JW1995 *yee*E	JW2105 *yeh*I		JW0988 *ycc*J			JW1167 *ycg*K	JW1251 *yci*G	JW1326 *yna*J		JW1411 *ydc*F	JW1432 *ync*J
C	JW2058 *yeg*L	JW2106 *yeh*K			JW1050 *yce*B	JW1133 *ymf*L	JW1183 *ycg*R			JW1359 *yna*K	JW1416 *ydc*A	JW1433 *ydc*Q
D	BW25113 **Wild type**				JW1054 *yce*H	JW1134 *ymf*M	JW1196 *ych*H	JW1265 *yci*N	JW1334 *yda*L	JW1360 *yda*Y		JW1441 *ydc*Y
E		JW2108 *yeh*M	JW5970 *ycc*V	JW1006 *ycd*P	JW1090 *ycf*L	JW1136 *ymf*R	JW1204 *ych*Q		JW1341 *yda*C	JW1367 *tfa*R		JW1442 *ydc*Z
F			JW0968 *ymc*B			JW1137 *ymf*O		JW1288 *ymj*A	JW1346 *yda*E			JW1447 *ync*E
G		JW2110 *yeh*Q	JW0976 *gns*A			JW1139 *ymf*Q	JW1247 *yci*C	JW1319 *mpa*A	JW1349 *yda*F	JW1376 *ydb*H	JW1424 *ydc*K	JW1452 *ydc*D
H	JW2095 *yeh*A		JW0984 *cbp*M	JW1034 m*do*C	JW1098 *ycf*R	JW1154 *ymg*C	JW1249 *yci*E	JW5960 *ymj*C	JW1353 *yda*T	JW1377 *ynb*E	JW1427 *ydc*L	JW1453 *ync*I

Plate #15/16

	1	2	3	4	5	6	7	8	9	10	11	12
A	JW1456 *ydc*E	BW25113 **Wild type**	JW0282 *ykg*J	JW0349 *yai*O	JW0382 *yai*E			JW0638 *ybe*L	JW0691 *ybf*B	JW0783 *ybi*A	JW0842 *ybj*O	JW1018 *ycd*Y
B	JW1468 *ydd*L	JW1545 *ydf*P		JW0355 *yai*P	JW0394 *yaj*B	JW0503 *ylb*A	JW0556 *ybc*H	JW0640 *ybe*R	JW0693 *ybf*C	JW0787 *ybi*J	JW0860 *ybj*D	
C	JW1469 *ydd*G	JW0239 *ykf*B	JW0284 *yag*W	JW0356 *yai*S	JW0400 *yaj*D	JW0508 *ylb*E	JW0562 *cus*F	JW0641 *djl*B	JW0694 *ybf*Q	JW0788 *ybi*I	JW0902 *ycb*J	JW1043 *yce*I
D		JW0242 *yaf*Z	JW0286 *yag*Y	JW0366 *yai*V		JW0509 *ylb*F		JW0643 *ybe*U			JW0924 *ycb*T	JW1044 *yce*J
E	JW1516 *yne*G	JW0259 *yag*B	JW0287 *yag*Z	JW0369 *yai*W	JW0455 *yba*M	JW0516 *ybc*I	JW0569 *ybd*J	JW0667 *ybf*M	JW0725 *ybg*E	JW0805 *ybi*U	JW0925 *ycb*U	JW1074 *yce*D
F	JW1520 *yne*K	JW0270 *yag*J	JW0311 *yah*E	JW0370 *yai*Y	JW0457 *yba*N	JW0535 *ybc*N	JW0591 *ybd*D		JW0736 *ybg*S	JW0827 *ybj*H		JW1114 *ycf*D
G	JW1534 *ydf*Z	JW0271 *yag*K	JW0313 *yah*G		JW0471 *yba*P	JW0537 *ybc*O	JW0594 *ybd*M			JW0834 *ybj*C		
H	JW1539 *tfa*Q	JW0281 *yag*U	JW0321 *yah*O	JW0380 *yai*A	JW0489 *ybb*D	JW0539 *ybc*Q	JW0595 *ybd*N		JW0773 *ybh*P	JW0837 *ybj*N	JW1004 *ycd*B	JW1140 *ycf*K

Plate #17/18

	1	2	3	4	5	6	7	8	9	10	11	12
A	BW25113 **Wild type**	JW1314 *ycj*X	JW1623 *rsx*G	JW2174 *yej*K	JW2346 *yfd*G	JW2738 *ygc*P	JW0113 *yac*H		JW0235 *yaf*W	JW2242 *yfa*X		JW0703 *ybg*L
B	JW1177 *ycg*B	JW1315 *ycj*F	JW1714 *yni*A	JW2175 *yej*L			JW0118 *yac*C	JW0203 *yaf*S	JW5956 *ykf*H			JW0903 *ycb*C
C		JW1419 *ydc*J	JW1781 *yea*O	JW2265 *yfb*K		JW2763 *yqc*C		JW0206 *yaf*T		JW2455 *yff*B	JW0348 *frm*R	
D		JW5961 *ync*K	JW1938 *yed*P	JW2292 *yfb*V	JW2424 *yfe*X	JW2777 *ygd*E	JW0132 *yad*K	JW0214 *yaf*K		JW2459 *ypf*I	JW0378 *yai*I	
E	JW1205 *yc*hA		JW1941 *yed*I	JW2298 *yfc*F	JW2508 *yfh*J	JW0004 *yaa*X	JW0133 *yad*L	JW0223 *yaf*O		JW2527 *yph*A		JW1574 *ynf*A
F	JW1240 *yci*U		JW1958 *yee*I		JW2599 *yfj*F	JW0012 *yaa*I	JW0159 *yae*H	JW0225 *ykf*J	JW1669 *suf*E	JW2625 *yfj*Y	JW0631 *ybe*A	
G	JW1243 *yci*I	JW1529 *yde*I	JW1989 *yee*X	JW2328 *yfc*N	JW2664 *yqa*A		JW0185 *yae*P	JW0229 *frs*A	JW5281 *ydj*M	JW2662 *lux*S		JW1778 *yea*L
H	JW1271 *yci*S	JW1606 *ydg*A	JW2139 *yei*B	JW2340 *yfc*Z	JW2707 *ygb*K	JW0099 *yac*F	JW0186 *yae*Q	JW0234 *ykf*I	JW1984 *yee*S	JW2782 *ygd*K	JW0642 *ybe*T	JW1916 *yed*K

Plate #19/20

	1	2	3	4	5	6	7	8	9	10	11	12
A	JW1945 *yed*J	JW2563 *yfi*D	JW0570 *ybd*K	JW1632 *ydh*H	JW0115 *yac*L	JW0493 *all*A	JW0821 *yli*I	JW0942 *ycc*R	JW0080 *mra*W		JW1674 *suf*A	JW2324 *yfc*A
B	JW2086 *yeg*U	JW0009 *yaa*H	JW0699 *ybg*H	JW1696 *ydi*U	JW0126 *yad*E		JW0831 *ybj*L	JW0944 *ycc*F		JW2670 *yga*D	JW1754 *ydj*A	JW2808 *yge*A
C	JW2092 *yoh*L	JW0153 *yad*S	JW0858 *ybj*E	JW1821 *yeb*R	JW0218 *yaf*M	JW0577 *ybd*Z	JW0851 *ybj*R	JW0947 *ycc*T			JW1767 *yea*A	JW0154 *btu*F
D	JW2129 *yoh*J	JW0215 *yaf*Q	JW0865 *clp*S	JW2145 *yei*H	JW0224 *yaf*P		JW0861 *ybj*X	JW1003 *ycd*O	JW0995 *ycd*K		JW2512 *isc*A	JW0276 *yag*P
E	JW2130 *yoh*K	JW0277 *yag*Q		JW2371 *frc*			JW0889 *yca*P	JW1853 *yeb*C			JW2708 *ygb*L	JW0763 *ybh*K
F	JW2148 *yei*J		JW1483 *ddp*X	JW2641 *yqa*E	JW0384 *rdg*C	JW0732 *ybg*F	JW0900 *yca*R	JW1942 *yed*A	JW1406 *ynb*B	JW0993 *ycd*I		
G	JW2151 *yei*M	JW0501 *ybb*Y	JW1619 *rsx*A	JW2778 *ygd*D	JW0472 *yba*Q	JW0750 *ybh*E	JW0908 *ycb*B	JW1964 *yee*N	JW1530 *yde*J	JW1017 *ycd*X	JW0756 *ybh*B	JW1308 *ycj*S
H	BW25113 **Wild type**	JW0504 *all*C	JW1626 *ydg*R		JW0491 *ybb*B	JW0752 *ybh*H		JW2230 *yfa*E	JW1762 *ydj*I	JW1258 *yci*V	JW1327 *usp*E	JW1333 *abg*R

Plate #21/22

	1	2	3	4	5	6	7	8	9	10	11	12
A	JW2521 *hca*R	JW1106 *cob*B	JW0079 *mra*Z	JW0403 *yba*D	JW2562 *yfi*K	JW0589 *ybd*B	JW2012 *wbb*L		JW2227 *yfa*L	JW2295 *yfc*C	JW2386 *yfe*O	JW2518 *yfh*R
B	JW2715 *tru*D			JW0850 *ybj*Q	JW2578 *yfi*A	JW0721 *mng*B		JW2119 *yeh*Z	JW2245 *yfa*O	JW2299 *yfc*G		JW2532 *yph*F
C	BW25113 **Wild type**	JW1318 *ycj*G	JW0433 *yba*W	JW0997 *ycd*M	JW2657 *yga*Z	JW0888 *yca*O	JW2052 *yeg*E			JW2301 *yfc*H	JW2420 *yfe*T	
D	JW0385 *mak*	JW2241 *yfa*W	JW0726 *ybg*C	JW1002 *ycd*N	JW0236 *ykf*G	JW1032 *ymd*B		JW2147 *yei*I	JW2248 *yfb*F	JW2319 *yfc*J	JW2427 *ype*A	JW2542 *yfh*D
E	JW0770 *ybh*M	JW2501 *yfg*B	JW1510 *lsr*F	JW1274 *yci*H	JW0247 *ins*O	JW1245 *yci*A	JW2061 *mdt*C	JW2161 *yei*R	JW2251 *arn*T	JW2347 *yfd*H	JW2451 *yff*H	JW2545 *yfh*H
F		JW2575 *yfi*H		JW1684 *ydi*F	JW0260 *yag*A	JW1435 *ydc*S	JW2062 *mdt*D	JW2165 *yej*A	JW2258 *yfb*B		JW2488 *yfg*F	JW2559 *yfi*C
G		JW2592 *ypj*D	JW2266 *yfb*L	JW1787 *yea*S	JW0278 *yag*R	JW1459 *ydd*E	JW2070 *yeg*S	JW2172 *yej*H	JW2289 *yf*bS	JW2378 *ypd*B		JW2568 *yfi*Q
H	JW1105 *ycf*X	JW2709 *ygb*M	JW0191 *yae*B	JW1890 *yec*I	JW0279 *yag*S	JW1994 *yee*D				JW2379 *ypd*C		

Plate #23/24

	1	2	3	4	5	6	7	8	9	10	11	12
A	BW25113 **Wild type**	JW2731 *ygc*B	JW2800 *ygd*Q	JW1682 *ydi*B	JW1261 *rlu*B	JW1052 *mdt*H		JW1272 *yci*M	JW1336 *yda*N	JW1437 *ydc*U	JW1652 *ydh*C	JW1716 *yni*C
B	JW2635 *yga*F		JW2803 *yge*D	JW2128 d*usC*		JW1086 *ycf*H		JW1278 *gmr*			JW1655 *mdt*K	JW1747 *ynj*F
C	JW2642 *yga*V		JW0910 *ycb*L	JW2706 *ygb*J	JW1593 *ydg*G		JW1168 *ycg*L	JW1291 *puu*D	JW1338 *yda*O	JW1486 *ydd*W	JW1664 *ydh*Y	JW1757 *pnc*A
D	JW2643 *yga*P				JW0977 *ycc*M	JW1120 *ymf*B	JW1193 *ycg*V	JW1292 *puu*R	JW5802 *ydb*A			
E	JW2655 *yga*X	JW2746 *yqc*E	JW1169 *ycg*M		JW0994 *rat*A			JW1303 *ycj*N	JW1402 *ydb*A	JW1527 *yde*E	JW1680 *ydi*M	JW1774 *yea*I
F		JW2748 *ygc*F	JW1457 *ydd*H	JW0798 *rht*A		JW1150 *ycg*F	JW1210 *ych*N	JW1309 *ycj*T	JW1405 *ynb*A	JW1636 *ydh*J	JW5274 *ydi*N	
G	JW2665 *yqa*B	JW2765 *yqc*D	JW2680 *nor*V		JW1007 *ycd*Q		JW1211 *ych*P	JW1323 *yna*I	JW1430 *ydc*N	JW1646 *ydh*D	JW1686 *ydi*P	JW1802 *yea*B
H	JW2681 *nor*W	JW2798 *nud*H	JW0497 *glx*R	JW1121 *ymf*C	JW1042 *yce*A		JW1221 *ych*J		JW1434 *ydc*R			JW1805 *yoa*E

Plate #25/26

	1	2	3	4	5	6	7	8	9	10	11	12
A	BW25113 **Wild type**	JW1917 *yedL*	JW2761 *yqcA*			JW0310 *yahD*	JW0432 *ybaV*		JW0702 *ybgK*	JW0779 *ybhG*	JW0822 *yliJ*	
B	JW1842 *yebK*		JW2791 *ppdC*	JW5904 *lomR*	JW0187 *yaeJ*	JW0312 *yahF*	JW0434 *ybaX*		JW0749 *ybhA*	JW0785 *ybiB*		JW0892 *ycaL*
C				JW1366 *stfR*	JW0200 *yafE*	JW0350 *yaiX*	JW0435 *ybaE*	JW0566 *ybdG*	JW0753 *ybhI*	JW0801 *mntR*	JW0829 *ybjJ*	JW0931 *ycbY*
D		JW1980 *yoeE*		JW1540 *stfQ*			JW0444 *ybaZ*	JW0621 *ybeM*	JW0771 *ybhN*	JW0803 *ybiS*		
E	JW1859 *yecO*	JW2649 *nrdI*	JW0527 *ybcD*	JW1551 *ydfT*	JW0213 *yafJ*	JW0373 *yaiB*		JW0626 *ybeD*	JW0772 *ybhO*	JW0806 *ybiV*		JW5898 *yccW*
F	JW1860 *yecP*	JW2659 *mprA*	JW0543 *essD*	JW0006 *yaaJ*	JW0255 *afuB*	JW0376 *yaiC*	JW0460 *ybaB*	JW0655 *ybeX*		JW0817 *yliE*	JW0875 *ycaJ*	JW0964 *yccC*
G	JW1896 *yecA*	JW2704 *pphB*		JW0066 *thiP*	JW0300 *ykgF*	JW0397 *yajC*	JW0467 *ybaL*	JW0659 *ubiF*		JW0818 *yliF*	JW0880 *ycaC*	
H	JW1915 *yedF*	JW2752 *mazG*	JW1361 *ynaA*	JW0068 *sgrR*	JW0307 *yahA*		JW0470 *ybaK*	JW0701 *ybgJ*	JW0777 *ybhS*	JW0819 *yliG*	JW0881 *ycaD*	JW2032 *wcaJ*

Plate #27/28

	1	2	3	4	5	6	7	8	9	10	11	12
A	JW2035 *wcaI*	JW2118 *yehY*	JW2204 *rcsD*	JW2516 *yfhQ*	JW5922 *ypjL*		JW0436 *cof*	JW1936 *dsrB*		JW3067 *yqjB*	JW5892 *yadB*	
B	BW25113 **Wild type**	JW2124 *yohD*	JW2243 *yfaY*	JW2522 *hcaE*			JW0536 *ninE*	JW2133 *yeiT*	JW2411 *pdxK*	JW3402 *yhhW*	JW0193 *metQ*	JW0409 *yajO*
C	JW2040 *wcaE*	JW2125 *yohF*	JW2287 *yfbQ*	JW2546 *yfhL*		JW2781 *csdA*	JW0600 *uspG*	JW2164 *rtn*	JW2422 *murP*	JW0005 *yaaA*	JW0216 *dinJ*	JW0424 *yajG*
D	JW2045 *wzc*	JW2153 *yeiC*	JW2339 *yfcY*	JW2561 *yfiE*	JW2705 *ygbI*		JW0605 *citG*	JW5378 *dedD*	JW2431 *yffI*	JW0010 *yaaW*		JW0437 *ybaO*
E	JW2049 *asmA*	JW2160 *yeiQ*	JW2376 *yfdZ*	JW2565 *yfiF*	JW2736 *ygcN*	JW2833 *ygeR*	JW0619 *crcB*	JW2314 *dedA*	JW2440 *cchB*	JW0065 *thiQ*	JW0308 *yahB*	JW0443 *ybaY*
F	JW2087 *yegV*	JW2166 *yejB*	JW2430 *yfeG*	JW2586 *yfiB*	JW2737 *ygcO*	JW0184 *rof*	JW0697 *ybgA*	JW2318 *flk*	JW2441 *cchA*	JW0125 *yadI*	JW0309 *yahC*	JW0474 *ybaS*
G	JW2093 *yohM*	JW2167 *yejE*	JW2438 *eutJ*	JW2615 *yfjR*		JW0210 *ivy*	JW1395 *paaY*	JW2381 *ypdE*	JW2515 *iscR*	JW0131 *yadC*	JW0317 *yahK*	
H	JW2116 *yehW*	JW2168 *yejF*		JW2619 *yfjU*		JW0325 *prpD*	JW1823 *yebT*	JW2383 *ypdG*	JW2640 *ygaU*	JW0137 *yadN*	JW0360 *tauD*	JW0534 *ybcM*

Plate #29/30

	1	2	3	4	5	6	7	8	9	10	11	12
A	JW0592 *ybd*H	JW0883 *yca*N	JW1276 *yci*T	JW1508 *lsr*D	JW1588 *ynf*M		JW1759 *ydj*F	JW1968 *erf*K	JW0849 *ybj*P	JW2030 *wca*K		
B	JW0645 *hsc*C	JW0884 *yca*K	JW1372 *ydb*K	JW1509 *lsr*B	JW1592 *mdt*J	JW1688 *ydi*R	JW1760 *ydj*G	JW1983 *yee*R	JW0923 *ycb*S		JW3891 *yii*Q	JW5604 *rep*
C	JW0673 *ybj*F		JW1403 *ydb*C	JW1517 *yne*H	JW1598 *fol*M	JW1689 *ydi*S	JW1763 *ydj*J	JW0054 *djl*A	JW0966 *ycc*Z	JW2329 *yfc*O	JW4110 *blc*	JW1849 *ruv*B
D	BW25113 **Wild type**	JW0938 *ycb*Z	JW1446 *ync*D	JW1519 *yne*J		JW1690 *ydi*T	JW1770 *yea*E	JW0173 *hlp*A	JW1020 *csg*G	JW2479 *yfg*C	JW1092 *ycf*N	JW3786 *uvr*D
E	JW0735 *zit*B			JW1533 *ydj*H	JW1639 *ydh*F	JW1732 *spy*	JW1779 *yea*M		JW1021 *csg*F	JW2618 *yfj*T	JW0141 *dks*A	JW1279 *rnb*
F	JW0835 *nfs*A	JW0967 *ymc*A	JW1498 *yde*S	JW1535 *ydf*I		JW1739 *ydj*X	JW1836 *yeb*F	JW0521 *sfm*D	JW1374 *hsl*J	JW2876 *pep*P	JW2511 *hsc*B	JW0786 *ybi*C
G	JW0862 *mac*A		JW1505 *yde*W	JW1546 *ydf*Q	JW1649 *ydh*P	JW1741 *ydj*Z	JW1949 *yed*S	JW0557 *nfr*A	JW1677 *ydi*J		JW0426 *tig*	JW3547 *yia*K
H	JW0863 *mac*B		JW1507 *lsr*C	JW1558 *flx*A	JW1672 *suf*C			JW0800 *ybi*P	JW1956 *yod*A	JW3183 *yhc*D	JW1875 *tar*	JW0505 *all*D

Plate #31/32

	1	2	3	4	5	6	7	8	9	10	11	12
A	JW3976 *ace*K	JW4011 *qor*	JW1648 *sod*B		JW0273 *yag*M	JW0498 *ybb*V	JW0658 *mia*B	JW1045 *yce*O	JW1152 *ymg*A		JW1466 *ydd*J	JW1742 *ynj*A
B	JW1772 *yea*G	JW4130 *hfq*	JW1638 *sod*C	JW2801 *ygd*R	JW0274 *yag*N	JW0507 *ylb*E	JW0676 *ybf*P	JW1123 *ymf*D	JW1153 *ymg*B	JW1352 *yda*S	JW1467 *ydd*K	BW25113 **Wild type**
C	JW1827 *pph*A	JW1667 *lpp*	JW1317 *tpx*			JW0532 *ybc*K	JW0724 *ybg*T		JW1156 *ymg*F	JW1369 *yna*E	JW1503 *yde*K	
D	JW3140 *arg*G	JW0599 *ahp*F		JW2819 *yge*G				JW1128 *ymf*H	JW1162 *ycg*I			
E	JW1241 *cls*	JW3467 *gor*	JW1329 *ogt*	JW2820 *yge*H		JW0548 *ybc*W			JW1185 *ycg*Y		JW1557 *ydf*V	JW1815 *yob*G
F	JW3331 *cys*G	JW1627 *gst*	JW0217 *yaf*L		JW0302 *ykg*H	JW0551 *ybc*Y		JW1130 *ymf*J			JW1635 *ydh*I	
G	JW1794 *fad*D	JW3914 *kat*G	JW2728 *ygc*J	JW0207 *yaf*U		JW0552 *ylc*E	JW0832 *ybj*M	JW1147 *elb*A			JW1713 *ydi*Z	JW1918 *yed*N
H	JW0008 *mog*	JW3879 *sod*A	JW2766 *ygd*H	JW0222 *yaf*N				JW1148 *ycg*X			JW1719 *ydj*O	JW5912 *yed*N

Plate #33/34

	1	2	3	4	5	6	7	8	9	10	11	12
A	JW1920 *yed*M	JW1306 *ycj*Q	JW2843 *yqe*B	JW2882 *yqf*E	JW2919 *ygg*T	JW2938 *ygh*G	JW2992 *ygi*W	JW3007 *zup*T	JW3035 *ygj*E	JW3053 *ygj*M	JW3073 *yqj*G	JW3118 *yra*O
B	JW1953 *yed*X	JW1765 *ydj*L	JW2849 *xdh*D	JW2887 *ygf*H	JW2921 *ygg*V	JW2952 *ygh*R	JW2995 *ygiZ*	JW3008 *ygi*E	JW3040 *ygj*F	JW3054 *ygj*N	JW3074 *yha*H	JW3119 *yra*P
C	JW1998 *yee*Z	JW3109 *aga*D	JW2864 *ygf*X	JW2889 *ygg*E	JW2922 *ygg*W	JW2954 *ygh*T	JW2996 *mda*B	JW3011 *ygi*L	JW3041 *yqj*H	JW3057 *ygj*Q	JW3075 *yha*I	JW3120 *yra*Q
D	BW25113 **Wild type**	JW2261 *ela*B	JW2865 *ygf*Y	JW2890 *arg*O	JW2923 *ygg*M	JW2966 *ygh*W	JW2997 *ygi*N	JW3022 *yqi*J	JW3042 *yqj*I	JW3060 *sst*T	JW3097 *gar*D	JW3123 *yhb*P
E	JW2268 *yfb*N	JW2262 *ela*A	JW2866 *ygf*Z	JW2891 *msc*S	JW2927 *ygg*H	JW2970 *ygh*Z	JW2999 *yqi*A	JW3023 *yqi*K	JW3045 *ygj*H	JW3061 *ygj*V	JW3099 *yha*V	JW3124 *yhb*Q
F	JW2269 *yfb*O	JW2802 *tas*	JW2867 *yqf*A	JW2895 *ygg*C	JW2929 *ygg*X	JW2985 *suf*I	JW3001 *yqi*B	JW3026 *ygi*F	JW5512 *ygj*I	JW3066 *yqj*A	JW3111 *yra*H	JW3125 *yhb*S
G	JW0601 *yb*dR	JW2835 *xdhB*	JW2868 *yqf*B	JW2896 *ygg*D	JW2934 *yqg*A	JW2990 *ygi*U	JW3002 *nud*F	JW3027 *htr*G	JW3050 *ygj*J	JW3069 *yqj*D	JW3114 *yra*K	JW3129 *yhb*W
H	JW1222 *rss*A	JW2841 *hyu*A	JW2870 *ygf*F	JW2897 *ygg*F	JW2935 *ygh*D	JW5502 *ygi*V	JW3006 *ygi*C	JW3031 *ygi*H	JW3051 *ygj*K	JW3070 *yqj*E	JW3116 *yra*M	JW3132 *nlp*I

Plate #35/36

	1	2	3	4	5	6	7	8	9	10	11	12
A	JW3147 *yhb*Y	JW3170 *yhb*H	JW3208 *yhcO*	JW3235 *yhd*V	JW3316 *yhe*T	JW3344 *yhf*X	JW3397 *yhg*N	JW3432 *yhh*M	JW3478 *hde*A	JW3491 *yhj*E	JW3532 *ysa*B	JW3568 *yib*A
B	JW3151 *yhb*E	JW3172 *yhb*J	JW3209 *aae*B	JW3241 *yrd*B	JW3317 *yhe*U	JW3351 *dam*X	JW3403 *yhh*X	JW3433 *yhh*N	JW3479 *hde*D	JW3503 *yhj*R	JW3533 *yia*H	JW3570 *yib*G
C	JW3159 *yrb*C	JW3174 *yrb*L	JW3210 *aae*A	JW3245 *sm*g	JW3318 *prk*B	JW3356 *yrf*B	JW3405 *yhh*Y	JW3435 *yhh*P	JW3481 *mdt*E	JW3506 *bcs*G	JW5653 *bax*	JW3571 *yib*H
D	JW3160 *yrb*D	JW3182 *yhc*A	JW3217 *yhd*E	JW3255 *yhd*N	JW3319 *yhf*A	JW3357 *yrf*C	JW3406 *yhh*Z	JW3455 *yhi*J	JW3482 *mdt*F	BW25113 **Wild type**	JW3546 *yia*J	JW3576 *yib*T
E	JW3161 *yrb*E	JW3188 *yhc*F	JW3222 *yhd*H	JW3305 *yhe*L	JW3325 *yhf*G	JW3360 *nud*E	JW3411 *yrh*B	JW3459 *yhi*N	JW3484 *gad*X	JW3508 *yhj*V	JW3549 *yia*M	JW3577 *yib*L
F	JW3163 *yrb*G	JW3189 *yhc*G	JW3225 *yhd*T	JW3306 *yhe*M	JW3327 *tsg*A	JW3365 *yhg*E	JW3413 *yhh*A	JW3463 *yhi*P	JW3486 *yhj*A	JW3519 *yia*C	JW3551 *yia*O	JW3586 *yib*N
G	JW3164 *kds*D	JW3190 *yhc*H	JW3228 *dus*B	JW3307 *yhe*N	JW3332 *yhf*L	JW3374 *yhg*A	JW3424 *yhh*K	JW3466 *yhi*R	JW3488 *yhj*B	JW5657 *yia*D	JW3558 *yia*V	JW3619 *yic*C
H	JW3165 *kds*C	JW3201 *yhc*M	JW3231 *yhd*U	JW3310 *sly*X	JW3339 *yhf*S	JW3377 *gnt*Y	JW3430 *yhh*F	JW3475 *yhi*F	JW3490 *yhj*D	JW3524 *yia*G	JW3559 *yia*W	JW3630 *yic*H

Plate #37/38

	1	2	3	4	5	6	7	8	9	10	11	12
A	JW3633 *setC*	JW3674 *yidA*	JW3733 *hsrA*	JW3809 *rmuC*	JW3849 *yihQ*	JW3892 *yiiR*	JW3963 *yjaG*	JW3990 *yjbA*	JW4025 *yjcD*	JW4069 *phnA*	JW4101 *yjeH*	JW4136 *yjeB*
B	JW5965 *yicS*	JW3688 *mdtL*	JW3737 *yijE*	JW3830 *yihD*	JW3850 *yihR*	JW3893 *yiiS*	JW3965 *yjaH*	JW3998 *yjbI*	JW4026 *yjcE*	JW4070 *yjdA*	JW4105 *yjeJ*	JW4138 *rlmB*
C	JW3640 *ade*	JW3690 *yieE*	JW3738 *yijB*	JW3834 *yihG*	JW3852 *yihT*	JW3899 *yiiU*	JW3972 *yjaB*	JW4005 *yjbJ*	JW4027 *yjcF*	JW4076 *adiC*	JW4106 *yjeK*	JW4139 *yjfI*
D	JW3651 *yidG*	JW3691 *yieF*	JW5597 *rffC*	JW3837 *yihI*	JW3853 *yihU*	JW3908 *yiiX*	JW3982 *yjbC*	JW4007 *yjbL*	JW4028 *actP*	JW4082 *yjdF*	JW4118 *yjeN*	JW4140 *yjfJ*
E	JW3652 *yidH*	JW3692 *yieG*	JW3779 *cyaY*	JW3843 *yihL*	JW3859 *yiiD*	JW3916 *yijF*	JW3983 *yjbD*	JW4008 *yjbM*	JW4029 *yjcH*	JW4087 *yjdI*	JW4119 *yjeO*	JW4141 *yjfK*
F	JW3653 *yidI*	JW3693 *yieH*	JW3783 *yigA*	JW3844 *yihM*	JW3867 *yiiG*	JW3927 *yijP*	JW3986 *yjbE*	JW4017 *yjbQ*	JW4039 *yjcO*	JW4088 *yjdJ*	JW4120 *yjeP*	JW4142 *yjfL*
G	JW3654 *yidJ*	JW3694 *yieI*	JW3785 *yigB*	JW3845 *yihN*	JW3871 *frvA*	JW3936 *yijD*	JW3988 *yjbG*	JW4018 *yjbR*	JW4041 *yjcP*	JW4089 *yjdK*	JW4124 *yjeS*	JW4143 *yjfM*
H	JW3655 *yidK*	JW3695 *cbrC*	JW3790 *yigF*	JW3846 *ompL*	JW3886 *fieF*	JW5548 *nudC*	JW3989 *yjbH*	JW4022 *yjcC*	JW4043 *yjcR*	JW4091 *yjdL*	JW4134 *yjeT*	JW4144 *yjfC*

Plate #39/40

	1	2	3	4	5	6	7	8	9	10	11	12
A	JW4148 *yjfP*	JW4179 *ytfM*	JW4207 *yjgI*	JW5968 *yjhX*	JW4303 *yjiR*	JW4350 *ytjB*	JW0698 *phr*	JW1831 *holE*	JW3835 *polA*	JW4312 *hsdM*	JW0102 *hofC*	JW0306 *betT*
B	JW4149 *ulaR*	JW4180 *ytfN*	JW4212 *yjgD*	JW4271 *yjhR*	JW4304 *yjiS*	JW4354 *yjjK*	JW1048 *dinI*	JW1850 *ruvA*		JW4314 *mrr*	JW0103 *hofB*	JW0327 *codB*
C	JW4157 *yjfY*	JW4181 *ytfP*	JW4220 *yjgR*	JW4288 *yjiC*	JW4316 *yjiX*	JW4365 *yjjY*	JW1100 mf*d*	JW1852 *ruvC*	JW4004 *dinF*	BW25113 **Wild type**	JW0108 *aroP*	JW0332 *cynX*
D	JW4162 *yjfZ*	JW4182 *yzfA*	JW4258 *yjhF*	JW4292 *yjiG*	JW4336 *yjjG*	JW4366 *yjtD*	JW1173 *umuC*	JW1854 *nudB*	JW4019 *uvrA*	JW4334 *holD*	JW0123 *yadG*	JW0358 *tauB*
E	JW4167 *ytfE*	JW4186 *ytfQ*	JW4259 *yjhG*		JW4340 *yjjU*	JW0387 *sbcC*	JW1343 *recT*	JW1944 *dcm*	JW4128 *mutL*	JW0018 *nhaA*	JW0147 *fhuC*	JW0359 *tauC*
F	JW4169 *ytfG*	JW4193 *yjgA*	JW4261 *yjhI*		JW4342 *yjjW*	JW0456 *priC*	JW1355 *ydaV*	JW1991 *sbmC*	JW4159 *priB*	JW0044 *yaaU*	JW0148 *fhuD*	JW0386 *araJ*
G	JW4175 *ytfJ*	JW4205 *pyrL*	JW4268 *yjhP*	JW4299 *yjiN*	JW4343 *yjjI*	JW0461 *recR*	JW1602 *tus*	JW2053 *alkA*	JW4216 *holC*	JW0046 *kefC*	JW0149 *fhuB*	JW0391 *brnQ*
H	JW4177 *ytfL*	JW4206 *yjgH*	JW4269 *yjhQ*	JW4300 *yjiO*	JW4348 *yjjJ*	JW0674 *seqA*	JW1752 *topB*	JW2200 *alkB*	JW4311 *hsdS*	JW0069 *setA*	JW0195 *metN*	JW0438 *mdlA*

Plate #41/42

	1	2	3	4	5	6	7	8	9	10	11	12
A	JW0441 *amt*B	JW0579 *fep*E	JW0077 *ilv*H	JW0593 *ybd*L	JW1253 *trp*B	JW1391 *paa*I	JW1736 *ast*A	JW2028 *wca*M	JW2414 *cys*M	JW2839 *yge*X	JW3645 *ilv*N	JW3910 *met*B
B	JW0451 *acr*B	JW0580 *fep*C	JW0232 *pro*B	JW0854 *lta*E	JW1255 *trp*D	JW1392 *paa*J	JW1750 *gdh*A	JW2029 *wca*L	JW2535 *gly*A	JW2880 *ser*A	JW3646 *ilv*B	JW3929 *arg*E
C	JW0454 *kef*A	JW0002 *thr*B	JW0233 *pro*A	JW0890 *ser*C	JW1256 *trp*E	JW1394 *paa*X	JW1789 *yea*U	JW2043 *wcaB*	JW2537 *gln*B	JW2975 *met*C	JW3722 *asn*A	JW3932 *arg*H
D	JW0473 *cop*A	JW0036 *cai*C	JW0253 *mmu*M	JW0891 *aro*A	JW1295 *puu*E	JW1576 *spe*G	JW2001 *his*G	JW2316 *usg*	JW2580 *phe*A	JW3194 *nan*A	JW3742 *ilv*M	JW3973 *met*A
E	JW0475 *yba*T	JW0070 *leu*D	JW0266 *arg*F	JW0911 *asp*C	JW1383 *paa*A	JW1683 *aro*D	JW2002 *his*D	JW2326 *aro*C	JW2581 *tyr*A	JW3242 *aro*E	JW5606 *ilv*E	JW3979 *met*H
F	JW0479 *ybb*L	JW0071 *leu*C	JW0377 *pro*C	JW0989 *wrb*A	JW1384 *paa*B	JW1694 *aro*H	JW2003 *his*C	JW2337 *six*A	JW2582 *aro*F	JW3322 *arg*D	JW3745 i*lv*A	JW3984 *lys*C
G	JW0484 *ybb*A	JW0073 *leu*A	JW0379 *aro*L	JW1046 *solA*	JW1385 *paa*C	JW1733 *ast*E	JW2007 *his*F	JW2370 *oxc*	JW2786 *arg*A	JW5652 *avt*A	JW3805 *metE*	JW4013 *alr*
H	JW0576 *fes*	JW0074 *leu*L	JW0381 *aro*M	JW1252 *trp*A	JW1387 *paa*E	JW1734 *ast*B	JW2008 *hisI*	JW2407 *cys*K	JW2806 *lys*A	JW3582 *cys*E	JW3841 *gln*A	JW4014 *tyr*B

Plate #43/44

	1	2	3	4	5	6	7	8	9	10	11	12
A	JW4351 *ser*B	JW0578 *ent*F	JW0758 *bio*B	JW0810 *moe*B	BW25113 **Wild type**	JW2187 *ccm*C	JW2558 *nad*B	JW3198 *ssp*A	JW3942 *coa*A	JW0231 *pho*E	JW0922 *ycb*R	JW1062 *flg*D
B	JW4355 *slt*	JW0585 *ent*C	JW0759 *bio*F	JW0811 *moe*A	JW1801 *pab*B	JW2188 *ccm*B	JW2566 *trx*C	JW3323 *pab*A	JW3953 *thi*H	JW0372 *ddl*A	JW1022 *csg*E	JW1063 *flg*E
C	JW0051 *pdx*A	JW0586 *ent*E	JW0760 *bio*C	JW0833 *grx*A	JW1969 *cob*T	JW2255 *men*E	JW2663 *gsh*A	JW3775 *hem*X	JW3957 *thi*E	JW0431 *ppi*D	JW1024 *csg*B	JW1064 *flg*F
D	JW0105 *nad*C	JW0587 *ent*B	JW0761 *bio*D	JW0914 *pnc*B	JW1970 *cob*S	JW2256 *men*C	JW2783 *ygd*L	JW5581 *ubi*E	JW3958 *thi*C	JW0519 *sfm*A	JW1025 *csg*A	JW1065 *flg*G
E	JW0129 *pan*C	JW0623 *lip*A	JW0765 *moa*B	JW1331 *abg*B	JW1971 *cob*U		JW2857 *idi*	JW3820 *fre*	JW4349 *lpl*A	JW0520 *sfm*C	JW1057 *flg*N	JW1067 *flg*I
F	JW0130 *pan*B	JW0633 *cob*C	JW0766 *moa*C	JW1388 p*aa*F	JW2041 w*ca*D	JW2317 *pdx*B	JW2863 *fld*B	JW3829 *mob*A	JW0135 *htr*E	JW0628 *rlp*A	JW1059 *flg*A	JW1068 *flg*J
G	JW0413 *thi*I	JW0733 *nad*A	JW0767 *moa*D	JW1389 *paa*G	JW2091 *thi*M	JW2429 *hem*F	JW2874 *vis*C	JW3900 *rra*A	JW0192 *rcs*F	JW0707 *ybg*P	JW1060 *flg*B	JW1069 *flg*K
H	JW0415 *pan*E	JW0757 *bio*A	JW0768 *moa*E	JW1628 *pdx*Y	JW2186 *ccm*D	JW2548 *pdx*J	JW2914 *gsh*B	JW3901 *men*A	JW0230 *crl*	JW0709 *ybg*D	JW1061 *flg*C	JW1093 *nag*Z

Plate #45/46

	1	2	3	4	5	6	7	8	9	10	11	12
A	JW1496 *ydeQ*	JW1869 *flhB*	JW1923 *fliG*	JW1935 *rcsA*	JW3112 *yraI*	JW3604 *rfaS*	JW5599 *rffD*	JW4277 *fimA*	JW0462 *htpG*	JW1283 *sapF*	JW1876 *cheW*	JW2764 *syd*
B	JW1500 *hipA*	JW1880 *flhC*	JW1925 *fliI*	JW2020 *wbbH*	JW3175 *mtgA*	JW3605 *rfaP*	JW5598 *rffG*	JW4279 *fimC*	JW0598 *ahpC*	JW1417 *trg*	JW1878 *motB*	JW2861 *dsbC*
C	JW1633 *slyB*	JW1905 *fliY*	JW1927 *fliK*	JW2022 *rfbX*	JW3594 *rfaD*		JW3763 *rffH*	JW4281 *fimF*	JW0941 *sulA*	JW1477 *osmC*	JW1879 *motA*	JW2988 *ygiS*
D	JW1660 *ydhU*	JW1908 *fliC*	JW1928 *fliL*	JW2163 *spr*	JW3595 *rfaF*	JW3607 *rfaQ*	JW3770 *rffM*	JW4283 *fimH*	JW0985 *cbpA*	JW1561 *dicC*	JW1886 *otsB*	JW3142 *secG*
E	JW1698 *nlpC*	JW1909 *fliD*	JW1929 *fliM*	JW2336 *yfcV*	JW3597 *rfaL*		JW3818 *rfaH*	BW25113 **Wild type**	JW1165 *minC*	JW1566 *dicB*	JW2183 *ccmG*	JW3146 *rrmJ*
F	JW1728 *osmE*	JW1910 *fliS*	JW1930 *fliN*	JW2428 *amiA*	JW3600 *rfaY*		JW4097 *cutA*	JW0014 *dnaJ*	JW1236 *oppB*	JW1720 *cedA*	JW2465 *bcp*	JW3286 *gspC*
G		JW1911 *fliT*	JW1932 *fliP*	JW2601 *smpB*	JW3601 *rfaJ*	JW3758 *rfe*	JW4103 *groL*	JW0303 *betA*	JW1239 *oppF*	JW1721 *katE*	JW2510 *hscA*	JW3288 *gspE*
H	JW1868 *flhA*	JW1922 *fliF*	JW1933 *fliQ*	JW2982 *yqhH*	JW3602 *rfaI*	JW5600 *rffE*	JW4192 *mpl*	JW0304 *betB*	JW1275 *osmB*	JW1873 *cheR*	JW2654 *proX*	JW3289 *gspF*

Plate #47/48

	1	2	3	4	5	6	7	8	9	10	11	12
A	JW3290 *gspG*	JW3684 *trmE*	JW0495 *gcl*	JW0987 *agp*	JW1595 *pntA*	JW2025 *rfbD*	JW2487 *ppx*	JW2734 *cysJ*	JW2924 *ansB*	JW3300 *chiA*	JW3794 *pldA*	JW4034 *nrfD*
B	JW3291 *gspH*	JW0116 *speD*	JW0510 *ybcF*	JW0999 *putA*	JW1611 *hdhA*	JW2026 *rfbB*	JW2525 *hcaB*	JW2759 *gudX*	JW2946 *glcD*	JW3414 *ugpQ*	JW5584 *pldB*	JW4036 *nrfF*
C	JW3293 *gspJ*	JW0181 *ldcC*	JW0661 *nagD*	JW1005 *phoH*	JW1643 *gloA*	JW2027 *galF*	JW2636 *gabD*	JW2768 *sdaB*	JW2947 *glcC*	JW3485 *gadA*	JW3913 *metF*	JW4037 *nrfG*
D	JW3294 *gspK*	JW0202 *gloB*	BW25113 **Wild type**	JW1178 *dadA*	JW1756 *ansA*	JW2033 *cpsG*	JW2720 *cysC*	JW2842 *yqeA*	JW2956 *gss*	JW3553 *sgbH*	JW4053 *phnP*	JW4040 *fdhF*
E	JW3309 *fkpA*	JW0315 *yahI*	JW0664 *nagB*	JW1179 *dadX*	JW1803 *sdaA*	JW2037 *fcl*	JW2721 *cysN*	JW2871 *gcvP*	JW2972 *yghA*	JW3591 *tdh*	JW3866 *fdhD*	JW4198 *treC*
F	JW3324 *fic*	JW0330 *cynT*	JW0680 *speF*	JW1310 *ycjU*	JW2010 *ugd*	JW2038 *gmd*	JW2722 *cysD*	JW2872 *gcvH*		JW3592 *kbl*	JW3895 *fpr*	JW4222 *idnT*
G	JW3513 *dppA*	JW0331 *cynS*	JW0808 *ybiY*	JW1488 *gadB*	JW2023 *rfbC*	JW2233 *glpQ*	JW2732 *cysH*	JW2873 *gcvT*	JW3181 *gltF*	JW5594 *aslB*	JW4031 *nrfA*	JW4223 *idnO*
H		JW0469 *ushA*	JW0963 *appA*	JW1594 *pntB*	JW2024 *rfbA*	JW2363 *dsdA*	JW2733 *cysI*	JW2905 *speA*	JW3192 *nanE*	JW3773 *aslA*	JW4033 *nrfC*	JW4224 *idnD*

Plate #49/50

	1	2	3	4	5	6	7	8	9	10	11	12
A	JW4225 *idn*K	JW0442 *tes*B	JW2031 *wzx*C		JW0156 *dgt*	JW0494 *all*R	JW0762 *uvr*B	JW5727 *phn*K	BW25113 **Wild type**	JW0567 *nfn*B	JW0955 *hya*B	JW1217 *nar*J
B	JW4285 *uxu*A	JW0465 *aes*	JW2218 *ato*B	JW4030 *acs*	JW0178 *rnh*B	JW0500 *all*B	JW0871 *trx*B	JW4060 *phn*I	JW0336 *lac*I	JW0606 *cit*X	JW0956 *hya*C	JW1218 *nar*I
C	JW4286 *uxu*B	JW0975 *ymc*E	JW2433 *eut*C	JW0028 *rih*C		JW0511 *pur*K	JW0893 *cm*k	JW4062 *phn*G	JW0338 *mhp*A	JW0609 *cit*D	JW0958 *hya*E	JW1224 *gal*U
D	JW0035 *cai*D	JW1077 *fab*H	JW2804 *aas*	JW0031 *car*B	JW0228 *gpt*	JW0512 *pur*E	JW0928 *pyr*D	JW4092 *cad*A	JW0342 *mhp*F	JW0740 *gal*K	JW0959 *hya*F	JW1293 *puu*C
E	JW0039 *cai*T	JW1081 *fab*F	JW3314 *kef*G	JW0048 *apa*H	JW0328 *co*dA	JW0602 *rnk*	JW1049 *pyr*C	JW4172 *cys*Q	JW0343 *mhp*E	JW0741 *gal*T	JW0981 *tor*C	JW1412 *ald*A
F	JW0041 *fix*B	JW1263 *yci*K	JW3765 *rff*A	JW0050 *ksg*A	JW0388 *sbc*D	JW0603 *rna*	JW1220 *pur*U	JW0043 *fix*X	JW0347 *frm*A	JW0742 *gal*E	JW0982 *tor*A	JW1439 *ydc*W
G	JW0042 *fix*C	JW1532 *ydf*G	JW3766 *wzx*E	JW0101 *gua*C	JW0412 *xse*B	JW0646 *rih*A	JW1226 *tdk*	JW0045 *kef*F	JW0393 *mal*Z	JW0879 *dms*C	JW1051 *grx*B	JW1460 *nar*V
H	JW0408 *pgp*A	JW1653 *cfa*	JW3889 *cdh*	JW0155 *pfs*	JW0466 *gsk*	JW0704 *nei*		JW0142 *sfs*A	JW0448 *maa*	JW0954 *hya*A	JW1184 *ymg*E	JW1461 *nar*W

Plate #51/52

	1	2	3	4	5	6	7	8	9	10	11	12
A	JW1462 *nar*Y	JW1605 *man*A	JW1792 *yea*X	JW2120 *bgl*X	JW2194 *nap*A	JW2439 *eut*E	JW2675 *gut*M	JW2697 *hyp*B	JW3033 *ttd*A	JW3328 *nir*B	JW3391 *glg*P	JW3543 *mal*S
B	JW1463 *nar*Z	JW1608 *uid*B	JW1816 *kdg*R	JW2155 *fru*K	JW2196 *nap*F	BW25113 **Wild type**	JW5433 *hyp*F	JW2698 *hyp*C	JW3034 *ttd*B	JW3329 *nir*D	JW3392 *glg*A	JW3545 *yia*I
C	JW1470 *fdn*G	JW1609 *uid*A	JW1839 *eda*	JW2182 *ccm*H	JW2215 *ato*D	JW2523 *hca*F	JW2683 *hyd*N	JW2699 *hyp*D	JW5511 *ebg*A	JW3342 *php*	JW3394 *glg*X	JW3552 *lyx*K
D	JW1472 *fdn*I	JW1614 *mal*Y	JW1840 *edd*	JW2184 *ccm*F	JW2216 *ato*A	JW2524 *hca*C	JW2686 *asc*B	JW2811 *kdu*I	JW3048 *ebg*C	JW3352 *aro*B	JW3395 *glg*B	JW3574 *mtl*D
E	JW1512 *tam*	JW1620 *rsx*B	JW1862 *tor*Y	JW2185 *ccm*E	JW2235 *glp*A	JW2526 *hca*D	JW2689 *hyc*G	JW2884 *yli*K	JW3052 *fad*H	JW3379 *mal*Q	JW3487 *tre*F	JW3579 *lld*R
F	JW1514 *uxa*B	JW1622 *rsx*D	JW1912 *amy*A	JW2190 *nap*C	JW2236 *glp*B	JW2536 *hmp*	JW2690 *hyc*F	JW2962 *hyb*C	JW3062 *uxa*A	JW5687 *glp*G	JW3536 *xyl*B	JW3585 *grx*C
G	JW1579 *ynf*E	JW1624 *rsx*E	JW2039 *wca*F	JW2192 *nap*H	JW2237 *glp*C	JW2648 *nrd*H	JW2691 *hyc*E	JW2965 *hyb*O	JW3063 *uxa*C	JW3388 *glp*E	JW3537 *xyl*A	JW3699 *bgl*B
H	JW1581 *ynf*G	JW1723 *chb*F	JW2075 *gat*D	JW2193 *nap*G	JW2436 *eut*H	JW2674 *srl*D	JW2696 *hyp*A	JW2978 *yqh*D	JW3155 *sfs*B	JW3389 *glp*D	JW3541 *xyl*R	

Plate #53/54

	1	2	3	4	5	6	7	8	9	10	11	12
A	BW25113 **Wild type**	JW3863 *fdo*I	JW1793 *rnd*	JW2171 *rsu*A	JW2553 *lep*A	JW3617 p*yr*E	JW4204 *pyr*B	JW0492 y*bb*S	JW1556 *rel*B	JW3076 *yh*aJ	JW4068 *phn*B	JW0647 *glt*L
B		JW3865 *fdo*G	JW1838 *pur*T	JW2309 *pur*F		JW3857 *rbn*	JW4313 *hsd*R	JW0549 *noh*B	JW2115 m*lr*A	JW3197 *ssp*B	JW4360 *cre*A	JW0648 *glt*K
C		JW1273 *pyr*F	JW1943 *vsr*	JW2397 *xap*B	JW2650 *nrd*E	JW3969 *pur*D	JW4344 *deo*C	JW0979 *tor*T	JW2231 *ina*A	JW3212 *aae*R	JW0205 *dna*Q	JW0649 *glt*J
D		JW1344 *rec*E	JW1963 *amn*	JW2398 *xapA*	JW2651 *nrd*F	JW4135 *pur*A	JW4345 *deo*A	JW1145 *mcr*A	JW2452 *aeg*A	JW3661 *yid*P	JW0221 *din*B	JW0665 *nag*E
E	JW3731 *rbs*K	JW1615 *add*	JW2050 *dcd*	JW2484 *pur*M		JW4171 *cpd*B	JW4347 *deo*D	JW1149 *ycg*E	JW2755 *rel*A	JW3702 *pho*U	JW0582 *fep*D	JW0679 *pot*E
F	JW5578 *fad*A	JW1625 *nth*	JW2131 *cdd*	JW2485 *pur*N	JW2809 *ara*E	JW4196 *nrd*G	JW0298 *ykg*D	JW1313 *ycj*W	JW2837 *yge*V	JW3778 *cya*A	JW0584 *fep*B	JW0684 *kdp*C
G	JW3822 *fad*B	JW1738 *xth*A	JW2146 *nfo*	JW2493 *xse*A	JW2860 *rec*J	JW4197 *nrd*D	JW0440 *gln*K	JW1379 *fea*R	JW3032 *ygi*P	JW3926 *yij*O	JW0604 *cit*T	JW0686 *kdp*A
H	JW3862 *fdh*E	JW1748 *nud*G	JW2149 *rih*B	JW2541 *pur*L	JW2912 *end*A	JW4203 *pyr*I	JW0476 *cue*R	JW1382 *mao*C		JW3977 *arp*A	JW0622 *tat*E	JW0734 *pnu*C

Plate #55/56

	1	2	3	4	5	6	7	8	9	10	11	12
A	JW0744 *mod*E	JW0815 *yli*C	JW0887 *foc*A	JW1110 *pot*C	JW1285 *sap*C	JW1438 *ydc*V	JW1521 *yde*A	JW1726 *chb*C	JW1888 *ara*G	JW2117 *ye*hX	JW3704 *pst*A	JW3888 *sbp*
B	JW0747 *mod*B	JW0826 *cmr*	JW0916 *ssu*B	JW1112 *pot*A	JW1286 *sap*B	JW1478 *ddp*F	JW1597 *ydg*I	JW1727 *chb*B	JW1889 *ara*F	JW2135 *mgl*C	JW3705 *pst*C	JW3898 *glp*F
C	JW0748 *mod*C	JW0838 *pot*F	JW0932 *uup*	JW1175 *nha*B	JW1287 *sap*A	JW1479 *ddp*D	JW1613 *malX*	JW1758 *ydj*E	JW1893 *ftn*	JW2136 mg*lA*	JW3706 *pst*S	JW3921 *frw*C
D	JW0769 *ybh*L	JW0841 *pot*I	JW0953 *ycc*A	JW1207 *cha*A	JW1304 *ycj*O	JW1480 *ddp*C	JW1699 *btu*D	JW1806 *man*X	JW1895 *tyr*P	JW2137 *mgl*B	BW25113 **Wild type**	JW3922 *frw*B
E	JW0794 *gln*Q	JW0845 *art*M	JW1001 *put*P	JW1208 *cha*B	JW1305 *ycj*P	JW1481 *ddp*B	JW1700 *btu*E	JW1808 *man*Z	JW1903 *yec*S	JW2143 *lys*P	JW3728 *rbs*A	JW3925 *frw*D
F	JW0795 *glnP*	JW0846 *art*Q	JW1040 *mdt*G	JW1238 *opp*D	JW1311 *ycj*V	JW1487 *gad*C	JW1701 *btu*C		JW1962 *shi*A	JW3658 *glv*G	JW3729 *rbs*C	JW3938 *btu*B
G	JW0796 *gln*H	JW0847 *art*I	JW1087 *pts*G	JW1242 *kch*	JW1358 *trk*G	JW1490 *ydd*B	JW1718 *ydj*N	JW1847 *znu*C	JW2076 *gat*C	JW3659 *glv*B	JW3789 *cor*A	JW3991 *xyl*E
H	JW0804 *ybi*T	JW0848 *art*P	JW1109 *pot*D	JW1284 *sap*D	JW1436 *ydc*T	JW1506 *ego*	JW1725 *chb*A	JW1848 *znu*B	JW2085 *yeg*T	JW3700 *bgl*F	JW3878 *rha*T	JW3992 *mal*G

Plate #57/58

	1	2	3	4	5	6	7	8	9	10	11	12
A	JW3993 *malF*	JW4072 *proP*	JW4247 *fecE*	JW0226 *prfH*	JW1053 *rimJ*	JW2173 *rplY*	JW2473 *hyfH*	JW2362 *dsdX*	JW2415 *cysA*	JW2531 *yphE*	JW2767 *sdaC*	JW2973 *exbD*
B	JW3994 *malE*	JW4081 *melB*	JW4249 *fecC*	JW0395 *queA*	JW1072 *rluC*	JW2249 *yfbG*	BW25113 **Wild type**	JW2380 *ypdD*	JW2417 *cysU*	JW2638 *gabP*	JW2772 *fucP*	JW2974 *exbB*
C	JW3995 *malK*	JW4084 *dcuB*	JW4251 *fecA*	JW0396 *tgt*	JW1075 *rpmF*	JW2315 *truA*	JW2154 *fruA*	JW2388 *mntH*	JW2418 *cysP*	JW2652 *proV*	JW2797 *ptsP*	JW3064 *exuT*
D	JW4038 *gltP*	JW4093 *cadB*	JW4264 *sgcA*	JW0514 *ppiB*	JW1423 *rimL*	JW2467 *hyfB*	JW2156 *fruB*	JW2389 *nupC*	JW2454 *acrD*	JW2653 *proW*	JW2813 *yqeG*	JW3101 *kbaZ*
E	JW4047 *alsC*	JW4166 *cycA*	JW4284 *gntP*	JW0836 *rimK*	JW5962 *sra*	JW2469 *hyfD*	JW2199 *yojI*	JW2406 *cysZ*	JW2477 *focB*	JW2673 *srlB*	JW2850 *ygfO*	JW3105 *agaS*
F	JW4049 *alsB*	JW4168 *ytfF*	JW4331 *fhuF*	JW0843 *rumB*	JW1707 *rpmI*	JW2470 *hyfE*	JW2217 *atoE*	JW2408 *ptsH*	JW2478 *yfgO*	JW5435 *ascF*	JW2900 *cmtA*	JW3106 *kbaY*
G	JW4066 *phnD*	JW4199 *treB*	JW4363 *creD*	JW0868 *aat*	JW1753 *selD*	JW2471 *hyfF*	JW2303 *hisP*	JW2409 ptsI	JW2482 *uraA*	JW2710 *ygbN*	JW2901 *cmtB*	JW3107 *agaB*
H	JW4067 *phnC*	JW4201 *mgtA*	JW0024 *ileS*	JW0936 *rmf*	JW1811 *rrmA*	JW2472 *hyfG*	JW2306 *hisJ*	JW2410 *crr*	JW2530 *yphD*	JW2760 *gudP*	JW2955 *pitB*	JW3108 *agaC*

Plate #59/60

	1	2	3	4	5	6	7	8	9	10	11	12
A	JW3110 *agaI*	JW3251 *trkA*	JW3416 *ugpE*	JW3443 *nikC*	JW3512 *dppB*	JW0033 *caiF*	JW0418 *cyoE*	JW0919 *ssuA*	JW1302 *ycjM*	JW1833 *exoX*	JW1934 *fliR*	JW2263 *elaC*
B	JW3130 *mtr*	JW3252 *mscL*	JW3417 *ugpA*	JW3444 *nikD*	JW3538 *xylF*	JW0067 *tbpA*	JW0499 *ybbW*	JW1039 *msyB*	JW1322 *mppA*	JW1861 *torZ*	JW1993 *sbcB*	JW2345 *intS*
C	JW3162 *yrbF*	JW3298 *bfr*	JW3418 *ugpB*	JW3445 *nikE*	JW3539 *xylG*	JW0076 *ilvI*	JW0597 *dsbG*	JW1111 *potB*	JW1380 *feaB*	JW1863 *cutC*	JW2004 *hisB*	JW2375 d*dg*
D	JW3168 *yhbG*	JW3313 *kefB*	JW3420 *livG*	JW3460 *pitA*	JW3540 *xylH*	BW25113 **Wild type**	JW0608 *citE*	JW1119 *trmU*		JW1870 *cheZ*	JW2006 *hisA*	JW2416 *cysW*
E	JW3171 *ptsN*	JW3315 *yheS*	JW3421 *livM*	JW3496 *dctA*	JW3573 *mtlA*	JW0254 *afuC*	JW0610 *citC*	JW1144 *pin*	JW1420 *mdoD*	JW1887 *araH*	JW2100 *mrp*	JW2434 *eutB*
F	JW3173 *npr*	JW3371 *feoA*	JW3422 *livH*	JW3509 *dppF*	JW3628 *gltS*	JW0340 *mhpC*	JW0743 *modF*	JW1254 *trpC*	JW5907 *yncB*	JW1898 *uvrC*	JW2240 *yfaV*	JW2437 *eutG*
G	JW3196 *dcuD*	JW3372 *feoB*	JW3423 *livK*	JW3510 *dppD*	JW3629 *yicE*	JW0357 *tauA*	JW0780 *ybiH*	JW1289 *puuP*	JW1474 *adhP*	JW1906 *fliZ*	JW2254 *pmrD*	JW2464 *gcvR*
H	JW3250 *rsmB*	JW5690 *gntT*	JW3441 *nikA*	JW3511 *dppC*	JW3641 *uhpT*	JW0374 *phoA*	JW0844 *artJ*	JW1296 *pspF*	JW1492 *ydeM*	JW1924 *fliH*	JW2260 *menF*	JW2466 *hyfA*

Plate #61/62

	1	2	3	4	5	6	7	8	9	10	11	12
A	JW2475 *hyfJ*	JW2915 *yqgE*	JW3102 *agaV*	JW3226 *panF*	JW3025 *glnE*	JW3611 *rpmG*	JW4107 *efp*	JW0538 *rusA*	JW3385 *rtcR*	JW0107 *ampE*	JW0496 *hyi*	
B	JW2483 *upp*	JW2917 *yggR*	JW3126 *yhbT*	JW3253 *yhdL*	JW3135 *truB*	JW3815 *tatC*	JW4129 *miaA*	JW0781 *rhlE*	JW3468 *arsR*	JW0275 *intF*	JW0526 *ybcC*	JW0728 *tolR*
C	JW2598 *smpA*	JW2926 *yggL*	BW25113 **Wild type**	JW3312 *yheV*	JW3227 *prmA*	JW3858 *dtd*	JW4158 *rpsF*	JW0983 *torD*	JW3756 *rho*	JW0316 *yahJ*	JW0531 *emrE*	JW0729 *tolA*
D	JW2639 *csiR*	JW2932 *nupG*	JW3148 *greA*	JW3330 *nirC*		JW3907 *rpmE*	JW4161 *rplI*	JW1586 *dgsA*	JW4178 *msrA*	JW0346 *frmB*	JW0544 *ybcS*	JW0864 *cspD*
E	JW2735 *ygcM*		JW3157 *yrbA*	JW3333 *frlA*	JW3311 *slyD*	JW3943 *tufB*	JW4194 *pmbA*	JW2088 *yegW*	JW4262 *sgcR*	JW0368 *sbmA*	JW0546 *borD*	JW0918 *ssuD*
F	JW2847 *ssnA*	JW3065 *exuR*	JW3176 *elbB*		JW3326 *ppiA*	JW3946 *rplK*	JW4333 *rsmC*	JW2554 *rseC*	JW4359 *rob*	JW0423 *ampG*	JW0558 *nfrB*	JW0933 *pqiA*
G	JW2869 *bglA*	JW5806 *tdcD*	JW3193 *nanT*	JW2713 *pcm*	JW3563 *selB*	JW4050 *rpiR*	JW4335 *rimI*	JW2555 *rseB*		JW0445 *ybaA*	JW0590 *cstA*	JW0934 *pqiB*
H	JW2913 *yggJ*	JW3091 *yhaB*	JW3216 *rng*	JW2858 *lysS*	JW3564 *selA*	JW4090 *lysU*		JW3000 *cpdA*	JW0106 *ampD*	JW0468 *fsr*	JW0720 *mngA*	JW0974 *cspG*

Plate #63/64

	1	2	3	4	5	6	7	8	9	10	11	12
A	JW1126 *intE*	JW1345 *racC*	JW1549 *cspB*	JW2067 *ogrK*	JW2480 *yfgD*	BW25113 **Wild type**	JW3525 *cspA*	JW3425 *livJ*	JW3627 *recG*	JW3897 *glpK*	JW4099 *aspA*	JW5967 *sgcB*
B	JW1127 *ymfG*	JW1381 *tynA*	JW1550 *cspF*	JW2132 *sanA*	JW2513 *iscU*	JW3234 *acrF*	JW3664 *ibpA*	JW3469 *arsB*	JW3662 *yidE*	JW3911 *metL*	JW4100 *fxsA*	JW4338 *osmY*
C	JW1297 *pspA*	JW1425 *tehA*	JW1573 *rspA*	JW2141 *yeiG*	JW2602 *intA*	JW3348 *gph*	JW3894 *yiiT*	JW3493 *yhjH*	JW3663 *ibpB*	JW3955 *thiS*	JW4108 *ecnB*	JW4341 *yjjV*
D	JW1298 *pspB*	JW1426 *tehB*	JW1642 *nemA*	JW2197 *eco*	JW2660 *emrA*	JW3363 *hslR*	JW3952 *htrC*	JW3499 *bcsZ*	JW3675 *yidB*	JW3956 *thiF*	JW4122 *rsgA*	JW4046 *alsE*
E	JW1299 *pspC*	JW1458 *nhoA*	JW1670 *sufS*	JW2246 *ais*	JW2661 *emrB*	JW3440 *acpT*	JW3369 *greB*	JW3534 *yiaA*	JW3686 *tnaA*	JW3978 *iclR*	JW4127 *amiB*	JW4111 *ampC*
F	JW1300 *pspD*	JW1525 *marB*	JW1812 *cspC*	JW2310 *cvpA*	JW2714 *surE*	JW3461 *yhiO*	JW3370 *yhgF*	JW3561 *aldB*	JW3725 *yieN*	JW4032 *nrfB*	JW4208 *yjgJ*	JW4152 *ulaB*
G	JW1301 *pspE*	JW1538 *pinQ*	JW1884 *yecG*	JW2364 *emrY*	JW2753 *chpA*	JW3462 *uspA*		JW3620 *dinD*	JW3813 *tatA*	JW4035 *nrfE*	JW4248 *fecD*	JW4153 *ulaC*
H	JW1339 *intR*	JW1544 *cspI*	JW2046 *wzb*	JW2365 *emrK*	JW2836 *xdhC*	JW3470 *arsC*	JW3415 *ugpC*	JW3621 *yicG*	JW3838 *hemN*	JW4042 *yjcQ*	JW4250 *fecB*	JW4154 *ulaD*

Plate #65/66

	1	2	3	4	5	6	7	8	9	10	11	12
A	JW4155 *ula*E	JW4236 *yjg*Z	JW1248 *omp*W	JW0669 *fur*	BW25113 **Wild type**	JW2074 *gat*R	JW2906 *yqg*B	JW3092 *yha*C	JW3236 *yhd*W	JW3622 *lig*B	JW3750 *yif*N	JW3935 *fab*R
B	JW4156 *ula*F	JW4327 *yjj*B	JW1926 *fli*J	JW2468 *hyf*C	JW1209 *cha*C	JW2102 *mol*R	JW2910 *gal*P	JW3093 *gar*K		JW5937 *ysd*C	JW3780 *yzc*X	JW4065 *phn*E
C	JW4184 *chp*B	JW4329 *yjj*Q	JW1037 *mdo*H	JW1142 *tfa*E	JW1484 *dos*		JW2925 *ygg*N	JW3095 *gar*L		JW3660 *glv*C	JW3781 *yif*L	JW4080 *mel*A
D	JW4265 *sgc*Q	JW0003 *thr*C	JW1237 *opp*C	JW0291 *eaeH*	JW1541 *noh*A	JW2514 *isc*S	JW2976 *ygh*B	JW3096 *gar*P	JW3449 *yhh*H	JW3740 *ilv*G	JW3803 *yig*M	
E	JW4266 *sgc*C	JW0660 *asn*B	JW2442 *eut*I	JW0657 *ybe*Z	JW1571 *int*Q		JW3058 *ygj*R	JW3103 *aga*W	JW3457 *yhi*L	JW3741 *ilv*G	JW3831 *yih*E	
F	JW3071 *yqj*K	JW0737 *aro*G	JW0482 *ybb*O					JW3179 *glt*B	JW3471 *yhi*S	JW3747 *ilv*C	JW3832 *dsb*A	JW4163 *ytf*A
G	JW3590 *yib*D	JW0127 *pan*D	JW2090 *thi*D	JW0857 *hcp*	JW1710 *arp*B	JW2774 *fuc*K	JW3087 *tdc*C	JW3184 *yhc*E	JW3526 *hok*A	JW3748 *ppi*C	JW3848 *yih*P	JW4211 *arg*I
H	JW3634 *yic*L	JW3961 *hem*E	JW0565 *phe*P	JW1035 *mdo*G		JW2886 *ygf*G	JW3088 *tdc*B	JW3187 *yhc*E	JW3618 *rph*	JW3749 *yif*O	JW3868 *frv*R	JW4227 *int*B

Plate #67/68

	1	2	3	4	5	6	7	8	9	10	11	12
A	JW4234 *yjg*X	JW0687 *kdp*F	JW2579 *phe*L	JW4233 *yjg*W			JW5087 *cit*F	JW5129 *mgs*A	JW5195 *ton*B	JW5230 *ync*N	JW5260 *ynf*F	JW5290 *ydj*K
B	JW4242 *yjh*E	JW1219 *tpr*	JW2878 *zap*A	JW4246 *yjh*V	JW5027 *mmu*P	JW5049 *yki*B	JW5092 *glt*I		JW5199 *yci*X		JW5261 *ynf*H	JW5293 *yea*V
C		JW1257 *trp*L	JW3642 *uhp*C	JW5001 *htg*A		JW5054 *psiF*		JW5141 *ycd*N	JW5201 *puu*A		JW5264 *ynf*K	JW5294 *yea*W
D	JW4302 *yji*Q	JW1390 *paa*H	JW3685 *tna*C	JW5004 *cai*E		JW5061 *mdl*B	JW5104 *yb*hF		JW5203 *ymj*B	JW5242 *ydd*A		JW5298 *yob*H
E		JW1607 *uid*C	JW3739 *ilv*L		JW5034 *ykg*M		JW5117 *hcr*	JW5156 *pls*X	JW5209 *sie*B	JW5244 *yne*L	JW5271 *ydh*X	JW5299 *yeb*Q
F		JW1705 *phe*M	JW3755 *rho*L	JW5011 *lig*T	JW5035 *ykg*M	JW5072 *sfm*F	JW5118 *dms*A		JW5218 *paa*K	JW5251 *ynf*O	JW5911 *yni*D	
G	JW0057 *rlu*A	JW1921 *fli*E	JW3997 *mal*M	JW5018 *mlt*D	JW5040 *ykg*C		JW5121 *ssu*C	JW5182 *dsb*B	JW5225 *hok*B	JW5254 *ynf*N	JW5282 *ast*D	JW5313 *yed*O
H	BW25113 **Wild type**	JW2000 *his*L			JW5046 *mhp*T	JW5078 *nmp*C	JW5122 *ycb*Q		JW5227 *ync*K	JW5257 *ynf*P	JW5286 *ynj*D	JW5913 *int*G

Plate #69/70

	1	2	3	4	5	6	7	8	9	10	11	12
A	JW5316 *fliO*	JW5343 *gatY*	JW5368 *yojL*	JW5401 *guaB*	BW25113 **Wild type**	JW5923 *ygfK*	JW5482 *speC*	JW5494 *hybB*	JW5510 *ygjG*	JW5528 *yraR*	JW5545 *yhdY*	JW5557 *yijE*
B		JW5915 *molR*	JW5374 *menD*		JW5449 amiC	JW5469 *ygfT*	JW5924 *yghE*	JW5926 *yghX*	JW5513 *ygjO*	JW5533 *yhbC*	JW5546 *zraP*	JW5560 *kdgT*
C			JW5387 *torI*			JW5470 *ygfU*	JW5484 *yghF*	JW5496 *yghY*	JW5514 *ygjP*	JW5534 *yhbX*	JW5547 *nfi*	JW5562 *frvB*
D	JW5328 *yoeF*	JW5359 *yeiS*			JW5453 *yqeF*				JW5515 *alx*	JW5538 *nanK*	JW5549 *thiG*	JW5929 *yiiE*
E	JW5330 *yeeF*		JW5394 *ucpA*	JW5421 *ypjJ*	JW5459 *ygeM*	JW5473 *ygfB*	JW5490 *yghQ*	JW5499 *dkgA*	JW5516 *yqjC*		JW5551 *sthA*	
F	JW5331 *yoeB*	JW5363 *bcr*	JW5397 *hda*	JW5425 *ygaQ*	JW5462 *xdhA*		JW5491 *yghS*	JW5927 *ygiB*	JW5519 *yhaO*	JW5540 *yhcN*	JW5553 *argB*	JW5566 *yihX*
G		JW5366 *ccmA*			JW5463 *ygeW*	JW5479 *yggU*	JW5492 *yghU*	JW5505 *yqiC*	JW5526 *garR*	JW5543 *yhdJ*		JW5567 *yihW*
H		JW5367 *napB*	JW5399 *yfgG*	JW5446 *exo*	JW5464 *yqeC*		JW5493 *hybF*	JW5508 *yqiH*	JW5527 *agaA*	JW5544 *yhdX*	JW5555 *ptsA*	JW5568 *yihV*

Plate #71/72

	1	2	3	4	5	6	7	8	9	10	11	12
A	JW5569 *yihS*	JW5590 *yigG*	JW5613 *yieK*	JW5636 *yicO*	JW5650 *sgbU*		JW5669 *hdeB*	JW5680 *yhhT*		JW5705 *gspL*	JW5716 *yjbO*	JW5730 *eptA*
B			BW25113 **Wild type**	JW5637 *yicN*	JW5651 *yiaN*		JW5670 *yhiD*	JW5945 *yhhS*	JW5696 *yhfY*	JW5706 *gspI*		JW5731 *adiA*
C	JW5571 *bipA*	JW5601 *wzzE*		JW5641 *ttk*	JW5654 *yiaB*	JW5663 *bcsF*	JW5672 *yhiQ*		JW5697 *yhfU*	JW5949 *yrdD*	JW5718 *yjcB*	JW5732 *yjdO*
D			JW5631 *cbrA*	JW5643 *yicR*	JW5655 *yiaF*	JW5941 *yhjQ*	JW5674 *yhiK*	JW5683 *yhhL*	JW5698 *frlR*	JW5711 *yjbF*		JW5734 *dipZ*
E	JW5574 *yihF*	JW5605 *ilvD*		JW5644 *htrL*	JW5656 *tiaE*	JW5665 *bcsA*			JW5700 *frlB*			JW5735 *dcuA*
F	JW5580 *tatB*	JW5609 *trkD*	JW5633 *yidQ*	JW5645 *yibQ*	JW5940 *bisC*	JW5942 *bcsC*	JW5676 *rbbA*	JW5691 *gntX*	JW5701 *yhfK*	JW5713 *ubiC*	JW5721 *yjcS*	JW5736 *yjeI*
G	JW5588 *yigI*	JW5611 *atpI*	JW5634 *emrD*	JW5648 *yiaY*	JW5659 *yhjY*	JW5943 *yhjK*	JW5677 *yhhJ*	JW5692 *hslO*	JW5703 *yheO*	JW5714 *zur*		JW5737 *ecnA*
H	JW5589 *rarD*	JW5612 *yieL*			JW5660 *eptB*	JW5668 *kdgK*	JW5678 *yrhC*	JW5694 *yrfA*	JW5704 *gspM*	JW5950 *yjbN*	JW5729 *yjcZ*	JW5738 *sugE*

Plate #73/74

	1	2	3	4	5	6	7	8	9	10	11	12
A	JW5739 *yjeM*	BW25113 **Wild type**	JW5764 *yjgX*	JW5778 *yjhA*	JW5791 *yjtY*	JW5801 *yjjX*	JW5925 *yghJ*	JW5576 *trkH*	JW5627 *dgoR*	JW5954 *yjiV*	JW5010 *yadD*	JW5022 *yafX*
B	JW5741 *rnr*	JW5753 *ytfT*		JW5779 *fimI*	JW5793 *yjjN*	JW0478 *ybbK*	JW5487 *glcE*	JW5931 *tatD*	JW5628 *dgoA*	JW5213 *rzoR*	JW5012 *clcA*	JW5023 *ykfF*
C	JW5743 *yjfO*	JW5754 *yjfF*			JW5794 m*doB*	JW2879 *ygfA*	JW5500 *yqhG*		JW5629 *dgoD*		JW5013 *cdaR*	
D	JW5744 *ulaA*	JW5756 *yjgK*	JW5768 *yjhB*	JW5782 *yjiD*	JW5795 *yjjA*	JW4263 *sgcE*	JW5501 *ygiQ*	JW5585 *rhtB*	JW5699 *frlC*	JW5382 *yfdI*	JW5014 *yaeI*	JW5030 *yagV*
E	JW5745 *ytfB*	JW5757 *yjgL*	JW5769 *yjhC*	JW5783 *yjiH*	JW5796 *yjjP*	JW5429 *srlA*	JW5509 *yqiI*	JW5586 *rhtC*	JW5708 *smf*	JW5386 *ypdJ*	JW5016 *yaeF*	JW5031 *ykgK*
F	JW5746 *fklB*	JW5758 *yjgM*	JW5770 *yjhD*	JW5784 *kptA*	JW5797 *yjjZ*	JW5430 *srlE*	JW5518 *yhaM*	JW5591 *yigE*		JW5946 *gntR*	JW5017 *yafD*	JW5033 *ykgL*
G	JW5747 *ytfH*	JW5759 *yjgN*	JW5952 *yjhU*	JW5785 *yjiL*		JW5467 *ygfQ*	JW5520 *tdcG*	JW5596 *rffT*	JW5748 *ytfI*	JW5005 *yabI*	JW5019 *yafV*	JW5037 *ykgA*
H	JW5749 *ytfK*	JW5763 *yjgX*	JW5775 *yjhH*	JW5786 *yjiM*		JW5477 *yggP*	JW5558 *cpxP*	JW5610 *yieM*	JW5752 *ytfR*	JW5008 *yacG*	JW5020 *fadE*	JW5039 *ykgI*

Plate #75/76

	1	2	3	4	5	6	7	8	9	10	11	12
A	JW5042 *ykgG*	JW5059 *yajR*	JW5082 *cusS*	JW5098 *ybgO*	JW5897 *yliA*	JW5126 *ycbX*	JW5139 *ycdL*	JW5158 *ycfP*	JW5173 *icdC*	JW5187 *dhaK*	JW5208 *lar*	
B	JW5893 *yahH*	JW5062 *ylaB*	JW5083 *ybdF*	JW5099 *ybgQ*	JW5113 *ybjI*	JW5127 *ymbA*	JW5147 *ycdZ*	JW5159 *ycfQ*	JW5174 *ycgG*	JW5196 *yciO*	JW5210 *ydaG*	JW5224 *cybB*
C	JW5044 *yahM*	JW5063 *ylaC*	JW5086 *fepA*	JW5102 *ybhT*	JW5114 *ybjK*	JW5128 *yccS*	JW5150 *ymdC*		JW5901 *ycgH*	JW5197 *yciQ*	JW5211 *ydaW*	JW5226 *ydcI*
D	BW25113 **Wild type**	JW5066 *ybbM*	JW5090 *ybeB*	JW5103 *ybhJ*	JW5116 *ybjT*	JW5130 *yccU*	JW5151 *yceK*	JW5164 *ymfA*	JW5178 *ymgG*	JW5200 *yciW*	JW5212 *rzpR*	JW5228 *ydcM*
E	JW5051 *yaiU*	JW5070 *ybcJ*	JW5091 *ybeQ*	JW5105 *ybiX*	JW5119 *ycaM*	JW5131 *yccX*	JW5152 *yceP*	JW5166 *ymfE*	JW5180 *ycgN*	JW5202 *ycjR*	JW5216 *ydbL*	JW5229 *ydcO*
F	JW5053 *yaiZ*	JW5073 *fimZ*	JW5094 *ybfG*	JW5107 *ybiN*	JW5120 *ycaI*	JW5133 *ymcD*	JW5153 *flgH*	JW5168 *ymfI*	JW5181 *hlyE*	JW5205 *abgA*	JW5217 *paaD*	JW5232 *ydcX*
G	JW5056 *yajI*	JW5079 *rzpD*	JW5095 *ybfH*	JW5108 *ybiO*	JW5123 *ycbV*	JW5136 *ymdF*	JW5155 *yceF*	JW5169 *ymfT*	JW5185 *dhaH*	JW5206 *ydaM*	JW5221 *ydbD*	JW5233 *yncA*
H	JW5058 *yajQ*	JW5081 *ybcV*	JW5096 *kdpE*	JW5109 *fsaA*	JW5124 *ycbF*	JW5137 *ycdG*		JW5172 *stfE*	JW5186 *dhaL*	JW5207 *ydaQ*		JW5177 *ymgD*

Plate #77/78

	1	2	3	4	5	6	7	8	9	10	11	12
A	JW5237 *yncM*	JW5248 *marR*	JW5265 *ydgJ*	JW5276 *ydiQ*	JW5291 *yeaJ*	JW5303 *yebW*	JW5317 *yodD*	JW5339 *yegP*	JW5352 *yehT*	JW5371 *yfaZ*	JW5388 *ypdA*	JW5405 *yphG*
B	JW5238 *sfcA*	JW5249 *marA*	JW5267 *slyA*	JW5280 *pfkB*	JW5292 *yeaP*	JW5306 *yebB*	JW5319 *yedS*	JW5340 *gatR*	JW5353 *yehU*	JW5372 *yfbE*	JW5389 *ypdH*	JW5406 *yphH*
C	JW5239 *bdm*	JW5250 *eamA*	BW25113 **Wild type**	JW5283 *ydjY*	JW5295 *yoaB*	JW5307 *yecD*	JW5323 *yodB*	JW5344 *fbaB*	JW5355 *pbpG*	JW5373 *yfbJ*	JW5391 *yfeA*	JW5407 *yfhK*
D	JW5240 *ddpA*	JW5252 *ydfO*		JW5284 *ynjB*	JW5296 *yoaC*	JW5308 *yecN*		JW5345 *yegX*	JW5356 *yohC*	JW5376 *yfbT*		JW5408 *yfhB*
E	JW5241 *yddV*	JW5253 *gnsB*	JW5270 *ydhO*	JW5285 *ynjC*		JW5309 *yecM*	JW5329 *dacD*	JW5346 *yohN*	JW5358 *yohH*	JW5377 *yfcE*	JW5395 *yfeW*	JW5409 *yfiP*
F	JW5243 *ydeN*	JW5255 *essQ*	JW5272 *ydhV*	JW5287 *ynjE*	JW5300 *proQ*	JW5310 *yecT*	JW5335 *nudD*	JW5349 *yehL*	JW5361 *yeiW*	JW5380 *trmC*	JW5400 *yfgH*	JW5412 *yfiL*
G	JW5245 *yneE*		JW5273 *sufB*	JW5288 *ynjI*	JW5301 *yebU*	JW5312 *otsA*	JW5336 *yegH*	JW5350 *yehP*	JW5362 *yeiP*	JW5381 *yfcM*	JW5402 *yfgJ*	JW5415 *yfjD*
H	JW5247 *yneI*	JW5263 *clcB*	JW5275 *ydiO*	JW5289 *ydjH*	JW5302 *yebV*		JW5338 *mdtA*	JW5351 *yehR*		JW5384 *yfdL*	JW5404 *sseB*	JW5418 *yfjO*

Plate #79/80

	1	2	3	4	5	6	7	8	9	10	11	12
A	JW5419 *yfjP*	JW5438 *ygbF*	JW5455 *yqeJ*	JW5481 *mltC*	JW5776 *sgcX*	JW5507 *yqiG*	JW0696 *ybfD*	JW1282 *ycjD*	JW2729 *ygcK*	JW0026 *fkpB*	JW1464 *narU*	JW5198 *yciX*
B	JW5422 *ypjA*	BW25113 **Wild type**	JW5456 *ygeI*	JW5503 *tolC*	JW5800 *nadR*	JW5542 *yhdP*	JW1455 *ydcC*	JW1822 *yebS*	JW0272 *yagL*	JW2875 *ubiH*	JW5948 *yhfZ*	
C	JW5424 *ypjC*	JW5440 *ygcQ*	JW5457 *pbl*	JW5529 *yhbO*	JW5441 *ygcR*	JW3566 *rhsA*	JW3451 *yhhI*	JW2528 *yphB*	JW0746 *modA*	JW2758 *gudD*	JW4064 *phnE*	JW2549 *recO*
D	JW5426 *yqaC*	JW5444 *ygcE*	JW5458 *ygeK*	JW5531 *deaD*	JW5805 *hyfI*	JW0692 *ybfO*	JW0194 *metI*	JW0055 *yabP*	JW3381 *malT*	JW4056 *phnM*	JW4367 *thrL*	JW2564 *ung*
E	JW5427 *ygaT*	JW5445 *ygcG*	JW5460 *ygeN*		JW5803 *ybhR*	JW0689 *rhsC*	JW0323 *prpB*	JW0285 *yagX*	JW3386 *glpR*	JW3518 *tag*		JW5416 *recN*
F	JW5428 *ygaY*	JW5450 *ygdB*	JW5461 *ygeQ*	JW5577 *yigZ*	JW5142 *ycdR*	JW5679 *rhsB*	JW1730 *ydjQ*	JW0345 *yaiL*	JW1651 *ydhB*	JW3530 *glyS*	JW5076 *ylcG*	JW2703 *mutS*
G	JW5431 *gutQ*	JW5451 *ppdB*	JW5475 *rpiA*			JW0486 *rhsD*	JW1780 *yeaN*	JW0820 *yliH*	JW3384 *rtcB*	JW1572 *rspB*		JW2799 *mutH*
H	JW5437 *rpoS*	JW5454 *yqeH*	JW5476 *ygfI*	JW5707 *gspD*	JW5442 *ygcU*	JW1451 *rhsE*	JW0952 *yccK*	JW1948 *yedS*	JW3650 *yidF*	JW2505 *sseA*		

Plate #81/82

	1	2	3	4	5	6	7	8	9	10	11	12
A	JW2928 *mut*Y	JW3718 *gid*B	JW5146 *ycd*W	JW0617 *crc*A	JW1769 *yea*D	JW1449 *ync*G	JW2054 *yeg*D	JW0533 *ybc*L	JW1693 *ydi*A	JW0487 *ybb*C	JW1985 *yee*T	JW2057 *yeg*K
B	BW25113 **Wild type**	JW3719 *gid*A	JW1321 *ycj*Z	JW1055 *mvi*M	JW1804 *yoa*D	JW1495 *yde*P	JW2060 *mdt*B	JW1229 *ych*E	JW1773 *yea*H	JW0620 *ybe*H	JW1986 *yee*U	JW2098 *yeh*D
C	JW3038 *dna*G	JW3720 *mio*C	JW1494 *yde*O	JW1347 *kil*	JW0124 *yad*H	JW1528 *yde*H	JW1089 *hin*T	JW0320 *yah*N	JW2134 *yei*A	JW0774 *ybh*Q	JW1987 *yee*V	JW2157 *set*B
D	JW3284 *pio*O	JW3784 *xer*C	JW1504 *yde*V	JW1370 *usp*F	JW0196 *gmh*B	JW1621 *rsx*C	JW0700 *ybg*I	JW0265 *yag*I	JW0134 *yad*M	JW0899 *yca*Q	JW2016 *wbb*L	JW2291 *yfb*U
E	JW3350 *dam*	JW0119 *cue*O	JW2097 *yeh*C	JW1536 *ydf*J	JW0802 *ybi*R	JW1668 *ynh*G	JW1678 *ydi*K	JW0280 *yag*T	JW0258 *ykg*N	JW1135 *ymf*N	JW2017 *wbb*K	JW2331 *yfc*Q
F	JW3610 *mut*M	JW0240 *yaf*Y	JW2333 *yfc*S	JW1553 *rem*	JW1096 *ycf*J	JW1671 *suf*D	JW0261 *yag*E	JW1676 *ydi*I	JW0362 *yai*T	JW1665 *ydh*Z	JW2019 *wbb*I	JW2344 *yfd*C
G	JW3626 *trm*H	JW0969 *ymc*C	JW2335 *yfc*U	JW1554 *hok*D	JW1407 *ynb*C	JW1784 *yea*Q	JW0262 *yag*F	JW1511 *lsr*G	JW0383 *yki*A	JW1955 *yed*Z	JW2055 *yeg*I	JW2356 *yfd*P
H	JW3677 *rec*F	JW0998 *ycd*C	JW0049 *apa*G	JW1555 *rel*E	JW1445 *ync*C	JW1965 *yee*O	JW2162 *yei*U	JW1954 *yed*Y	JW0450 *yba*J	JW1961 *yee*L	JW2056 *yeg*J	JW2359 *yfd*S

Plate #83/84

	1	2	3	4	5	6	7	8	9	10	11	12
A	JW2374 *yfd*Y	JW1591 *mdt*I	JW2284 *lrh*A	JW0859 *aqp*Z	JW2907 *yqg*C	JW3373 *yhg*G	JW3774 *hem*Y	JW0001 *thr*A	JW1070 *flg*L	JW3233 *acr*E	JW2637 *gab*T	JW0339 *mhp*B
B	JW2399 *yfe*N	JW1813 *yob*F	JW2573 *clp*B		JW2918 *ygg*S	JW3390 *yzg*L	JW3872 *yii*L	JW0812 *iaa*A	JW1312 *omp*G		JW2944 *glc*G	JW0878 *dms*B
C	JW2490 *yfg*I	BW25113 **Wild type**	JW0063 *ara*C	JW2343 *vac*J	JW2971 *yqh*A	JW3480 *gad*E	JW3971 *yja*A	JW1737 *ast*C	JW1368 *pin*R	JW3599 *rfa*Z	JW3180 *glt*D	JW1215 *nar*G
D	JW2607 *yfj*J	JW0718 *suc*D	JW0719 *mng*R	JW2817 *yqe*K	JW3117 *yra*N	JW3483 *gad*W	JW3980 *yjb*B	JW0588 *ent*A	JW1497 *yde*R	JW3603 *rfa*B	JW3555 *sgb*E	JW1216 *nar*H
E	JW5921 *yfj*S	JW1095 *ndh*	JW2779 *gcv*A	JW2831 *yge*P	JW3178 *yhc*C	JW3492 *yhj*G	JW4272 *yjh*S	JW0904 *smt*A	JW1867 *flh*E	JW3635 *nlp*A	JW4054 *phn*O	JW1294 *puu*B
F	JW2626 *yfj*Z	JW0799 *omp*X	JW3876 *rha*S	JW2400 *yfe*R	JW3221 *yhd*A	JW3548 *yia*L	JW4295 *yji*J	JW1082 *pab*C	JW1881 *flh*D	JW4282 *fim*G	JW4057 *phn*L	JW1471 *fdn*H
G	JW1151 *ycg*Z	JW1125 *lit*	JW3698 *bgl*H	JW2845 *ygf*J	JW3337 *frl*D	JW3565 *yib*F	JW4310 *yji*W	JW2257 *men*B	JW2503 *pbp*C	JW4318 *tsr*	JW4059 *phn*J	JW2018 *wbb*J
H	JW1568 *ydf*E	JW1531 *dcp*	JW0784 *din*G	JW2848 *ygf*M	JW3340 *yhf*T	JW3572 *yib*I	JW4319 *yji*Z	JW0136 *ecp*D	JW2794 *ppd*A	JW0264 *yag*H	JW4061 *phn*H	JW2021 *glf*

Plate #85/86

	1	2	3	4	5	6	7	8	9	10	11	12
A	JW2082 *gatZ*	JW2701 *fhlA*	JW2960 *hybE*	JW0326 *prpE*		JW0581 *fepG*	JW2304 *hisM*	JW4048 *alsA*	JW0525 *intD*	JW0040 *fixA*	JW5009 *hpt*	JW5234 *ansP*
B	JW2195 *napD*	JW2770 *fucO*	JW2964 *hybA*	JW1409 *azoR*	JW3808 *udp*	JW0685 *kdpB*	JW2305 *hisQ*	JW2756 *rumA*	JW0618 *cspE*	JW0333 *lacA*	JW5052 *ampH*	JW5278 *arpB*
C	JW2338 *yfcX*	JW2771 *fucA*	JW3299 *bfd*	JW0030 *carA*	JW3970 *purH*	JW0816 *yliD*	JW2307 *argT*		JW0920 *ssuE*	JW0341 *mhpD*	JW5057 *yajL*	JW5354 *yohO*
D	JW2692 *hycD*	JW2773 *fucI*	JW5689 *malP*	JW0097 *mutT*	JW3656 *yidL*	JW1214 *narK*	JW2885 *argK*	JW3213 *tldD*	JW5963 *blr*	JW2051 *udk*	JW5071 *sfmH*	JW5423 *pinH*
E	JW2693 *hycC*	JW2775 *fucU*	JW3575 *mtlR*	JW0458 *apt*	JW0059 *polB*	JW1807 *manY*	JW2942 *yghK*	JW3301 *tufA*	JW2300 *folX*	JW2368 *yfdE*		JW5466 *guaD*
F	JW2694 *hycB*	JW2810 *kduD*	JW3864 *fdoH*	JW2461 *purC*	JW2502 *ndk*	JW1902 *yecC*	JW3239 *yhdZ*	JW0453 *acrR*	JW2604 *alpA*	JW3419 *livF*	JW5134 *cspH*	JW5468 *ygfS*
G	JW2695 *hycA*	JW2894 *epd*	JW0037 *caiB*	JW2491 *guaA*	JW0334 *lacY*	JW2077 *gatB*	JW3442 *nikB*	JW2668 *recX*	JW3029 *bacA*	JW4116 *poxA*	BW25113 **Wild type**	JW5517 *yhaL*
H	JW2700 *hypE*	JW2958 *hybG*	JW0038 *caiA*	JW2787 *recD*	JW0452 *acrA*	JW2234 *glpT*	JW3578 *lldP*	JW3446 *nikR*	JW4015 *aphA*	JW2571 *kgtP*	JW5184 *cvrA*	JW5522 *tdcE*

Plate #87/88

	1	2	3	4	5	6	7	8	9	10	11	12
A	JW5541 *aaeX*	BW25113 **Wild type**	JW5777 *yjhT*	JW5038 *ykgB*	JW5189 *ychM*	JW5383 *tfaS*	JW5807 *leuB*	JW5816 *ybfE*	JW5908 *yddM*	JW5833 *yeeJ*	JW5842 *yphC*	JW5850 *yqjF*
B		JW5944 *yhiM*	JW5787 *yjiT*	JW5041 *ykgE*	JW5215 *ydbJ*	JW5385 *yfdN*	JW5808 *pcnB*		JW5825 *yneF*	JW5834 *yeeY*	JW5843 *norR*	
C	JW5556 *gldA*	JW5693 *yrfD*	JW5789 *mcrC*	JW5060 *bolA*	JW5235 *yncH*			JW5818 *potG*	JW5826 *asr*	JW5836 *cld*	JW5844 *ygcI*	JW5852 *yihO*
D	JW5559 *yiiM*	JW5710 *yrdA*	JW5790 *yjiA*	JW5084 *hokE*	JW5304 *yebA*	JW5420 *ypjM*	JW5811 *fhiA*	JW5819 *ybjS*	JW5827 *ydhL*	JW5837 *yegR*	JW5845 *ygcS*	JW5853 *ysgA*
E	JW5563 *yiiF*	JW5733 *yjdC*	JW5792 *yjjM*	JW5143 *ycdT*	JW5325 *yeeL*	JW5448 *ygdI*	JW5812 *mbhA*	JW5820 *ycfS*	JW5910 *ydiD*	JW5838 *yohG*	JW5846 *ygeO*	JW5854 *yigL*
F	JW5575 *mobB*	JW5742 *yjfN*	JW5486 *glcF*	JW5145 *ymdE*	JW5326 *yoeA*	JW5525 *tdcR*	JW5813 *ykfC*	JW5821 *emtA*	JW5830 *yebN*	JW5839 *yejO*	JW5847 *prfB*	JW5855 *recQ*
G	JW5608 *yieP*	JW5755 *yjgF*	JW5619 *tnaB*	JW5170 *ymfP*	JW5916 *molR*	JW5607 *hdfR*	JW5814 *yaiF*	JW5822 *abgT*	JW5831 *znuA*	JW5840 *elaD*	JW5848 *yghO*	JW5856 *trxA*
H	JW5938 *yicM*	JW5761 *yjgB*		JW5171 *ymfS*	JW5375 *nuoC*	JW0488 *ylbH*	JW5815 *tfaD*	JW5823 *ydcH*	JW5832 *yedQ*	JW5841 *prmB*	JW5849 *yqhC*	JW5857 *rbsD*

Plate #89/90

	1	2	3	4	5	6	7	8	9	10	11	12
A	JW5858 *yid*X	JW5867 *aid*B	JW0485 *ybb*P	JW0616 *dcu*C	JW5179 *ymg*H	JW1501 *hip*B	JW1559 *ydf*W	JW3516 *yhj*X				JW5434 *asc*G
B	JW5859 *dgo*T	JW5868 *ula*G	JW0688 *ybf*A	JW5067 *ybb*N	JW5686 *gnt*U		JW0197 *dkg*B	JW3581 *yib*K	JW5688 *rtc*A			JW5165 *hfl*D
C	JW5860 *yid*R	JW5869 *yji*K	JW1015 *ycdU*	JW5097 *abr*B		JW3647 *ivb*L	JW2460 *ypf*J	JW3631 *yic*I	JW5322 *yed*W	JW5125 *ycb*W		JW0695 *ybf*L
D	JW5939 *yic*J	JW5953 *yji*P	JW2730 *ygc*L	JW5112 *ybj*G	JW3375 *bio*H	JW5080 *rzo*D	JW0644 *djl*C	JW5002 *hok*C	JW5396 *ypf*H	JW0502 g*lx*K		JW5874 *ydh*M
E	BW25113 **Wild type**	JW5871 *mcr*B	JW1267 *cys*B	JW5132 *etp*		JW5089 *lip*B	JW0668 *ybf*N	JW5003 *yaa*Y	JW5443 *ygc*W	JW5603 *gpp*	JW5055 *pro*Y	JW5876 *yfe*H
F		JW5955 *bgl*J	JW0162 *gln*D	JW5135 *tor*S	JW2904 *spe*B	JW5111 *yli*B	JW1166 *ycg*J		JW0939 *ycb*G	JW1246 *yci*B	JW5258 *ynf*C	JW5877 *ype*B
G	JW5864 *yrh*A	JW5873 *prf*C	JW2042 *wca*C	JW5138 *ycd*H	JW0022 *rps*T	JW5106 *ybi*M	JW1083 *yce*G		JW3037 *rps*U	JW2413 *yfe*S	JW5259 *ynf*D	JW5878 *csi*E
H	JW5947 *aro*K	JW1830 *yob*A	JW0613 *dcu*C	JW5176 *ycg*H	JW1522 *mar*C	JW5262 *dms*D	JW3489 *yhj*C	JW5188 *dha*R	JW3937 *trm*A	JW2064 *bae*R	JW5327 *yeeP*	JW1058 *flg*M

Plate #91-94

	1	2	3	4	5	6	7	8	9	10	11	12
A	JW4253 *fec*I	JW4125 *yje*F	JW0090 *ddl*B	BW25113 **Wild type**							JW3713 *atp*H	JW5592 *dap*F
B	JW2556 *rse*A	JW3959 *rsd*	JW1026 *csg*C									JW0870 *cyd*D
C	JW4252 *fec*R	JW1982 *flu*	JW1031 *ymd*A							JW1630 *pdx*H	JW3715 *atp*E	JW1041 *lpx*L
D	JW1656 *ydh*Q	JW5865 *yrf*G								JW2308 u*biX*	JW3716 *atp*B	JW3711 *atp*G
E	JW0583 *ybd*A	JW5065 *ybb*J								JW3709 *atp*C	JW3039 *rpo*D	
F	JW1537 *ydf*K	JW0738 *gpm*A								JW3710 *atp*D	JW3030 *fol*B	
G	JW1907 *fli*A	JW1107 *ycf*Z								JW4055 *phn*N	JW3400 *gnt*K	
H	JW3682 *yid*D	JW1731 *ydj*R										

Plate #95

	1	2	3	4	5	6	7	8	9	10	11	12
A	JW3368 *ompR*	JW3584 *secB*	JW3144 *folP*	JW5413 *rimM*	JW3136 *rbfA*	JW0656 *ybeY*	JW3906 *priA*					
B	JW0145 *mrcB*		JW2667 *alaS*	JW5539 *yhcB*	JW5851 *pnp*	JW2226 *ubiG*	JW3712 *atpA*					
C		JW4002 *dgkA*	JW3261 *rpmJ*	JW5682 *dcrB*	JW3933 *oxyR*	JW3985 *pgi*	BW25113 **Wild type**					
D	JW0909 *ycbK*		JW0406 *nusB*		JW3947 *rplA*	JW0157 *degP*						
E	JW0182 *yaeR*	JW0212 *lpcA*	JW0052 *surA*	JW2862 *xerD*	JW3134 *rpsO*	JW2496 *yfgL*	JW5157 *ycfM*					
F	JW2500 *yfgA*	JW2509 *fdx*	JW0727 *tolQ*	JW2987 *parC*	JW3714 *atpF*	JW1194 *ychF*	JW4326 *dnaT*					
G	JW0013 *dnaK*	JW2576 *rluD*	JW3024 *rfaE*	JW3596 *rfaC*	JW2795 *thyA*	JW3606 *rfaG*						
H		JW2788 *recB*	JW5100 *tolB*	JW2790 *recC*	JW1225 *hns*	JW0663 *nagA*						

Supplementary data 2 *Layouts of all the KEIO 96-well plates showcasing gene distribution from the KEIO collection, accompanied by mean chlorophyll-a fluorescence values for each gene when co-cultured with microalgae, C. sorokiniana for two days (n=3).*

Plate #1/2

	1	2	3	4	5	6	7	8	9	10	11	12
A	0.793	0.839	0.923	1.009	0.967		0.970	0.904	0.881	1.060	1.048	0.709
B	1.000	0.934	0.932	0.957	0.897		0.955		0.907		0.876	0.843
C	0.786	0.891	0.901	0.864	0.955	0.903	0.905	0.894	0.883	0.880	1.020	1.000
D	0.760	0.844	0.929	0.918	0.889	0.666	0.896	0.873	0.910	0.890	0.927	0.928
E	0.772	0.898	0.933		0.927	0.886	0.935	0.848	0.861	0.873	0.948	1.000
F	0.809	0.873	0.990	1.001	0.993	0.927	0.867	0.860	0.887	0.866	0.943	0.864
G	0.786	0.951	0.962		0.938	0.951		0.887	0.919	0.999	1.096	0.836
H	0.891	0.922	0.922	0.868	0.894		0.892	0.877	0.866	0.906	0.941	0.856

Plate #3/4

	1	2	3	4	5	6	7	8	9	10	11	12
A	0.803	0.799	0.889	0.901	1.057	0.810	0.830	0.848		0.903	0.853	0.859
B		0.918	1.000	0.892	0.895	0.861	0.936	0.879	0.814	0.874	0.911	0.896
C	0.905	0.863	1.252	0.915	0.890	0.924	0.891	0.790	0.811	0.756	0.860	0.896
D	0.877	0.941	0.938	0.922	0.922	0.833	0.768	0.862		0.825	0.864	0.918
E			1.259	0.924	0.894	0.839	0.794	0.868	0.864	0.857		0.887
F	0.814	0.907	0.822	0.825	0.900	0.880		0.813	0.858	0.816	0.878	0.848
G	0.807	0.874	0.910	0.884	0.815	0.825	0.899	0.794		0.886	0.897	
H	0.860	0.873	0.863	0.877	0.785	0.824	0.800	0.730	0.811	0.842	0.906	

Plate #5/6

	1	2	3	4	5	6	7	8	9	10	11	12
A	0.905	0.885	1.086	0.859	0.949	1.016	0.804	0.802	0.947	0.811		
B	0.823	0.994	0.923	0.916	1.026	0.943	0.836	0.931	0.917	0.871	0.860	0.986
C	0.954	0.908	0.892	0.929	1.038	0.905	0.823			0.867		
D	0.971	0.952	0.930	0.883	0.962			0.803		0.892		
E	0.826	0.978	0.898	0.946	0.848	1.057		0.920	0.890	0.884	0.845	0.822
F	1.000	0.989	0.873	0.956	1.020	0.894	0.823	0.871	0.962	0.900		
G	0.898	1.011	0.920		0.876	0.920	0.982	1.101	0.878	0.957		0.893
H	0.821	0.905		0.786		0.761	0.782	0.761	1.536	1.125	0.875	

Plate #7/8

	1	2	3	4	5	6	7	8	9	10	11	12
A		0.836	0.914		0.882			0.871	0.921	0.885	1.022	0.859
B		1.000	0.855	0.882	0.865	0.876	0.898		0.899			
C		0.827	0.926		0.812			0.863	0.927		0.832	1.011
D		0.865	0.910	0.914	0.904		0.925	0.876	0.876	0.878	0.904	0.966
E			0.949	0.933	0.802	0.893			0.947	1.018	0.899	0.838
F		0.955		0.806	0.703	0.988	0.863	0.906	0.919	0.986	0.914	
G		0.762	0.926	0.822	0.820			0.944	1.041	0.911	0.860	
H	0.811	0.877	0.922	1.072	0.938	0.825	0.856	0.892	0.954	1.205	0.927	1.209

Plate #9/10

	1	2	3	4	5	6	7	8	9	10	11	12
A	0.901	1.000	0.935	0.821	0.885	1.017	0.836	0.808	0.881	0.760	0.809	0.808
B	1.001	0.903	0.906	0.863	0.857	0.915	0.804	0.855	0.884	0.811	0.815	0.840
C	0.866	0.941	0.962	0.841	0.804	0.956	0.848	0.801	0.852	0.807	0.847	0.878
D	0.849	0.938	0.919	0.835		0.842		0.818		0.806	0.879	0.838
E	0.817	0.954	0.886	0.908	0.871	1.037	0.704	0.810	0.820	0.879		0.882
F		0.870	0.819		0.857	0.856	0.859	0.827	0.878	0.886	0.814	0.856
G	0.926	0.960	0.974	1.067		0.951	0.822	0.808		0.892	0.876	0.822
H	0.833	0.868	0.825	0.841	0.821	0.827	0.841	0.808	0.823	0.835	0.919	0.871

Plate #11/12

	1	2	3	4	5	6	7	8	9	10	11	12
A	1.030		0.816	1.054	1.166	0.939	1.017	0.930		1.089	0.945	1.090
B	1.057		1.040	1.070	1.105	0.966	0.841	0.932	0.940	1.191	0.860	1.202
C	0.955	1.079	1.060	0.973		0.958	0.952	1.246		1.020		1.079
D	0.991		1.002		0.945	0.822	1.011	1.021	0.985		1.080	1.025
E	1.000	1.228		1.009	1.063	0.922	0.801	1.049	0.995			
F	1.000	0.955	1.049	1.073				0.926	1.020	1.041		1.047
G	1.188	1.082	1.290	0.980	0.869	0.913	1.040	0.992	1.209	1.037	1.034	1.122
H	1.083	1.000		1.086	1.211	1.189	1.226		0.983	1.300	1.321	1.130

Plate #13/14

	1	2	3	4	5	6	7	8	9	10	11	12
A	0.816	1.102	0.940	0.905		0.813		0.893	0.871	0.847	0.856	
B	0.968	1.032		0.923			0.844	0.871	1.005		0.861	0.899
C	0.959	0.942			0.857	0.791	0.722			0.820	0.868	1.082
D	1.000				0.928	0.811	0.858	0.895	0.817	0.874		0.881
E		0.926	0.858	0.831	0.821	0.801	0.826		0.826	0.854		0.844
F			1.043			0.870		0.873	0.880			0.866
G		1.035	1.023			0.856	0.922	0.841	0.877	0.948	0.870	0.851
H	1.040		0.900	0.918	0.895	0.858	0.884	0.904	0.772	0.956	0.963	1.207

Plate #15/16

	1	2	3	4	5	6	7	8	9	10	11	12
A	0.998	1.000	0.975	1.133	1.054			1.020	1.147	0.967	1.057	1.043
B	1.084	1.213		1.117	1.027	1.090	1.062	0.838	1.184	1.177	1.301	
C	1.074	1.191	1.208	1.239	1.035	1.044	1.079	0.895	1.080	0.931	1.039	1.163
D		1.188	1.021	1.237		1.059		0.887			0.962	1.110
E	1.105	1.147	1.131	1.176	0.998	1.090	0.846	0.912	1.079	0.882	0.998	0.966
F	0.922	1.102	1.164	0.993	1.219	1.133	0.929		0.972	1.016		1.098
G	1.049	1.100	1.021		1.067	1.180	0.716			0.950		
H	1.008	1.093	1.069	1.169	1.068	0.999	0.889		1.026	1.029	0.874	1.143

Plate #17/18

	1	2	3	4	5	6	7	8	9	10	11	12
A	1.000	0.994	0.955	0.980	0.915	0.904	0.836		0.804	0.817		0.851
B	0.755	0.877	0.850	0.903			0.852	0.857	0.870			0.813
C		0.905	0.992	0.960		0.873		0.838		0.828	0.885	
D		0.925	0.954	0.914	0.882	0.879	0.887	0.824		0.848	0.838	
E	0.915		0.847	0.950	0.874	0.942	0.901	0.845		0.829		0.832
F	0.837		0.903		0.769	0.894	0.757	0.774	0.851	0.777	0.750	
G	0.824	0.876	0.917	0.979	0.881		0.867	1.143	0.849	0.858		0.806
H	0.732	0.867	0.873	0.868	0.891	1.114	0.904	0.822	0.804	0.819	0.808	0.807

Plate #19/20

	1	2	3	4	5	6	7	8	9	10	11	12
A	0.950	1.078	0.998	0.972	0.868	0.805	0.969	0.867	0.836		1.066	0.887
B	1.000	0.992	0.860	0.936	0.841		0.870	1.016		1.026	1.065	1.021
C	0.802	1.005	0.872	1.024	0.963	0.814	1.026	0.913			1.013	0.985
D	0.895	0.998	0.954	0.925	1.024		0.829	0.911	0.862		0.926	0.939
E	0.915	1.021		0.967			0.980	0.777			0.938	0.997
F	0.964		0.921	0.940	0.821	0.929	1.009	0.941	0.971	0.924		
G	1.035	1.021	1.044	1.047	1.033	1.150	0.974	0.834	0.981	1.010	0.967	0.960
H	1.000	1.094	1.104		0.802	0.950		0.945	0.832	0.932	0.857	1.024

Plate #21/22

	1	2	3	4	5	6	7	8	9	10	11	12
A	1.047	1.257	0.929	1.113	0.910	0.946	1.089		0.817	0.873	0.817	0.992
B	1.050			0.849	0.807	0.880		0.950	0.934	0.990		0.853
C	1.000	0.902	0.953	0.679	0.969	1.024	0.840			0.863	0.804	
D	1.012	0.996	0.919	1.301	1.057	0.726		0.889	0.898	0.969	0.819	0.920
E	0.937	1.136	1.049	1.196	0.809	1.016	0.843	0.738	0.946	0.962	0.812	1.008
F		1.093		1.211	0.901	1.127	0.922	0.662	0.801		0.875	0.887
G		1.099	1.120	1.048	0.928	0.918	0.913	0.810	0.910	0.908		1.078
H	1.094	1.142	1.547	1.128	0.775	0.822				1.155		

Plate #23/24

	1	2	3	4	5	6	7	8	9	10	11	12
A	1.000	0.988	0.985	1.026	1.153	0.893		0.867	1.188	0.994	1.129	1.202
B	0.917		0.938	0.948		0.908		1.241			1.014	0.885
C	1.335		0.899	0.999	0.914		0.962	0.884	0.981	0.933	1.058	1.005
D	0.882				0.905	1.154	0.912	1.135	0.907			
E	0.830	0.895	1.090		1.217			0.937	1.055	1.053	1.075	1.127
F		0.968	1.251	0.972		1.170	0.903	1.173	0.845	0.964	1.056	
G	0.989	1.234	1.008		1.077		0.937	0.900	1.072	1.195	1.006	1.168
H	0.877	0.988	0.996	1.138	1.151		0.883		0.956			0.911

Plate #25/26

	1	2	3	4	5	6	7	8	9	10	11	12
A	1.000	1.177	1.037			0.988	0.975		0.841	0.991	1.173	
B	1.072		0.956	1.003	0.879	0.875	0.940		1.058	1.028		0.987
C				0.820	0.805	0.850	0.856	0.993	0.961	0.828	0.929	1.051
D		0.893		0.875			0.894	0.848	0.833	1.312		
E	0.930	0.986	0.930	0.946	0.970	1.025		0.875	0.933	0.901		0.884
F	0.962	0.967	0.873	0.749	0.920	0.914	0.909	0.980		0.840	0.953	0.971
G	0.959	0.822		0.824	1.023	0.874	0.954	0.912		0.933	1.065	
H	0.888	1.059	1.088	0.979	1.169		0.862	1.016	1.068	1.141	0.925	1.058

Plate #27/28

	1	2	3	4	5	6	7	8	9	10	11	12
A	1.125	1.071	1.201	0.971	1.012		0.991	0.902		0.983	0.815	
B	1.000	1.287	1.012	0.888			0.965	1.221	1.075	0.875	0.711	0.804
C	1.165	1.036	1.413	0.922		0.877	0.950	0.881	0.837	0.992	0.803	0.809
D	0.860	1.104	1.146	1.142	0.964		0.986	0.987	0.854	0.972		0.826
E	0.882	1.100	1.420	1.020	0.881	0.930	0.930	0.933	0.808	0.989	0.817	0.800
F	0.828	1.122	1.006	1.048	0.913	0.956	0.971	0.961	0.862	0.892	0.826	0.812
G	1.020	1.166	1.318	0.995		0.940	1.069	0.919	0.917	0.998	0.955	
H	0.882	1.128		1.175		1.266	1.021	1.073	0.804	0.991	0.838	0.814

Plate #29/30

	1	2	3	4	5	6	7	8	9	10	11	12
A	1.133	0.933	1.037	1.028	1.008		1.061	1.241	0.860	0.966		
B	0.903	0.972	0.997	1.201	0.899	1.003	1.004	1.061	1.190		1.134	1.199
C	1.001		0.945	1.027	0.839	1.031	1.138	0.943	1.022	1.192	1.209	1.049
D	1.000	0.902	0.950	0.959		0.947	0.992	0.970	1.202	1.130	0.948	1.063
E	1.069			0.924	1.009	0.919	1.054		1.177	1.221	0.989	1.093
F	0.899	1.076	1.003	0.988		1.001	0.986	1.091	0.870	1.079	0.975	0.918
G	1.109		1.007	0.988	1.012	1.080	0.979	1.093	1.140		1.330	1.348
H	1.012		0.926	1.225	1.190			1.097	1.217	1.167	1.051	0.988

Plate #31/32

	1	2	3	4	5	6	7	8	9	10	11	12
A	1.052	1.079	1.113		1.014	0.820	1.112	0.812	0.901		0.987	0.814
B	1.130	1.178	1.171	1.090	1.151	0.985	0.803	1.012	1.025	0.816	1.050	1.000
C	1.176	0.927	1.048			0.931	1.146		0.950	1.029	1.016	
D	1.026	1.243		1.033				0.876	1.091			
E	1.138	0.980	1.149	1.175		1.093			1.060		0.982	0.850
F	1.127	0.922	1.235		1.019	1.158		1.006			0.971	
G	0.976	1.080	1.087	1.221		1.202	1.118	1.022			1.066	1.029
H	1.042	1.052	1.092	1.076				0.949			0.931	1.026

Plate #33/34

	1	2	3	4	5	6	7	8	9	10	11	12
A	1.112	0.949	0.981	0.868	1.032	0.933	1.129	0.984	0.885	0.921	0.919	0.842
B	1.209	1.134	1.005	0.979	1.142	0.997	1.079	0.914	0.947	0.934	0.943	0.913
C	0.804	0.968	1.015	0.943	0.979	0.913	0.974	1.005	0.985	1.196	1.037	0.802
D	1.000	1.035	0.965	1.210	0.953	1.016	1.007	0.851	0.988	0.899	0.999	0.883
E	1.001	0.911	0.972	1.025	1.197	0.928	0.955	1.027	0.934	0.918	0.837	0.801
F	1.031	0.804	1.038	0.931	1.079	0.991	0.968	0.919	0.810	0.950	0.908	1.174
G	0.979	1.118	1.115	0.982	1.053	0.921	0.868	0.952	1.058	1.032	1.011	0.831
H	0.970	0.997	1.078	0.974	0.835	1.034	0.978	0.853	0.992	1.031	1.060	0.814

Plate #35/36

	1	2	3	4	5	6	7	8	9	10	11	12
A	0.956	1.095	1.069	1.133	1.154	0.932	1.060	1.070	1.100	1.012	1.083	0.832
B	1.039	1.185	1.073	1.178	0.821	0.951	0.963	0.995	0.899	0.979	0.953	0.919
C	1.073	1.140	0.931	1.030	1.117	1.183	0.879	0.990	1.081	0.967	0.917	0.975
D	1.024	1.157	0.941	0.856	0.982	1.245	1.052	1.037	0.954	1.000	0.894	0.989
E	0.949	1.035	0.961	1.118	0.939	1.128	0.805	0.815	0.897	0.968	0.921	0.814
F	0.835	0.984	0.900	1.031	0.947	0.977	0.899	0.954	1.131	1.021	0.963	1.048
G	1.005	1.471	0.919	1.203	0.991	0.888	0.971	1.020	1.195	1.040	0.872	1.064
H	0.900	0.963	0.942	0.891	0.986	1.081	1.537	1.023	1.013	1.059	0.958	1.018

Plate #37/38

	1	2	3	4	5	6	7	8	9	10	11	12
A	0.987	1.073	1.065	1.025	1.004	1.081	1.102	1.186	1.129	1.048	1.159	1.067
B	1.000	1.140	0.981	0.960	1.062	1.037	0.981	1.028	1.044	1.052	1.056	1.175
C	1.029	1.008	1.049	1.086	1.104	0.908	1.013	1.089	1.004	1.085	1.086	1.114
D	1.000	1.000	1.096	1.001	0.944	0.937	1.027	1.034	1.011	1.060	1.134	1.156
E	0.882	0.872	0.874	0.919	1.025	1.035	1.077	1.043	1.095	1.072	1.035	1.183
F	0.877	1.044	1.050	0.972	0.992	1.107	1.089	0.954	1.115	1.104	1.051	1.097
G	0.919	1.124	1.059	1.066	1.075	1.060	1.088	1.113	1.082	1.073	1.053	1.072
H	0.856	0.984	0.983	0.938	1.017	1.050	1.012	1.042	1.059	1.108	0.921	1.208

Plate #39/40

	1	2	3	4	5	6	7	8	9	10	11	12
A	0.839	0.916	0.963	0.831	1.227	0.916	0.954	1.074	0.998	0.880	0.982	0.966
B	0.907	0.958	0.907	0.900	1.070	1.109	1.017	0.909		0.882	1.131	0.914
C	0.860	0.921	0.978	0.876	1.204	0.929	1.042	0.806	1.032	1.000	0.891	0.908
D	0.977	0.901	1.026	0.868	0.900	1.019	0.977	1.080	0.879	0.902	0.985	1.008
E	0.976	0.866	1.068		1.029	0.953	0.986	0.887	1.057	0.805	0.846	0.835
F	0.889	1.055	1.098		0.924	1.046	0.829	0.950	1.022	0.866	1.089	0.998
G	0.863	0.994	0.974	0.961	0.934	0.854	0.906	1.010	0.990	0.891	0.944	0.940
H	0.812	0.927	0.884	1.127	0.818	0.938	0.903	1.093	1.185	0.959	1.013	1.009

Plate #41/42

	1	2	3	4	5	6	7	8	9	10	11	12
A	0.951	1.000	0.864	1.029	0.993	0.946	0.998	0.935	1.225	1.077	1.081	1.195
B	0.972	1.091	1.115	1.032	0.992	1.057	1.070	1.232	1.109	1.115	1.216	1.099
C	0.926	1.030	1.017	0.920	1.027	1.007	1.002	0.995	0.992	1.150	1.129	1.091
D	0.991	1.018	0.897	1.021	0.976	1.030	1.031	0.996	1.052	1.106	1.090	1.127
E	0.954	1.023	0.987	0.885	0.905	1.062	1.033	1.056	1.111	0.992	1.054	1.076
F	0.930	1.036	1.004	1.001	1.004	1.072	1.079	1.062	0.958	0.928	1.054	1.115
G	0.924	1.096	0.990	0.883	0.963	1.097	1.030	1.039	1.067	0.968	0.994	1.000
H	0.986	1.024	0.914	1.005	0.940	1.167	0.993	0.801	0.896	0.810	1.029	0.931

Plate #43/44

	1	2	3	4	5	6	7	8	9	10	11	12
A	0.915	1.112	1.439	1.056	1.000	1.096	0.968	1.113	0.972	1.076	1.048	0.834
B	0.920	1.087	1.262	1.103	1.141	1.094	1.222	1.007	1.009	1.067	1.024	1.174
C	0.944	1.090	1.252	0.988	1.100	1.084	1.082	1.042	1.009	1.094	0.878	1.078
D	1.035	1.104	1.250	0.924	1.087	1.040	1.031	1.150	1.014	1.096	1.059	1.161
E	1.043	0.939	1.050	0.998	1.256		1.011	1.102	1.112	1.192	0.915	1.159
F	0.878	1.253	1.105	0.958	1.075	1.059	1.049	1.025	1.114	1.045	1.135	1.053
G	0.982	1.135	1.198	1.102	1.075	1.048	1.027	1.035	1.047	1.086	1.207	1.072
H	1.023	1.079	1.124	0.946	0.991	1.005	0.963	0.820	1.028	0.899	1.093	1.035

Plate #45/46

	1	2	3	4	5	6	7	8	9	10	11	12
A	1.158	1.079	1.178	1.103	1.085	0.941	1.058	0.888	1.147	1.101	1.028	1.036
B	1.014	1.117	1.176	1.013	1.117	0.864	1.078	0.940	1.210	1.095	0.966	1.026
C	1.010	0.997	0.985	0.965	0.840		0.946	0.849	0.999	0.949	0.964	0.962
D	1.003	1.094	0.967	0.807	0.846	0.903	1.014	0.943	1.017	0.997	0.983	1.005
E	0.985	0.989	0.976	0.961	0.810		0.923	1.000	0.943	0.984	0.996	1.006
F	0.926	1.004	0.862	1.014	0.837		1.089	0.991	1.029	1.025	0.996	0.915
G		0.948	0.893	0.964	0.811	0.845	1.002	0.989	1.008	0.950	0.883	0.978
H	0.948	1.102	1.122	1.126	1.118	0.989	1.054	1.033	0.977	1.152	0.962	1.022

Plate #47/48

	1	2	3	4	5	6	7	8	9	10	11	12
A	0.825	0.908	0.853	0.866	0.935	0.888	0.878	0.867	0.907	0.885	0.822	0.919
B	0.985	0.827	0.884	0.859	0.919	0.923	0.895	0.972	0.914	0.916	0.906	1.063
C	0.838	0.926	0.947	0.832	0.857	0.925	0.963	0.960	0.903	0.890	0.996	1.012
D	0.853	0.991	1.000	0.869	0.911	0.934	0.932	1.036	0.955	0.883	0.859	0.931
E	0.812	0.867	0.851	0.898	0.972	0.928	0.911	0.920	0.890	0.934	0.948	1.012
F	0.894	0.841	0.853	0.804	0.826	0.914	0.985	0.871		0.956	0.950	0.954
G	0.879	0.905	0.877	0.852	0.932	0.909	0.989	1.031	0.990	0.965	1.034	0.881
H		0.954	0.899	0.823	0.856	0.822	0.903	0.845	0.898	0.848	0.959	0.906

Plate #49/50

	1	2	3	4	5	6	7	8	9	10	11	12
A	0.815	0.847	0.842		0.856	0.802	0.860	0.867	1.000	0.866	0.918	0.983
B	0.804	0.866	0.913	0.847	0.889	0.917	0.948	0.865	0.923	0.832	0.950	1.023
C	0.810	0.852	0.928	0.891		0.791	0.828	0.854	0.897	0.818	0.860	0.928
D	0.766	0.785	0.853	0.809	0.759	0.840	0.779	0.805	0.865	0.870	0.826	0.829
E	0.816	0.800	0.886	0.803	0.825	0.909	0.785	0.823	0.855	0.834	0.895	0.877
F	0.801	0.843	0.828	0.917	0.840	0.925	0.872	0.862	0.898	0.847	0.873	1.010
G	0.843	0.889	0.908	1.069	0.886	0.962	0.905	0.946	0.976	0.892	0.942	0.841
H	0.833	0.915	0.910	0.897	0.842	0.979		0.849	0.905	0.944	0.845	0.877

Plate #51/52

	1	2	3	4	5	6	7	8	9	10	11	12
A	1.149	1.109	0.899	1.068	1.008	0.942	0.954	0.855	0.914	0.804	0.949	0.919
B	1.017	1.053	1.116	1.064	0.901	1.000	0.996	0.899	0.985	0.947	0.929	1.005
C	0.992	0.912	1.067	0.972	0.950	0.953	1.034	0.933	0.983	0.810	0.962	0.986
D	1.085	1.027	1.042	0.977	0.895	0.888	1.066	1.049	0.992	0.834	0.911	0.852
E	1.065	1.105	0.949	1.163	1.070	0.974	0.949	1.085	0.946	0.825	0.989	0.939
F	1.012	1.071	1.008	1.164	1.078	0.978	0.874	1.050	0.996	0.969	0.942	0.922
G	0.929	1.153	1.018	1.134	1.141	1.121	1.024	1.028	1.015	1.001	0.885	0.883
H	1.095	1.123	1.080	1.123	0.862	0.934	1.013	0.915	1.006	0.869	0.817	

Plate #53/54

	1	2	3	4	5	6	7	8	9	10	11	12
A	1.000	0.964	1.052	1.110	0.970	0.881	1.056	0.893	0.866	0.863	0.939	1.032
B		0.986	1.004	1.006		1.055	0.980	0.958	0.925	0.969	1.007	0.932
C		0.997	0.984	0.937	0.966	0.955	0.972	0.959	1.006	0.948	0.924	0.897
D		1.045	1.002	1.027	1.053	0.772	0.970	0.977	0.876	0.938	0.962	0.965
E	0.993	1.030	0.977	0.967		0.945	0.946	0.984	0.837	0.957	0.910	1.005
F	0.943	0.980	1.009	0.985	0.982	0.941	0.992	0.962	0.958	0.883	0.971	0.959
G	0.904	1.037	1.113	0.993	0.867	0.951	1.025	0.936	0.954	1.109	1.005	0.908
H	0.857	0.878	0.974	0.947	0.892	0.882	0.973	0.895		0.922	0.935	1.037

Plate #55/56

	1	2	3	4	5	6	7	8	9	10	11	12
A	1.009	0.873	1.103	1.122	1.018	1.039	0.948	0.983	0.810	0.877	0.804	0.877
B	0.865	1.094	1.031	1.025	1.004	0.978	0.852	0.898	0.905	0.848	0.863	0.840
C	0.848	0.868	0.897	0.994	0.952	0.935	0.926	0.923	0.816	0.814	0.822	0.851
D	1.027	1.063	0.914	0.959	1.021	0.991	1.017	0.889	0.879	0.805	1.000	0.874
E	0.878	0.882	0.979	0.918	0.936	0.995	0.900	0.843	0.907	0.875	0.816	0.874
F	0.990	0.933	0.944	1.059	1.015	0.911	0.907		0.942	0.893	0.847	0.921
G	0.950	1.018	0.865	0.895	0.971	0.851	0.901	0.942	0.899	0.915	0.911	0.965
H	1.069	0.904	1.082	1.209	1.170	1.343	1.053	1.009	0.963	0.849	0.826	1.156

Plate #57/58

	1	2	3	4	5	6	7	8	9	10	11	12
A	1.073	0.969	1.078	1.016	0.991	0.922	0.928	0.840	0.895	0.936	0.941	0.801
B	0.976	0.807	0.996	0.881	0.996	0.878	1.000	0.853	0.858	0.932	0.905	0.808
C	0.937	0.872	0.996	0.907	0.965	0.879	0.937	0.804	0.927	0.995	0.989	0.953
D	1.057	1.026	0.886	0.981	0.886	0.848	0.915	0.928	0.907	0.876	0.885	0.921
E	0.991	0.994	0.855	0.937	0.980	0.910	0.920	0.882	0.927	0.996	0.907	0.830
F	1.075	0.866	0.873	0.955	0.907	0.960	0.855	0.896	1.059	0.906	0.958	0.961
G	1.065	0.961	0.907	0.892	0.867	0.909	0.800	0.865	0.925	0.962	0.820	0.971
H	0.968	0.942	0.907	0.893	0.893	0.820	0.835	1.083	0.884	0.873	0.817	0.975

Plate #59/60

	1	2	3	4	5	6	7	8	9	10	11	12
A	0.985	1.062	0.968	0.915	0.900	0.876	0.957	0.935	0.982	0.949	1.026	0.910
B	0.896	0.951	0.994	1.015	0.972	0.971	0.952	0.985	0.979	0.975	0.967	0.986
C	0.919	0.855	0.987	0.968	0.963	0.943	0.961	0.910	1.058	0.979	0.951	0.958
D	1.003	0.966	0.954	0.945	0.943	1.000	0.909	0.969		0.986	0.937	0.964
E	0.969	0.954	1.060	0.933	0.994	0.952	1.017	0.996	1.041	1.086	0.924	0.947
F	0.985	0.996	1.009	0.999	0.973	1.090	0.951	0.920	1.028	0.998	0.984	0.957
G	0.939	0.917	1.071	1.026	1.039	0.949	0.980	0.966	1.089	1.013	0.962	0.950
H	1.114	0.947	0.802	0.895	0.851	0.873	0.963	0.871	0.984	0.829	0.814	0.858

Plate #61/62

	1	2	3	4	5	6	7	8	9	10	11	12
A	1.114	1.091	0.867	0.856	0.875	0.944	1.075	0.983	0.999	1.037	0.890	
B	1.067	0.861	0.915	0.893	0.948	0.977	0.858	0.945	0.999	1.001	0.968	1.071
C	0.962	1.073	1.000	0.903	0.914	0.848	1.113	0.913	0.887	1.025	0.884	1.012
D	1.043	0.817	0.951	0.880		0.895	0.960	0.813	1.003	1.166	0.817	1.086
E	0.900		0.941	0.982	0.956	0.881	0.979	0.874	0.925	1.023	0.903	0.979
F	0.963	0.860	0.946		0.982	0.919	0.922	0.859	0.905	0.933	0.824	0.889
G	0.945	0.825	0.982	0.925	0.994	0.934	0.893	0.867		1.144	0.950	0.862
H	1.037	0.884	0.873	0.872	0.936	0.862		0.756	0.888	0.983	0.933	0.877

Plate #63/64

	1	2	3	4	5	6	7	8	9	10	11	12
A	0.890	1.035	1.209	1.060	1.042	1.000	0.967	1.004	0.992	0.986	1.245	1.040
B	1.128	0.916	0.915	1.033	0.973	1.002	1.024	0.984	1.056	1.050	1.088	1.036
C	1.147	1.047	1.105	1.061	1.111	0.919	1.025	1.033	0.948	1.008	1.016	1.014
D	1.013	0.990	1.102	0.980	1.056	0.990	1.088	0.859	0.962	1.048	1.027	1.018
E	0.897	0.903	1.058	1.002	1.090	0.957	0.885	0.920	1.048	0.894	0.997	0.980
F	0.955	0.958	0.981	0.995	1.082	0.985	0.916	0.914	0.994	1.012	1.004	0.993
G	1.085	0.990	1.039	1.087	0.993	0.926		0.929	1.066	1.020	1.073	1.031
H	0.979	0.905	1.033	0.984	1.072	0.898	1.051	0.863	0.967	1.077	0.961	1.003

Plate #65/66

	1	2	3	4	5	6	7	8	9	10	11	12
A	1.049	1.204	1.176	1.036	1.000	0.974	0.972	1.032	0.972	0.978	0.963	0.940
B	1.126	1.155	1.194	1.077	1.116	1.174	1.100	1.070		1.026	1.114	1.076
C	1.073	1.180	1.147	1.146	1.126		1.037	1.022		1.021	1.005	1.087
D	1.033	1.065	1.118	1.091	1.158	1.026	1.027	1.008	0.977	1.065	1.153	
E	0.973	1.218	1.160	1.022	1.035		0.976	1.059	1.001	1.011	0.995	
F	0.937	1.072	1.215					1.002	0.996	0.917	1.064	1.090
G	1.103	1.147	1.198	1.011	1.025	1.098	1.035	1.046	0.967	1.023	1.019	1.160
H	1.121	0.959	1.039	1.202		0.956	0.942	0.946	0.951	0.989	0.949	0.990

Plate #67/68

	1	2	3	4	5	6	7	8	9	10	11	12
A	1.195	1.044	1.159	1.238			1.106	1.138	1.112	0.993	0.946	1.166
B	1.000	0.827	1.001	1.013	0.995	0.955	1.032		0.987		1.007	1.068
C		0.809	1.038	1.141		0.854		0.898	0.928		1.139	1.190
D	1.181	0.853	0.936	1.033		0.890	0.943		1.063	0.803		1.130
E		0.878	1.042		0.980		0.981	0.959	0.984	0.958	1.054	1.175
F		0.805	0.890	0.918	0.976	0.819	1.065		1.014	1.229	1.134	
G	1.209	0.809	1.041	0.887	0.922		0.856	1.053	0.927	1.014	1.148	1.164
H	1.000	0.983			1.242	0.998	1.116		1.147	1.109	0.963	0.994

Plate #69/70

	1	2	3	4	5	6	7	8	9	10	11	12
A	1.183	1.162	0.844	1.482	1.000	1.040	0.853	0.925	1.108	0.951	1.216	0.973
B		1.190	1.177		1.178	1.207	0.998	1.105	0.948	1.007	1.088	0.992
C			1.238			1.020	0.994	0.975	0.956	0.992	0.970	0.951
D	0.913	1.233			1.011				0.925	0.957	0.998	1.020
E	1.126		0.920	0.899	1.019	1.069	0.957	1.038	0.820		0.848	
F	1.057	0.937	1.026	0.932	0.826		0.970	0.911	0.958	0.922	1.030	1.061
G		1.036			1.051	0.914	1.072	1.025	1.118	0.924		0.827
H		1.184	1.222	1.046	0.882		1.095	0.979	0.835	1.135	0.838	0.992

Plate #71/72

	1	2	3	4	5	6	7	8	9	10	11	12
A	1.086	1.054	0.949	1.001	1.050		0.988	1.027		0.928	1.051	0.993
B			1.000	1.085	1.034		1.051	1.031	1.046	1.039		1.049
C	1.036	1.039		1.072	0.983	1.075	1.056		0.996	0.859	1.002	0.991
D			1.017	1.064	1.009	1.017	0.994	0.979	1.016	0.925		1.004
E	0.965	1.073		1.081	1.065	1.049			1.012			1.013
F	1.019	1.051	1.107	1.109	1.102	1.086	0.986	0.992	0.978	0.973	0.952	0.968
G	1.022	1.039	1.109	1.052	1.070	1.084	1.048	1.073	1.140	0.975		0.952
H	0.986	1.009			0.975	0.962	0.997	0.929	0.896	0.953	1.062	1.006

Plate #73/74

	1	2	3	4	5	6	7	8	9	10	11	12
A	1.021	1.000	1.017	1.047	0.924	1.016	1.014	1.077	0.960	1.071	0.847	0.860
B	0.833	0.979		0.924	0.985	0.981	0.958	0.974	1.010	0.924	0.969	0.981
C	0.813	0.945			0.849	0.972	0.896		0.896		0.967	
D	0.855	0.926	0.938	0.991	0.907	0.959	0.897	0.953	0.948	0.978	1.004	0.970
E	0.842	0.945	0.998	1.009	1.017	0.992	0.942	0.858	1.010	1.016	0.988	0.950
F	0.886	0.964	1.054	0.978	0.899	1.014	0.990	0.987		1.043	1.011	1.002
G	0.959	0.981	1.014	1.067		1.009	0.965	0.934	1.051	0.919	1.119	0.976
H	0.899	1.045	1.031	1.022		0.921	0.983	1.062	1.122	1.089	0.980	1.192

Plate #75/76

	1	2	3	4	5	6	7	8	9	10	11	12
A	0.976	1.032	0.982	1.020	0.965	0.850	1.080	0.966	0.903	0.896	0.988	
B	0.924	0.955	1.101	1.083	1.008	0.884	1.068	0.886	0.988	0.893	0.967	1.056
C	0.945	0.880	1.056	0.978	0.887	0.897	0.909		0.871	0.946	0.897	0.855
D	1.000	0.974	0.969	1.091	0.931	0.909	0.919	0.854	0.889	0.910	0.945	0.945
E	0.932	1.065	1.097	1.019	1.000	0.966	0.960	0.919	0.875	0.808	0.889	0.943
F	1.001	0.909	1.097	1.147	0.946	0.953	1.069	0.892	0.918	0.891	0.896	1.022
G	0.901	1.045	1.161	0.988	0.951	0.924	1.019	1.001	0.930	0.918	1.011	0.875
H	0.990	1.152	1.085	1.073	0.891	0.895		1.097	0.979	1.033		1.020

Plate #77/78

	1	2	3	4	5	6	7	8	9	10	11	12
A	1.243	0.945	0.956	1.056	0.918	1.095	0.903	0.917	0.901	1.021	0.875	1.014
B	1.164	1.024	0.966	0.935	0.985	1.067	1.027	0.985	1.014	0.982	0.971	1.008
C	1.156	0.938	1.000	1.055	1.060	1.057	1.049	0.970	1.059	1.047	1.055	1.082
D	0.993	1.017		1.100	1.056	1.003		0.996	0.994	1.009		1.128
E	0.979	1.048	0.965	1.014		0.936	1.010	1.064	0.968	1.046	0.916	1.104
F	1.096	0.966	1.046	0.979	1.003	0.932	0.926	1.001	0.963	1.053	0.955	1.007
G	0.943		0.926	1.035	0.971	1.082	0.953	0.908	0.982	1.041	1.073	1.008
H	0.903	0.978	0.995	0.954	0.935		0.910	0.936		0.954	1.056	1.089

Plate #79/80

	1	2	3	4	5	6	7	8	9	10	11	12
A	0.933	0.855	0.974	0.998	1.034	0.956	0.899	0.859	1.036	0.878	1.015	0.976
B	0.846	1.000	0.988	1.112	1.102	0.972	0.983	0.935	1.032	0.944	1.073	
C	0.853	0.948	1.072	1.106	0.987	0.957	0.862	0.887	0.871	0.866	0.951	0.968
D	0.948	0.973	1.097	0.996	0.899	0.880	0.971	0.842	0.940	0.914	0.959	0.894
E	0.935	1.039	1.049		0.999	0.985	1.004	1.002	0.938	0.935		0.899
F	1.094	1.013	1.140	1.094	1.015	1.079	0.956	0.911	0.975	0.921	0.980	0.867
G	0.885	1.063	1.130			0.986	0.880	0.967	0.974	1.004		0.843
H	0.918	0.812	1.036	0.868	0.857	1.025	0.847	0.899	0.951	1.040		

Plate #81/82

	1	2	3	4	5	6	7	8	9	10	11	12
A	0.857	0.935	0.963	0.961	0.899	0.926	0.868	0.885	0.818	0.927	0.944	0.907
B	1.000	1.034	0.946	0.936	0.912	0.931	1.003	0.899	0.924	0.858	0.907	0.955
C	0.989	0.903	0.920	0.845	0.894	0.936	0.979	0.873	0.865	0.882	0.879	1.038
D	1.019	0.887	0.897	0.804	0.824	0.955	0.946	0.868	0.894	0.880	0.897	0.876
E	1.051	0.946	0.965	0.890	0.950	0.856	0.899	0.874	0.867	0.892	0.802	0.966
F	0.976	1.028	0.947	0.911	0.859	0.869	0.856	0.892	0.845	0.853	0.868	0.966
G	0.875	0.808	0.948	0.835	0.894	0.852	0.802	0.841	0.834	0.852	0.814	1.026
H	0.842	0.726	0.852	0.724	0.790	0.804	0.848	0.881	0.847	0.869	0.945	1.140

Plate #83/84

	1	2	3	4	5	6	7	8	9	10	11	12
A	1.045	1.157	0.932	0.848	0.914	1.000	0.913	0.878	0.802	0.858	0.928	0.931
B	1.128	1.132	1.170		1.148	1.042	0.911	0.801	0.813		0.832	0.870
C	1.138	1.000	1.099	1.004	1.014	0.969	0.868	0.803	0.836	0.813	0.941	0.912
D	1.114	1.108	1.094	1.099	1.055	0.963	0.804	0.876	0.815	0.833	0.819	0.983
E	1.115	1.072	1.149	1.166	1.107	0.958	0.897	0.873	1.021	0.848	0.974	0.897
F	1.121	1.133	1.001	1.126	0.986	0.956	0.819	0.847	0.868	0.867	0.903	0.949
G	1.125	1.062	1.076	1.024	0.952	1.024	0.937	0.912	0.887	0.924	0.874	1.043
H	1.148	1.169	0.886	1.073	1.055	0.901	0.918	0.926	0.949	0.942	0.952	0.842

Plate #85/86

	1	2	3	4	5	6	7	8	9	10	11	12
A	0.870	0.818	0.862	0.854		0.803	0.849	0.896	0.886	0.849	0.865	0.869
B	0.839	0.885	1.009	0.976	0.994	1.024	1.060	0.973	0.981	0.923	0.926	0.884
C	0.871	0.908	1.017	0.757	1.061	0.979	1.030		0.967	0.979	0.923	0.877
D	0.829	0.909	0.931	0.936	1.001	0.771	1.185	0.936	1.001	1.054	0.980	0.827
E	0.833	0.829	1.059	0.948	0.754	0.817	1.048	1.026	0.967	1.111		0.926
F	0.826	0.891	0.856	0.904	0.912	0.848	0.948	0.998	0.954	0.931	0.878	0.924
G	0.831	0.862	1.158	1.258	0.930	0.935	0.948	0.935	0.897	0.974	1.000	0.866
H	0.844	0.822	0.760	0.817	0.815	0.830	0.804	0.882	0.804	0.823	0.805	0.806

Plate #87/88

	1	2	3	4	5	6	7	8	9	10	11	12
A	0.872	1.000	0.945	0.981	1.004	1.096	0.936	0.995	0.957	0.939	0.917	0.943
B		1.147	0.891	1.034	1.023	1.064	1.021		0.918	0.944	0.888	
C	0.871	0.948	1.019	0.965	0.982			0.815	0.918	0.933	0.899	0.895
D	1.055	0.971	0.949	0.980	0.983	1.018	0.996	0.954	0.969	0.947	0.874	0.853
E		0.849	1.014	1.016	0.984	1.036	0.970	0.935	0.897	0.894	0.851	0.883
F	0.960	0.995	0.966	0.942	1.033	1.003	0.934	0.963	0.945	0.983	0.864	0.879
G	0.928	1.010	0.953	0.880	1.018	1.035	0.897	0.896	0.975	1.034	0.844	0.891
H	1.099	0.954		0.862	1.032	1.082	0.862	0.975	0.847	0.945	0.910	0.858

Plate #89/90

	1	2	3	4	5	6	7	8	9	10	11	12
A	0.925	0.936	0.960	0.943	0.863	1.008	0.979	1.022				0.808
B	0.926	0.949	0.908	1.007	1.043		1.297	0.986	0.905			0.920
C	0.826	0.954	0.964	0.936		0.905	0.833	0.894	0.988	0.988		0.917
D	0.826	0.903	0.954	0.953	1.058	0.887	0.900	0.982	0.871	0.877		0.945
E	1.000	0.929	1.096	1.037		0.817	0.913	0.969	0.880	0.905	0.963	0.959
F		0.974	0.892	0.970	0.897	0.949	0.923		0.806	0.910	0.848	0.976
G	0.937	0.998	0.965	0.947	1.065	0.927	0.817		0.848	1.035	1.051	1.039
H	0.950	1.020	0.909	0.909	0.887	0.989	0.870	0.954	0.804	0.812	1.068	0.914

Plate #91-94

	1	2	3	4	5	6	7	8	9	10	11	12
A	1.201	0.984	1.046	1.000							0.924	1.227
B	1.113	0.987	1.053									0.979
C	0.994	0.918	1.116							0.826	1.071	1.051
D	1.013	0.971								0.879	1.066	1.116
E	0.943	1.030								0.956	0.976	
F	0.920	0.966								1.084	0.907	
G	0.952	0.924								0.864	0.969	
H	0.890	1.054										

Plate #95

	1	2	3	4	5	6	7	8	9	10	11	12
A	0.936	0.908	0.963	0.908	0.950	0.950	0.942					
B	0.940		0.936	0.907	0.944	0.966	0.926					
C		0.939	0.920	0.894	0.940	0.950	1.000					
D	0.961		0.911		0.964	0.930						
E	0.935	0.948	0.916	0.927	0.950	0.918	0.997					
F	0.937	0.951	0.920	0.943	0.897	0.909	0.992					
G	0.916	0.969	0.955	0.928	0.918	0.942						
H		0.980	0.925	0.940	0.917	0.935						

Supplementary data 3 *Corresponding fold change values displayed in 96-well plates layout.*

Supplementary data 4 *Primers used for plasmid construction in this study.*

Designation	**Primer sequences (5' to 3')**
pET-*zwf*	
zwf-MCS2-Fwd	TAAGAAGGAGATATAATGGCGGTAACGCAA
zwf-MCS2-Rev	TAAGAAGGAGATATAATGGCGGTAACGCAA
pET-*zwf*-MCS2-Fwd	TAACTGCTGCCACCGCTGAG
pET-*zwf*-MCS2-Rev	CCGCCATTATATCTCCTTCTTATACTTAAC
pET-*fbp*	
fbp-MCS2-Fwd	TAAGAAGGAGATATAATGAAAACGTTAGGT
fbp-MCS2-Rev	TGGCAGCAGTTACGCGTC
pET-*fbp*-MCS2-Fwd	TAACTGCTGCCACCGCTG
pET-*fbp*-MCS2-Rev	ACCTAACGTTTTCATTATATCTCCTTCTTA
pET-*zwf-fbp*	
zwf-MCS1-Fwd	GAAGGAGATATAATGGCGGTAA
zwf-MCS1-Rev	CTGTTCGATTACTCAAACTCATTCC
pET-*fbp*-MCS1-Fwd	TGAGTAATCGAACAGAAAGTAATCGTATT
pET-*fbp*-MCS1-Rev	GCCATTATATCTCCTTCTTAAAGTTAAACA

Supplementary data 5 *Initial organic substrate concentration detected in the mixed medium at D0.*

Culture medium	Riboflavin (mg L^{-1})	Soluble carbohydrate (mg L^{-1})	Soluble protein (mg L^{-1})
Mono	0.1±0.04	33±2	0.8±0.01
NT	0.3±0.1	215±0.3	13. 2 ±6.7
R3-0 mM	0.8±0.2	218±3.3	8.3±6.3
R3-0.01 mM	0.9±0.1	228±12	14.6 ±3.6
R3-0.1 mM	1.3±0.2	227±12	25±5.5

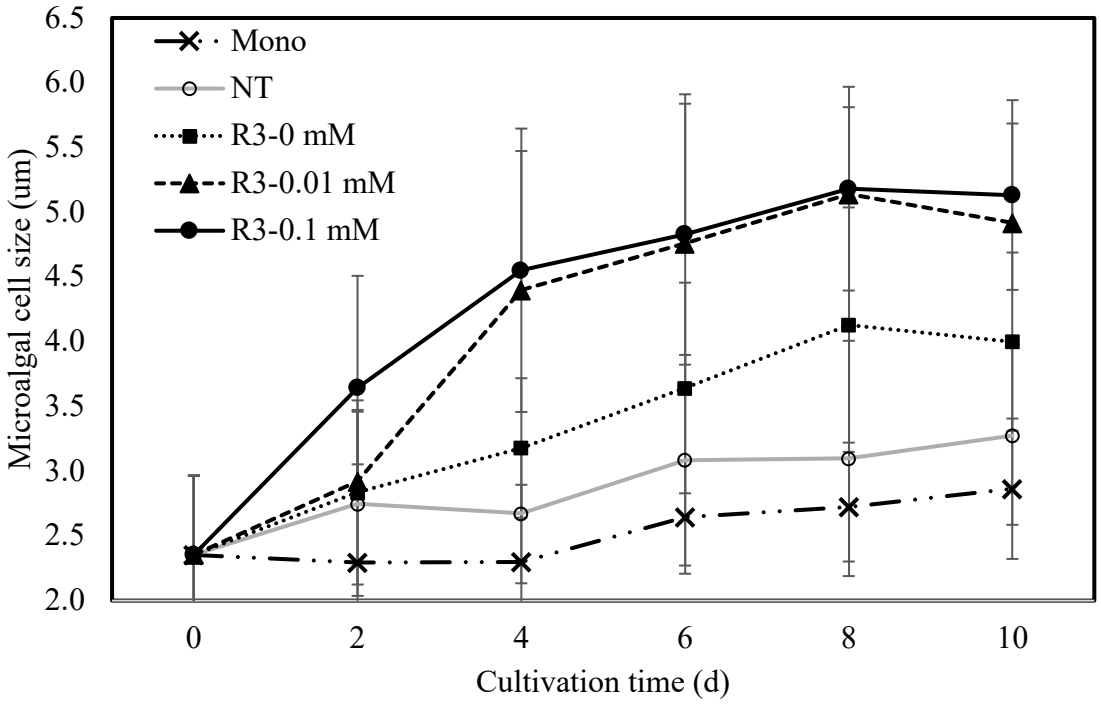

Supplementary data 6 *Algal cell size measurement over time, n=3.*

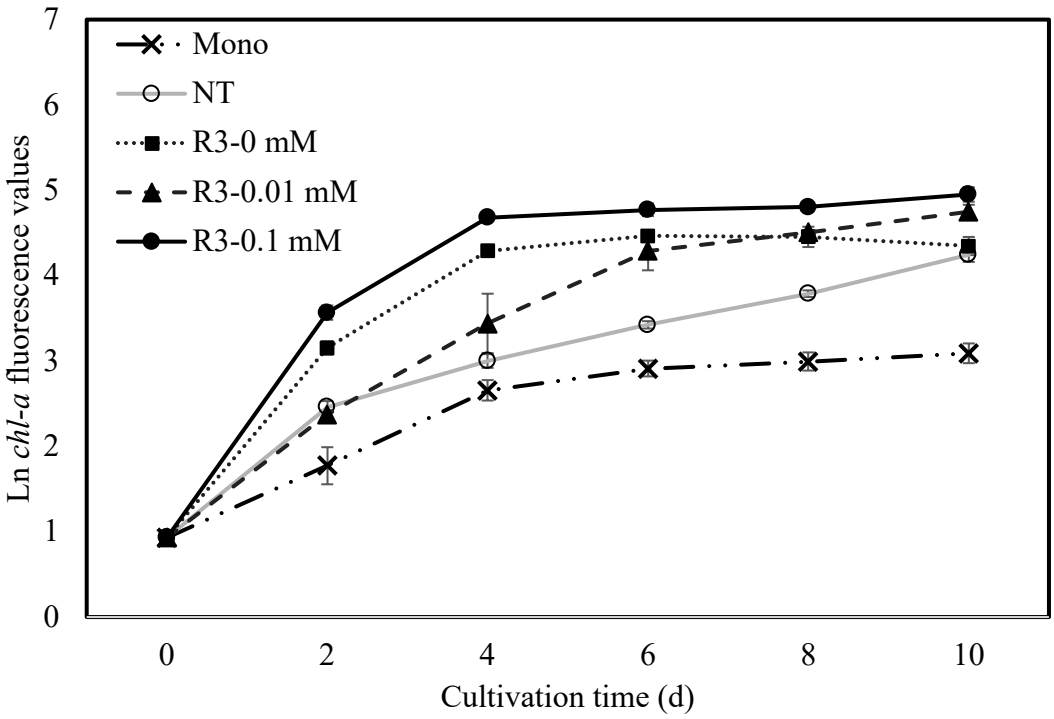

Supplementary data 7 *Plot of log of algal growth based on chl a fluorescence measurements over time, n=3.*

Supplementary data 8 *Primers used for plasmid construction in this study.*

Designation	Primer sequences (5' to 3')
pETDuet-1-*zwf-fbp*	
zwf-MCS1-Fwd	GAAGGAGATATAATGGCGGTAA
zwf-MCS1-Rev	CTGTTCGATTACTCAAACTCATTCC
pET-*fbp*-MCS1-Fwd	TGAGTAATCGAACAGAAAGTAATCGTATT
pET-*fbp*-MCS1-Rev	GCCATTATATCTCCTTCTTAAAGTTAAACA
fbp-MCS2-Fwd	TAAGAAGGAGATATAATGAAAACGTTAGGT
fbp-MCS2-Rev	TGGCAGCAGTTACGCGTC
pET-*fbp*-MCS2-Fwd	TAACTGCTGCCACCGCTG
pET-*fbp*-MCS2-Rev	ACCTAACGTTTTCATTATATCTCCTTCTTA
pACYCDuet-1-*cob*U-*cob*C	
*cob*U-MCS1-Fwd	GGAGATATAATGATGATTTTGGTGAC
*cob*U-MCS1-Rev	TCTGTTCGTCATTTGATTTTTACTC
pACYC-*cob*U-MCS1-Fwd	TCAAATGATCGAACAGAAAGT
pACYC-*cob*U-MCS1-Rev	AATCATCATTATATCTCCTTATTAAAGTT
*cob*C-MCS2-Fwd	TAAGAAGGAGATATAATGCGACTGTGGTT
*cob*C-MCS2-Rev	GGCAGCAGTCATGCATTCTC
pACYC-*cob*C-MCS2-Fwd	TGCATGACTGCTGCCACCG

pACYC-*cob*C-MCS2-Rev	AACCACAGTCGCATTATATCTCCTTCTTA
pCDFDuet-1-*bio*F-*bio*D	
*bio*F-MCS1-Fwd	GAGATATAATGAGCTGGCAGGAG
*bio*F-MCS1-Rev	CTGTTCGATTAACCGTTGCCA
pCDF-*bio*F-MCS1-Fwd	ACGGTTAATCGAACAGAAAGTAATCG
pCDF-*bio*F-MCS1-Rev	GCCAGCTCATTATATCTCCTTAT
*bio*D-MCS2-Fwd	GATATAGTGAGTAAACGTTATTTTGTCACC
*bio*D-MCS2-Rev	CAGCAGCTACAACAAGGCAA
pCDF-*bio*D-MCS2-Fwd	TGTTGTAGCTGCTGCCAC
pCDF-*bio*D-MCS2-Rev	CGTTTACTCACTATATCTCCTTCTTATACT

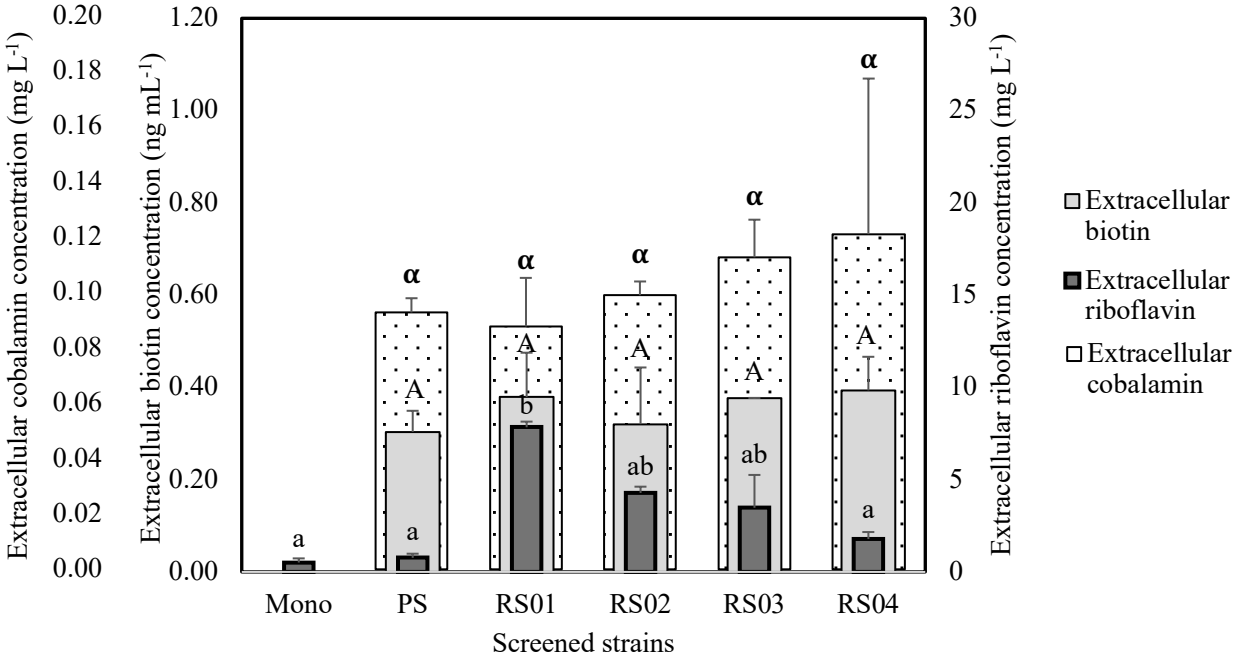

Supplementary data 9 *Quantification of metabolite concentrations in the extracellular medium of recombinant bacterial strains compared to monoculture and parental strain controls. The extracellular medium was prepared by mixing the culture supernatant with an equal volume of BG11 medium. Data are stated as mean ± standard deviation, n=3. Lowercase alphabets, uppercase alphabets, and Greek letters stand for significant differences across different time points within the same strain, detected by Tukey test.*

List of Publications

Osaka University (PhD study-related)

1. **C. Y. Tong**, H. Tomita, K. Miyazaki, C. J. C. Derek, K. Honda. KEIO Knockout Collection Reveals Metabolomic Crosstalk in *Chlorella* spp.-*Escherichia coli* Co-cultures. *Journal of Phycology* (2025). In Press.
2. **C. Y. Tong**, H. Tomita, K. Miyazaki, C. J. C. Derek, K. Honda. Impacts of Riboflavin-overproducing Engineered *Escherichia coli* towards *Chlorella sorokiniana* Growth in Co-cultivation Approach. *Algal Research* (2025). 103938.

Universiti Sains Malaysia (PhD study-related)

1. **C. Y. Tong**, Chai Ying Kee, Kohsuke Honda, C. J. C. Derek. Microalgal-bacterial Co-cultivation on Novel Bio-coated Supports: Evaluation of Growth Performance in Submerged and Permeated Biofilm Cultivation System with Cost-benefit Assessment. *Algal Research* (2024). **84**, 103792.
2. **C. Y. Tong**, Kohsuke Honda, Norhidayah Ahmad Wazir, C. J. C. Derek. Co-culture of *Chlorella vulgaris* and *Escherichia coli* Enhance Intracellular Organic Matter in Biofilm Mode. *ASEAN Engineering Journal* (2024). **14(4)**, 161-166.
3. **C. Y. Tong**, Kohsuke Honda, C. J. C. Derek. Enhanced Microalgal Growth and Metabolites through Co-cultivation with *Escherichia coli* in Algal Organic Matter Solution. *Algal Research* (2023). **77**, 103351.
4. **C. Y. Tong,** Chai Ying Kee, Kohsuke Honda, C. J. C. Derek. Bio-coatings in Permeated Cultivation Systems: Unprecedented Impacts on Microalgal Monoculture Growth and Organic Matter Yield. *Environmental Research* (2023). **239**, 117403.
5. **C. Y. Tong,** Kohsuke Honda, C. J. C. Derek. Enhancing Organic Matter Productivity in Microalgal-bacterial Biofilm using Novel Bio-coating. *Science of the Total Environment* (2023). **906,** 167576.
6. **C. Y. Tong**, C. J. C. Derek. Bio-coatings as Immobilized Microalgae Cultivation Enhancement: A Review. *Science of the Total Environment* (2023). **887**, 163857.
7. **C. Y. Tong**, Kohsuke Honda, C. J. C. Derek. A Review on Microalgal-bacterial Co-culture: The Multifaceted Role of Beneficial Bacteria towards Enhancement of Microalgal Metabolite Production. *Environmental Research* (2023). **228**, 115872.
8. **C. Y. Tong**, M. X. Chua, Win Hung Tan, C. J. C. Derek. Microalgal extract as bio-coating to enhance biofilm growth of marine microalgae on microporous membranes. *Chemosphere* (2022). **360***,* 137712.

Others

1. Win Hung Tan, **C. Y. Tong**, M. X. Chua, C. J. C. Derek. Modelling and Optimizing Secondary Metabolites Production in *Spirodela polyrhiza* using Machine Learning. *Journal of Cleaner Production* (2024). **478**, 143986.
2. **C. Y. Tong,** Huai Z Li, C. J. C. Derek. A Microscale System for In-situ Investigation of Immobilized Microalgal Cell Resistance against Liquid Flow. *Lab on Chip*, (2023). **23(18)**, 4052-4066.
3. **C. Y. Tong**, C. J. C. Derek. "Cultivation of Diatoms in Photobioreactors." Diatoms: Ecology and Biotechnological Applications (1st Ed), edited by Tiwari A., Pandey, A., Show, P.-L., & Binod, P. (Eds.) CRC Press, 2023.
4. Mei Xia Chua, **Yi Tong Cheah,** Win Hung Tan, Derek Juinn Chieh Chan. A novel cultivation platform of duckweed (*Lemna minor*) via application of beeswax superhydrophobic coatings. *Environmental Research* (2023). **224**, 115544.
5. **C. Y. Tong**, S. L. Lim, M. X. Chua, C. J. C. Derek. Uncovering the Role of Algal Organic Matter Biocoating on *Navicula incerta* Cell Deposition and Biofilm Formation. *Bioengineered* (2023). **14(1),** 2252213.
6. **Cheah Yi Tong,** Noorul Aisyah Md Suhaimi, Derek Chan Juinn Chieh. Effect of Bioturbation on Biomass Concentration, Total Lipid and Eicosapentaenoic Acid (EPA) Yield of *Navicula* sp. *AIP Conference Proceedings* (2023). **2785**, 040001.
7. **C. Y. Tong**, C. J. C. Derek. Marine Microalgal Biofilm Development and Its Adhesion Propensities on Commercial Membrane via XDLVO Approach. *Journal of Biotechnology* (2022). **360***,* 37-44.
8. **C. Y. Tong**, C. J. C. Derek. Novel Extrapolymeric Substances Biocoating on Polyvinylidene Fluoride Membrane for Enhanced Attached Growth of *Navicula incerta*. *Microbial Ecology* (2022). **86**, 549-562.
9. **C. Y. Tong,** J. K. Lew, C. J. C. Derek. Algal Extracellular Organic Matter Pre-treatment Enhances Microalgal Biofilm Adhesion onto Microporous Substrate. *Chemosphere* (2022). **307***,* 135740.
10. **Yi Tong Cheah,** Bee Wah Ng, Tze Ling Tan, Zi Sheng Chia, Derek Juinn Chieh Chan. Biomass and Eicosapentaenoic Acid (EPA) Production from *Amphora* sp. under Different Environmental and Nutritional Conditions **.** *Biotechnology and Applied Biochemistry* (2022). **70(2)**, 568-580.
11. **C. Y. Tong**, Fakhira Huda Binti Che Yusuf , C. J. C. Derek. Optimization of *Moringa Oleifera* Seed Extract and Chitosan as Natural Coagulant in Treatment of Fish Farm Wastewater. *Desalination and Water Treatment* (2022). **256***,* 99-113.
12. **C. Y. Tong,** C. J. C. Derek, Membrane Surface Roughness Promotes Rapid Initial Cell Adhesion and Long Term Microalgal Biofilm Stability. *Environmental Research* (2022). **206***,* 112602.

13. **C. Y. Tong,** C. J. C. Derek, A Methodological Review on the Characterization of Microalgal Biofilm and Its Extracellular Polymeric Substances. *Journal of Applied Microbiology* (2022). **132(5)**, 3490-3514.
14. **C. Y. Tong**, Ying Shi Chang, Boon Seng Ooi, C. J. C. Derek. Physico-chemistry and Adhesion Kinetics of Algal Biofilm on Polyethersulfone (PES) Membrane with Different Surface Wettability. *Journal of Environmental Chemical Engineering* (2021). **9(6),** 106531.
15. **Yi Tong Cheah**, Derek Juinn Chieh Chan. Physiology of Microalgal Biofilm: A Review on Prediction of Adhesion on Substrates. *Bioengineered* (2021). **12(1)**: 7577-7599.
16. **C. Y. Tong**, C. J. C. Derek. The Role of Substrates Towards Marine Diatom *Cylindrotheca fusiformis* Adhesion and Biofilm Development. *Journal of Applied Phycology* (2021). **33(2)**: 2845-2862.
17. Chang Ying Shi, **Cheah Yi Tong**, Lyly Leow Hui Ting, Ishak Nur Ir Imani, Ng Yin Sim, Ahmad Abdul Latif, Leo Choe Peng, Derek Chan Juinn Chieh, Ooi Boon Seng. Microalgal Exopolymeric Substances Fouling in Submerged Vacuum Membrane Distillation and its Mitigation via Enhanced Air Bubbling. *Desalination* (2021). **508**, 115047.
18. **C. Y. Tong**, C. J. C. Derek. Biofilm Formation of Benthic Diatoms on Commercial Polyvinylidene Fluoride Membrane. *Algal Research* (2021). **55**, 102260.
19. **C. Y. Tong**, H.K.K. Lakbir Singh, C. J. C. Derek. Effect of High Temperature towards Microalgal Organic Matter and its Impact towards Membrane Distillation Application. *Water Environment Research* (2021). **93(7)**: 1107-1115.
20. **Cheah Yi Tong**, Fakhira Huda Binti Che Yusuf, C. J. C. Derek. Fish Farm Wastewater Treatment using *Moringa oleifera* Seed Powder as Natural Coagulant. *IOP Conference Series: Earth and Environmental Science* (2021). **945(1)**, 012070.

Acknowledgement

Enrolling myself into a double-degree program between Osaka University and Universiti Sains Malaysia was the best decision that I have made in my PhD journey. It gave me a golden opportunity to explore a new research field, with the aids of all the advanced equipment and guidance from the experts.

I acknowledge the people who mean a lot to me since I was born, my parents for giving me liberty to choose what I desired in my life. They know I have strong interest in my research and always be the first person to share my moment of obvious joy.

Next, I am extremely grateful to my main thesis advisor in Osaka University, Professor Dr. Kohsuke Honda, and advisor in Universiti Sains Malaysia, Associate Professor Dr. Derek Chan Juinn Chieh, for their supports in my research.

Following that, I would like to send my appreciation to my co-advisors in Osaka University, Professor Dr. Hiroya Tomita, and Specially Appointed Professor Dr. Kentaro Miyazaki for their guidance in my research.

I sincerely thank all the members of Honda Lab for their support and assistance during my stay in Japan. I extend my special gratitude to Prof. Dr. Honda and Prof. Dr. Tomita for their generosity and care during the conference trip to Okinawa in December 2024. That was one of my best memories of the study life in Japan. Special thanks to Prof. Dr. Honda for giving me another research opportunity in Bielefeld University, Germany too. I truly appreciated my studies in Japan, and it has been a rewarding experience for me.